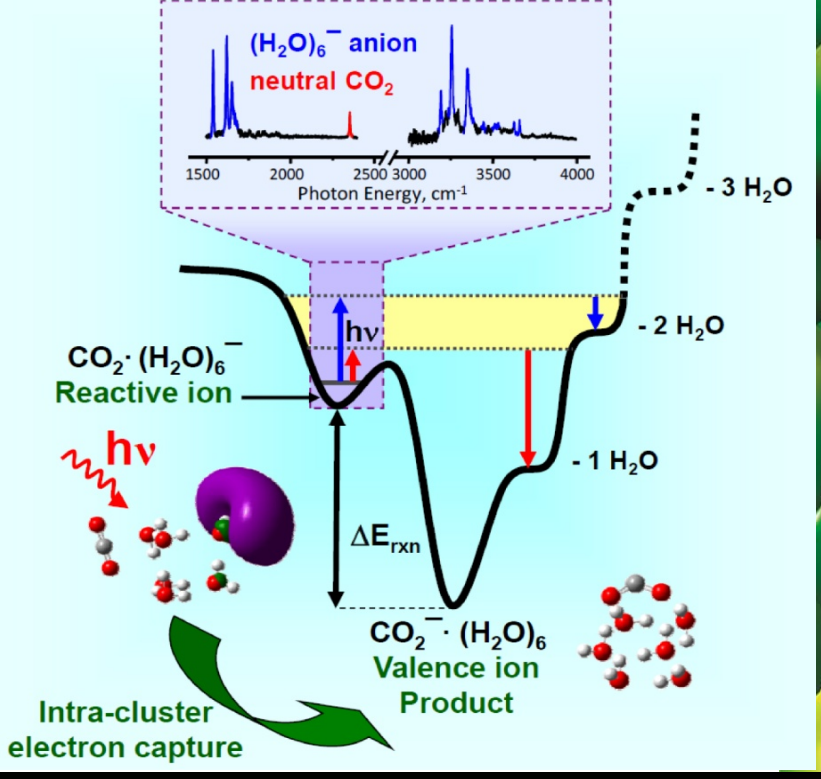

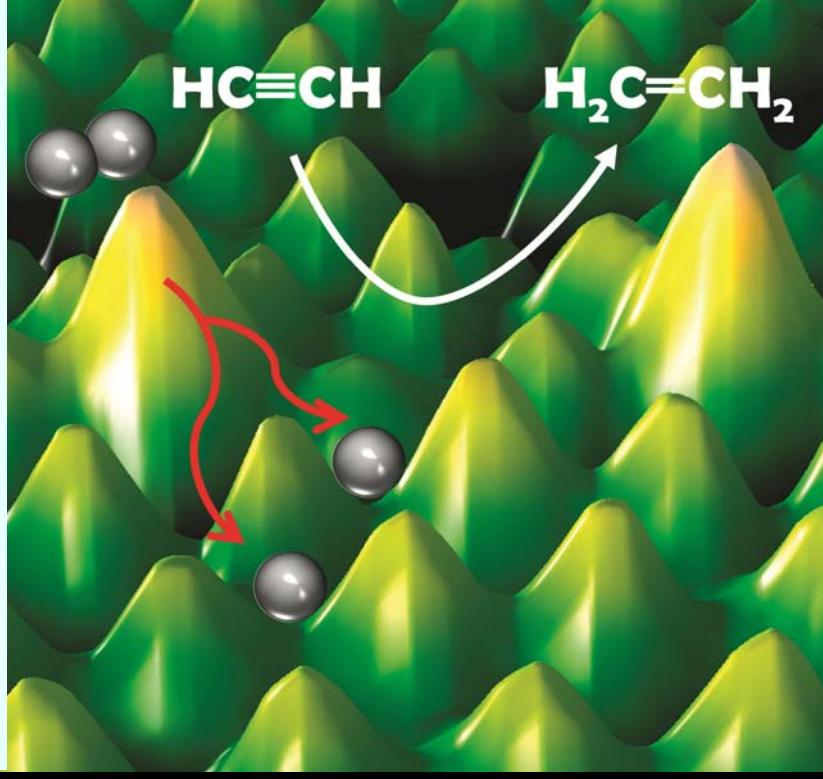

CPIMS 8

U.S. DEPARTMENT OF ENERGY | Office of Science

Office of Basic Energy Sciences
Chemical Sciences, Geosciences & Biosciences Division

Eighth Condensed Phase and Interfacial Molecular Science (CPIMS) Research Meeting

Bolger Conference Center, Potomac, MD
October 21 - 24, 2012

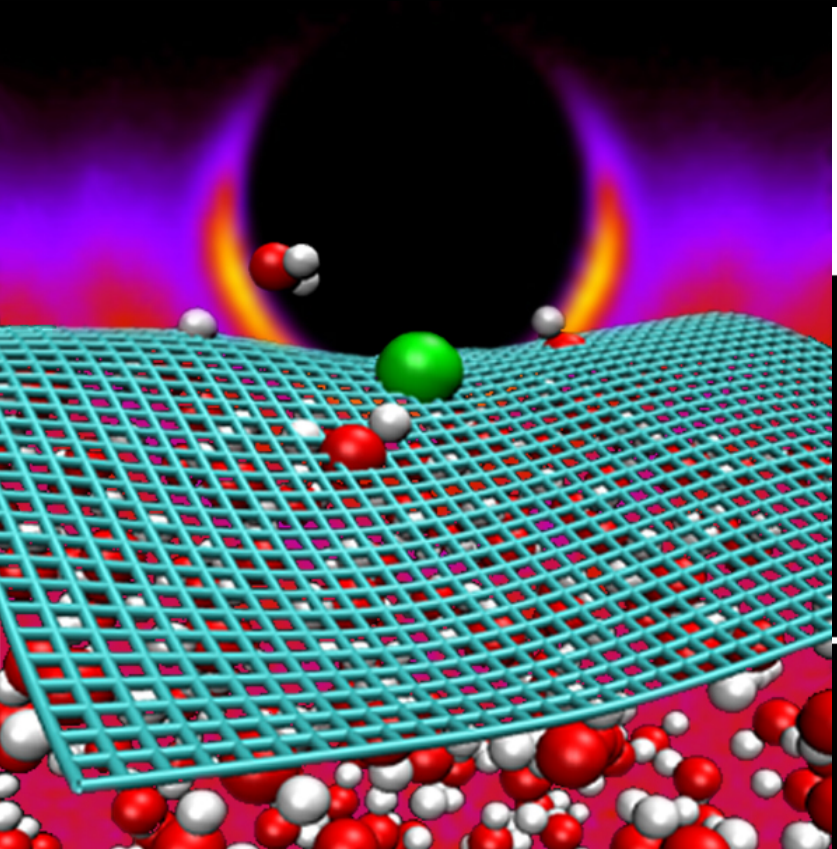

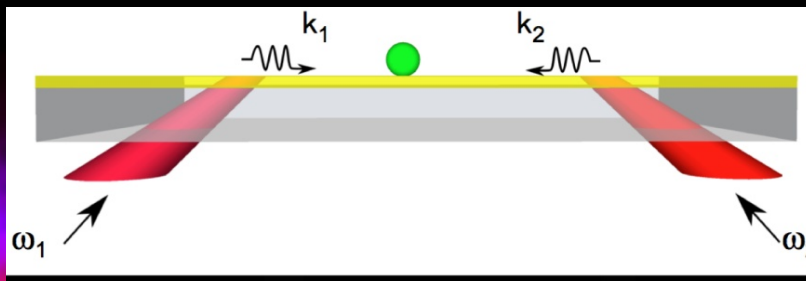

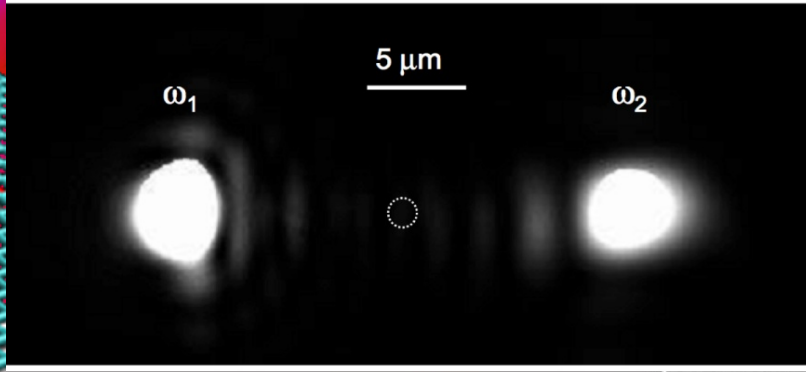

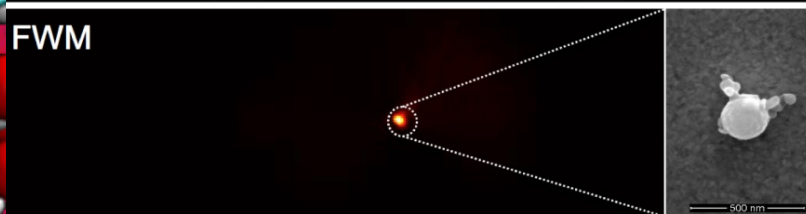

Program and Abstracts for

CPIMS 8

Eighth Research Meeting of the Condensed Phase and Interfacial Molecular Science (CPIMS) Program

Bolger Conference Center
Potomac, MD
October 21-24, 2012

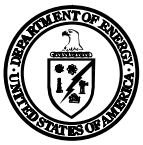

U.S. DEPARTMENT OF ENERGY | Office of Science

Office of Basic Energy Sciences
Chemical Sciences, Geosciences & Biosciences Division

The research grants and contracts described in this document are supported by the U.S. DOE Office of Science, Office of Basic Energy Sciences, Chemical Sciences, Geosciences and Biosciences Division.

Potential energy landscape of the $(H_2O)_6^-$•CO_2 cluster. Using supersonic expansion techniques the cluster is prepared with the excess electron localized on the water cluster. Excitation of the asymmetric CO stretch of the CO_2 or of the OH stretch of bending vibrations of a water monomer results in electron transfer to CO_2 followed by loss of one or two water molecules. Direct dynamics simulations show that the electron transfer process is triggered by formation of an H bond between a water molecule and the CO_2.

Reprinted with permission from K. J. Breen, A. F.DeBlase, T. L. Guasco, V. K. Voora, K. D. Jordan, T. Nagata, and M. A. Johnson "Bottom-Up View of Water Network-Mediated CO_2 Reduction Using Cryogenic Cluster Ion Spectroscopy and Direct Dynamics Simulations", *The Journal of Physical Chemistry A*, January 1, 2012.

Submitted by Kenneth D. Jordan (University of Pittsburgh and Mark A. Johnson (Yale University)

For further information, see abstract on pages 99-102.

Catalytic hydrogenations are critical to many industrial processes including agricultural chemicals, foods and pharmaceuticals. Typical heterogeneous hydrogenation catalysts involve nanoparticles composed of expensive noble metals or alloys based on platinum, palladium, rhodium, and ruthenium. Small quantities of individual, isolated palladium atoms can convert the otherwise catalytically inert surface of an inexpensive metal like copper into an ultraselective catalyst. The mechanism involves facile dissociation of molecular hydrogen at individual palladium atom sites followed by spillover onto the copper surface, where ultraselective catalysis occurs by virtue of weak binding. The reaction selectivity is in fact much higher than that measured on palladium alone, illustrating the unique synergy of the system. This approach is a promising strategy for designing novel bi-functional heterogeneous catalysts in which a catalytically active element is atomically dispersed in a more inert matrix. Moreover, some of the best industrial alloy catalysts to date may already be operating via this mechanism, but there is currently no way to directly probe the atomic scale geometry of an alloyed nanoparticle of a working catalyst.

G. Kyriakou, M. B. Boucher, A. D. Jewell, E. A. Lewis, T. J. Lawton, A. E. Baber, H. L. Tierney, M. Flytzani-Stephanopoulos and E. C. H. Sykes, *Science*, 2012, 335, 1209-1212.

Submitted by E. Charles H. Sykes (Tufts University)

For further information, see abstract on pages 175-178.

CPIMS 8

About the Cover Graphics

Influence of a dissolved ion on the structure and thermodynamics of the air-water interface. The model anion (green), comparable in size to an iodide ion and slightly less charged, resides near the mean interfacial height in this snapshot from a molecular simulation. Instantaneous topography of the interface (blue wire mesh, determined by coarse-graining the solvent's molecular configuration) highlights, however, that fluctuations about the average surface are substantial.

The energy and entropy of adsorbing such a solute at the interface are both surprisingly negative, suggesting that entropy changes arise from the ion's suppression of capillary-like fluctuations. Computed energy changes, depicted in the background color pattern, originate instead from shifting populations of water molecules in surface, bulk, and solvation environments. By occupying space in the high-energy surface region, a solute effectively reduces the contact area between liquid and vapor. The resulting decrease in surface energy can be large, but is neglected by traditional perspectives such as dielectric continuum theory.

D. E. Otten, P. R. Shaffer, P. L. Geissler, and R. J. Saykally, *Proceedings of the National Academy of Science*, 109, 701 (2012).

Submitted by Phillip L. Geissler and Richard J. Saykally (Lawrence Berkeley National Laboratory)

For further information, see abstracts on pages 67-60 and pages 151-154.

Nonlinear optics with surface waves. Upper panel: two femtosecond pulses are coupled into a gold film to form two counter-propagating surface plasmon polarition (SPP) waves. A silicon nanotarget is placed in the middle. Middle panel: reflection image on the CCD showing the launching points of the SPP waves. Lower panel: Fourwave mixing signal (electronic coherent anti-Stokes Raman scattering) of the nanotarget, excited by the two SPP waves. Note that the particle is excited by surface waves only, and not by freely propagating photons. The inset shows a SEM image of the Si nanoparticle.

X. Liu, Y. Wang, and E. O. Potma, "Surface-mediated four-wave mixing of nanostructures with counterpropagating surface plasmon polaritons", *Optics Letters* 36, 2348-2350 (2011).

Submitted by Eric O. Potma (University of California, Irvine)

For further information, see abstract on pages 147-149.

Foreword

This volume summarizes the scientific content of the Eighth Research Meeting on Condensed Phase and Interfacial Molecular Science (CPIMS) sponsored by the U. S. Department of Energy (DOE), Office of Basic Energy Sciences (BES). The research meeting is held for the DOE laboratory and university principal investigators within the BES CPIMS Program to facilitate scientific interchange among the PIs and to promote a sense of program identity.

During past CPIMS research meetings, investigators from other research programs have been invited to present their work. The hope is that the cross-fertilization of ideas is promoted, and the invited presentations have been well received during prior CPIMS meetings. Unfortunately, budget cuts have resulted in the need to drop temporarily the inclusion of outside speakers from the CPIMS meeting agenda. It is hoped that budget reductions can be reversed before future meetings are held. In the meantime, several CPIMS investigators have graciously agreed to present their research in the time slots freed by this decision. We are indebted to these investigators for agreeing to prepare presentations on this occasion.

Reductions in budgets available for conferences have also meant that there were no hardcopies of this book printed, and that no electronic copies of the book were provided on CD-ROMs. As a consequence, the need to deliver the book in pdf format entirely by electronic means led to the extensive use of file compression. It is hoped that the resulting visual quality is acceptable to readers.

We are deeply indebted to the members of the scientific community who have contributed valuable time toward the review of proposals and programs. These thorough and thoughtful reviews are central to the continued vitality of the CPIMS Program. We appreciate the privilege of serving in the management of this research program. In carrying out these tasks, we learn from the achievements and share the excitement of the research of the many sponsored scientists and students whose work is summarized in the abstracts published on the following pages.

This year's speakers are gratefully acknowledged for their investment of time and for their willingness to share their ideas with the meeting participants. Special thanks are reserved for the staff of the Oak Ridge Institute for Science and Education, in particular, Connie Lansdon and Tim Ledford. We also thank Diane Marceau, Robin Felder, and Michaelene Kyler-Leon in the Chemical Sciences, Biosciences, and Geosciences Division for their indispensable behind-the-scenes efforts in support of the CPIMS program. Finally, we thank Dawn Adin (BES/AAAS Fellow) for expert advice on the design of this pdf file.

Gregory J. Fiechtner, Mark R. Pederson, and Michael P. Casassa
Chemical Sciences, Geosciences and Biosciences Division
Office of Basic Energy Sciences

Agenda

U. S. Department of Energy
Office of Basic Energy Sciences
Eighth Condensed Phase and Interfacial Molecular Science (CPIMS) Research Meeting

Sunday, October 21

3:00-6:00 pm	**** Registration ****
6:00 pm	**** Reception (No host, Pony Express Bar & Grill) ****
7:00 pm	**** Dinner (Osgood's Restaurant) ****

Monday, October 22

7:30 am **** Breakfast (Osgood's Restaurant) ****

All Presentations held in Stained Glass Hall

8:30 am *Introductory Remarks*
Gregory J. Fiechtner, **Mark R. Pederson, and Eric A. Rohlfing,**
DOE Basic Energy Sciences

Session I Chair: **Michael D. Fayer,** Stanford University

9:00 am *The Ultrafast Infrared Spectroscopy of Protons in Water*
Andrei Tokmakoff, Massachusetts Institute of Technology

9:30 am *Equilibria and Dynamics at Aqueous Interfaces - SHG and SFG Studies*
Kenneth B. Eisenthal, Columbia University

10:00 am *Correlating Electronic and Nuclear Motions during Photoinduced Charge Transfer Processes using Multidimensional Femtosecond Spectroscopies and Ultrafast X-ray Absorption Spectroscopy*
Munira Khalil, University of Washington

10:30 am **** Break ****

Session II Chair: **Gregory K. Schenter,** Pacific Northwest National Laboratory

11:00 am *Understanding Nanoscale Confinement Effects in Solvent-Driven Chemical Reactions*
Ward H. Thompson, University of Kansas

11:30 am *Computational Studies of Aqueous and Ionic Liquids Interfaces*
Liem X. Dang, Pacific Northwest National Laboratory

12:00 noon *Nucleation Chemical Physics*
Shawn M. Kathmann, Pacific Northwest National Laboratory

12:30 pm **** Lunch (Osgood's Restaurant) ****

1:30–4:00 pm Free/Discussion Time

Session III Chair: **Jay A. LaVerne,** Notre Dame Radiation Laboratory

4:00 pm *Fundamentals of Solvation under Extreme Conditions*
John L. Fulton, Pacific Northwest National Laboratory

4:30 pm *Laboratory Studies of Nuclear Reactor Chemistry: The Equilibrium $H + H_2O \leftrightarrow H_2 + OH$*
David M. Bartels, Notre Dame Radiation Laboratory

5:00 pm *Reactivity and Dynamics in Ionic Liquids*
James F. Wishart, Brookhaven National Laboratory

5:30 pm *Rapid Capture of Charges in Pulse-Radiolysis Experiments at LEAF*
Andrew R. Cook, Brookhaven National Laboratory

6:00 pm **** Reception (no host, Pony Express Bar & Grill) ****

6:30 pm **** Dinner (Osgood's Restaurant) ****

Tuesday, October 23

7:30 am **** Breakfast (Osgood's Restaurant) ****

Session IV Chair: **Mark S. Gordon,** Ames Laboratory

8:30 am *Atomistic and Coarse-Grained Modeling of Catalytic Reactions on Surfaces and in Nanoporous Materials*
James W. Evans, Ames Laboratory

9:00 am *Correlations between Core Level Binding Energies and Activity for Catalytic and Electrocatalytic Oxidation*
Scott L. Anderson, University of Utah

9:30 am *Dynamics in the Electronic Continuum*
John C. Tully, Yale University

10:00 am **** Break ****

Session V Chair: **E. Charles H. Sykes,** Tufts University

10:30 am *Surface Chemical Dynamics*
Michael G. White, Brookhaven National Laboratory

11:00 am *Ultrafast Chemical Dynamics on Nanoscale Surfaces*
Nicholas Camillone III, Brookhaven National Laboratory

11:30 am *Molecular Dynamics on the Angstrom Scale*
Richard Osgood, Columbia University

12:00 noon **** Lunch (Osgood's Restaurant) ****

1:00–4:00 pm Free/Discussion Time

Session VI Chair: **Greg A. Kimmel,** Pacific Northwest National Laboratory

4:00 pm *Transient Excitons at Metal Surfaces: Fact or Fiction?*
Hrvoje Petek, University of Pittsburgh

4:30 pm *Atomic-Scale Characterization of Optically-Active Nanoscale Systems*
Jeffrey R. Guest, Argonne National Laboratory

5:00 pm *In situ Microscopy and Spectroscopy at the Molecular Environmental Science Beamline at the ALS*
Hendrik Bluhm, Lawrence Berkeley National Laboratory

5:30 pm *The Quest for Non-Fluorescent Optical Detection of Single Molecules*
Sunney Xie, Harvard University

6:00 pm **** Reception (No Host, Pony Express Bar & Grill) ****

6:30 pm **** Dinner (Osgood's Restaurant) ****

Wednesday, October 24

7:30 am **** Breakfast (Osgood's Restaurant) ****

Session VII Chair: **Mark A. Johnson,** Yale University

8:30 am *Structural and Chemical Properties of Group 6 Transition Metal Suboxide Clusters*
Caroline Chick Jarrold, Indiana University

9:00 am *Reactions of Group 6 Transition Metal Oxide and Sulfide Clusters with Water: Theoretical Insights*
Krishnan Raghavachari, Indiana University

9:30 am *Probing Molecular and Cluster Anions using Low Temperature Photoelectron Spectroscopy*
Xue-Bin Wang, Pacific Northwest National Laboratory

10:00 am **** Break ****

10:30 am *Electronic Structure and Proton Transfer in Hydrogen Bonded, Pi Stacked and Micro-Hydrated Systems*
Musahid Ahmed, Lawrence Berkeley National Laboratory

11:00 am *Computational Studies of Transition Metal Clusters & Actinide Complexes*
Krishnan Balasubramanian, California State University, East Bay and University of Houston

11:30 am **** Lunch (Osgood's Restaurant) ****

Session VIII Chair: **Bruce D. Kay,** Pacific Northwest National Laboratory

1:00 pm *Nonlinear Optics with Surface Plasmon Polaritons*
Eric O. Potma, University of California, Irvine

1:30 pm *Correlated Scanning and Photoemission Electron Microscopy of Nanoparticles and Structures*
Wayne P. Hess, Pacific Northwest National Laboratory

2:00 pm *Closing Remarks*
Gregory J. Fiechtner, DOE Basic Energy Sciences

Table of Contents

Table of Contents

CPIMS
Principal Investigator
Abstracts

Imaging Mass Spectrometry and Electronic Structure of Organic Molecules

Musahid Ahmed
MS 6R-2100, 1 Cyclotron road, Chemical Sciences Division
Lawrence Berkeley National Laboratory, Berkeley, CA 94720
mahmed@lbl.gov

The evolution and manipulation of natural systems requires detailed knowledge of complex heterogeneous chemical reactions that typically cannot be understood by simple bulk analysis. Chemical imaging methods provide simultaneously information of a sample's chemical composition and spatial heterogeneity. In this program, imaging mass spectrometry is being performed with ion sputtering and laser desorption in conjunction with tunable vacuum ultraviolet (VUV) radiation generated at the Advanced Light Source. Knowledge gained from studies of fundamental (5,9,17) desorption and ionization mechanisms are being applied to imaging lignin and plant biomass, following molecular transformations in soil organic matter, establishing microbial decomposition of plant biomass, observing antibiotic action on bacterial biofilms (6, 8, 13), and establishing the chemical composition and structure of biological material (*i.e.* melanin and lignin). Parallel to this effort, VUV photoionization in conjunction with theoretical calculations are being used to gain insight into proton transfer mechanisms, solvation and electronic structure in organic molecules and clusters relevant to biofuel production (1, 2, 4, 7, 10, 16, 18, 20). This is performed via molecular beam mass spectrometry, and electronic structure methods being developed by Anna Krylov at University of Southern California. A major focus is on the effects of non-covalent interactions, i.e., hydrogen bonding, stacking, and electrostatic interactions, on the IEs of the individual molecules and the changes in electronic structure (i.e., hole localization) upon clustering and solvation induced by these interactions. Laser ablation molecular beam mass spectrometry was applied to the study of carbon-nitrogen clusters (15), poly-acetylenes (14), silicon (19), silicon carbide, and organo-silicon (11) clusters. A high repetition rate (25 kHz) IR-OPO laser system has been commissioned and preliminary IR-VUV double resonance experiments on methane have been performed.

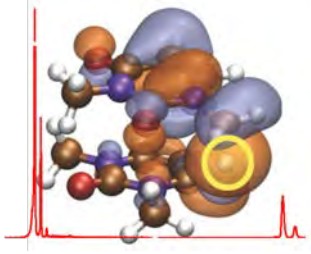

VUV photoionization mass spectra of dimethyluracil dimer and molecular orbital of its ion. (1)

Lignin is the second most abundant biopolymer on Earth, after cellulose, and it interacts closely with cellulose and hemicelluloses in plant cell walls. It is responsible for conferring strength and rigidity to plants and is also resistant to bacterial and fungal degradation, which has implications for its role in the environment. From a practical point of view, lignin presents problems in the production of products such as paper and lignocellulose-based biofuels and fundamental information on the decomposition and chemical reactivity of lignin is necessary to improve the production of biofuels. Previous investigations of lignin decomposition from this lab centered around the fragmentation and energetics of two lignin monomers, coniferyl and sinapyl alcohol, using ion sputtering followed by photoionization (9). However, moving to lignin polymers, the photoionization spectra are quite complex with rich signal not only in the monomer region but in the dimer region as well. Signal is also dependent on the type and extraction method of the lignin. For this reason, future investigations (with Mark Nimlos and Gregg Beckham of NREL) will focus on the decomposition of lignin model compounds. These dimer compounds were synthesized using derivatives of both coniferyl and sinapyl alcohol using an 8-O-4 linkage between the two monomer units. There are two competing fragmentation pathways where the dominant dissociation is breaking along the linkage followed by subsequent fragmentation whereas the minor channel is losing smaller fragments from the dimer (i.e. loss of H_2O, CH_2CO, CH_3, etc.). Calculations using NERSC supercomputing facilities will also investigate the low energy structures of the dimers and their products along with calculations mapping the reaction coordinate of the dissociation mechanisms. Experimentally measured ionization and appearance energies will be compared to theoretical numbers as has been done for the lignin monomers (9) and deoxyribose, a sugar (4).

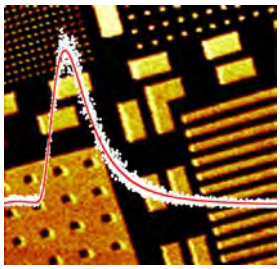

VUV LDPI image of a polymer photoresist and TOF of laser desorbed adenine. (5)

In this program, the decomposition of plant cell wall components can be imaged with high spatial resolution and molecular specificity. In collaboration with Mark Nimlos (NREL), *Populus* cell wall chemistry will be imaged at the cellular level. *Populus* is a Department of Energy (DOE) target for biofuels feedstock and was chosen as one of the two plant species targeted for genetic improvement within the context of three national Bioenergy Research Centers (BRCs) established by DOE to address biological challenges to biofuels production. Using vacuum ultraviolet-laser desorption post-ionization (VUV-LDPI), we have demonstrated imaging using a 30 μm laser spot size (5) from organic surfaces and this lends itself well for extracting mass spectra from individual plant cells which typically are between 20-100 μm in diameter. By decoupling the desorption step from photoionization, it was also demonstrated that imaging resolution of 5 μm could be obtained from a 30 μm laser spot size (5). Future improvements to this resolution will be performed by using better optics and possibly femtosecond UV laser radiation.

Lignin and sugars are not only of interest for biofuel development; they also play a fundamental role in soil chemistry. Globally, soils store more than three times as much carbon in soil organic matter (SOM) as is found in either the atmosphere or in living plants. When plant biomass degrades, microbes deconstruct it and integrate the resulting organic carbon into the soil. How this process occurs is still a major question that may affect how soils respond to global climate change and may provide a natural model for effective methods of degrading lignin for biofuel production. Building on our previous knowledge of the photoionization and desorption of model lignocellulose compounds and biomolecules, investigations into the decomposition of plant biopolymers in soils have resulted in new projects (with Peter Nico (LBNL), and Markus Kleber (Oregon State)), which take a top-down and bottom-up approach. In the first project, microbial decomposition of plant biomass will be followed in different environmental samples. In the second project, model mineral-organic interfaces will be studied. In both cases, of particular interest is the chemistry and transport that occur on heterogeneous inorganic/organic interfaces that comprise these complicated systems.

In the soil matrix, plant fragments enter the soil as plant debris that are progressively decomposed and incorporated into aggregates of minerals and organic compounds. As a test case, VUV-LDPI mass spectroscopy has been applied to probe the organic matter in a well-documented soil system (Susua (Oxisol)) at various density fractions (1.6 ~ 3.0 g/cm^3). The mass spectra at different density fractions reflect the soil changes from being plant-like (lignin or plant lipids) to microbial-like (long chain aliphatic hydrocarbons). The ultimate goal of these experiments will be to perform mass spectrometry on non-fractionated soil samples, and directly image the chemical composition of a soil ecosystem. But these density fraction experiments are necessary to build up a database and library of the different chemical components and their signatures with VUV photoionization to allow identification in a heterogeneous and complicated system such as soil.

A recent model “multi-layer concept” suggests that organic moieties associate with mineral surfaces in a predictable, complex, multi-layered fashion. The model draws upon understanding of organic matter as a continuum of amphiphilic molecular fragments which become progressively more hydrophilic with oxidation. So, an organic compound or metal may not directly interact with a soil mineral; rather, the compound may interact with a multi-layered sequence of organics and ions positioned on top of a deeply buried mineral surface. Though popular, this model has not been rigorously tested experimentally. To this end, our specific objectives are to determine conditions under which a mixture of organic compounds will exhibit a complex, layered structure when associated with mineral surfaces and map the spatial distribution of organic moieties.

In collaboration with scientists from LBNL (Hugo Destaillats and Mohamad Sleiman) a project to study the oxidation of soot and other atmospheric particles deposited on model surfaces has been initiated.

These processes are involved in the soiling and weathering (aging) of “cool” roofing materials and other urban surfaces. The use of highly reflective cool roofing materials can save air conditioning energy in buildings and help mitigate the urban heat island effect. Widespread adoption of highly reflective urban surfaces has the potential to slow global warming. The solar reflectance of an initially "cool" building envelope surface can be significantly reduced (by 20% to 60%) due to deposition of airborne particles. These aging processes can increase the need for conditioning energy by making surfaces hot, but can be minimized with self-cleaning or soil-repelling materials. Mass spectral differences of soot samples deposited on surfaces coated with a photo-catalyst (TiO_2), before and after exposure in the environment over days have been observed. Mass spectrometry of model systems studied in a controlled environment in a laboratory show very similar results.

Melanin is the most pervasive and widespread pigment in all living organisms and creates a broad range of black, brown and grey colors. Furthermore, it possesses an intriguing set of physical-chemical properties including: broad band monotonic absorbance; extremely low radiative quantum yield; and condensed phase electrical and photoconductivity. This has led to the suggestion that melanin could be useful as a bio-inspired high-tech material in applications such as bioelectronics, chemical sensing, and photon detection. However, although extensive experimental studies have been conducted on both natural and synthetic melanin, the structure, composition, and how these units are put together to form oligomers of melanin are not well understood. Hence a program is being initiated to study the chemical composition of melanin using VUV-LDPI in collaboration with Matt Shawkey, University of Ohio, Akron. Extracts from bird feathers will be used to build a database from which the structure of melanin will be elucidated. Melanin from different feathers provides distinct and consistent patterns in the mass spectrum upon VUV-LDPI. In future work, more samples from different color feathers will be tested in order to clarify the relationship between the color of the feather and the chemical structure of melanin, while also building up the classification of mass spectra of melanosomes. Preliminary results show that some melanosomes exhibit complex polymer structure, but others not, UV-Vis absorption, and atomic force microscope (AFM) measurements on a set of feather samples will be performed. These measurements, statistical analysis of mass spectra, and theoretical calculations based on the chemical structure observed in the VUV-LDPI experiment, will allow profound insight into the chemistry and physics of melanin.

Proton transfer is ubiquitous in chemistry and biology, but has always been described in the context of hydrogen-bonding networks (“proton wires”) acting as proton conduits. Using VUV photoionization in molecular beams and electronic structure calculations (Anna Krylov, USC), we showed efficient intramolecular ionization-induced proton transfer for a system with no hydrogen bonds: 1,3 dimethyuracil dimer (1). Methylation blocks the H-bonding sites and eliminates the H-bonded conformers in the neutral. Upon photoionization, the dimethyuracil dimer undergoes proton transfer and dissociates producing a protonated monomer. Deuterated dimethyluracil experiments reveal that proton transfer occurs from the methyl groups and not from the aromatic CH sites. Calculations illuminate qualitative differences in the proton transfer reaction coordinate in the π-stacked and hydrogen-bonded base pairs. Proton transfer in methylated dimers involves significant rearrangements of the two fragments facilitating a relatively low potential energy barrier of only 0.6 eV in the ionized dimer.

Micro-hydration of 1, 3-dimethyluracil reveals that proton transfer is initiated via ionization of the water moiety. The initial proton transfer that occurs from pi-stacked dimers is eliminated, and a sequential proton transfer from water is initiated. Electronic structure calculations reveal that the water molecules bond to the hydrogen acceptor sites in 1, 3-dimethyluracil dimers (the oxygen atoms) and hence eliminate the possibility for proton transfer. Both calculations and experiments show that when the excited electron orbital is localized at the water molecule, the water cluster surrounding the monomer or dimer begins to dissociate. Furthermore, the water bond to the 1, 3-dimethyluracil dimer makes the structure rigid and prevents the structural rearrangement necessary for proton transfer between the pi-stacked molecules.

Publications based on DOE support (2010-present)

1. A. Golan, K. B. Bravaya, R. Kudirka, O. Kostko, S. R. Leone, A. I. Krylov, and M. Ahmed *"Ionization of stacked dimethyluracil dimers leads to facile proton transfer in the absence of H-bonds"*. Nature Chem. (2012), **4**, 323
2. A. Golan and M. Ahmed "*Ionization of water clusters mediated by exciton energy transfer from argon clusters",* J. Phys. Chem. Lett. (2012) **3**, 458
3. M. J. Berg, K. R. Wilson, C. Sorensen, A. Chakrabarti, and M. Ahmed "*Discrete Dipole Approximation Model for Low-Energy Photoelectron Emission from NaCl Nanoparticles"* J. Quant. Spectrosc. Radiat. Transfer (2012) **113**, 259
4. D. Ghosh, A. Golan, L.K. Takahashi, A.I. Krylov and M. Ahmed *"An experimental and theoretical determination of the ionization energy of deoxyribose",* J. Phys. Chem. Lett. (2012) **3**, 97
5. O. Kostko, L. K. Takahashi, and M. Ahmed "*Desorption Dynamics, Internal Energies and Imaging of Molecules from Surfaces with Laser Desorption and Vacuum Ultraviolet (VUV) Photoionization",* Chem. Asian. J. (2011) **6**, 3066
6. M. T. Blaze, L.K. Takahashi, J. Zhou, M. Ahmed, F. D. Pleticha, and L. Hanley "*Brominated Tyrosine and Polyelectrolyte Multilayer Analysis by Laser Desorption VUV Postionization and Secondary Ion Mass Spectrometry"*. Anal. Chem. (2011) **83**, 4962
7. K. Khistyev, K. B. Bravaya, E. Kamarchik, O. Kostko, M. Ahmed, and A. I. Krylov "*The effect of microhydration on ionization energies of thymine"* Faraday Disc. (2011) **150**, 313
8. G. L. Gasper, L. K. Takahashi, J. Zhou, M. Ahmed, J. F. Moore, and L. Hanley "*Comparing Vacuum and Extreme Ultraviolet Radiation for Postionization of Laser Desorbed Neutrals from Bacterial Biofilms and Organic Fullerene"* Nuclear Instruments and Methods in Physics Research Section A (2011) **649**, 222
9. L.K. Takahashi, J. Zhou, O. Kostko, A. Golan, S. R. Leone and M. Ahmed "*VUV Photoionization and Mass Spectrometric Characterization of the Lignin Monomers Coniferyl and Sinapyl Alcohol"* J. Phys. Chem. A (2011) **115**, 3279
10. K. B. Bravaya, O. Kostko, S. Dolgikh, A Landau, M. Ahmed, and A. I. Krylov *"Electronic structure and spectroscopy of nucleic acid bases: Ionization energies, ionization-induced structural changes, and photoelectron spectra"* J. Phys. Chem. A (2010) **114**, 12305
11. R. I. Kaiser, P. Maksyutenko, C. Ennis, F. Zhang, X. Gu, A. Mebel, O. Kostko, M. Ahmed **"***Untangling the Chemical Evolution of Titan's Atmosphere and Surface: From Homogeneous to Heterogeneous Chemistry"* Faraday Disc. (2010) **147**, 429
12. K. R. Wilson, H. Bluhm, M. Ahmed "*Aerosol Photoemission"*, in Fundamentals and Applications in Aerosol Spectroscopy, edited by J.P. Reid and R. Signorell, Taylor and Francis, (2010) pp 367-417
13. G. L. Gasper, L. K. Takahashi, J. Zhou, J. Moore, M. Ahmed, L. Hanley *"Laser Desorption Postionization Mass Spectrometry of Antibiotic-Treated Bacterial Biofilms using Tunable Vacuum Ultraviolet Radiation"* Anal. Chem. (2010) **82,** 7472
14. R. I. Kaiser, B. J. Sun, H. M. Lin, A. H. H. Chang, A. Mebel, O. Kostko and M. Ahmed *"An Experimental and Theoretical Study on the Ionization Energies of Polyynes (H-(C≡C)$_n$-H; n = 1 - 9)"* Astrophys. J. (2010) **719** 1884
15. O. Kostko, J. Zhou, A. Chang, B. J. Sun, J. S. Lie, A. H. H. Chang, R. I. Kaiser and M. Ahmed "*Determination of ionization energies of C_nN (n=3-12) clusters: Vacuum-ultraviolet (VUV) photoionization experiments and theoretical calculations"* Astrophys. J. (2010) **717**, 674
16. E. Kamarchik, J. M. Bowman, O. Kostko, M. Ahmed, and A. I. Krylov "*Spectroscopic signatures of proton transfer dynamics in the water dimer cation"*. J. Chem. Phys. (2010) **132,** 194311
17. J. Zhou, L. K. Takahashi, K. R. Wilson, S. R. Leone and M. Ahmed "*Determination of Internal Energies of Ion Desorbed Neutral Organic Molecules with Tunable Vacuum Ultraviolet Photoionization"* Anal. Chem. (2010) **82**, 3905
18. O. Kostko, K. B. Bravaya, A. I. Krylov, and M. Ahmed "*Ionization of cytosine monomer and dimer studied by VUV photoionization and electronic structure calculations."* Phys. Chem. Chem. Phys., (2010), **12**, 2860
19. O. Kostko, S. R. Leone, M. A. Duncan and M. Ahmed "*Determination of ionization energies of small silicon clusters with vacuum-ultraviolet (VUV) photoionization."* J. Phys. Chem. A (2010), **114**, 3176
20. K. B. Bravaya, O. Kostko, M. Ahmed, and A. I. Krylov "*The effect of pi-stacking, h-bonding, and electrostatic interactions on the ionization energies of nucleic acid bases: adenine-adenine, thymine-thymine and adenine-thymine dimers"* Phys. Chem. Chem. Phys. (2010) **12,** 2261

Model Catalysis by Size-Selected Cluster Deposition

PI: Scott L. Anderson
Chemistry Department, University of Utah
315 S. 1400 E. Rm 2020
Salt Lake City, UT 84112
anderson@chem.utah.edu

Program Scope

The goal of our research is to explore correlations between supported cluster size, electronic and morphological structure, the distributions of reactant binding sites, and catalytic activity, for model catalysts prepared using size-selected metal cluster deposition. The work to date has focused on catalysts with catalytically active metal clusters deposited on metal oxide supports, and on electrocatalysis by metal clusters on glassy carbon electrodes. We are also looking at effects of cluster size on Pd-catalyzed H_2 splitting and uptake in metals.

The experimental setup is quite flexible. The main instrument has a mass-selecting ion deposition beamline fed by a laser vaporization source that produces high fluxes at low deposition energies (~10^9 Pd_{10}/sec in a 2 mm diameter spot at 1 eV/atom, for example). Typical samples with 0.1 ML-equivalent of metal, deposited in the form of M_n^+ can be prepared in 10 – 20 minutes, and our analysis methods are also quite fast. Speed is important, because even in UHV these samples are highly efficient at collecting adventitious contaminants, due to substrate-mediated adsorption. Sample morphology is probed by low energy He^+ ion scattering (ISS), electronic structure is probed by x-ray and UV photoelectron spectroscopy and ion neutralization spectroscopy (XPS, UPS, INS), and reactivity is studied using a differentially pumped mass spectrometer surrounded by a cluster of pulsed and cw gas inlets that can be used to dose the sample while various temperature programs are executed.

The main UHV analysis chamber has a port in the bottom, equipped with a gate valve, a triple differential seal, and one of several interchangeable small chambers with their own pumping systems. When the sample is positioned in the lower chamber is it isolated from the main UHV system, enabling high pressures procedures such as film growth or *in situ* electrochemical studies.

Recent Progress

Strong Effects of Cluster Size and Air Exposure on Platinum Electrocatalysis

We studied the O_2 reduction reaction (ORR) in 0.1 M $HClO_4$, catalyzed by Pt_n ($n \leq 11$) deposited on glassy carbon electrodes (GCEs). Very strong effects of cluster size and air exposure were observed, with all clusters except Pt_7 showing high activity for carbon oxidation by water when studied *in situ*, without air exposure. Only Pt_7 showed the expected ORR activity. If the same size clusters were deposited on GCEs in vacuum, but exposed briefly to laboratory air before electrochemistry, then the high carbon oxidation activity was

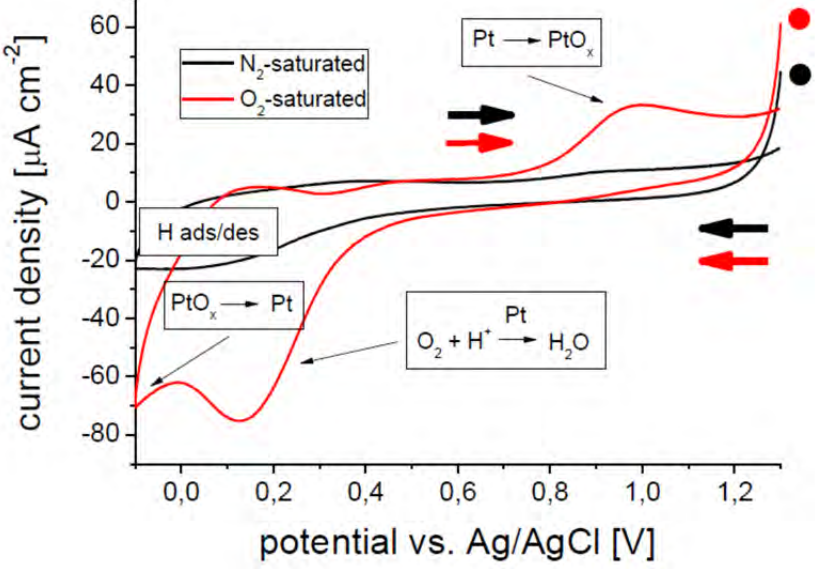

Fig. 1: Pt_7/GCE: CVs in nitrogen- and oxygen-saturated 0.1*M* $HClO_4$ at a sweep rate of 0.1 Vs^{-1}, starting at 1.3 V (indicated by dot), and scanning to -0.1 V vs. Ag/AgCl and back.

entirely quenched, presumably due to reaction of the highly active Pt_n with species in the air. For Pt_7, air exposure leads to quenching of ORR activity, replaced by reversible redox of adventitious organic species.

The instrument was modified to allow *in situ* electrochemical studies to be made in the lower chamber. A retractable electrochemical cell was constructed of PEEK, consisting of a 4 mm diameter working section that contains a Pt counter electrode (working cell volume ≈ 15 μL). One end of the working section is open, with a lip holding a 3 mm diameter O-ring that is used to seal the cell against the surface of the GCE. The other end of the working section is sealed to a reference electrode section, communicating via a fritted Vycor disk. The reference electrode was Ag/AgCl. Both working and reference sections of the cell are equipped with Teflon tubes used for injecting electrolyte, and ports to allow electrolyte solution to flow out of the cell. Electrolyte flows are controlled by a syringe pump located outside the vacuum system.

To allow *in situ* electrochemical measurements, an electrode is first prepared by depositing Pt_n on a clean, degassed GCE in UHV, which is then lowered through the triple seal into the lower chamber while the electrochemical cell is retracted. The electrochemical cell is then pushed against the surface of the GCE, sealing via the O-ring at the open end of the working section. For *in situ* experiments, the lower chamber was vented with high purity Ar, then the working and reference sections were filled with 0.1 M $HClO_4$, and 3 M NaCl, respectively. Cyclic voltammograms (CVs) were acquired using a CH Instruments model 600D potentiostat.

The ORR results for Pt_7/GCE are show in Fig. 1, in the form of CVs taken in both N_2- and O_2-saturated $HClO_4$. The structure of the CV is similar to that seen both in our *in situ* cell and in the literature for Pt nanoparticles on GCE, and the activity *per* Pt atom is roughly twice that of Pt nanoparticles, probably because the small clusters have essentially all the Pt on the surface, and are highly dispersed on the GCE. Optical microscopy of the electrode after several hundred CV cycles showed no signs of any degradation.

Fig. 2 shows CVs for Pt_4/GCE, and also a post-electrochemistry optical micrograph of

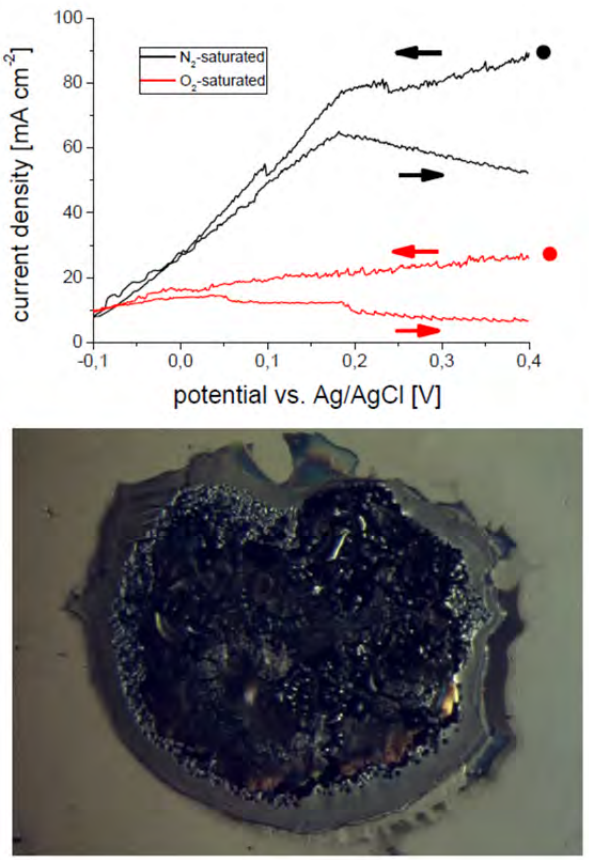

Fig. 2: Top. CV of Pt_4/GCE in N_2- and O_2-saturated 0.1*M* $HClO_4$ at a scan rate of 1 Vs^{-1} from 0.4 to -0.1 V vs. Ag/AgCl and back. Bottom. Optical micrograph of the electrode after electrochemical cycling.

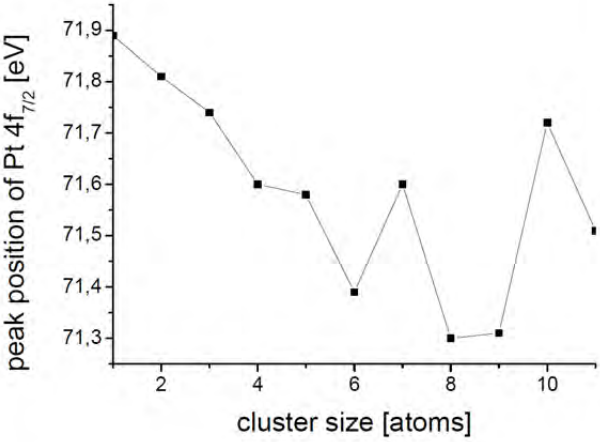

Fig. 3 XPS of as-deposited Pt_n/GCE in UHV

the electrode. Both the huge oxidative currents (note change in scale), and the dramatic degradation of the electrode are typical of all Pt_n/GCE samples other than Pt_7. The glitches in the CVs are due to partial blockage of the small volume cell by bubbles, leading to complete shut-down of the cell after a few CV cycles. Gas generation occurs in both N_2- and O_2-saturated $HClO_4$, and also in H_2SO_4 electrolytes, even though we are careful to stay out of the potential regions where water splitting occurs. The electrode degradation occurs only in the central 2 mm region of the electrode, where clusters were deposited, and not in the surrounding region of GCE also exposed to electrolytes. The appearance is of a combination of blistering of the GCE and etching of the surface, which is initially found to have roughness of only ~±2 nm by AFM. The conclusion is that for Pt_n, $n \neq 7$, the small clusters are highly active for carbon oxidation by water, generating CO_2 which eventually blocks further current flow, and destroying the electrode surface.

Exposure to air after cluster deposition, and prior to electrochemistry, has a huge effect on the activity of these small clusters. For Pt_7, the ORR and Pt redox signals are essentially gone, replaced by a symmetric pair of redox waves that look like slow, reversible redox of some adventitious adsorbate. This effect is not unexpected, because any sample exposed to atmosphere even briefly is always covered with carbonaceous adsorbates. For the other size clusters, which are highly reactive in absence of air exposure, the effect is even more dramatic. There is essentially no electrochemical current, other than capacitive currents on the order of 0.1 μA, essentially identical to what is seen on clean Pt-free GCEs. It appears, therefore, that these clusters must react with adventitious adsorbates in such a way to completely passivate the electrode. As expected from the lack of electrochemical currents, these air-exposed electrodes show no sign of degradation in repeated cycling.

XPS of the Pt_n/GCE samples, as prepared in UHV, is shown in Fig. 3. In addition to the trend, expected from final state screening considerations, of an overall drop in Pt $4f_{7/2}$ binding energy with increasing size, there are also strong oscillations indicating that the different clusters have different electronic properties. The relative inactivity of Pt_7 may be correlated with the observation that it is a local maximum in the XPS binding energy (which may indicate a particularly stable, unpolarizable valence structure), however, Pt_{10} also has a high Pt 4f binding energy, and it highly active. Calculations on Pt_n structures and electronic properties are underway in the group of Shiv Khanna at VCU.

Electronic Structure

We previously demonstrated a one-to-one correlation between the binding energy of the Pd 3d core level, and the activity for CO oxidation of $Pd_n/TiO_2(110)$. The strong correlation was somewhat surprising in that chemical reactions are expected to depend only to the valence electronic structure, and core levels are only an indirect probe of the valence structure. Therefore, we have been using a combination of ultraviolet photoelectron spectroscopy (UPS), and ion neutralization spectroscopy (INS) to look at the valence structure of metal clusters deposited on supports, and looking for correlations with activity. Fig. 4 shows an example of UPS for two different sizes of Pd_n deposited on $TiO_2(110)$, taken in the course of a study of of methanol decomposition over $Pd_n/TiO_2(110)$. Here data are shown only for Pd_n/TiO_2, however, we also have data for $MeOH/Pd_n/TiO_2$ taken at temperatures corresponding to different steps in the decomposition/desorption process.

In this case, we take advantage of the band gap of TiO_2 to use UPS to look at the onset of photoemission from Pd_n in the region between the Fermi level, and the onset of the large oxygen peak from TiO_2. The small peak just below the Fermi level for clean TiO_2 results from Ti^{3+} at vacancies and interstitial sites. The lower left inset shows the near-Fermi level region for two example clusters, where the signal from the TiO_2 substrate has been subtracted. Note that the onset of emission is well below the Fermi level, and is size dependent. As shown in the upper right inset, which gives *preliminary* emission onset energies obtained from a rather crude spectral deconvolution method, the onset moves closer to the Fermi level with increasing size, however, there is still a significant shift, indicating that these small clusters are not yet metallic. We are currently working on a more quantitative approach to deconvoluting the spectrometer function from the data.

Future Plans

In addition to the TiO_2 work, we have very interesting results for Pd_n on different alumina supports, and are planning to go back and look at these systems with UPS and INS with the goal of understanding how interaction with different supports influences the valence structure in different size clusters.

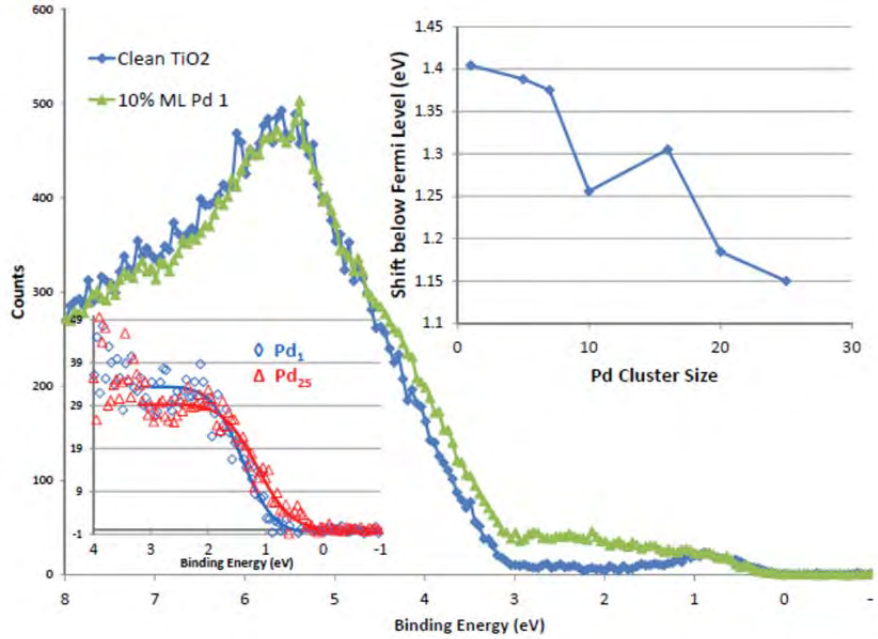

Fig. 4. UPS data for $Pd_n/TiO_2(110)$. **Main frame:** raw data for TiO_2 and 0.1 ML Pd_1/TiO_2. **Lower Left Inset:** Comparison of near Fermi level portion of subtracted spectra for Pd_1/TiO_2 and Pd_{25}/TiO_2. **Upper Right Inset:** Fitted shift in Pd_n absorption edge, relative to Fermi level (results from preliminary fitting).

We also have carried out a series of non-size selected catalysis experiments (using a second, "test" instrument) focusing on hydrogen activation over Pd, and subsequent spillover to underlying metal films for storage. The intention is to examine hydrogen storage via hydride formation in magnesium, however, we also observed reversible hydrogen uptake for Pd deposited on MoO_x on Mo(110), with efficiency many times greater than that for a 100 layer Mg film. Given work by Ceyer indicating that unique chemistry can be driven by escaping subsurface hydrogen in other metals, this seems like a potentially interesting system, and we will look at some selective hydrogenation chemistry on size-selected $Pd_n/MoO_x/Mo$. Finally, we are considering another round of electrochemistry experiments, probably in a non-aqueous solvent, to avoid the highly efficient destruction of the electro by oxidation from water.

Publications acknowledging DOE support

"Size-dependent oxidation of Pd_n ($n \leq 13$) on alumina/NiAl(110): Correlation with Pd core level binding energies." Tianpin Wu, William E. Kaden, William A. Kunkel, and Scott L. Anderson, Surf. Sci. 603 (2009) 2764-77.

"Electronic Structure Controls Reactivity of Size-Selected Pd Clusters Adsorbed on TiO_2 Surfaces", William E. Kaden, Tianpin Wu, William A. Kunkel, Scott L. Anderson, Science. 326 (2009) 826 - 9.

"CO Adsorption and Desorption on Size-Selected Pd_n/TiO_2 Model Catalysts: Size Dependence of Binding Sites and Energies, and Support-Mediated Adsorption" William E. Kaden, William A. Kunkel, F. Sloan Roberts, Matthew Kane and Scott L. Anderson, J. Chem. Phys. 136 (2012) 204705 12 pages, doi: 10.1063/1.4721625

Electronic Structure of Transition Metal Clusters and Actinide Complexes and Their Reactivity- DEFG2-05ER15657 –

K. Balasubramanian,
California State University East Bay, Hayward CA 94542 & University of Houston Down Town, Houston, TX

Program Scope

We have made substantial progress in three areas of our computational studies, viz., the electronic structure of actinide complexes, carbon nanotubes and fullerene encapsulation of actinides, and subnano silver-metal clusters. We have made progress in (a) Computing the binding properties of environmentally occurring actinides with carbon nanotubes and mesoporous silica as possible means of actinide sequestrations (b) electronic structure and spectroscopy of subnano gold, silver particles and alloys of silver and gold particles up to 25 atoms, which are found to have very interesting fluorescent emissions (c) properties of open 5d- transition metal clusters especially tantalum. The research work on silver and gold nanocluster was carried out in collaboration with experimentalists. We are providing here only a brief summary of major highlights, in each of the categories. Significant part of our findings have been published or submitted for publication with a recent work being featured as a "hot paper" [1] in Angewante Chemie, communications.

Computational Studies of Actinide Sequestration with carbon nanotubes and mesoporous materials.

Challenges of nuclear waste disposal and the management of nuclear fuel is attributed to the understanding of actinides behaviors in aqueous systems and the development of novel procedures for successful elemental separation, extraction and sequestration. In most common forms, actinides in their high oxidation states exist as actinyl ions, such as actinyl(V) and actinyl(VII), but common form is the actinyl(VI) ion, AnO_2^{2+}. Actinyl ions are either found in solutions or in crystals. Moreover, actinide contamination in biological and geological environments is a topic of considerable importance to the United States and many around the world. Bioremediation microbiological, chemical and geological strategies processes, have been investigated experimentally and sometimes combined and/or complemented molecular simulations to measure and elucidate, the sensitive nature of the structural, bonding and energetic characteristics of actinides. However, comprehensive strategies for elimination and remediation of contaminated lands and facilities are still lacking.

Carbon nanotubes (CNTs) have been considered for many different applications in terms of their chemical, electronic and mechanical properties, as well as their unique tubular structure and large length/diameter ratio. CNTs for gas and biosensing applications have attracted great attention. They possess excellent adsorption ability to form strong interactions with foreign molecules. In addition, their inner cavities and active and topological defective sites on their surfaces can contribute to the high pollutants removal capability of CNTs. The interaction between actinides and CNTs is a subject of intense current interest. Among the actinides, the most extensively studied and characterized by both experiment and theory is uranyl(VI). Uranium exists in aqueous solutions and acidic pH conditions (between 3 and 4) as the actinyl ion UO_2^{2+}. This ion has received considerable interest because of its increased nuclear activity that produces high-level nuclear wastes.

We have carried out computational studies of UO_2^{2+} CNT interactions using high level relativistic computations.[4] The uranyl ion was introduced onto the exterior (EX) and interior (IN) surfaces of a (6, 6) pristine (defect-free, **DF**) and Stone-Wales (**SW**) defect CNT. Topological defects, such as the SW defect in CNTs, were examined as a potential driving force for enhanced binding for foreign atoms and molecules. In addition, to elucidating the magnitude of uranyl binding to the SW, defect we have carried out further calculations on hexagons labeled **6N** (**N=A**, **B**, **C**, **D** and **E**) which neighbor the SW defect. We have computed the DFT/B3LYP-optimized structures of the uranyl ion absorbed on the exterior and interior of the (6, 6) CNT complexes. In order to access the degree of rotational barriers around the curvature of the tube as a function of uranyl's initial orientation, we have considered full optimizations for UO_2^{+2} along the tube axis (*act* -CNT) and perpendicular to the tube's axis (*act*$\perp$-CNT). For the CNT complexes the uranyl ion bond length (O_x-U-O_y) remained linear with the maximum displacement of ~.05° for all complexes. Also, for all act-complexes the average U-O distances ranged from 1.77 Å to 1.80 Å.

The relative path indexes of the uranyl ion traversing the CNT frameworks were also computed and plotted. These computations show the **SW-5A** configurations to be the most favorable compared to **SW-5B** for both **par** and **per** orientations. For the **par** and **per** complexes, the **SW-5A-EX** binding energies are 133.81 and 158.74 kcal mol^{-1} lower than **SW-5B-EX**. A critical factor governing the stability of endohedral versus exohedral complexes is the local charge depletion that the framework experiences as the ion transverses "outside" and "inside" of the nanotube. That means that even though UO_2^{2+} prefers enegetically endohedral rather than exhohedral positions, a complete understanding is lacking unless and until UO_2^{2+} donation and the CNTs back-donation is assessed. We can deduce the charge contributions (donation) from the Mulliken charge populations of these complexes. In this manner, a slight donation (0.80 e^-) is observed for the **ex** complexes, while higher donation together with predominant back-donation (up to 0.91 e^-) is revealed for **en** systems. More interesting is that such effects explains why the uranyl ion tends to exhibit enhanced absorption for endhohedral complexes while for similar systems the dopant prefers to deabsorb (exit) the tube.

We have also studied aqueous complexes of Cm (III), U(VI), Np(VI) and Pu(VI) with OH^-.The effects of the aqueous solvent in the configuration preferences of these complexes have been investigated. The free energies of solvation were predicted using a self-consistent reaction-field model and a combined discrete-continuum model. Spectroscopic studies on many of these species are carried out by a fluorescence emission spectroscopy at Berkeley, by Professor Heino Nitsche's group, our experimental collaborators. Extensive *ab initio* calculations have been carried out to study equilibrium structures, vibrational frequencies, and bond characters of hydrated Cm(III) carbonates and hydroxide complexes in aqueous solution and the gas phase. The structures have been further optimized by considering long-range solvent effects as a polarizable continuum dielectric model. Our results reveal that it is necessary to include water molecules bound to the complex for proper treatment of the hydrated complex and the dielectric cavity. Structural reoptimization of the complex in a dielectric cavity seems inevitable to seek subtle structural variations in the solvent and to correlate with the observed spectra. The optimized structure of some of these complexes is not the same in the gaps phase and aqueous solution illustrating the importance of carrying out these computations in solution.

Electronic Structure & Spectroscopy of Subnano Silver & Gold Clusters.

We have carried out joint experimental-computational studies on gas-phase subnano silver clusters and gold clusters. The bimetallic 13 atom core QC with a composition, Ag_7Au_6 protected with mercaptosuccinic acid (H_2MSA) are experimentally found to be unusually stable and exhibited very interesting luminescent spectra.[1] This alloy cluster points to the diverse category of materials which may be useful in catalytic and photophysical applications. Theoretical calculations for $(Ag_7Au_6)SCH_3)_{10}$ suggest a distorted icosahedral core exhibiting well defined transitions in its absorption profile. Our computational work on this alloy cluster was fueled by these experimental luminescence spectra of Ag-Au alloy clusters obtained by our experimental collaborators at IIT, Madras, India. The lowest energy structure of $Ag_7Au_6(SCH_3)_9$ has a Ag_7Au_6 core with a distorted icosahedral core and the geometries and detailed bond lengths of the two lowest energy structures are shown in Figures 1 and 2. The lowest energy structure of $Ag_7Au_6(SCH_3)_{10}$ has a Ag_7Au_6 distorted icosahedron, and the 2nd lowest energy structure has a Ag_7Au_6 core with initial symmetry of C_2, lying 0.151eV higher on the potential energy surface.

Figure 1: Lowest energy structure of $Ag_7Au_6(SCH_3)_9$ before and after optimization. Luminescence spectra &structure of$Ag_7Au_6(SCH_3)_{10}$

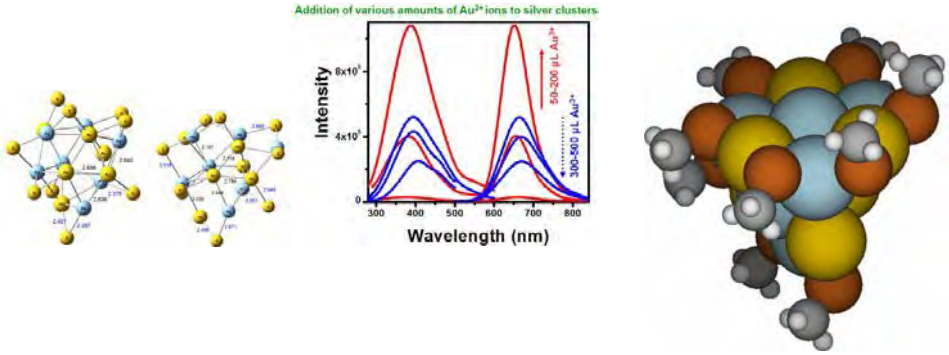

We have carried out a joint experimental and theoretical study[3] of two luminescent molecular quantum clusters of silver, $Ag_7(H_2MSA)_7$ and $Ag_8(H_2MSA)_8$ (H_2MSA is the protonated dicarboxilic acid of mercaptosuccinic acid in thiolate form). Global optimizations and property calculations are performed in the framework of density-functional theory (DFT-PBE) resulted in lowest energy structures shown in Fig 2. The simulated excitation spectra of these two clusters are in good agreement with the corresponding experimental spectra. The presence of –RS-Ag-RS- as a stable motif has been confirmed in all of the lowest energy structures. Our computed vibrational spectra are also consistent with experimental findings.

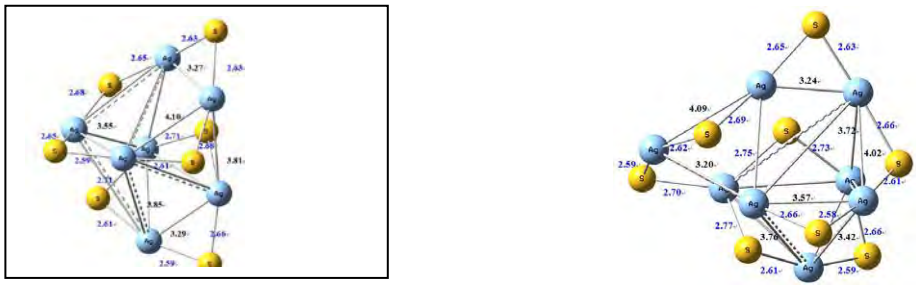

Fig 2 Optimized Structures of $Ag_7(SCH_3)_7$ (Left) and $Ag_8(SCH_3)_8$ (Right)

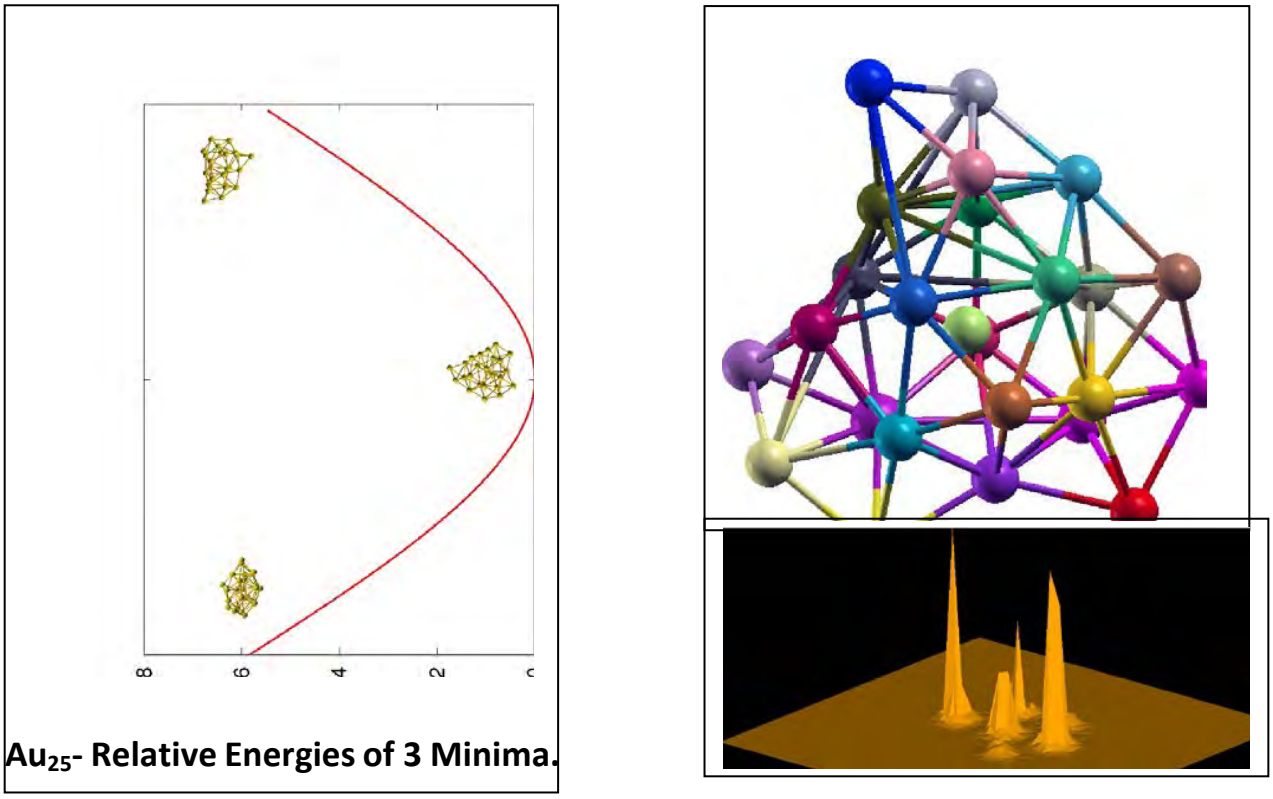

Fig 3 Au_{25}-(Left)-Three most stable Structures and their Energetic. Top(Right)-Optimized geometry of the most stable Structure of Au_{25} with color coding based on charges- different colors demonstrate aurophilicity due to relativity. Bottom (right) –Laplacian of Charge Density demonstrates reactive sites in Au_{25}.

We have recently carried out molecular dynamics followed by relativistic ab initio DFT studies of Au_{25} cluster in the gas phase.[12] We have optimized the preliminary structures obtained from MD using relativistic DFT. Three competitive structures have been obtained for Au_{25} . Fig 3 shows the relative energy Plots of various structures of Au_{25} clusters during their evolution with emphasis on three optimized structures, the lowest structure with color coded reactive sites and the Laplacian of the charge density for Au_{25}'s optimized structure. Our relativistic computations reveal three minima within 0.58 eV among which the structure shown on the top right of Fig 3 is the lowest in energy. Both Lowdin population analysis and Laplacian charge densities reveal that electronic charges on the various centers of the distorted Au_{25} structure are not equally distributed among the atoms owing to relativity. Moreover such unequal distribution of electronic charges unfold the existence of reactive centers on the gas-phase Au_{25} cluster thus providing significant new insight into reactivity of gold such nanoclusters of gold.

Recent Publications from the DOE BES Grant

[1] *Thalappil Pradeep, Thumu. Udayabhaskararao, Yan Sun, Nirmal Goswami, Samir K. Pal, K. Balasubramanian, "Ag7Au6: A 13 atom alloy quantum cluster". Angewante Chemie., International Edition (2012) "Hot Paper", published on-line* http://dx.doi.org/10.1002/anie.201107696

[2] *Xiang Li, Weijun Zheng, Angela Buonaugurio, Allyson Buytendyk, Kit Bowen, and Krishnan Balasubramanian, "Photoelectron Spectroscopy of the Molecular Anions, ZrO^-, HfO^-, $HfHO^-$, and $HfO2H^-$, J. Chem. Phys.* ***136****, 154306 (2012);* http://dx.doi.org/10.1063/1.4704127

[3] *Y. Sun, K. Balasubramanian, T. Uday. B. Rao T. Pradeep, and, "First principle studies of two luminescent molecular quantum clusters of silver, $Ag_7(H_2MSA)_7$ and $Ag_8(H_2MSA)_8$ based on experimental fluorescence spectra", J. Phys. Chem. C,115 (42), pp 20380–20387, (2011) http://pubs.acs.org/doi/abs/10.1021/jp203545t*

[4] *T. Simeon, K. Balasubramanian, and C. Welch, "New Computational Insights into Interaction of Uranyl ion (UO_2^{2+}) with Stone-Wales Defect Single-Walled Carbon nanotubes", J. Phys Chem. C., 2012 (submitted)*

[5] *M. Benavides, K. Balasubramanian, "Binding of Plutonium to Human Serum Apotransferrin: Structural Insights and IR Spectra", Chem. Phys. Lett. (2012) in press.*

[6] *T. Simeon, K. Balasubramanian, and C. Welch, "Computational Studies of Interaction of In and In^{3+} with Stone-Wales Defect Single-Walled Carbon nanotubes", J. Phys. Chem. Lett., 2010, 1 (2), pp 457–46*

[7] *D. M. David Jaba Singh, T. Pradeep, K. Thirumoorthy and K. Balasubramanian, "Closed-cage Tungsten oxide Clusters in the Gas Phase", J. Phys. Chem. A, 2010, 114 (17), pp 5445–5452*

[8] *Z. Cao, K. Thiumoorthy, and K. Balasubramanian, "Curium(III) hydroxide Complexes in Aqueous Solution",*

(2012) Submitted.

[9] *Manoj Yadav and K. Balasubramanian, "First principles study of structure and stability of small tantalum clusters", Chemical Physics Letters, (2012) Submitted*

[10] *Himadri De, K. Balasubramanian, S. Pal, and T. Pradeep, "A Theoretical Study of Structures and Energetics of Au_{25} Clusters: A Relativistic Density Functional Investigation", (2012) submitted.*

[11] *Manoj Yadav and K. Balasubramanian, "Theoretical Study of Chemisorption of H_2 and CH_4 on Tantalum Clusters", To be Submitted for Publication.*

[12] *Himadri De, K. Balasubramanian, S. Pal, T. Pradeep, "Equilibrium Geometry and Spectroscopy of thiol stabilized Au_{25} Clusters: A Relativistic Density Functional Investigation", (2012) to be submitted.*

FUNDAMENTAL ADVANCES IN RADIATION CHEMISTRY

Principal Investigators:

DM Bartels (bartels.5@nd.edu), I Carmichael, DM Chipman, I Janik, JA LaVerne, S Ptasińska
Notre Dame Radiation Laboratory, University of Notre Dame, Notre Dame, IN 46556

SCOPE

Research in fundamental advances in radiation chemistry is organized around two themes. First, energy deposition and transport seeks to describe how energetic charged particles and photons interact with matter to produce tracks of highly reactive transients, whose recombination and escape ultimately determine the chemical effect of the impinging radiation. The work described in this part is focused on fundamental problems specific to the action of ionizing radiation. Particular projects include measurement of radiolytic product yields in low temperature aqueous ices, experimental study and theoretical treatment of the VUV spectrum of water up to supercritical conditions, investigation of spur and track recombination and radiolytic yields in aromatic hydrocarbon liquids and the determination of recombination and yields in various supercritical fluids. The second thrust deals with structure, properties and reactions of radicals in condensed phases. Challenges being addressed include the experimental and theoretical investigation of solvated electron reaction rates, measurement of radical reaction rates as a function of density in supercritical fluids, theoretical characterization of free radical structure and solvation, and time-resolved resonance Raman investigation of free radical transients.

PROGRESS AND PLANS

VUV absorption measurements of the first absorption band of water at elevated temperatures as a function of density were performed at the Synchrotron Radiation Center, University of Wisconsin. The work is aimed at measuring, for the first time, the entire breadth of the first absorption band in the vacuum UV in the range of densities from 0.007 g/cm^3 (gas-like) to 0.45 g/cm^3 (liquid like). Coverage of such a broad optical density range necessitated the construction of cells with pathlengths varying from 100 µm to 0.63 µm. At the lowest density ranges of supercritical conditions (up to 20 bar, 392.7 °C) the spectrum appears to be unchanged from that of the water monomer measured *in vacuo* at room temperature, in terms of both shape and molar absorptivity. Upon increase of density from 0.006-0.1 g/cm^3 (pressure 20-200 bar), the lower energy shoulder of the monomer absorption band fades, the peak maximum shifts 0.06 eV towards higher energies, and broadens slightly without change in molar absorptivity. Further increase of the density from 0.1 to 0.45 g/cm^3 causes a further shift of the maximum peak position to the blue and further broadening in the lower energy range. The overall shift of the maximum peak position from the gas-like to the liquid-like phase is about 0.3 eV and follows, surprisingly closely, the water density dependence. The molar absorptivity initially increases in the density range of 0.1-0.3 g/cm^3 but then appears to decrease upon further increase of the density above 0.3 g/cm^3 (for pressures higher than 280 bar). Electronic structure calculations are being carried out on excited states of water clusters to help interpret these experiments.

Hydroxyl radicals are the main transient oxidizing species formed in the radiolysis of water. We have measured the quantitatively challenging yield of $^{\bullet}$OH using formic acid as a scavenger with a wide variety of types of radiation. By varying the formic acid concentration one can infer the time dependence of the $^{\bullet}$OH in the particle track. Extensive analysis of these scavenger concentration results in combination with Monte Carlo track-diffusion calculations are currently underway to obtain a consistent set of hydroxyl radical kinetics in pure water. Reasonable results

have been obtained with γ-rays suggesting that the overall kinetics of the scavenging system is relatively well understood. $^{\bullet}$OH yields are found to decrease with decreasing He ion energy. Agreement between the model and experiments with heavier ions is more problematic because of the difficulty in precisely determining the particle charge state of the impinging ion. Completion of the modeling is expected in the near future and the results will be used to better understand the formation and short time chemistry of $^{\bullet}$OH in the radiolysis of water.

The study of hydrogen atoms in high temperature water was initiated with measurement of the hyperfine coupling constant (hfc) and *g*-factor vs. temperature. Water saturated with H_2 at 70 bar was recirculated using high-pressure syringe pumps through a sapphire irradiation tube in an EPR cavity and irradiated with 3MeV electrons to produce H atoms. The magnetic field was carefully calibrated using an NMR probe and the well-characterized single line from the $SO_3^{\bullet-}$ radical. Below 100 °C the measured coupling decreased linearly with increase in temperature. The hfc is several parts per thousand below the value in vacuum due to interactions with the solvent. It is possible to treat the low temperature linear region in terms of a quantized atom vibrating in a three-dimensional harmonic solvent potential well. This simple model breaks down above 120 °C. At about 240 °C, the hfc reaches a minimum and begins to swing back toward the vacuum value. Similar temperature dependence is found in the *g*-factor. The H-atom signals are strongly polarized by the chemically induced dynamic electron polarization (CIDEP) phenomenon, and the relaxation times are dominated by spin exchange encounters. In the coming year these properties of the time-resolved H-atom signals will be analyzed to obtain a more detailed picture of the H-atom spin-dependent reaction dynamics.

To help understand these experimental observations, the solvation environment of a hydrogen atom in water has been characterized from ambient to supercritical conditions using classical molecular dynamics simulations based on a potential energy surface previously fitted to high level electronic structure calculations. The diffusion constant and free energy of solvation calculated for the H atom in water are found to be in close agreement with experiment at low temperatures where comparison is possible, giving confidence that the calculations will provide a reliable prediction of these properties at high temperatures. Clusters of the hydrogen atom surrounded by many water molecules are being further analyzed through quantum mechanical calculations of the electron paramagnetic hyperfine coupling constants and *g*-factors, the latter including both paramagnetic orbital Zeeman and spin-orbit coupling contributions and both relativistic mass and diamagnetic (gauge) corrections to the underlying tensor. Though the scatter in the computed data at each temperature is large, a clear trend is noted which roughly mimics the experimentally observed behavior.

A program to investigate radiolysis reactions of transition metal cations M^{2+} was initiated to support studies of nuclear reactor corrosion. Metal ions initially chosen for study are the aqueous complexes of Mn^{2+}, Fe^{2+}, Co^{2+}, Ni^{2+}, Cu^{2+} and Zn^{2+}. Kinetics of solutions of the M^{2+} ion perchlorate salts have been systematically recorded with near-UV transient absorption following electron pulse radiolysis, with variation of dose, metal ion concentration, and temperature to 300 °C. In most cases we also recorded kinetics in the presence of methanol as a scavenger for the OH radicals. Reaction (1) for most of the M^{2+} ions has been measured with pseudo-first-order

$$e^-_{aq} + M^{2+}_{aq} \rightarrow M^{+}_{aq} \qquad (1)$$

kinetics by following absorption of the hydrated electron at 800 nm as a function of temperature. At room temperature only the reduction of Cu^{2+} approaches the diffusion limit, but the activation

energy indicates that this reaction, like the others, is limited by the ΔG and reorganization energy. We were astonished to learn that the redox potentials of the resulting M^+ aquo-ions are not established and experiments are underway to rectify this deficiency.

Dissociative electron attachment to simple alkyl and aryl triflates in the gas phase, models of nonionic photoacid generators for modern electron beam lithography, was investigated by mass spectrometry of the anionic products formed. Several reaction channels were observed upon electron capture involving single or multiple bond cleavages or intramolecular rearrangement. Major dissociation channels involved C–O, S–O, or C–S bond scissions in the triflate moiety and both energetics and yields are strongly influenced by the aryl substituents.

Mixtures of methane and nitrogen embedded in helium droplets have been irradiated with a 70 eV electron beam. The mass spectrum obtained from the ions produced has been measured at very high resolution, and high level electronic structure calculations have been carried out to identify the structures and binding energies of the ions observed. For the separate pure gases the most intense series of peaks are assigned to homogeneous molecular clusters. For the mixture of gases the mass spectrum shows strong cluster formation of heterogeneous peaks, the largest assigned to $CH_3N_2^+$ and lower yields of the homogeneous species. The high resolution of this experiment allows a reassignment to $CH_4N_2^+$ of a peak (mass 44) that was previously attributed to CO_2 in the gas chromatograph mass spectrum obtained from the Cassini/Huygens mission to Titan in 2004.

Cationic resins commonly used in separations systems and in reactor filters often contain quaternary ammonium groups and are highly basic. To aid in understanding the radiolytic decomposition of these ammonium groups, a series of investigations have examined the radiolysis of a variety of dry quaternary ammonium salts. Most of the focus at this stage has been on the radiolytic production of H_2 since this compound presents the greatest hazard in waste separation systems. The yield of H_2 increases from about 1 in methylammonium chloride to greater than 4.4 molecules/100 eV in trimethylammonium chloride. However adding a fourth methyl drops the yield to 0.07 molecules/100 eV. N-H bond breakage seems to be the precursor to most of the H_2, and yields of H_2 are very small without this possibility. Little effect is found with variation in the anion of the salt. The addition of an aromatic group as in benzyl trimethylammonium chloride also leads to significant reduction in H_2 yields. Current work is attempting to identify residual products following the formation of H_2.

A series of instrumental advances were made in the pulse radiolysis/time resolved resonance Raman (TR^3) experimental facility in order to allow studies of inorganic transient species absorbing in the deep UV region. The existing fused silica flow cell design proved unsuitable for this type of measurement, because in the ionizing radiation field the cell material became increasingly opaque in the UV. Application of a variety of fused silica materials with the highest purity available did not show any improvement in this respect. To avoid cell material problems a liquid micro jet was used instead. Initial experiments with liquid jets presented their own challenges, but made long averaging of weak TR^3 signals possible. The structural properties of the superoxide radical (O_2^-) dissolved in water and its protonated form have been investigated by deep UV TR^3 spectroscopy. Attention was focused on the vibration of the radiolytically-produced radical itself and solvent shifts and models are being constructed to rationalize the observations.

Two novel plasma devices have been designed which enable production of atmospheric pressure plasma jets operated in nitrogen and nitrogen with oxygen admixtures. Plasma jets are generated by dielectric barrier discharge inside a quartz tube and launched into the open atmosphere. Both plasma sources have been constructed with the same materials and dimensions, the only difference is the shape of the electrodes: spiral and 4-strip. A distinction that is responsible for dramatically different electrical, optical and thermal properties of the jets, Emission spectra taken at an axial distance of 1 mm from the orifice of the quartz tube show regions attributable to the NO-γ system between 200 – 300 nm, to the N_2 2nd positive system between 300 – 420 nm, to the green transition $N_2{:}O\left({}^1S \rightarrow {}^1D\right)$ with a maximum at 557.7 nm and to the N_2 first positive system above 570 nm.

PUBLICATIONS WITH BES SUPPORT SINCE 2010

Bazin M.; Ptasińska S.; Bass A.D.; Sanche L.; Burean E.; Swiderek P. *J. Phys. Conden. Mat.* **2010**, **22**, 084003 Electron induced dissociation in the condensed-phase nitromethane: II. Desorption of neutral fragments.

do Couto P.C.; Chipman D.M. *J. Chem. Phys.* **2010**, **132** Insights into the UV spectrum of liquid water from model calculations.

Hare P.M.; Price E.A.; Stanisky C.M.; Janik I.; Bartels D.M. *J. Phys. Chem. A* **2010**, **114**, 1766-75 Solvated electron extinction coefficient and oscillator strength in high temperature water.

Haygarth K.; Bartels D.M. *J. Phys. Chem. A* **2010**, **114**, 7479-84 Neutron and beta/gamma radiolysis of water up to supercritical conditions. II. SF_6 as a scavenger for hydrated electron.

Haygarth K.H.; Marin T.; Janik I.; Kanjana K.; Stanisky C.M.; Bartels D.M. *J. Phys. Chem. A* **2010**, **114**, 2142-50 Carbonate radical formation in radiolysis of sodium carbonate and bicarbonate solutions up to 250℃ and the mechanism of its second order decay.

Schmitt C.; LaVerne J.A.; Robertson D.; Bowers M.; Lu W.; Collon P. *Nucl. Inst. Meth. Phys. Res. A* **2010**, **268**, 1551-7 Equilibrium charge state distributions for boron and carbon ions emerging from carbon and aluminium targets.

Stanisky C.M.; Bartels D.M.; Takahashi K. *Radiat. Phys. Chem.* **2010**, **79**, 64-5 Rate constants for the reaction of hydronium ions with hydrated electrons up to 350 ℃.

Baidak A.; Badali M.; LaVerne J.A. *J. Phys. Chem. A* **2011**, **115**, 7418-27 Role of the low-energy excited states in the radiolysis of aromatic liquids.

Balcerzyk A.; LaVerne J.A.; Mostafavi M. *J. Phys. Chem. A* **2011**, **115**, 4326-33 Direct and indirect radiolytic effects in highly concentrated aqueous solutions of bromide.

Chipman D.M. *J. Phys. Chem. A* **2011**, **115**, 1161-71 Hemibonding between hydroxyl radical and water.

Ferreira da Silva F.; Ptasińska S.; Denifl S.; Gschliesser D.; Postler J.; Matias C.; Märk T.D.; Limao-Vieira P.; Scheier P. *J. Chem. Phys.* **2011**, **135**, 174504 Electron interaction with nitromethane embedded in helium droplets: attachment and ionization measurements.

Hug G.L.; Mozumder A. Electron localization and trapping in liquid hydrocarbons: The Anderson model. In *Charged Particle and Photon Interactions with Matter: Recent Advances, Applications, and Interfaces*; Hatano, Y., Katsumura, Y., Mozumder, A., Eds.; CRC Press, Taylor & Francis Group: Boca Raton, FL, 2011; pp 209-35.

Ptasińska S.; Gschliesser D.; Bartl P.; Janik I.; Scheier P.; Denifl S. *J. Chem. Phys.* **2011**, **135**, 214309 Dissociative electron attachment to triflates.

Roth O.; LaVerne J.A. *J. Phys. Chem. A* **2011**, **115**, 700-8 Effect of pH on H_2O_2 production in the radiolysis of water.

Schmitt C.; LaVerne J.A.; Robertson D.; Bowers M.; Lu W.T.; Collon P. *Nucl. Instrum. Methods Phys. Res., Sect. A* **2011**, **269**, 721-8 Target dependence for low-Z ion charge state fractions.

LaVerne J.; Baidak A. *Radiat. Phys. Chem.* **2012**, **81**, 1287-90
Track effects in the radiolysis of aromatic liquids.

Surface Chemical Dynamics

N. Camillone III,[a] A.L. Harris,[b] and M. G. White[a]
Brookhaven National Laboratory, Chemistry Department, Building 555, Upton, NY 11973
(nicholas@bnl.gov, alexh@bnl.gov, mgwhite@bnl.gov)

1. Program Scope

This program focuses on fundamental investigations of the dynamics, energetics and morphology-dependence of thermal and photoinduced reactions on planar and nanostructured surfaces that play key roles in energy-related catalysis and photocatalysis. Laser pump-probe methods are used to investigate the dynamics of interfacial charge and energy transfer that lead to adsorbate reaction and/or desorption on metal and metal oxide surfaces. State- and energy-resolved measurements of the gas-phase products are used to infer the dynamics of product formation and desorption. Time-resolved correlation techniques follow surface reactions in real time and are used to infer the dynamics of adsorbate–substrate energy transfer. Measurement of the interfacial electronic structure is used to investigate the impact of adsorbate–surface and interadsorbate interactions on molecular orbital energies. New capabilities to synthesize and investigate the surface chemical dynamics of arrays of supported metal nanoparticles (NPs) on oxide surfaces include the deposition of size-selected clusters from ion beams as well as solution-phase synthesis and deposition of narrow-size-distribution nanometer-scale particles.

2. Recent Progress

Ultrafast Surface Chemical Dynamics. The ultimate goal of this work is to follow surface chemical processes in real time. As a step forward, we are investigating the dynamics of substrate–adsorbate energy transfer by injecting energy with ~100-fs near-IR laser pulses that initiate surface reactions by substrate-mediated processes such as DIMET (desorption induced by multiple electronic transitions) and heating via electronic friction. Time-resolved monitoring of the complex is achieved by a two-pulse correlation (2PC) method wherein the surface is excited by a "pump" pulse and a time-delayed "probe," and the delay-dependence of the product yield reports on the energy transfer rate.

We are currently focused on using the 2PC method to follow desorption and reaction dynamics on small (nanometer-diameter) metal NPs supported on oxide surfaces. NPs on wide band gap oxides are photoexcited much more efficiently than the support. Thus time-resolved measurements should probe the rate of energy transfer from the NP to the support and to adsorbates on the NP surfaces. Such systems serve as more realistic model catalysts for surface dynamics studies and also provide the opportunity to explore the size-dependence of the dynamics in the metal-to-nonmetal transition size regime.

Our first step in this undertaking has been to explore the use of inverse micelle synthesis for the preparation of robust palladium NP assemblies supported on TiO_2(110). We have prepared NPs by segregation of a metal salt [$Pd(OAc)_2$] in the hydrophilic core of inverse micelles of an amphiphilic diblock copolymer [polystyrene-b-poly(4-vinylpyridine)] in an organic solvent and spin coated them onto UHV-cleaned TiO_2(110) supports. The polymer is removed by oxygen plasma treatment and heating in low (10^{-6} Torr) oxygen partial pressures. This approach yields high monodispersity and also allows, in principle, control of NP size and interparticle distance through choice of polymer block lengths and metal salt concentrations.

We have employed scanning electron microscopy (SEM, Figure 1), atomic force microscopy (AFM), Auger electron spectroscopy (AES) and temperature-programmed desorption (TPD) to characterize the NP arrays. We have established one preparation protocol that yields a bimodal distribution of 4-nm and 11-nm particles; the NPs are predominantly metallic Pd and expose clean surface sites. Thermal desorption yields are consistent with the surface area expected based on SEM and AFM measurements; they are also reproducible from run to run, showing that the arrays are stable to ~ 900 K. O_2 and CO

[a] Principal Investigator; [b] Collaborating Investigator

(Figure 2) can be adsorbed exclusively on the NPs. Such arrays are almost ideal for our surface kinetics and dynamics studies.

The thermal desorption of O_2 and CO from these NP arrays show desorption activation energies similar to those for desorption from extended Pd(111) single crystal surfaces. The O_2 + CO and O_{ad} + CO thermal reaction kinetics are complex and suggest that there are at least two distinct types of O-atom binding sites on the NP surfaces, as well as multiple CO binding sites. A unique aspect of the O_{ad} + CO reaction is the absence of a desorption feature associated with O_{ad}–CO phase segregation on Pd(111). An intriguing possibility is that this phase segregation requires (111) terraces > 10 nm in diameter, pointing to a fundamental change in the phase diagram of this mixed adlayer system at the nanoscale.

We are currently investigating the dynamics of NP–adsorbate energy transfer by femtosecond time resolved 2PC desorption and reaction. Thus far we have found that loosely-bound adsorbates (O_2) show dynamics similar to those on extended single crystal surfaces. However, more tightly-bound adsorbates (CO) show complex dynamics on the NPs. In particular, we found a dependence of the dynamics on surface temperature. Specifically, we have observed a local minimum in the 2PC yield at zero delay (Figure 3, inset) that suggests that the relative importance of phonon-mediated desorption as compared to electron-mediated desorption increases with temperature.

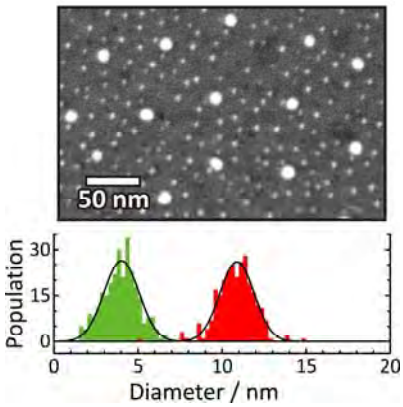

Figure 1. SEM and diameter distribution for Pd_{NP}/TiO_2 prepared by inverse micelle synthesis.

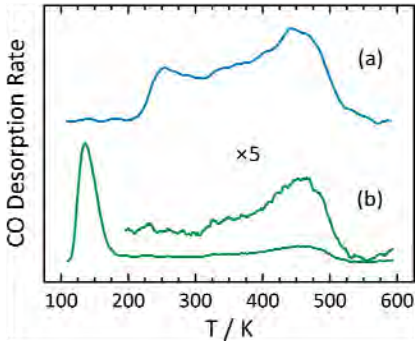

Figure 2. CO TPD from Pd_{NP}/TiO_2 following adsorption at (a) 200K and (b) 100 K. Desorption from the TiO_2 surface occurs at low temperature (~ 140-K feature) while desorption from the Pd NPs occurs at higher temperatures.

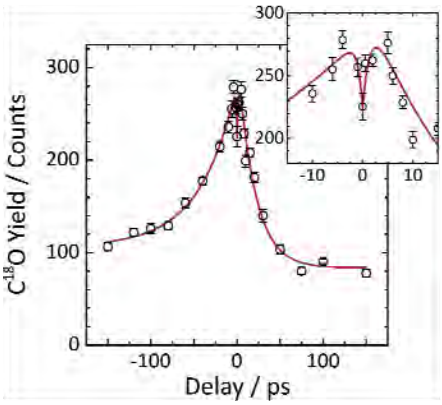

Figure 3. Ultrafast time-resolved CO desorption dynamics from Pd_{NP}/TiO_2.

Pump-Probe Studies of Photodesorption and Photooxidation on TiO_2(110) Surfaces. Measurements of the final state properties of gas-phase products are being used as a probe of the mechanism and dynamics of photodesorption and photooxidation on well-characterized TiO_2(110) surfaces. Recent studies have focused on the photooxidation of a series of related $R(CO)CH_3$ molecules (acetaldehyde, R = H; acetone, R = CH_3; butanone, R = C_2H_5; and acetophenone, R = C_6H_5) co-adsorbed with oxygen on a reduced TiO_2(110) surface. Laser pump-probe measurements show that the kinetic distributions for the methyl radical fragments ($CH_3^{\bullet}$) from all four molecules are very similar, with a "slow" and "fast" component. The "fast" methyl dissociation channel is attributed to a prompt fragmentation process involving an excited intermediate $[R(COO)(CH_3)_{(ad)}]^*$ which is formed by charge transfer at the TiO_2(110) following UV photoexcitation. The average translational energies of the "fast" methyl fragments are also found to increase with the size of the R-group, even though the C-CH_3 bond energies are essentially the same for all four molecules. This apparent correlation between methyl kinetic energy with the mass of the remaining surface fragment is indicative of a simple two-body fragmentation process. The latter suggests that the excited intermediate is

only weakly coupled to the titania surface, whose primary role is to provide near-surface charge carriers (h^+, e^-) that initiate photoreaction.

Preliminary pump-probe experiments for the photoreactions of the alcohols, ethanol and 2-propanol, on TiO_2(110) provide evidence for multistep mechanism. Previous studies using thermal desorption measurements have shown that in the presence of co-adsorbed oxygen, ethanol and 2-propanol undergo partial oxidation (dehydrogenation) on a TiO_2(110) surface to form acetaldehyde and acetone during UV exposure. Based on the results presented above, the acetaldehyde and acetone dehydrogenation products would be expected to undergo further photoreaction by the loss of a methyl fragment. By measuring the translational energy distributions of the methyl photoproducts from adlayers of ethanol and 2-propanol co-adsorbed with oxygen, we are able show that they precisely match those of methyl fragments from photooxidation of acetaldehyde and acetone, respectively. These measurements provide strong support for a secondary photofragmentation step involving the dehydrogenation products in the overall photodecomposition of the original alcohol. Moreover, the role of molecular oxygen must also include the formation of an oxygen complex (e.g., diolate) with the primary photoproducts (acetaldehyde or acetone) in order for these surface species to become photoactive.

Two-Photon Photoemission Studies of Interfacial Electronic Structure. Two-photon photoemission (2PPE) spectroscopy is being used to probe the valence band structure of supported metal compound clusters as a function of size and composition. Our recent efforts have focused on Mo_xS_y clusters deposited on a Al_2O_3 thin film surface, which are being used as model nanocatalysts for desulfurization reactions. On bulk alumina surfaces, the bonding of MoS_2 particles can involve strong Mo–O bond linkages (Type I) that generally increase the Mo oxidation state via charge transfer to the support. In this work, charge transfer at the cluster-alumina interface is probed by work function (Φ) measurements using 2PPE as a function of cluster size (structure) and coverage. For clusters on ultrathin oxide films, work function changes provide a direct probe of charge transfer resulting from cluster-oxide bonding interactions or electron tunneling from the NiAl metal substrate through the ultrathin oxide film. The latter has been observed for surface species with high electron affinities (e.g., Au adatoms) and ultrathin oxide films on metals which have low work functions (e.g., MgO(100)/Ag(100)).

In these experiments, mass-selected Mo_xS_y clusters are soft-landed onto the Al_2O_3/NiAl(110) substrate, with a surface coverage that varies smoothly from the center to the edges of the substrate. With a small focused laser spot size (250 μm), it is possible to measure the work function as a function of cluster coverage by rastering it across the face of the crystal. The coverage dependent work function data was used to extract the intrinsic interfacial dipole moments for the individual Mo_xS_y clusters supported on the alumina surface. The derived interfacial dipole moments are consistent with charge transfer from the Al_2O_3/NiAl(110) surface to the Mo_xS_y clusters, which is not expected for Type I interactions with the alumina support. We attribute the direction of charge transfer to electron tunneling through the ultrathin alumina film which is favored by the high electron affinities of the Mo_xS_y clusters and the relatively low NiAl work function induced by the presence of the alumina film. These results extend previous observations of electronic charging to non-metallic clusters and suggest a novel way to modify the electronic structure and reactivity of nanocatalysts for heterogeneous chemistry.

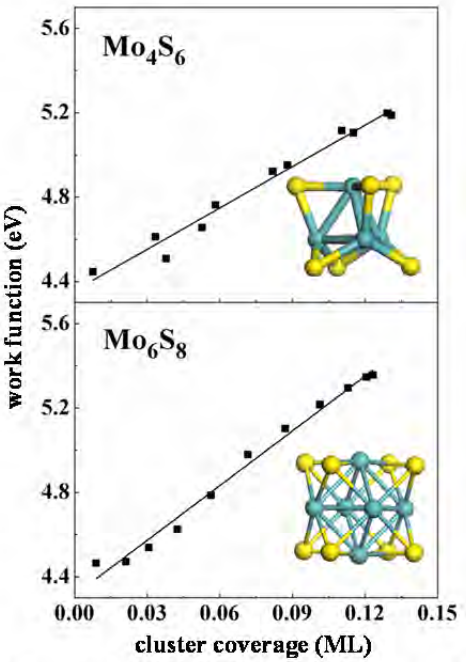

Figure 4: Coverage dependent work function for the Mo_4S_6 and Mo_6S_8 clusters deposited on an ultrathin alumina film on NiAl(100) surface.

3. Future Plans

Our planned work develops three interlinked themes: (i) the chemistry of supported NPs and nanoclusters (NCs), (ii) the exploration of chemical dynamics on ultrafast timescales, and (iii) the photoinduced chemistry of molecular adsorbates. The investigations are motivated by the fundamental need to connect chemical reactivity to chemical dynamics in systems of relevance to catalytic processes—in particular metal and metal-compound NPs and NCs supported on oxide substrates. They are also motivated by fundamental questions of physical changes in the electronic and phonon structure of NPs and their coupling to adsorbates and to the nonmetallic support that may alter dynamics associated with energy flow and reactive processes.

Future work on ultrafast photoinduced reactions will involve modeling of the energy transfer rates to elucidate the novel dynamics we have observed. In addition, further experiments on progressively smaller nanoparticles (towards sub-nm) will be pursued to further explore fundamental changes in surface reaction kinetics and dynamics as the size of the metal substrate material is reduced from macroscopic (planar bulk surfaces) to the nanoscale. Future studies in surface photochemistry using pump-probe techniques continue to explore mechanistic aspects of semiconductor photoreactions through measurements of final state properties of gas-phase products, with added capabilities for ion imaging that can provide mass resolved angular distributions of photoproducts. New studies in size-selected clusters will focus on metal oxide nanoclusters (Ti, Ce, Mo, W) supported on single crystal metal supports (e.g., Cu), so called "inverse" catalysts, to explore cluster-support electronic interactions that can provide a basis for understanding reactivity.

DOE-Sponsored Research Publications (2010–2012)

Infrared Study of Triruthenium Dodecacarbonyl Interactions with Gold, F. M. Hoffmann, Y. S. Hoo, T. H. Cai, M. G. White, J. Hrbek, *Surf. Sci*., accepted for publication.

CO oxidation on nanostructured SnO_x /Pt(111) surfaces: unique properties of reduced SnO_x, S. Axnanda,W.-P. Zhou, M. G. White, *Phys. Chem. Chem. Phys*., accepted for publication.

Final State Distributions of Radical Photoproducts from the Photooxidation of Acetone on TiO_2(110), D. Sporleder, D. P. Wilson and M. G. White, *J. Phys. Chem. C*, Just Accepted Manuscript, **DOI:** 10.1021/jp303947q.

Local Work Function of Size-Selected Mo_xS_y Clusters on Al_2O_3/NiAl(110), J. Zhou, J. Zhou, N. Camillone III and Michael G. White*, Phys. Chem. Chem. Phys*.**, 14,** 8105-8110 (2012).

Adsorption structures and electronic properties of 1,4-phenylene diisocyanide on Au(111) surface, J. Zhou, D. Acharya, N. Camillone III, P. Sutter and M.G. White, *J. Phys. Chem. C*, **115**, 21151–21160 (2011).

Electronic Structure of the Thiophene/Au(111) Interface Probed by Two-Photon Photoemission, J. Zhou, Y. Yang, N. Camillone and M. G. White, *J. Phys. Chem. B*, **114**, 13670-13677 (2010).

Hydrogenation of Carbon Dioxide by Water: Alkali-Promoted Synthesis of Formate, F. M. Hoffmann, Y. Yang, J. Paul, M. G. White, J. Hrbek, *J. Phys. Chem. Lett*.,**1**, 2130-2134 (2010).

Fundamental Studies of Methanol Synthesis from CO_2 Hydrogenation on Cu(111), Cu Clusters and Cu/ZnO(0001), Y. Yang, J. Evans, J. A. Rodriguez, M. G. White and P. Liu, *Phys. Chem. Chem. Phys.*, **12**, 9909-9917 (2010).

Methanol Synthesis from H_2 and CO_2 on a Mo_6S_8 Cluster: A Density Functional Study, P. Liu, Y.-M. Choi, Y. Yang and M. G. White, *J. Phys. Chem. A* 114, pp 3888–3895 (2010)

Theory of Dynamics of Complex Systems

David Chandler

Chemical Sciences Division, Lawrence Berkeley National Laboratory
and
Department of Chemistry, University of California, Berkeley CA 94720

chandler@berkeley.edu

DOE funded research in our group concerns the theory of dynamics in systems involving large numbers of correlated particles. Glassy dynamics is a quintessential example. Here, dense molecular packing severely constrains the allowed pathways by which a system can rearrange and relax. The majority of molecular motions that exist in a structural glass former are trivial small amplitude vibrations that couple only weakly to surrounding degrees of freedom. In contrast, motions that produce significant structural relaxation take place in concerted steps involving many particles, and as such, dynamics is characterized by significant heterogeneity in space and time. Our recent contributions to this topic have established that these heterogeneities are precursors to a non-equilibrium phase transition, and that this transition underlies the glass transition observed in laboratory experiments [4,11,12,15].[1] We have also shown that relaxation leading up to this transition exhibits a surprising degree of universality [5,11]. Theory on this topic involves complicated esoteric mathematical methods, yet we have been able to produce a review of its essential concepts [3] that should be accessible to a broad audience of chemists and physicists.

Liquid interfacial dynamics is another important example, and here too our Group has made several new contributions. Much of this latest work is based upon two advances: i. a general and efficient procedure for identifying instantaneous interfaces from molecular coordinates [2], and ii. a generalization of umbrella sampling methods for collecting statistics on rare but important density fluctuations [1,8]. Work is underway characterizing pathways of water evaporation (an example of which is illustrated in the top panel of the Figure 1), the structure and dynamics of water at a Pt surface (lower-right panel), and the structure and dynamics of water at an oily surface (lower-left panel).

An insightful perspective on the nature of hydrophobic effects, created in our Group's work over the last decade, focuses on the role of interfacial fluctuations in dynamics and forces of assembly. Quantitative detail on this perspective is found in our recent advances [1,7, 9,13,14]. These studies were made possible by the developments noted in the previous paragraph. The principal effects of interfacial fluctuations can be captured with coarse-grained modeling, as illustrated in Publication [7]. The fact that this understanding can be used to formulate a quantitatively accurate and computationally

[1] Numbers in square brackets refer to papers in the list of Recent DOE Supported Research Publications.

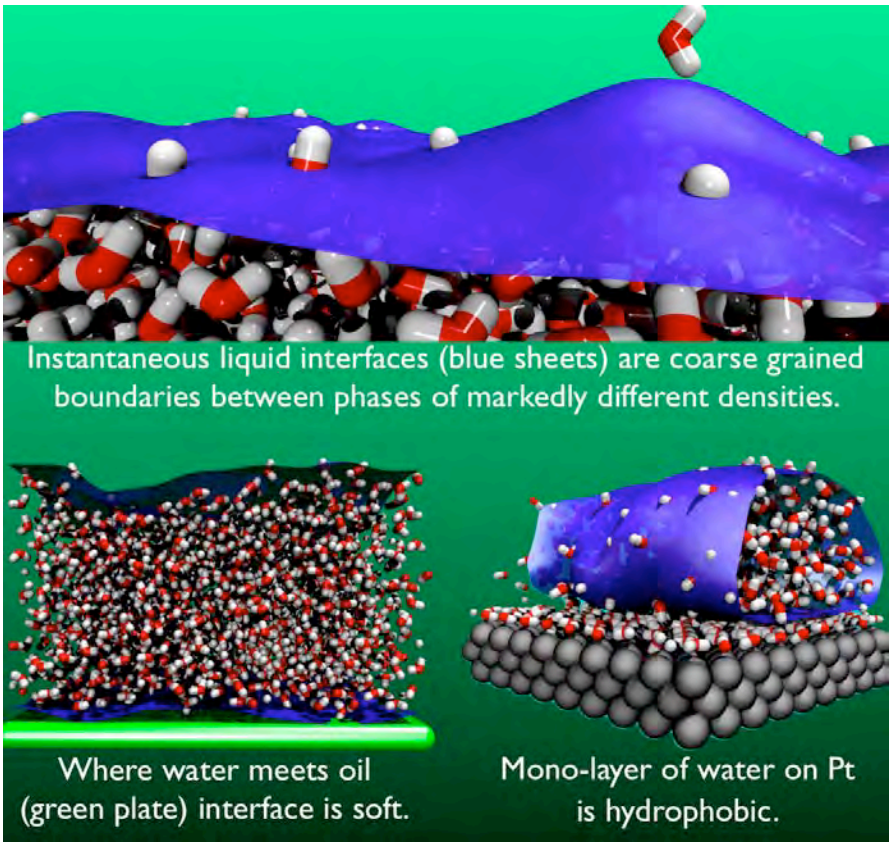

Figure 1: Snap shots from molecular dynamics trajectories showing some of the systems examined by the Chandler research group in their DOE funded studies of liquid interfaces.

convenient theory of solvation and hydrophobic effects is established for the first time in Publication [6].

Finally, we have embarked upon a program of understanding the properties of water at supercooled conditions. Just as hydrophobicity is controlled by interfaces because of the proximity of liquid-vapor coexistence, the behaviors of cold water in bulk, in confinement and in non-equilibrium, depend upon interfaces because of the proximity of crystal-liquid coexistence. Figure 2 illustrates some of our recent results on this topic [10,16]. H. E. Stanley and his many coworkers and followers have widely written on how properties of cold and supercooled liquid water might reflect a metaphysical liquid-liquid transition and critical point. The need for such an unseemly explanation is no longer, as all these properties are now shown to reflect nothing more than easily observed water-ice coexistence and associated pre-melting phenomena [10,16]. This newly developed understanding of confined cold water sets the stage for interpreting crystal, liquid and amorphous-solid phase behaviors of aerosols, a topic of significant importance to climate science, and a topic we plan to examine in the near future.

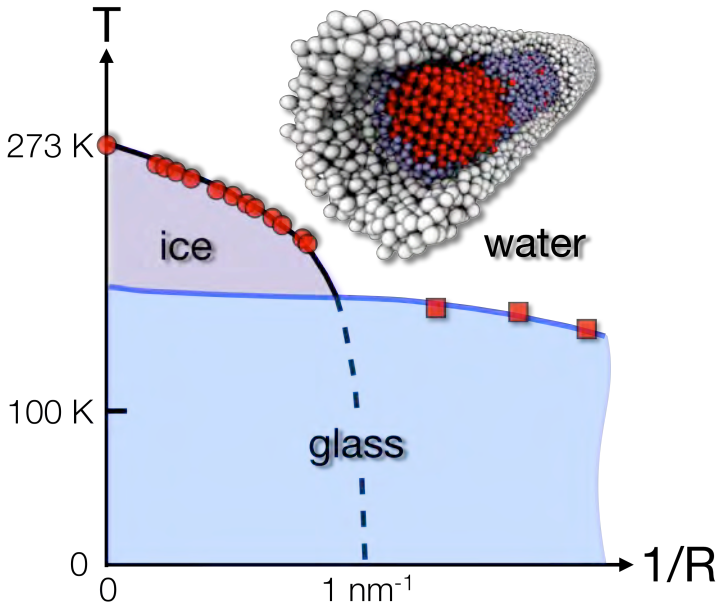

Figure 2: A phase diagram for water confined to a disordered hydrophilic nano-pore of radius R. [Adapted from Ref. 16.] In this pictured case, the external pressure is 1 atm. Lines are theoretical curves derived from effects of the interfaces present as the result of confinement (there are no adjustable parameters, only measured bulk transport properties, thermodynamics and liquid-ice interfacial tension enter the theoretical analysis). Experimental data points are from calorimetric observations of the water-ice and water-glass transitions.

Recent DOE Supported Research Publications

1. Patel, A. J., P. Varilly and D. Chandler, "Fluctuations of water near extended hydrophobic and hydrophilic surfaces," *J. Phys. Chem. B*, ***114***, 1632–1637 (2010).

2. Willard, A.P. and D. Chandler, "Instantaneous Liquid Interfaces," *J. Phys. Chem. B*, ***114***, 1954–1958 (2010).

3. Chandler, D. and J.P. Garrahan, "Dynamics on the Way to Forming Glass: Bubbles in Space-time" *Annu. Rev. Phys. Chem*., **61**, 191-217 (2010).

4. Elmatad, Yael S., R.L. Jack, J.P. Garrahan and D. Chandler, "Finite-temperature critical point of a glass transition," *Proc. Natl. Acad. Sci. USA* **107,** 12793-12798 (2010).

5. Elmatad, Y.S., D. Chandler, and J.P. Garrahan, "Corresponding States of Structural Glass Formers II", *J. Phys. Chem. B* **114**, 17113-17119 (2010).

6. Varilly, P., A. J. Patel and D. Chandler, “Improved coarse grained model of solvation and the hydrophobic effect,” *J. Chem. Phys.* **134**, 074109.1-15 (2011).

7. Patel, A. J., P. Varilly, S. N. Jamadagni, H. Acharya, S. Garde and D. Chandler, “Hydrophobic effects in interfacial environments,” *Proc. Natl. Acad. Sci. USA* **108**, 17678-17683 (2011).

8. Patel, A. J., P. Varilly, S. Garde and D. Chandler, “Quantifying density fluctuations in volumes of all shapes and sizes using indirect umbrella sampling,” *J. Stat. Phys.* **145**, 265-275 (2011).

9. Patel, A. J., P. Varilly, S. N. Jamadagni, H. Acharya, S. Garde and D. Chandler. “Extended surfaces modulate hydrophobic interactions of neighboring solutes” *Proc. Natl. Acad. Sci. U.S.A.* **108**, 17678-17683 (2011).

10. Limmer, D.T., and D. Chandler, "The Putative Liquid-Liquid Transition is a Liquid-Solid Transition in Atomistic Models of Water," *J. Chem. Phys.* **135,** 134503.1-10 (2011). Addendum discussing issues of equilibration and proper sampling techniques is found in the Appendix to the arXiv version of this paper: arXiv:1107.0337v2.

11. Keys, A.S., L.O. Hedges, J.P. Garrahan, S.C. Glotzer, and D. Chandler, "Excitations are localized and relaxation is hierarchical in glass-forming liquids," *Phys. Rev. X* **1**, 021013.1-15 (2011).

12. Jack, R. L., L. O. Hedges, J. P. Garrahan, and D. Chandler, “Preparation and relaxation of very stable glassy states of a simulated liquid” *Phys. Rev. Lett* **107**, 275702.1-4 (2011).

13. Rotenberg, B., A. J. Patel, and D. Chandler, “Molecular explanation for why talc surfaces can be both hydrophilic and hydrophobic” *J. Am. Chem. Soc.* **113**, 20521-20527 (2011).

14. Patel A. J., P. Varilly, S. N. Jamadagni, M. Hagan, D. Chandler and S. Garde, “Sitting at the edge: How biomolecules use hydrophobicity to tune their interactions and function” *J. Phys. Chem. B* **116**, 2498-2503 (2012).

15. Speck, T., and D. Chandler, “Constrained dynamics of localized excitations causes a non-equilibrium phase transition in an atomistic model of glass formers” *J.Chem.Phys*. **136**, 184509.1-9.

16. Limmer, D. T., and D. Chandler, “Phase diagram of supercooled water confined to hydrophilic nanopores,” *J. Chem. Phys.* **137**, 045509.1-11 (2012).

Rapid capture of charges by polyfluorenes in pulse-radiolysis experiments at LEAF

Principal Investigators: Andrew R. Cook and John R. Miller

Department of Chemistry, Brookhaven National Laboratory, Upton, NY, 11973 USA

acook@bnl.gov, jrmiller@bnl.gov

Program Scope:

This program applies both photoexcitation and ionization by short pulses of fast electrons to investigate fundamental chemical problems relevant to the production and efficient use of energy and thus obtain unique insights not attainable with other techniques. These studies may play an important role in the development of safer, more effective, and environmentally beneficial processes for the chemical conversion of solar energy. Picosecond pulse radiolysis is employed to generate and study reactive chemical intermediates or other non-equilibrium states of matter in ways that are complementary to photolysis and electrochemistry and often uniquely accessible by radiolysis. This program also develops new tools for such investigations, applies them to chemical questions, and makes them available to the research community. Advanced experimental capabilities, such as Optical Fiber Single-Shot detection system, allow us to work on fascinating systems with 5-10 ps time-resolution that were previously prohibitive for technical reasons.

Current focuses are studies of transport of charges and excitons in conjugated polymers, which are of interest due to their applications in "plastic" electronics and organic photovoltaic devices. Pulse radiolysis is almost unique in its ability to rapidly inject charges into conjugated polymer chains and observe them with optical spectroscopy.

Recent Progress:

Ion-Pairing by Protons and Avoiding this drag on Mobility. Ionization of THF, one of the best solvents for conjugated polymers, produces free ions, which move independently of each other, and a somewhat larger amount of geminate (or spur) ions consisting of electrons and holes that are separated by 1-7 nm, but are bound by their mutual Coulomb attraction. When THF was used in past work to investigate electron transfer and the Marcus theory, the geminate ion-pairs presented only a minor problem because they annihilate upon recombination. Electrons in long conjugated molecules behave differently. Experiments with oligomers of fluorene, F_n, n=1-4 gave rise to ion pairs ($F_n^{-\bullet}$,RH_2^+), where the solvated proton, RH_2^+, (THF=RH) is the positive counter-ion in THF, formed by proton transfer from THF radical cations ($RH^{+\bullet}$+RH$\rightarrow$ $R^\bullet$+ RH_2^+). The ($F_n^{-\bullet}$,RH_2^+) ion-pairs disappear immediately for F_1, but have long (~100 ns) lifetimes for F_2-F_4 and longer. The results determine unexpectedly slow rates, k_{pt}, of highly-exoergic proton transfer within the ion-pairs. They also furnish rates of escape, k_{esc}, to form free ions. They additionally make comparisons to several smaller molecules. The dependence of k_{esc} on length of the oligomer gives a valuable first look into the

hypothesis that delocalized charges can enhance escape by Coulomb-bond charges. These results tell us that in THF ionization of conjugated polymers creates two kinds of anions: a) highly-mobile free $pF^{-\bullet}$ free ions and b) slower moving ($pF^{-\bullet}$,RH_2^+) pairs, in which the electron can move only by dragging a more massive proton with it.

Radiation chemistry of chloroform. The nature and mobilities of holes in conjugated polymers and aggregates is central to their application in OPV devices. Holes are readily studied by pulse radiolysis in halogenated solvents, where electrons are converted rapidly to relatively inert chloride ions. An important criterion for the selection of solvents is polymer solubility; chloroform excels in this capability. While many reports of oxidation following pulse radiolysis are in the literature, there is no comprehensive understanding of this complex chemistry. Results determined the relationship between solute IP and which species they can be oxidized by: $CHCl_3^{+\bullet}$, $Cl^{\bullet}$, and $CCl_3^{\bullet}$. A key result for low IP polymers and aggregates is that cations will be formed as ion pairs; some initially solvent-separated, but likely ultimately contact ion pairs. The yield of free ions is low, < 10%. Ion pairing will likely effect charge motion in polymers.

"Step" capture of holes. In order to study charge transport in molecular wires, charges must first be captured; the rate at which they are captured largely determines the time-resolution for transport measurements with molecules with pendant trap groups. Capture by diffusion can limit time resolution to a few ns. In previous work, it was found that large numbers of electrons could be captured by pF in THF before they were solvated at times faster than observable in our experiments. This resulted in "Step" increases in absorption is pulse radiolysis experiments with ~15 ps time-resolution, providing the ability to probe much faster electron transport than would be possible by diffusive capture alone.

Electrons in some molecular liquids have mobilities as large as 100 cm2/Vs, but this is not true for holes, so it is natural to assume that very fast "step" capture is exclusive to electrons, which are initially mobile and delocalized after they are produced by ionization. Therefore fast injection into conjugated polymer chains, known for electrons, might not be available for holes, greatly limiting time-resolution in possible subsequent hole transfer experiments. To test this, experiments examined polyfluorenes dissolved in chloroform. The surprising result was very prominent "steps" in OFSS absorption data where polyfluorene radical cations absorb, seen to the right. At the highest concentration, the yield of $pF^{+\bullet}$ is quite high, with G~1 ions/100eV absorbed. Similar "step" capture results are found for small molecules. The mechanism of capture is not known; it is tempting to draw parallels to that for electrons described in previous work, invoking extended hole wavefunctions before solvation and possibly coherent hole wavefunction propagation. It should be noted

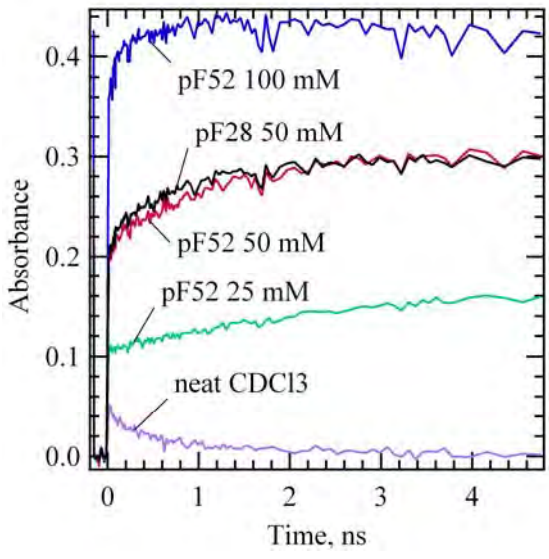

that however despite the encouragingly high yields of $pF^{+\bullet}$ formed in 15 ps, a persistent issue is that most will be geminate ions, thus paired to a counterion.

Spectra of Singly- and Doubly-Reduced Oligofluorenes. While the nature of polarons is crucial to operation of organic photovoltaics it is not well understood, and the question of whether two polarons readily combine to make a bipolaron is not yet clear. We obtained absorption spectra of

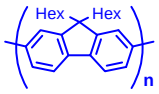

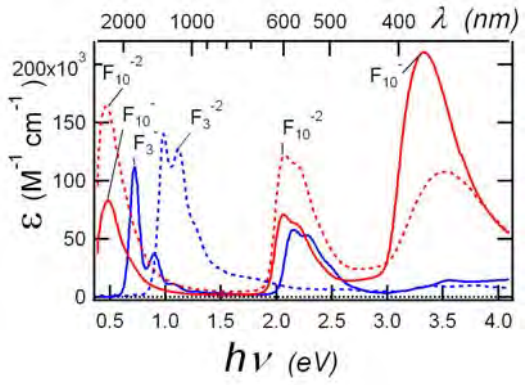

anions and dianions of F_1 through F_{10} that gave new insights. Polarons were found to have a length of 4.3±0.5 repeat units. In short oligomers (<4.3 units) polarons had sharp spectral bands which broadened in long oligomers. This result points to a variable polaron length when polarons are not confined by the length of the oligomer. Double reduction produced bipolarons in short oligomers but two side-by-side-polarons in long oligomers. These results were reproduced in long-range-corrected DFT calculations, but not with standard functionals like B3LYP. Long oligomers also contain bands at approximately the energy of the neutral, but these novel "vestigial neutral" (VN) bands shift with length.

Rapid triplet transport along polyfluorenes? Triplet excitons in pFs with AQ or NI end traps have intense optical bands at the same wavelength as pF without end traps, but with smaller extinction coefficients. Experiment tests and computations confirmed that triplet excitons were trapped at both AQ and NI, although the triplet energy of AQ is higher than that of pF. The role of charge-transfer triplet states explained the trapping energetics and the coincidence of absorption bands. In polymers more than 100 units long triplet excitons reached the end traps in <40 ns; slow diffusive triplet attachment rates prevented measurement of the actual rate and kinetics.

Future Plans:

The fast step capture of holes is presently contrary to our intuition. Like those for electron capture the mechanism is not clearly identified. Experiments will utilize both polymers and small molecules in a variety of solvents with different IP's as well as mixtures to shed some light on the mechanism.

Research will seek methods to rapidly attach large numbers of triplet excited states to solutes without singlet precursors, which will enhance time resolution for measurements of triplet transport by 1-3 decades, and enable fast measurements of triplets of molecules with low yields of intersystem crossing. Preliminary OFSS data show rapid production of pF* in both THF and isooctane, though far more in isooctane, with a very large amount of triplet remaining after a few ns at high [pF], completely obscuring any singlet decay. A plausible conclusion is that much ^{3}pF* is formed in "Steps". We will examine the mechanisms and yields of such rapid triplet production, with a hypothesis that step capture of electrons and holes is intimately connected to fast triplet production. Future work will model the dynamics and learn how fast triplets are produced and what conditions maximize their numbers, in order to enable subsequent measures of triplet transport in conjugated polymers with time resolution as fast as 15 ps.

Efforts will be made to observe electrons and holes attached to aggregates and crystallites, that may simulate the behavior of charges in films. We will also be seeking to investigate production of charges in actual films comprised of or containing conjugated polymers.

.

Publications of DOE sponsored research that have appeared since 10/1/2009:

1. Grills, D. C.; Cook, A. R.; Fujita, E.; George, M. W.; Preses, J. M.; Wishart, J. F. Application of External-Cavity Quantum Cascade Infrared Lasers to Nanosecond Time-Resolved Infrared Spectroscopy of Condensed-Phase Samples Following Pulse Radiolysis. *Appl. Spectrosc.* **2010,** *64*, 563-570.
2. Cook, A. R.; Sreearunothai, P.; Asaoka, S.; Miller, J. R. "Sudden, "Step" Electron Capture by Conjugated Polymers" *J. Phys. Chem. A* **2011**, *115*, 11615-11623. doi:10.1021/jp205790k.
3. Sreearunothai, P.; Estrada, A.; Asaoka, S.; Kowalczyk, M.; Jang, S.; Cook, A. R.; Preses, J. M.; Miller, J. R. "Triplet Transport to and Trapping by Acceptor End Groups on Conjugated Polyfluorene Chains" *J. Phys. Chem. C* **2011**, *115*, 19569-19577. doi:10.1021/jp205828q.
4. Wishart, J. F.; Funston, A. M.; Szreder, T.; Cook, A. R.; Gohdo, M. "Electron Solvation Dynamics and Reactivity in Ionic Liquids Observed by Picosecond Radiolysis Techniques" *Faraday Discuss.* **2012**, *154*, 353-363. doi:10.1039/C1FD00065A.
5. Musat, R.; Crowell, R. A.; Cook, A. R.; Renault, J.-P. "Nanosecond Pulse Radiolysis of Nano-Confined Water," *J. Phys. Chem. C*, accepted.

Reactive Intermediates in the Condensed Phase: Radiation and Photochemistry

Robert A. Crowell
Chemistry Department, Brookhaven National Laboratory, P.O. Box 5000, Upton NY, 11973; crowell@bnl.gov

Scope

The scope of this program is to study and gain an understanding of the fundamental processes associated with the interaction of ionizing radiation within bulk liquids, the liquid/solid and solid/solid interface. Specific emphasis is placed upon developing detailed knowledge of the role of the solvent, the interface and nano-confinement on charge recombination, electron transfer, energy transfer and ion-radical chemistry. One of the most common sources of chemical reactivity in our universe is ionizing radiation. Radiation chemists typically study the rapid, energetic reactions that are initiated by the interaction of ionizing radiation, such as high-energy electrons, with matter. The processes that control these reactions, such as excited state chemistry, thermalization, solvation and energy transfer, are among the most fundamental events that occur in condensed phase chemistry and the related areas of energy sciences, physics and biology. The processes are the key steps for efficient energy conversion, catalysis, and energy storage. Understanding of the basic processes that control these reactions impacts many DOE related fields including the design of nuclear reactors, radioactive waste management, development energy storage devices, radiation therapy, polymer processing, and planetary- and astrophysics. While much is now understood about radiation chemistry in bulk liquids, there is still a significant gap in our knowledge of the many fundamental processes that lead to radiation damage. This is particularly true for the radiation chemistry of nanoconfined and interfacial systems. Detailed mechanisms for these processes are not known and it is commonly accepted that these (and many other) radiation induced processes involve exotic chemistry that occurs on an ultrafast timescale ($<10^{-10}$ s). In this program the approach utilizes a wide array of experimental techniques including ultrafast optical transient absorption, time resolved x-ray absorption spectroscopy, and ultrafast pulse radiolysis, The work proposed here will take advantage of a variety of DOE user facilities, including LEAF, NSLS and the APS.

Our progress has already shown that the combination ultrafast laser spectroscopy, nanosecond pulse radiolysis and x-ray absorption spectroscopy (XAS) are a powerful combination of techniques that will help this program achieve its goals. Specifically, ultrafast transient absorption (TA) measurements of the charge transfer (CT) band in ionic liquids have shown that CT is followed by a very complex series of chemical reactions. Recently, we have succeeded in our first time resolved XAS experiments on this system. Although the results are preliminary, the data suggest that the bromine atom undergoes a reaction in less than 500 ps. Future work will continue to use these techniques unravel the details of this complex chemistry. Nanosecond pulse radiolysis studies of nanoconfined water show that both nanoconfinement and the liquid solid interface dramatically affect the reactions of the solvated electron. Currently, we are entering into the picosecond regime to get more information on the details of the mechanism of electron generation and reactivity. Additional work will utilize XAS and TA spectroscopy to understand ion solvation and CT in nanoconfined water.

Recent Progress

To meet the main objectives of our program we are focused on two specific areas: the photochemistry of room temperature ionic liquids and more recently we have begun to study the radiation chemistry of aqueous systems under nano-confinement. In order to achieve our goals we use the techniques of ultrafast pulse radiolysis, ultrafast optical and x-ray spectroscopies.

Photochemistry and Solvation Dynamics of Ionic Liquids

The photochemistry of the charge transfer (CT) band of the room-temperature ionic liquid (RTIL) 1-hexyl-3-methylimidazolium bromide ([hmim$^+$][Br$^-$]) has been investigated using near-IR to Vis ultrafast transient absorption (TA) and steady-state UV absorption spectroscopies. Continuous irradiation of the CT band at 266 nm results in the production of photoproducts that absorb strongly at 266 nm. We have shown that these photoproducts, which are apparently very stable, adversely affect ultrafast TA measurements. Elimination of these effects reveals at least two transient species that exist within the TA detection window of 150 fs to 3 ns and 500 nm to 1250 nm (b in figure below). One of the components is a short-lived (<1ps) specie that absorbs at 1080 nm, which we assign to a caged ion pair. A second band exhibits a multicomponent spectrum that is very broad with an absorption maximum around 600 nm and a lifetime that is longer than the 3ns window of our TA spectrometer. Initial interpretation of the data indicate that no solvated electrons are produced by the CT mechanism, but the initial CT process is results in complex reactions involving radical ions and possibly the generation of reactive excited states.

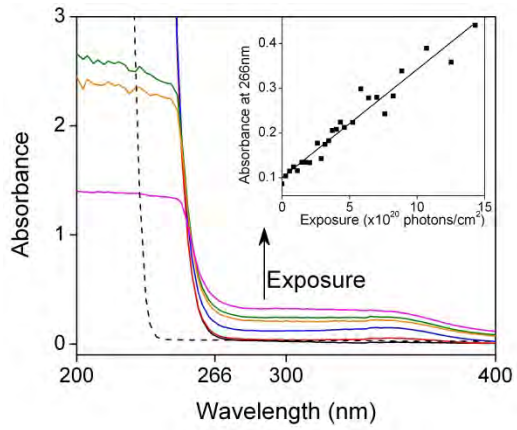

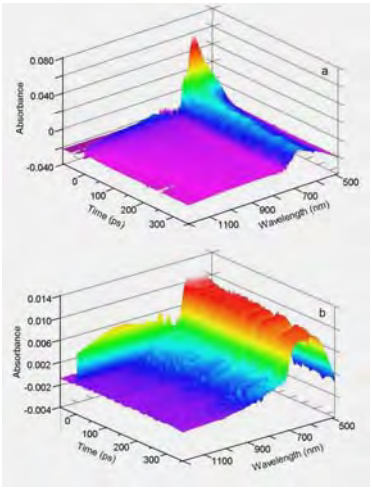

Additionally, we have studied the kinetic salt effect on the disproportionation reaction between diiodide anions in methanol has been examined using two ionic liquids and one inorganic salt. The ionic reaction was accelerated significantly, depending on the cation of the salt, and the ionic liquids enhanced the reaction more effectively. At higher concentrations the reaction rates decrease owing to increasing viscosities.

The radiation chemistry of nanoconfined water

In this project, we have studied the production and evolution of the aqueous electron in water confined in porous silica (1 nm and 57 nm pore sizes) and compare these results to bulk water. The pulse radiolysis technique was used to investigate the evolution of the hydrated electron formed in water trapped in silica with 2 ns time resolution. The spectrum of the solvated electron is measured at 20 ns following the passage of ionizing radiation. Within the signal to noise of our experiment the spectrum of the solvated electron is the same in both the bulk and confined media indicating that within 20 ns the electron solvates in the region of the pore that has bulk like properties and not at the interface. It is observed that the reaction rates of the solvated electron increase with decreasing pore size going from 6.8×10^6 s^{-1} in the bulk to 34.7×10^6 s^{-1} in a 1 nm pore. The yield at 20 ns increases by a factor of 2.03±0.01 relative to the bulk. We interpret these results with respect to effects of confinement on the water structure and dynamics as well as the surface energetics. Studies using picosecond resolution and better signal to noise are needed to evaluate a potential delocalization of the electron under confinement.

The evolution of the hydrated electron in bulk and confined water is followed up to one microsecond. The confinement induces an acceleration of the decay of the hydrated electron with increasing confinement degree. Upon confinement the rate increases by a factor of 1.25 in the 57 nm pore relative to the bulk. In the 1 nm pore the difference is much more dramatic and increases from 6.8×10^6 s^{-1} in the bulk to 34.7×10^6 s^{-1} in the 1 nm pore, a factor of 5.

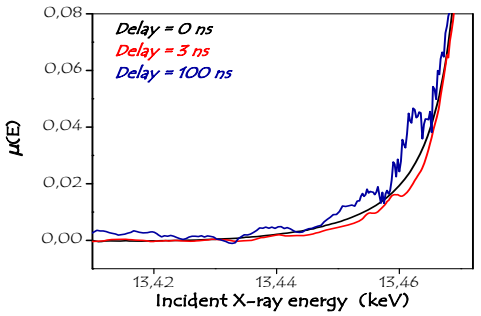

TR-XANES of hmim Br showing no bromine at t<1ns after excitation of the CT

Future Plans

Photochemistry and Solvation Dynamics of Ionic Liquids

Future work will focus on two main areas of interest. First, we will continue to study both the photochemistry and solvation dynamics of selected room temperature ionic liquids. We are in the process of extending the detection range of our ultrafast laser system further down into the UV (this will help detect radical dications) as well out into the mid-IR. We will continue our TA experiments using a variety of scavengers to help identify the origin of the bands that are observed. The ultimate goal is to understand the degradation pathways (mechanisms) of the RTILs so that more robust systems can be developed.

In the second part of this effort we will complement the TA experiments using both static and time-resolved XAS to study the solvation structure and dynamics of the bromide ion. This work is being carried out at Sector 7 of the APS. We have used static EXAFS in combination with DFT calculations to investigate the equilibrium solvation structure of the bromide ion in a series of imidazolium RTILs. The solvation location of the bromide ion lies primarily above the C2 and H2 entities. The separation between the bromide and the C2 (3.12Å) and nitrogens (3.94Å) is nearly independent of the RTILs that were investigated. In attempt to learn more about the CT process we have performed our first TR-XAS on ([hmim$^+$][Br$^-$]). In the figure above we observe no pre-edge feature in the TR-XANES spectra at times greater than 500ps following excitation of the CT band. This suggests that on this timescale no bromine atom is formed (exists), and that the CT process is accompanied by a fast reaction of the bromine atom. One possibility is abstraction of the H2 hydrogen (which is acidic) by the initially formed bromine atom to form HBr. Future work on1,2-dimethyl-3hexyl imidazolium bromide, where the H2 is replaced by a methyl group, should provide more insight on this possible mechanism.

The radiation chemistry of nanoconfined water

To understand the role of confinement on the radiation chemistry of water we must, understand the role of confinement of solvation, its effect on reaction kinetics and mechanisms, and its effect on ion/radical diffusion. To develop an accurate description of nano-confined water and its effect on solvation we propose to use a combination of static and time resolved XAS on salt solutions that we have previously developed at the APS and the static XAS capabilities of the NSLS. Specifically, we will start with the aqueous bromide system that we have previously characterized by both ultrafast optical and XAS methods in the bulk. By using strontium bromide we will initially study the solvation structure of both the cation and anion at the interface. Experiments will be carried out as a function of both pore size and humidity to gain specific information about the interactions of charged species with the interface and the role of water. We will use commercially available and well characterized material that include zeolites and Vycors (also known as controlled porous glasses) to cover pore sizes from 1 nm out to 50 nm.

Concurrent experiments will utilize ultrafast UV pump/NIR to mid-IR probing to study the effect of surface hydration on the reactivity of caged ion pairs. Time resolved XAS will also be used to gain more detailed insight to the structural and dynamics nature of surface hydration effects. This will be

complementary to work we have carried out in the bulk. We also propose to continue to utilize the ultrafast pulse radiolysis and single shot detection capabilities available to us at LEAF to study the effect of confinement on water radiolysis. Our preliminary results have been successful, but we need to modify our current cell design to eliminate contributions from the cell windows. We will also study the effect of pore size and humidity on the formation and reactions of the hydrated electron. We will also measure the spectrum of the confined hydrated electron at early times. Previous work in zeolites indicates a significant blue shift in the absorption maximum as the electron becomes more confined. A blue shift of 0.28eV has been observed for an electron trapped in a 13Å zeolite supercage. From the fundamental studies of the hydrated electron we will progress to more complex systems. Dilute solutions have the same early stages of their radiation chemistry as neat liquids and, as such, are of little interest for the studies of primary events. Because there are no analogs of chromophore groups in radiolysis, to have an effect on the picosecond time scale, the solute has to be present in very high concentration. In this regime ultrafast radiation chemistry becomes the chemistry of concentrated solutions and mixtures. Radiolysis of concentrated solutions and nano-confined systems has important practical implications since most of the radiation chemistry involved in radioactive waste management, fuel reprocessing and reactor design occurs in highly acidic systems, at interfaces and in nanoporous environments. Due to the high ion concentration, ionization and excitation events in spurs involve both the water and the ions, and cross reactions that involve the species derived from either one of these two components are very rapid, occurring on the time scale that is presently available using the LEAF facility. As previously mentioned, we will initially focus our efforts on bulk water we will then progress to the unique reactions that occur between electrons (both solvated and pre-solvated) in more complex systems such as the nitric acid/nitrate system.

DOE Publications/Manuscripts 2009-present

1. R. Musat, A. R. Cook, J-P Renault, R. A. Crowell, "Nanosecond Pulse Radiolysis of Nanoconfined Water, " J. Phys. Chem. C 116, 13104 (2012).
2. R Musat, R. A. Crowell, K. Takahashi, D. Polyanskiy, M. Thoas, J. F. Wishart, Y. Katsumura "Ultrafast transient absorption spectrum of the room temperature ionic liquid 1-hexyl-3-methylimidazolium bromide: Confounding effects of photodegredation" to be submitted to Chem. Phys. Lett
3. J. Belloni, R. A. Crowell "Ultrafast Pulse Radiolysis," Recent Trends in Radiation Chemistry Chapter 5 (2010)
4. K. Takahahsi, K. Suda, T. Seto, Y. Katsumura, R. Katoh, R. A. Crowell, J. F. Wishart "Photo-detrapping of solvated electrons in an ionic liquid," Rad. Phys. Chem., 1129, 78 (2009)
5. K. Takahashi, H. Tezuka, T. Sato, Y. Katsumumra, M. Watanabe, R. A. Crowell, J. F. Wishart "Kinetic salt effects on an ionic reaction in ionic liquid/methanol mixtures," Chem. Lett. 38, 236 (2009)
6. C. G. Elles, I. A. Shkrob, R. A. Crowell, D. A. Arms. E. C. Landahl "Transient x-ray absorption spectroscopy hydrated halogen atom," J. Chem. Phys. 128, 061102 (2008)

Kinetics of charge transfer in a heterogeneous catalyst-reactant system: the interplay of solid state and molecular properties

Tanja Cuk

Chemical Sciences Division, Lawrence Berkeley National Laboratory

D46 Hildebrand, Department of Chemistry, University of California Berkeley, Berkeley, CA 94720

tanjacuk@berkeley.edu

Program Scope: One of the greatest challenges in the design of efficient and selective catalysis technologies is the limited fundamental understanding of how interfacial properties at solid state/reactant interfaces guide catalytic reactions. The central research question is to determine how molecular properties of reactants influence charge dynamics in solid state catalysts, and conversely, how these charge dynamics induce molecular changes; likely, it is this synergy that results in catalytic efficiency. There are two perspectives on the solid state catalyst/reactant interface. From the solid state perspective, interfacial properties are described by band alignment and Fermi levels; from the molecular perspective, interfacial properties are described by oxidation states and reactant adsorption. The characterization of catalytic materials has either focused on molecular changes such as adsorption, dissociation, and new bond formations occurring on the reactant side of the interface or the changes in interfacial band alignment and passivation of surface states on the solid state side. While these properties are useful for understanding catalytic performance, a causal link between the changes observed on each side of the interface is lacking. What is needed is to directly follow the trajectory of how charge carriers in solid state catalysts initiate interfacial charge capture by reactant molecules—from the creation of the charge carrier in the bulk, to its accumulation at the interface, and to the moment at which a reactant molecule transforms and, in the process, consumes the charge carrier.

Recent Progress: Recent progress has been made in two areas related to the study of water oxidation on Co_3O_4. This catalyst has proven efficient for O_2 evolution from H_2O when activated by visible light absorbing $Ru(bpy)_3$. Co_3O_4 has two highly absorbing band gaps in the visible range, though it alone has not been shown to initiate a reaction. We have characterized the transient optical spectroscopy of these two band gaps for the first time. The transient spectrum provides insight into the dispersion of the valence and conduction bands that initiate reactions at the interface. Further, the transient kinetics provide the time scales of thermalization and electron hole recombination that compete with charge capture by reactant molecules. Secondly, we have attempted several p-n junctions with Co_3O_4 in order to separate the photogenerated electron hole pairs and initiate molecular reactions at the interface. The successful formation of such a junction will allow for ultrafast, laser initiated charge injection into the catalyst, important for the larger goal of this program. The transient optical and infrared spectroscopy of already well-separated charges will describe the detailed balance between the flow of charge carriers to catalyst-reactant interfaces and the dynamics of interfacial charge capture by reactant molecules.

The Co_3O_4 films for the optical pump-probe experiments were deposited on quartz with varying film thicknesses between 10 nm-200 nm. They were deposited by reactive sputtering in an Argon/O_2 (4.5 mTorr/ 0.5 mTorr) atmosphere from a heated cobalt target (500° C) at the Joint Center for Artificial Photosynthesis. These polycrystalline films of approximately 20 nm crystallites have been characterized by X-ray Diffraction, Scanning Electron Microscopy, ellipsometry, Mott-Schottky, cyclic voltammetry, and infrared, Raman, and optical absorption.

The transient spectrum after pumping above both band gaps (at 600 nm (2.1 eV) and 800 nm (1.6 eV)) with 520 nm light is shown in Figure 1. In the past, transient spectra such as these have been used to determine the nature of the band curvature responsible for singularities in electronic structure in both semiconductors and noble metals [1]. We are in the process of applying this same theoretical description—which involves as inputs a calculated band dispersion and the change in the occupied and unoccupied band filling due to the pump pulse—to replicate the transient spectrum. Already one can see that the two band gaps behave differently: while there is a maximum change in transmission and reflection at 600 nm, there is a zero-crossing in the spectra around 800 nm. The transmittance and reflectance spectra allow for the experimental determination of both the real and imaginary parts of the index of refraction, constraining the theoretical description. Understanding these spectral signatures will provide the benchmark for investigating Co_3O_4 exposed to different reactant environments and within a p-n junction device.

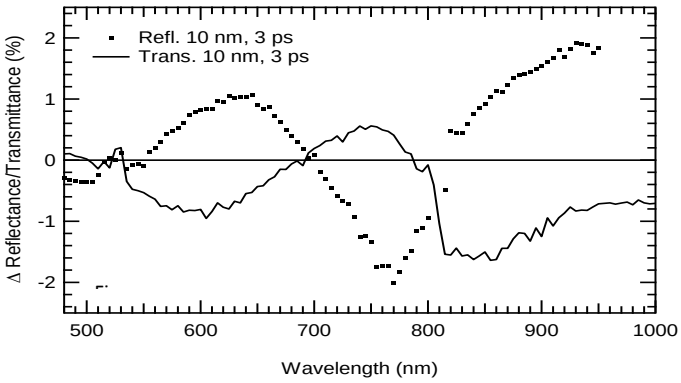

Figure 1: Transient optical spectrum of Co_3O_4 measured in reflection and transmission for the 10 nm film. Pumped at 520 nm.

The transient kinetics associated with the thermalization and electron hole recombination across these two band gaps are shown in Figure 2. The kinetics depends on the thickness of the film and differs in reflectance and transmission for all but the thinnest, 10 nm film. For the thicker 100-200 nm films, the electrons and holes recombine on the 100's of ps time scale when probed in reflection. On the other hand, when the same film is probed in transmission, a longer, ns time scale is measured. Since in the 10 nm films the two time scales agree in both measurement geometries, we take the difference to be an effect related to surface versus bulk recombination in the thicker films. Currently we are testing this hypothesis by putting the films in different chemical environments (e.g. water, methanol) in a controlled vacuum chamber to change the surface terminations. The surface recombination is also likely related to surface roughness of the films. In order to test this, we will be growing the films epitaxially on a lattice matched spinel, $MgAl_2O_4$, to control for the crystal face and surface roughness of the sputtered films [2].

The kinetics associated with charge capture at the water interface has been previously studied in n-type TiO_2 using second harmonic generation and transient gratings [3]. There, the photogenerated

electron-hole pairs are separated by the large electric field that exists at the water interface. A 100's of ps time scale is measured for hole capture at the interface. Given the longer time scales of electron hole recombination that we measure, one would think that water oxidation could then compete with recombination. However water oxidation on Co_3O_4 cannot be initiated efficiently without a separate light absorber. There could be two potential reasons for this: (1) the time scale for hole capture at the Co_3O_4/water interface is slower due possibly to the higher lying valence band and (2) visible light driven excitation by $Ru(bpy)_3$ that does result in high quantum efficiencies (50-60%) preferentially creates holes on the surface of the oxide. These are some of the questions that we will be investigating in the coming year using both a controlled environment for surface terminations and p-n junctions to separate the electron hole pair at longer time scales.

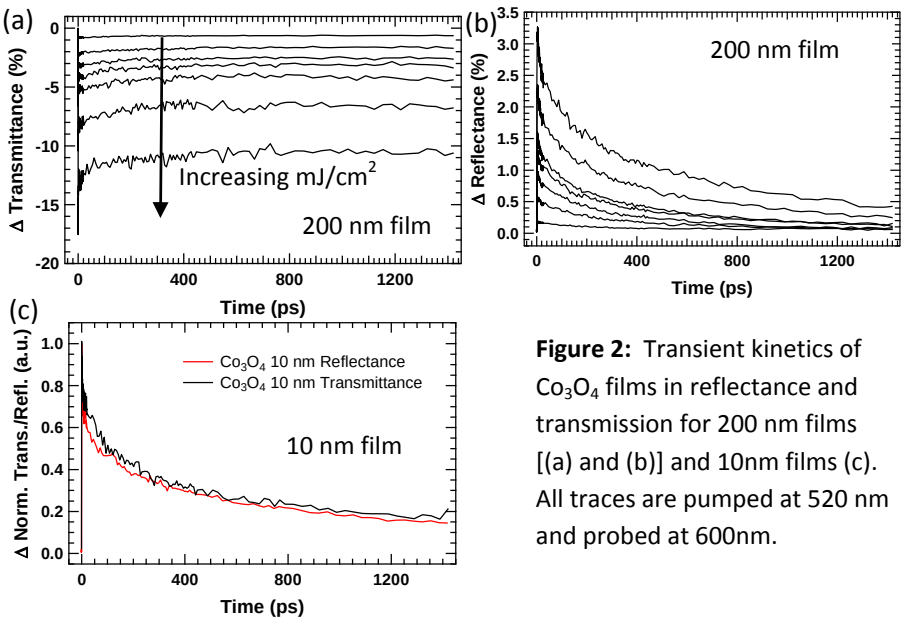

Figure 2: Transient kinetics of Co_3O_4 films in reflectance and transmission for 200 nm films [(a) and (b)] and 10nm films (c). All traces are pumped at 520 nm and probed at 600nm.

The second area in which our efforts have been devoted is the creation of a Co_3O_4 p-n junction. So far we have tried both indium tin oxide and lightly doped n-type Silicon as the n-type semiconductor. The former gives a good contact and no rectifying behavior while the n-type Silicon does give rectifying behavior though no change upon illumination. The lack of light activation may be due to: (1) the built in electric field lying largely in the lightly doped n-type Silicon since Co_3O_4 is highly p-type (2) poor interfacial characteristics, possibly due to a SiO_2 layer in between the silicon and Co_3O_4. Efforts currently involve finding a more lattice matched n-type semiconductor with a higher n-type doping and work function on which to grow the Co_3O_4 films. The lattice matching will help with interfacial issues, by providing the right substrate for preferential Co_3O_4 growth over other, competing phases; it could also help with creating less transition metal defects and lowering the p-type carrier density that makes junction formation difficult. The higher n-type doping and work function will enhance the ability of the junction to create an electric field within Co_3O_4 itself.

Future Plans: The plans for the next year involve finishing up experimental and theoretical transient optical pump-probe spectroscopy on Co_3O_4 in air, adding temperature control to the vacuum chamber, pump-probe experiments of Co_3O_4 with different surface terminations (in methanol and water environments), and creating a more controlled p-n junction with Co_3O_4. Finishing up the transient pump probe spectroscopy in air will involve probing the d-d transitions lying in the near infrared regime and theoretical input from electronic structure calculations [4]. Adding temperature control to the vacuum

chamber will allow us to heat the samples to create a clean, organic free interface before the reactant environment is changed. We also plan to either cool or raster the samples to ensure that the methanol/water does not desorb between laser pump pulses.

The current plan for creating a more controlled p-n junction involves depositing Co_3O_4 on n-type ZnO. While ZnO has a hexagonal and not spinel structure, it has been grown on $MgAl_2O_4$ epitaxially with a relative rotation of the two substrates [5]; since Co_3O_4 is lattice matched to the spinel $MgAl_2O_4$, the same could occur there. However, alloy formation of Zn-Co-O is common and there is a possibility that a non-Co_3O_4 interface forms despite the lattice matching. Controlling for this will be related to different oxygen/argon partial pressures and the use of a completely Co_3O_4 target. In parallel, we will attempt a p-n junction with a lattice matched, n-type spinel or n-type cubic substrate.

Publications:

[1] Sun, C.-K. *et. al.* "Femtosecond-tunable measurement of electron thermalization in gold," Phys. Rev. B. **50**, pp. 15337 (1994); Rosei, R. Antonangeli, F., and Grassano, U.M., "d-bands position and width in gold from very low temperature thermomodulation measurements", Surface Science **37**, pp. 689 (1973).

[2] Vaz, C. A. F. et. al. "Interface and electronic characterization of thin epitaxial Co_3O_4 films," Surface Science, **603**, pp. 291 (2009).

[3] Lantz, J., Corn, R, "Time-Resolved Optical Second Harmonic Generation Measurements of Picosecond Band Flattening Processes at Single Crystal TiO_2 Electrodes". J. Phys. Chem., **98**, pp. 9387 (1994); Kasinski, J. *et. al.,* "Picosecond dynamics of surface electron transfer processes: Surface restricted transient grating studies of the n-TiO_2/H_2O Interface". J. Phys. Chem., **90**, pp. 1253 (1990).

[4] Chen, J., Wu, X., and Selloni, A., "Electronic structure and bonding properties of cobalt oxide in the spinel structure," Phys. Rev. B, **83**, 245204 (2011).

[5] Andeen, D. et al., "Crystal chemistry of epitaxial ZnO on (111) $MgAl_2O_4$ produced by hydrothermal synthesis," J. of Crystal Growth, **259**, pp. 103 (2003).

Computational Studies of Aqueous and Ionic Liquids Interfaces

Liem X. Dang
Chemical and Materials Sciences Division
Pacific Northwest National Laboratory
Richland, WA 93352
liem.dang@pnnl.gov

Background and significance

A quantitative description of the ion distribution and how to describe ion interactions in different environments remains a challenge, and are subject to current debate. We found that the interionic potentials of mean force (PMF), as well as the interfacial properties, are very sensitive to ion-ion interaction potential models. We performed simulations using polarizable potential models to study the Ca^{2+}-Cl^- ion-pair interaction and examine the dependence of the computed PMFs on the model used. The resulting PMF was very sensitive to the magnitude of the Ca^{2+}-Cl^- ion-pair interaction. When the ion-ion interaction was modeled using parameters adjusted to fit the electronic structure results, our simulation predicted a Ca^{2+}-Cl^- and Sr^{2+}-Cl PMFs with no contact ion-pair (CIP) state and a shallow solvent-separated ion-pair state (SSIP) state. We were able to quantitatively capture the experimentally measured x-ray reflectivity of the aqueous salt interface for $SrCl_2$ using the modified ion-ion interaction model. We also computed the reflectivity for $SrBr_2$, and SrI_2, systems and provided a detailed physical description of the interfacial structure of these systems.

Room temperature ionic liquids (RTILs) have been shown to be versatile and tunable solvents that can be used in many chemical applications. In this study, we developed a dynamical, molecular-scale picture of the gas dissolution and interfacial processes in RTILs using molecular simulations. From these simulations, we can calculate the free energies associated with transporting a gas solute across various RTIL interfaces and gain physical insight into the interfacial properties and transport molecular mechanism of the gas sorption processes. For CO_2 sorption, the features in the PMF of CO_2, are qualitatively similar for both the polarizable and non-polarizable force fields. However, we observed some quantitative differences, and in this paper, we describe the possible causes of these differences. We also show that ionic-liquid chemical structures have significant impact on the gas sorption process, and we discuss this influence on the H_2O transport mechanism.

Recent Progress and Future Plans

Computational Studies of Aqueous Interfaces of $SrCl_2$ Salt Solutions

The sensitivity of the modeled chemistry on ion-ion interactions and its consequence were studied using molecular dynamics (MD) and PMF approaches. In this report, we describe in detail our simulation studies of the inter-ionic PMF for the Sr^{2+}-Cl^- ion pair in bulk water, as well as the interfacial properties of aqueous interface salt solutions. Two sets of potential parameters were used to describe the Sr^{2+}-Cl^- interactions; because of the availability of experimental data on the x-ray reflectivity of the aqueous interface, we believe this is an ideal system to benchmark ion-ion interactions.

In Figure 1, the computed PMF that used the standard mixing rules (green line) shows that there are stable CIP and solvent-separated ion pair (SSIP) states centered at 2.75 Å and 5.00 Å, respectively. The CIP and SSIP calculated from this simulation have free energies of -3.2 kcal/mol and -0.6 kcal/mol, respectively, with a 5.5 kcal/mol barrier to CIP dissociation. The CIP well depth is much deeper than the corresponding SSIP well depth, which is indicative of the CIP being fairly stable. As stated above, the cross-term Lennard-Jones parameters for the ion-ion potential model were initially constructed using standard mixing rules. However, we found that this approach usually over-estimates the minimum interaction energy when compared to accurate, high-level electronic structure calculations. We are interested in the accuracy of the intermolecular interaction and what effect it has on the computed ion-pair PMFs in aqueous solutions. To this end, we performed electronic structure calculations on the Sr^{2+}-Cl^- complex to determine its minimum energy and distance. The *ab initio* calculations using MP2 method in conjugation with DGDZVP basis sets give a minimum potential energy of 258.4 kcal/mol for the $SrCl^+$, and a distance $r_{(Sr\text{-}Cl)}$=2.6 Å. We also benchmarked these results against the higher level CCSD(T) level of theory, and found the results to be in excellent agreement. We adjusted the Sr^{2+} and Cl^- Lennard-Jones parameters to match the quantum mechanics

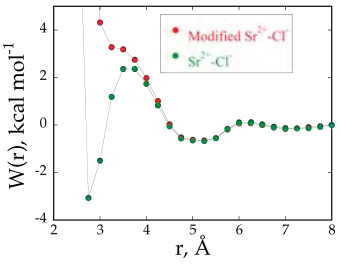

Figure 1. Computed interionic PMFs for the Sr^{2+}-Cl^- ion pair in water.

calculations. Additional PMF calculations were carried out using this new set of parameters for the Sr^{2+}-Cl^- potential model to assess its effect on the computed PMF. The resultant PMF also is shown in Figure 1 (red line). This PMF is significantly different from the original PMF, and with these parameters, we found that the CIP is greatly diminished. There is a very small and repulsive residual of the CIP near 3 Å. It also is interesting to note that beyond the barrier to the CIP (at r = 3.75 Å), the computed PMFs for both models are essentially the same.

Figure 2 compares the structure factors calculated from simulations that used standard mixing rules (green line), the new set of parameters (red line), and experiment (black triangles). As mentioned in the theoretical background section and in previous studies, the structure factor can be accurately calculated from both experiment and simulation. Furthermore, it links the experimentally measured spectrum directly to the molecular-level interfacial structure determined from the MD simulations. As such, it is the appropriate property for comparison between experiment and simulation, which can improve our understanding of the relationship between the x-ray reflectivity and the interfacial structure. However, in the computational procedure, there are some uncertainties in calculating the intrinsic structure factors from both experiment and simulation. The uncertainties are caused mainly by estimates of the induced wave amplitudes and have little effect on the characteristic of the structure factors. Therefore, the comparison between experimental and simulation results focuses on the features of the structure factor, such as resonance frequency and the curvature trend. The calculated structure factors from both experiments and MD simulations are less accurate in the higher q regions. In simulations, the electron density could be accurately computed from the atomic number of species only when q is small. In experiments, the signal is reduced significantly with increased q, and the fluctuations increase significantly, introducing large error bars in the measured values. Consequently, the comparison of the structure factor calculated from experiment and MD simulation at the low q value is more meaningful and accurate.

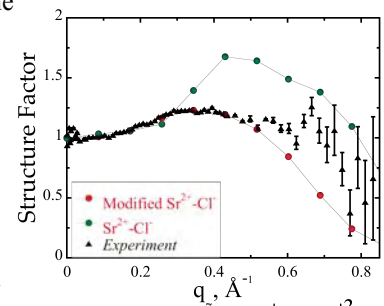

Figure 2. Simulated $|\Phi(q_z)|^2$ of 2.7 M of $SrCl_2$ salt

The structure factor calculated from simulation using a modified potential shows very similar features with experimental results. Especially when q is smaller than 0.5 Å^{-1}, the simulation quantitatively reproduces the experimental results. This is strong evidence that the electron density profile calculated from the MD simulation captures the same features as the experimental profile, and the corresponding ion distribution and interfacial structure may reasonably represent the experimental results. The resonance frequency at 0.35 Å^{-1} of the structure factor corresponds to a wavelength of ~18 Å^{-1} for the electron density profile. This long wavelength is attributed to the fluctuation of the number density profile across the interface in the simulation, including both strong ion double layer at the interface and the weak ion double layer towards the bulk phase. The simulation results suggest the enhancement of the electron density at the interface compared to the bulk phase is prerequisite to reproducing the experimental results. However, the precise fine structure of liquid/vapor interface for ion-aqueous solution in MD simulation is essential for the structure factor to be consistent with the experimental results. In principle, one electron density profile could be derived from different sets of number densities, as the contribution to the total electron density profile is from three species, and the structure factor can be calculated with different combinations of electron density profiles, thickness of the interface, and surface roughness. However, to the best of our knowledge, this MD simulation study, using a modified ion-ion potential model, provides the most reasonable prediction on the ions distribution across the liquid/air interface in $SrCl_2$ aqueous solution.

We propose to refine our current ion-water and ion-ion polarizable potential parameters. To do so, we have calculated the effective ion-ion potentials in water or potentials of mean force (see Figure 1), along with the calculation of radial distribution functions, which will then be used to calculate the known osmotic and activity coefficients of concentrated electrolytes solution. These properties can be compared with the corresponding experimental osmotic pressure, activity coefficients of electrolyte solution, and x-ray reflectivity of concentrated aqueous salt interfaces values to enhance the confidence in the simulation results for concentrated solutions. Further efforts to improve ion-ion and ion-water interactions using electronic structure techniques should be addressed in the future.

Anion Effects on Interfacial Absorption of Gases in Ionic Liquids

Gas Adsorbed at the Interface. The constrained mean force technique is applied to construct a free energy profile (i.e., the PMF) for transporting a gas solute (CO_2 or H_2O) across the air-RTIL interface. The PMF for CO_2 transfer across the air-[bmim][Tf_2N] interface was computed. For a CO_2 molecule that is ~10 Å away from the liquid phase, the average force acting on the solute will be small, and the free energy value is set to be zero. As the

CO_2 approaches within 10 Å of the liquid region, a monotonic decay is observed in the PMF. After reaching a minimum around the Gibbs dividing surface (GDS), the PMF starts to increase toward the bulk region, passes through a barrier, and eventually oscillates about a constant value. Similar PMF features were observed in a previous study of the transfer free energy of a single CO_2 molecule across the vapor/liquid interface of [bmim][BF_4]. The fact that the shape of the PMF is similar in these two ionic liquids, along with the results of the density profile, and specific orientation at the interface, may suggest that the [bmim] cation is mainly responsible for the qualitative features of the CO_2 PMF in the interfacial region.

The minimum in the CO_2 PMF near the GDS clearly reveals the stability of CO_2 at the interface, which may lead to the tendency of CO_2 to form an adsorbed layer at the interface. In addition, the barrier located at 5 Å from the liquid phase indicates that CO_2 accommodation is an activated process. In a recent study of a CO_2-[bmim][Tf_2N] system, Perez-Blanco and Maginn found that CO_2 indeed forms an adsorbed layer at the interface with density higher than in the bulk and the liquid phases. Their observation is consistent with our PMF results, and may be attributed to the favorable molecular interaction between CO_2 and the fluorines of the anions at the RTIL/air interface. The free energy of solvation of CO_2 in [bmim][Tf_2N], determined from the difference between the PMF in the bulk and in the vapor region, are estimated to be -0.30 ±0.15 kcal/mol and -0.12 ±0.15 kcal/mol at 350 K and 400 K, respectively. These results are in reasonable agreement with the experimental values of -0.29 kcal/mol and -0.02 kcal/mol at 350 K and 400 K, respectively, based on the Henry's laws constant used in solubility measurements. PMFs calculated from simulations at the two temperatures are very similar, indicating that the temperature does not significantly affect the free energy of transporting CO_2 across the air/ionic-liquid interface. The main effect on the PMF is a shallower minimum at the interface and a smaller solvation free energy, which would be expected because the gas solubility in a liquid typically decreases as the temperature increases.

Figure 3 shows the PMFs for H_2O across the RTIL/vapor interfaces, with the dashed line indicating the GDS. The PMF value is larger in the vapor phase and decreases monotonically toward the RTIL. The lowest PMF value in [bmim][Tf_2N] is reached when H_2O is just below the GDS towards the RTIL. Farther into the bulk region, modest oscillations are found in the PMF value around the minimum. These results clearly demonstrate that there is a preference for H_2O to be solvated by the RTIL, possibly because of favorable electrostatic interactions. The monotonic decay of H_2O PMF from the vapor phase toward the bulk RTIL is different from the solvation of CO_2 in the same RTIL, where a minimum PMF value is observed at the interfacial region, which is indicative of the interfacial activity of CO_2. The average PMF in the bulk region can be used to estimate the free energy of solvation, giving a value ~-1.3 kcal/mol for H_2O. In a recent study, we examined the transport of a single H_2O molecule across [bmim][BF_4] and [bmim][PF_6] liquid/vapor interfaces and found more negative solvation free energies for H_2O in both ionic liquids. These results are consistent with the hydrophobic properties of the anions. [Tf_2N] is considered to be a more hydrophobic anion, leading to a lower H_2O solubility and a smaller negative solvation free energy in [bmim][Tf_2N]. Even though the PMFs of H_2O molecules exhibit the same monotonic decay from the vapor phase into liquid phase, some subtle differences are observed. At the air-[bmim][BF_4] interface, the free energy decays further into the bulk region, while the free energy is similar both at the interface and in the bulk at the air-[bmim][PF_6] and air-[bmim][Tf_2N] interfaces. This result may be attributed to strong interactions between the H_2O molecule and the [BF_4] anion. Because the [BF_4] anion is present in higher concentrations when it is more than 5 Å from the GDS of the air/[bmim][BF_4] interface towards the liquid bulk (as indicated by the number density profile), the free energy of H_2O reaches the bulk value in this region and increases as the H_2O molecule moves towards the air. These simulation results clearly demonstrate that the anion has pronounced effects in these systems and shape our understanding of gas dissolution and transport mechanism in the bulk, as well as the surface processes in these ionic liquids. In this work, we briefly report recent advances in theory and experiments that shed light on gas sorption processes in RTILs. However, many aspects of these processes are not fully understood, making this an exciting time for collaborations to further explore the molecular solvation of interfacial processes.

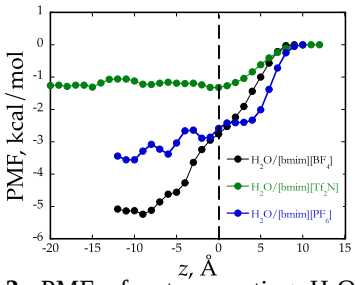

Figure 3. PMFs for transporting H_2O across the [bmim][Tf_2N], [bmim][BF_4] and [bmim][PF_6] liquid/air interfaces.

Future Direction and Outlook. RTILs are versatile, tunable, and reasonably economical solvents for CO_2 capture and sequestration. Computational simulations were undertaken to provide molecular-level information and improve our understanding of gas sorption and selectivity in RTILs. However, most of the studies have been restricted to such processes in neat RTILs. In the capture of CO_2 from flue gas, H_2O often is absorbed, creating a humid condition. Therefore, it would be desirable to understand the effect of H_2O on gas sorption and selectivity. Because

the gas solute first needs to cross the interface before it can be absorbed into the liquid, we plan to investigate the molecular structures and properties of the vapor/liquid interface of ionic-liquid/H_2O mixtures. Depending on where the H_2O molecules reside and the mutual interaction between the gas and H_2O, the gas solubility and selectivity can be modified. We will further examine the influence of varying H_2O content on the free energies associated with a gas solute crossing the interface. Additionally, certain amines can react with CO_2 to form carbamate salts. In the future, we hope to add functional amines into the RTILs and examine their impact on gas solubility and interfacial properties. Molecular simulation provides a valuable tool for obtaining molecular-level information of all of these processes.

Previous work on the RTIL-based CO_2 capture technique has established that both the anion-CO_2 interaction and the entropic free volume play important roles in determining CO_2 solubility and selectivity. Computer simulations have started examining the influence of anions on the interfacial properties of RTILs and the gas sorption process at the RTIL/air interface. Further studies to include other anions may be warranted. It will be informative to examine the role that the cations play in the sorption process. Other types of RTILs, such as phosphonium or ammonium salts, should also be considered to address the effect of the alkyl chain length of the imidazolium cation on the solubility or the interfacial activity. Given the complex nature of the gas sorption process, additional simulation studies will be required to develop a molecular-level understanding of the mechanism of these processes.

References to publications of DOE sponsored research (2010-Present)

1. The Behavior of NaOH at the Air-Water Interface: A Computational Study. Wick CD, Dang LX. *J. Chem. Phys.*, 133, 024705 **(2010)**.

2. Interpreting Vibrational Sum-Frequency Spectra of Sulfur Dioxide at the Air/Water Interface: A Comprehensive Molecular Dynamics Study. Baer M, Mundy CJ, Chang TM, Tao FM, Dang LX. *J. Phys. Chem.* B, 114, 7245-7249 **(2010)**.

3. Grand Canonical Monte Carlo Studies of CO_2 and CH_4 Adsorption in p-tert-Butylcalix[4]Arene. Daschbach JL, Sun XQ, Thallapally PK, McGrail BP and Dang LX, *J. Phys. Chem.* B, 114, 5764-5768 **(2010)**.

4. Computational Investigation of the Influence of Organic-Aqueous Interfaces on NaCl Dissociation Dynamics. Wick CD, Dang LX. *J. Chem. Phys.*, Volume: 132 Issue: 4 Article Number: 044702 **(2010)**.

5. Probing the Hydration Structure of Polarizable Halides: A Multi-Edge XAFS and Molecular Dynamics Study of the Iodide Anion. Fulton, John; Schenter, Gregory; Baer, Marcel; Mundy, Christopher; Dang, Liem; Balasubramanian, Mahalingam. *J. Phys. Chem.* B 114, 12926-12937 **(2010)**.

6. Structure and Dynamics of N, N-Diethyl-N-Methyl Ammonium-Triflate Ionic Liquid, Neat and with Water from Molecular Dynamics Simulations. Chang, Tsun; Dang, Liem; Devanathan, Ram; Dupuis, Michel. *J. Phys. Chem.* B 114, 12764-12774 **(2010)**.

7. Molecular Mechanism of CO_2 and SO_2 Molecules Binding to the Air/Liquid Interface of 1-Butyl-3-methylimidazolium Tetrafluoroborate Ionic Liquid: A Molecular Dynamics Study with Polarizable Potential Models. Wick, Collin; Chang, Tsun-Mei; Dang, Liem. *J. Phys. Chem*. B 114, 14965-14971 **(2010)**. (**Journal Cover**)

8. Computational Study of Ion Distributions at the Air/Liquid Methanol Interface" Sun, Xiuquan; Wick, Collin; Dang, Liem. *J. Phys. Chem*. A 115, 5767-5773 (**2011**).

9. Computational Study of Hydrocarbon Adsorption in Metal–Organic Framework Ni_2(dhtp). Sun XQ, Wick CD, Thallapally PK, Dang, Liem; McGrail, Benard. *J. Phys. Chem*. B, 115, 2842-2849 **(2011)**.

10. Molecular Mechanism of Hydrocarbons Binding to the Metal-Organic Framework. Sun XQ, Wick CD, Thallapally, PK, Dang, Liem; McGrail, Benard; *Chemical Physics Letters*, 501, 455-460 **(2011)**.

11. Molecular Mechanism of Gas Adsorption into Ionic Liquids: A Molecular Dynamics Study. Dang Liem and Chang, Tsun-Mei, *J. Phys. Chem. Letters,* 3, 175-181 (**2012**). (**Journal Cover**)

12. Molecular Mechanism of Specific Ion Interactions between Alkali Cations and Acetate Anion in Aqueous Solution: A Molecular Dynamics Study. Annapureddy Harsha V. R.; Dang Liem X. *J. Phys. Chem.* 116, 7492-7498 (**2012**).

13. Note: Interionic Potentials of Mean Force for Ca2+-Cl- in Polarizable Water. Dang Liem X.; Tai Ba Truong; Ginovska-Pangovska Bojana. *J. Chem. Phys.,* 136, 126101 (**2012**).

14. Quantitative Analysis of Aqueous Nanofilm Rupture by Molecular Dynamic Simulation. Peng Tiefeng; Nguyen Anh V.; Peng Hong; Tsun-Mei Chang and Liem X. Dang, *J. Phys. Chem.* B, 116, 1035-1042 (**2012**).

15. Development of Ions-TIP4P-Ew Force Fields for Molecular Processes in Bulk and at the Aqueous Interface using Molecular Simulations. Tiefeng Peng, Tsun-Mei Chang, Xiuquan Sun, Anh V. Nguyen, Liem X. Dang, *J. Mol. Liqs.* 173, 47–54 (**2012**).

Transition Metal-Molecular Interactions Studied with Cluster Ion Infrared Spectroscopy

DE-FG02-96ER14658

Michael A. Duncan

Department of Chemistry, University of Georgia, Athens, GA 30602

maduncan@uga.edu

Program Scope

Our research program investigates gas phase metal clusters and metal cation-molecular complexes as models for heterogeneous catalysis, metal-ligand bonding and metal cation solvation. The clusters studied are molecular sized aggregates of metal or metal oxides. We focus on the bonding exhibited by "physisorption" versus "chemisorption" on cluster surfaces, on metal-ligand interactions with benzene or carbon monoxide, and on solvation interactions exemplified by complexes with water, acetonitrile, etc. These studies investigate the nature of the metal-molecular interactions and how they vary with metal composition and cluster size. To obtain size-specific information, we focus on ionized complexes that can be mass selected. Infrared photodissociation spectroscopy is employed to measure the vibrational spectroscopy of these ionized complexes. The vibrational frequencies measured are compared to those for the corresponding free molecular ligands and with the predictions of theory to reveal the electronic state and geometric structure of the system. Experimental measurements are supplemented with calculations using density functional theory (DFT) with standard functionals such as B3LYP or BP86.

Recent Progress

The main focus of our recent work has been infrared spectroscopy of transition metal cation-molecular complexes with carbon monoxide or water, e.g., $M^+(CO)_n$ and $M^+(H_2O)_n$. These species are produced by laser vaporization in a pulsed-nozzle cluster source, size-selected with a specially designed reflectron time-of-flight mass spectrometer and studied with infrared photodissociation spectroscopy using an IR optical parametric oscillator laser system (OPO). In studies on complexes of a variety of transition metals, we examine the shift in the frequency for selected vibrational modes in the adsorbate/ligand/solvent molecule that occur upon binding to the metal. The number and frequencies of IR-active modes reveal the structures of these systems, while sudden changes in spectra or dissociation yields reveal the coordination number for the metal ion. In some systems, new bands are found at a certain complex size corresponding to intra-cluster reaction products. In small complexes with strong bonding, we use the method of rare gas "tagging" with argon or neon to enhance dissociation yields. In all of these systems, we employ a close interaction with theory to investigate the details of the metal-molecular interactions that best explain the spectroscopy. We perform density functional theory (DFT) calculations (using Gaussian 03W or GAMESS) and when higher level methods are required, we collaborate with theorists (e.g., Prof. Laura Gagliardi, Minnesota). Our infrared data on these metal ion-molecule complexes provide many examples of unanticipated structural and dynamical information. A crucial aspect of these studies is the infrared

laser system, which is an infrared optical parametric oscillator/amplifier system OPO/OPA; Laser Vision). This system covers the infrared region of 600-4500 cm^{-1} with a linewidth of ~1.0 cm^{-1}.

$M^+(H_2O)_n$ complexes and those tagged with argon have been studied previously in our lab for a number of the first-row transition metals. Over the past year or so, we have extended these studies to additional metals and particularly have been able to make doubly charged metal-water complexes for comparison to the corresponding singly charged systems. In the vanadium system, we have studied multiple water complexes. Hydrogen bonding bands appear for the first time for the complex with five water molecules, establishing that four water molecules is the coordination for V^+. Similar measurements establish that the coordination of Zn^+ is three waters. Silver, scandium and chromium complexes were rotationally resolved, providing the H-O-H bond angle in these systems. We have been able to produce multiply charged transition metal cation-water complexes for chromium, manganese, scandium and niobium systems tagged with multiple argons. IR spectra of these systems have very different intensity patterns and O-H shifts than those for the singly charged systems, and we are able to study the charge dependence of the cation-water interaction. We find that O–H stretch vibrations are more red-shifted for the doubly charged complexes, the symmetric stretch vibration gains additional IR intensity compared to the asymmetric stretch, and the H-O-H bond angle expands more for the doubly charged complexes. All of these effects are attributed to the added polarization on the water molecule coming from the higher charged ion.

Transition metal carbonyls provide classic examples of metal-ligand bonding, and carbon monoxide is the classic probe molecule for surface science and catalysis. We have investigated transition metal cation carbonyls to compare these to corresponding neutral carbonyls known to be stable. The stability of these systems is conveniently explained with the 18-electron rule, and this is a guiding principle for our cation work. We studied the $Co^+(CO)_n$ complexes, for which the n=5 species is isoelectronic to neutral $Fe(CO)_5$, and the $Mn^+(CO)_n$ system, for which the n=6 complex is isoelectronic to $Cr(CO)_6$. In both cases, the cation complexes had a filled coordination at the expected n=5 and 6 complexes, respectively, and they had the same structures as the corresponding neutrals (trigonal pyramid and octahedral). However, the frequencies of the CO stretch vibrations, which are strongly red-shifted in the neutrals, were hardly shifted at all for the cations. This trend was attributed to the reduced π back-bonding in the cation systems. We also studied the $Cu^+(CO)_n$ complexes, for which the n=4 species is isoelectronic to neutral $Ni(CO)_4$. Again, the n=4 complex has a closed coordination, with the expected tetrahedral structure. Unlike the nickel complex, but similar to the gold system, the copper complex has a blue-shifted carbonyl stretch, consistent with the behavior for so-called "non-classical" carbonyls.

A longstanding goal in inorganic chemistry has been to test the limits of the 18-electron rule in situations requiring unusual coordination numbers. Early transition metals with fewer *d* electrons need more carbonyls to achieve a closed-shell configuration. Specifically, the vanadium group cations (d^4) need seven carbonyls. We therefore made and studied the carbonyl cations of V, Nb and Ta. We found that vanadium did not produce the seven-coordinate (7-C) carbonyls, but instead formed a 6-C complex (even though DFT predicted the 7-C complex to be stable). Nb^+ produced both 6-C and 7-C carbonyls, while the tantalum cation formed only the desired 7-C species, providing the first example of a 7-C all-carbonyl complex. Apparently, the size of the ion and its growth mechanism are both important in such a system. Scandium, titanium, zirconium and hafnium cations, which all have fewer still *d* electrons, also formed carbonyls with a coordination of only six. However, the red shift of the carbonyl stretch was

found to be greatest for hafnium. Although rhodium is isoelectronic to cobalt, the $Rh(CO)_n^+$ complexes were found to have a primary coordination number of four, with a square-planar structure for the n=4 species.

In an unusual example of metal-carbonyl interactions, we studied the uranium system, using a depleted rod sample. Uranium carbonyls were formed easily and found to dissociate efficiently upon infrared excitation. In addition to the $U^+(CO)_n$ species, we also detected $UO_2^+(CO)_n$ complexes. We found that the uranium carbonyls have red-shifted CO stretch vibrations, whereas the oxides have blue-shifted vibrations. The fragmentation behavior and spectral patterns confirmed that the $U^+(CO)_8$ ion is the fully coordinated species, and the spectrum for this ion was consistent with a square antiprism structure predicted by theory. The $UO_2^+(CO)_5$ species was the fully coordinated oxide carbonyl, and its spectrum is consistent with the D_{5h} structure predicted by theory (five equivalent CO's around the UO_2^+ waist). In the course of this work, we also found uranium complexes with multiple oxygens attached. Spectra for UO_4^+ and UO_6^+ showed that each contained a UO_2 core with one η^2 coordinated "superoxide" O_2 ligand. Professor Laura Gagliardi (Univ. of Minnesota) collaborated with us on these uranium systems.

Extending the metal carbonyl work, we examined metal *oxide* carbonyls, i.e., $VO^+(CO)_n$ and $VO_3(CO)_n$. We found that the coordination of VO^+ is five CO's, while that of VO_3^+ is three. The carbonyl stretching frequencies in these systems are less shifted than in the V^+ carbonyl complex. The VO^+ system has a CO stretch that is virtually unshifted with respect to free CO, while the VO_3^+ carbonyl stretches are blue shifted. Increased oxidation apparently leads to reduced available *d* electron density and consequently less back-bonding.

Previous work in our lab had identified intracluster reactions in several metal ion complexes with CO_2, i.e., $M^+(CO_2)_n$ (M=V, Ni, Mg, Al) Vibrational bands in the asymmetric stretch region of CO_2 (near 2350 cm^{-1}) were assigned to coordinated CO_2 in the small clusters (n=1-4) and other bands were assigned to second sphere ligands in the slightly larger clusters (n=5-7). In larger clusters still, however, new bands grew in suggesting that the core ion identity had somehow changed, producing a different environment for some CO_2 ligands. We speculated that the reaction might be the formation of an oxide-carbonyl species, which would have the same mass as the selected $M^+(CO_2)_n$ species, but at that time we could not scan the lower frequency region of the spectrum to investigate this further. Recently, using the new longer wavelength coverage of our IR system, we scanned this region for the $V^+(CO_2)_n$ system. We also intentionally produced the oxide carbonyl species of the form $VO^+(CO)_n$ (see above) to see where the carbonyl and oxide stretches for these systems would come. The lower frequency region of the spectrum also had new bands appearing at the same critical cluster size seen before, but the bands were not those of an oxide carbonyl. Instead, we found that the intracluster reaction had produced an oxalate species in the cluster by coupling two CO_2 molecules in the second sphere (remote from the metal).

Future Plans

Continuing the work above, we will focus future efforts on doubly charged metal-water complexes, and we will include metal-acetonitrile complexes which might stabilize higher charge states more effectively. Metal carbonyl work will attempt to extend the atomic complex studies to diatomic and triatomic metal species. Metal-benzene and metal-CO_2 studies will employ the long wavelength laser coverage to examine higher resolution spectroscopy in these systems and to further elucidate the intracluster reaction systems for other metals.

Publications (10/1/2009–present) for this Project

1. Z. D. Reed and M. A. Duncan, "Infrared spectroscopy and structures of manganese carbonyl cations, $Mn(CO)_n^+$ (n=1-9)," *J. Am. Soc. Mass Spectrom.* **21**, 739-749 (2010). **DOI:** 10.1016/j.jasms.2010.01.022

2. A. M. Ricks, L. Gagliardi and M. A. Duncan, "Infrared spectroscopy of extreme coordination: The carbonyls of U^+ and UO_2^+," *J. Am. Chem. Soc.* **132**, 15905-15907 (2010). **DOI:** 10.1021/ja1077365

3. P. D. Carnegie, B. Bandyopadhyay and M. A. Duncan, "Infrared spectroscopy of $Sc^+(H_2O)$ and $Sc^{2+}(H_2O)$ via argon complex predissociation: The charge dependence of cation hydration," *J. Chem. Phys.* **134**, 014302-1 to 014302-9 (2011). **DOI:** 10.1063/1.3515425

4. M. A. Duncan, "IR spectroscopy of gas phase metal carbonyl cations," *J. Mol. Spec.* **266**, 63-74 (2011) (invited feature article; cover art). **DOI:**10.1016/j.jms.2011.03.006

5. B. Bandyopadhyay, P. D. Carnegie, and M. A. Duncan, "Infrared spectroscopy of $Mn^+(H_2O)_n$ and $Mn^{2+}(H_2O)$ complexes via argon complex predissociation," *J. Phys. Chem. A* **115**, 7602-7609 (2011). **DOI:** 10.1021/jp203501n.

6. A. M. Ricks, L. Gagliardi and M. A. Duncan, "Oxides and superoxides of uranium detected by IR spectroscopy in the gas phase," *J. Phys. Chem. Lett.* **2**, 1662-1666 (2011). **DOI:** 10.1021/jz2006868.

7. A. D. Brathwaite, Z. D. Reed and M. A. Duncan, "Infrared spectroscopy of copper carbonyl cations," *J. Phys. Chem. A* **115**, 10461-10469 (2011). **DOI:** 10/1021/jp206102z.

8. J. D. Mosley, T. C. Cheng, S. Hasbrouck, A. M. Ricks and M. A. Duncan, "Electronic Spectroscopy of Co^+-Ne via Mass-selected Photodissociation," *J. Chem. Phys.* **135**, 104309-1 to 104309-6 (2011). **DOI:** 10.1063/1.3633472.

9. A. D. Brathwaite and M. A. Duncan, "Infrared spectroscopy of $Si(CO)_n^+$ complexes: Evidence for asymmetric coordination," *J. Phys. Chem. A* **116**, 1375-1382 (2012). **DOI:** 10.1021/jp211578t.

10. R. Garza-Galindo, M. Castro and M. A. Duncan, "Theoretical study of nascent hydration in the $Fe^+(H_2O)_n$ system," *J. Phys. Chem. A* **116**, 1906-1913 (2012). **DOI:** 10.1021/jp2117533l.

11. B. Bandyopadhyay and M. A. Duncan, "Infrared spectroscopy of $V^{2+}(H_2O)$ complexes," *Chem. Phys. Lett.* **530**, 10-15 (2012). **DOI:** 10.1016/j.cplett.2012.01.048.

12. M. A. Duncan, "Laser Vaporization Cluster Sources," *Rev. Sci. Instrum.* **83**, 041101/1-19 (2012)(invited review). Selected for April 23, 2012 issue of *Virtual Journal of Nanoscale Science & Technology*, published by AIP.

13. A. M. Ricks, A. D. Brathwaite and M. A. Duncan, "Spin states and coordination of $V^+(CO)_n$ clusters revealed by IR spectroscopy," *J. Phys. Chem. A*, in press (2012). **DOI:** 10.1021/jp301679m. Final publication pending, P. B. Armentrout Festschrift.

Electronic Structure and Reactivity Studies for Aqueous Phase Chemistry

Michel Dupuis
Chemical and Materials Sciences Division
Pacific Northwest National Laboratory, Richland WA
michel.dupuis@pnnl.gov

Program scope: We are broadly interested in charge and ion transport in complex molecular environments for chemistries relevant to the DOE. For this research we use *ab initio* electronic structure, dynamics, and classical simulation methods. Our recent efforts have focused on protons. Proton movement and transport play key roles in the inter-conversion of chemical and electrical energies. Specifically for this CPIMS program, our current focus is on amine-based protic ionic liquids. Brønsted acid-base ionic liquids based on alkyl-substituted amines are in fact being considered as possible water-free proton exchange membranes for low-temperature fuel cells. In this context we are interested in characterizing the proton transport capabilities of this type of ionic liquids. Because of the accepted belief that proton transport is critically dependent on the level of hydration in the molecular environment, proton transport in ionic liquids is an intriguing theoretical challenge. The inherent complexity of the process (*e.g.*, a combination of vehicular and Grotthuss mechanisms in an aqueous environment), the morphology of the environment, the level of hydration, and the multiple length and time scales involved all contribute to the difficulty of this problem.

Recent progress: *Proton transport in ammonia-water mixtures (with Bojana Ginovska-Pangovska and Liem Dang)*

Polymer gel electrolytes based on a polymer infused with protic ionic liquids have been the focus of emerging experimental research about proton membranes for fuel cell applications [1-2]. Nakamoto and Watanabe [2] have identified triflic acid (TfOH) and diethyl methyl amine (*dema*) as the ionic liquid denoted *dema-IL* (with ion pairs TfO^-/dema-H^+) with the greatest potential for PEMFC applications under anhydrous conditions at 150 ºC based on an analysis of thermal properties and ionic conductivity. However the level of understanding of proton transport in such systems is limited [3].

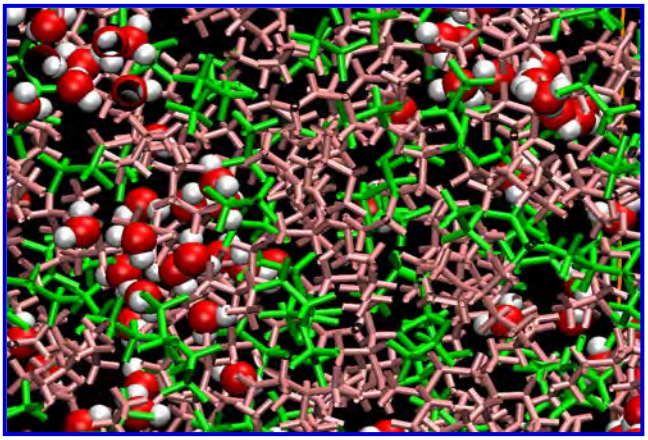

Fig. 1 Close-up snapshot of dema-IL-water mixture for mole fraction x_W=0.20. The dispersed water molecules can be seen; a layered structure stands out, with pink layers of $[Tfl]^-$ and green layers of $[dema]^+$. T.M. Chang *et al.* J. Phys. Chem . A 114, 12764 (2010)

Proton transport in aqueous environments combines vehicular transport of H_3O^+ with the Grotthuss mechanism that gives rise to the unusually high diffusion of the proton in aqueous media. In contrast, it is known that structural deformation of the Grotthuss mechanism does not take place in neat ammonia [4-5]. Furthermore the similarity between the proton NMR signals and nitrogen NMR signals suggest that proton transport is mostly vehicular, and that diffusion of deprotonated amines (after O_2 reduction at the cathode) is also involved in the global charge transport process. Older work by Meiboom et al. [6-7] showed that water catalyzes proton transfer in ammonium/amine mixtures. Thus it is of interest to investigate in detail the dynamics of proton transfer in ammonium-amine-water mixtures. Questions of

interest are: (*i*) What is the diffusion rate of neutral amines in the ionic liquid? (*ii*) How do trace amounts of water affect the structure of the ionic liquid? (*iii*) Is the water miscible? (*iv*) Does water affect the diffusion of ammonium ions and neutral amines? (*v*) Does water influence proton transport? (*vi*) How fast do the rates of diffusion change with temperature?

We are currently extending our work on the structure on *dema*-IL-water mixtures [8] to carry out systematic investigations of proton dynamics in ammonium-ammonia-water mixtures using ab initio molecular dynamics simulations.

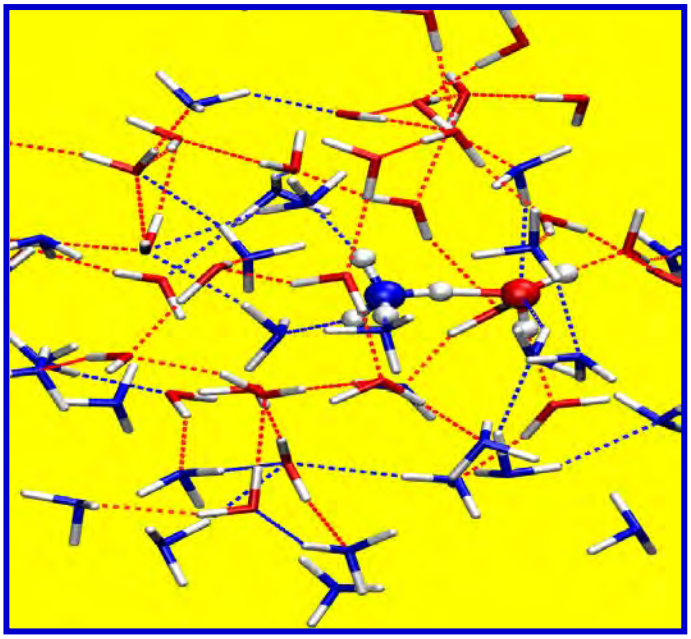

Fig. 2 Snapshot of an ab initio MD simulation of one excess proton in a water-ammonia mixture showing the proton transferring between a water molecule and an ammonia molecule.

1. Sekhon, S. S., P. Krishnan, et al. (2006). "Proton conducting membrane containing room temperature ionic liquid." Electrochimica Acta **52**(4): 1639-1644.
2. Nakamoto, H. and M. Watanabe (2007). "Bronsted acid-base ionic liquids for fuel cell electrolytes." Chemical Communications(24): 2539-2541.
3. S.-Y. Lee, T. Yasuda, and M. Watanabe, "Fabrication of protic ionic liquid/sulfonated polyimide composite membranes for non-humidified fuel cells," *Journal of Power Sources* **195**, 5509 (2010).
4. Baldwin, J., J. Evans, et al. (1971). "Solutions of electrolytes in liquid ammonia. 6. mean molal ion activity coefficients and ion transference numbers of ammonium iodide", Journal of the Chemical Society a -Inorganic Physical Theoretical(21): 3389
5. Y. Liu and M. E. Tuckerman, "Protonic defects in hydrogen bonded liquids: structure and dynamics in Ammonia and comparison with water," *Journal of Physical Chemistry B* **105**, 6598 (2001).
6. Z. Luz and S. Meiboom, "Nuclear Magnetic Resonance Study of the Protolysis of Trimethylammonium ion in aqueous solution – Order of the reaction with respect to solvent," *Journal of Chemical Physics* **39**, 366 (1963).
7. A. Loewenstein and S. Meiboom, "Rates and mechanisms of protolysis of di- and trimethylammonium ions studied by proton magnetic resonance", *Journal of Chemical Physics* **27**, 1067 (1957).
8. T.M. Chang, L. Dang, R. Devanathan, **M. Dupuis**, "Structure and Dynamics of N, N-Diethyl-N-Methyl Ammonium-Triflate Ionic Liquid, Neat and with Water, from Molecular Dynamics Simulations", J. Phys. Chem . A 114, 12764 (2010).

References to publications of DOE Chemical Physics sponsored research (2010-present)

1. D. M. Camaioni, B. Ginovska, **M. Dupuis**, "Modeling the Reaction of Zero-Valent Fe with CCl4", J. Phys. Chem. C 113, 1830 (2009). (cover)
2. T.M. Chang, L. Dang, R. Devanathan, **M. Dupuis**, "Structure and Dynamics of N, N-Diethyl-N-Methyl Ammonium-Triflate Ionic Liquid, Neat and with Water, from Molecular Dynamics Simulations", J. Phys. Chem . A 114, 12764 (2010).
3. B. Ginovska, D. M. Camaioni, and **M. Dupuis**, About the Barriers to Reaction of CCl4 with HFeOH and FeCl2 , J. Phys. Chem. A 115, 8713 (2011).

Photochemistry at Interfaces

Kenneth B. Eisenthal
Department of Chemistry
Columbia University
New York, NY 10027
kbe1@columbia.edu

Program Scope

The objective of the program is to increase knowledge of the chemical and physical properties, both equilibrium and time dependent, of liquid interfaces.

Recent Progress

Dynamics of Excited State Electron Transfer at a Liquid Interface Using Time-Resolved Sum Frequency Generation

Femtosecond time resolved vibrational sum frequency generation has been used for the first time to probe a chemical reaction of interfacial molecules pumped into their excited electronic states. The ultrafast dynamics of electron transfer from ground state N,N-dimethylaniline (DMA) to photoexcited coumarin 314 (C314) at a water/DMA monolayer interface was obtained. Because of the immiscibility of DMA and water, the DMA molecules are at the interface and translational diffusion of interfacial C314 and DMA is not required. As a consequence translational diffusion of the reactants does not contribute to the observed dynamics. The electron transfer process was monitored by detection of the C314 carbonyl SFG signal. The time constant of the forward electron transfer process was found to be 16 ± 2ps, which is approximately twice as fast as the forward electron transfer of a closely related on photoexcitation of a closely related coumarin in bulk DMA. The faster rate at the interface is attributed to the interface having a lower polarity than bulk DMA; this is supported by the measured blue shift of C314 at the interface in the presence of DMA with respect to the spectrum of C314 in bulk DMA. As a consequence of the lower polarity it is surmised that the free energy of reorganization is smaller at the interface, which would favor a faster electron transfer at the interface. It is concluded, on comparing the electron transfer rates at the interface and bulk DMA that the free energy of reorganization dominates the electronic coupling factor that could favor a faster rate in bulk DMA because there are more DMA molecules surrounding C314 in the bulk liquid. The back electron transfer process in which an electron is returned from the C314 radical anion to the DMA radical cation was found to have a time constant of 174 ± 21 ps. There was no evidence that the frequency of the ring –C=O stretch vibration was different in excited state C314 from its value in ground state C314. To our knowledge, this is the first time-resolved SFG experiment to examine electron transfer at a liquid interface.

Excited state energy relaxation at a colloidal microparticle/water interface

The excited-state relaxation dynamics of molecules adsorbed to the surface of colloidal microparticles suspended in water have been measured for the first time using time-resolved second harmonic generation. The S_1 excited-state lifetime of malachite green at the surface of negatively charged polystyrene sulfate microparticles suspended in water has been determined to be 5.7 ± 0.4 ps. This lifetime is longer than the corresponding results at the air/water and alkane/water interfaces by a factor of two and three, and is within experimental error of the MG lifetime at the water/silica interface, which is also negatively charged. The excited state relaxation involves torsional motions of the phenyl

and anilino groups attached to the central carbon, which bring about the change in structure required for transition from the excited state potential energy surface to the ground electronic state where the phenyl and anilino groups are in a "propeller orientation" with respect to each other. The attractive interaction between the positively-charged MG and the negatively-charged polystyrene sulfate could impose a thermodynamic restriction on the orientation of MG, and thus restrict the orientations of the phenyl and anilino groups, which would inhibit the torsional motions necessary for the energy relaxation process. The rigidity of the polystyrene and silica surfaces may limit the torsional motions required for relaxation, whereas the absence of a rigid interface for the air/water and alkane/water interfaces permits a more rapid relaxation. Although the charged colloidal particle creates a significant electric field that extends into the water solution, our calculations based on our measurements of the colloid surface charge density, the known viscoelectric constant of water, and the low electrolyte concentration, indicate that the viscosity increase in the interfacial water is negligible. We therefore conclude that the slower decay of excited state MG at the colloid/water interface is not due to an increased local friction arising from the interfacial the orientation of molecules at interfaces is

Molecular Orientational Distribution at Interfaces Using Pump-Probe SHG

At the present time the orientation of interfacial molecules is obtained from measurement of the intensities of two linear polarization combinations. From a single measurement one cannot obtain both the average orientation and the orientational distribution. It is typically assumed that the distribution is a delta function. In any case the polarization measurements can be described by an orientation parameter $R_{eq} = <\cos\theta>_{\rho g}/<\cos^3\theta>_{\rho g}$ where the brackets indicate the average for the equilibrium ground state orientational distribution. To fit our data to an orientational distribution function, e.g. a Gaussian distribution, requires two variables. They are the mean orientational angle and a quantity σ, which is related to the full width at half-maximum. In order to obtain these two parameters requires two independent measurements. The second measurement is for an equilibrium distribution that is perturbed by a circularly polarized pump pulse that is incident normal to the interface. By using this arrangement the equilibrium in plane isotropic orientational distribution is not perturbed. The perturbed ground state distribution is directly dependent on the probability of excitation of a molecule whose transition dipole makes an angle $90^0 - \theta$ with the interface normal, i.e. $|\mu \cdot E_c|^2$. Measurements of two polarization combinations immediately after the pump pulse yields a second measured parameter

$$R_{(t=0)} = <\cos^3\theta>_{\rho g}/<\cos^5\theta>_{\rho g}$$

It is to be noted that the interfacial molecules, both ground and excited state have not reoriented during the time of the measurements because the time scale for reorientation of aromatic molecules at the air/water interface has been shown in our laboratory to be several hundred picoseconds. The fitting of the two measurements of the organic dye molecule, coumarin 314, at the air/water interface, to a Gaussian distribution, yields a mean angle of 55^0 and a full width at half maximum of 16^0. The method we have used can be applied to other two variable orientational distributions. For example, using the wobbling in a cone model to describe orientational diffusion at an interface, we found the tilt angle of

the cone relative to the interface normal, and the half –cone angle, which is the mean of the angle from one side of the cone to the center. Interestingly the results are very close to those we obtained from a Gaussian model.

Competitive Adsorption at the Air/Water Interface

The coexistence of surface active organics at the air/water interface significantly changes the chemical and physical properties of the interface. Measurement of the population and adsorption free energy of a single species in the presence of others in a complex mixture is not straight forward. Surface tension measurements can yield the surface excess but not identify the composition of the interface. We have used SHG to selectively measure the competitive adsorption of the aromatic dye molecule, coumarin 314, with acetonitrile at the air/water interface. C314 is an aromatic molecule containing carbonyl, ethyl ester, lactone groups, and C≡N bonds, which can be viewed as a model for environmental humic – like substances. By tuning the incident light frequency to achieve resonance of the second harmonic frequency with the $S_0 \rightarrow S_1$ transition in C314 enabled us to differentiate it from acetonitrile whose electronic transitions are in the far UV, and as a consequence its contribution to the SHG intensity is negligible. The displacement of interfacial C314 by acetonitrile was manifested by a decrease in the SHG intensity. The experimental findings are well represented by a Frumkin – Fowler – Guggenheim model, which is basically a Langmuir model that includes lateral interactions. With this model we obtained the free energies of adsorption of C314 and acetonitrile for a range of different C314 and acetonitrile concentrations. It was found that the C314 – acetonitrile interactions were weak, whereas attractive interactions among C314 molecules were obtained using the FFG model. A possible factor in these attractive interactions, are dipole-dipole interactions between C314 molecules, noting that the C314 dipole moment is large, 8 Debye. If the orientation of the C314 molecules was closer to being normal to the interface, the interaction would be repulsive. However if the orientation was closer to parallel to the interface the interaction would be attractive. Using our orientational measurements of C314 at the air/water interface we find the interactions would be attractive between two dipoles oriented at 55^0 with respect to the interface normal.

Interfacial Population and Organization of Surfactants with SFG and Surface Tension

The complementery interface sensitive methods of sum frequency generation (SFG) and surface tension have been used in our lab to investigate the surface reorganization of a tailor made surfactant at the air/water interface. SFG yields information on the density and orientation of surfactants at the interface, whereas surface tension yields information on the surface excess of surfactants, which is not their interfacial density. The rapid rise in the SFG signal to its maximum value at 1mM, which remained essentially constant thereafter, was attributed to the formation of large surfactant domains. Above 1mM the domains, all of which have the same density, dominated the SFG signal. As a consequence, the SFG signal remained essentially constant. The surface excess had an equally rapid rise to its maximum value at 1mM, which remained constant until reaching a concentration of 3mM where it dropped to a zero value, indicating that a full surfactant monolayer

had been formed. This coincides with the formation of bulk micelles, which is commonly referred to as the critical micelle concentration. The orientation of the surfactant carbonyl chromophore was obtained from polarization measurements of the SFG signal, and showed a small change above a 1mM concentration. The SFG results and the surface tension results, though inherently different, were found to be consistent and useful.

Publications : 2010 - 2012

Rao, Y.; Xu, M; Jockusch, S; Turro, N.J. and Eisenthal, K.B., **Dynamics of Excited State Electron Transfer at a Liquid Interface Using Time-Resolved Sum Frequency Generation,** Chemical Physics Letters, 2012**,** in press **(selected as frontier article**).

Haber, L. H. and Eisenthal, K.B., **Molecular Excited-State Relaxation Dynamics at the Colloidal Microparticle/WateInterface Monitored with Pump-Probe Second Harmonic Generation,** submitted to Journal of Physical Chemistry B, 2012.

Rao, Y.; Hong, S. Y.; Turro, N. J.; Eisenthal, K. B., **Molecular Orientational Distribution at Interfaces Using Second Harmonic Generation**. Journal of Physical Chemistry C 2011**,** *115* (23), 11678-11683.

Haber, L. H.; Kwok, S. J. J.; Semeraro, M.; Eisenthal, K. B., **Probing the colloidal gold nanoparticle/aqueous interface with second harmonic generation.** Chemical Physics Letters 2011**,** *507* (1-3), 11-14.

Sahu, K.; Eisenthal, K. B.; McNeill, V. F., **Competitive Adsorption at the Air-Water Interface: A Second Harmonic Generation Study.** Journal of Physical Chemistry C 2011**,** *115* (19), 9701-9705.

Rao, Y.; Li, X.; Lei, X. G.; Jockusch, S.; George, M. W.; Turro, N. J.; Eisenthal, K. B., **Observations of Interfacial Population and Organization of Surfactants with Sum Frequency Generation and Surface Tension.** Journal of Physical Chemistry C 2011**,** *115* (24), 12064-12067

Sahu, K.; McNeil,V. Faye,; Eisenthal, K.B.; **Effect of Salt on Adsorption Affinity of an Aromatic Carbonyl Molecule to the Air/Aqueous Interface : Insight for Aqueous Environmental Interfaces.** Journal of Physical Chemistry C 2010, 114(42), 18258-18262

Future Plans

Femtosecond SHG and SFG studies of the chemical and physical channels for energy redistribution and degradation by interfacial molecules pumped into excited electronic states. Apply these nonlinear spectroscopic methods to both planar and nano-microparticle liquid interfaces.

The research described in the above publications was supported, in part by NSF and DTRA. The NSF support was chiefly equipment and J.Roscioli, the DTRA was supplies, and DOE chiefly supported Yi Rao and Sung -Young Hung. Although the objectives of the research supported by the three agencies are different the research is leveraged by their support.

Time Resolved Optical Studies on the Plasmonic Field Effects on Bacteriorhodopsin Proton Pump Function and Other Light-Harvesting Systems

Mostafa A. El-Sayed
School of Chemistry and Biochemistry, Georgia Institute of Technology
Atlanta, GA 30332
melsayed@gatech.edu

Program Scope

Bacteriorhodopsin is the light-transducing membrane protein found in two-dimensional crystalline patches of the purple membrane, or PM, of *Halobacterium halobium*. This light-driven proton pump moves protons from the cytoplasmic to the extracellular side of its membrane via a series of isomerizations of its interior retinal chromophore and thermodynamic relaxations of its alpha helices. Under continuous wavelength (cw) illumination, bR exhibits a stationary photocurrent as it transforms light energy into electrochemical energy in the form of a proton gradient across its membrane. A limitation of bR for solar energy applications arises from its relatively poor native solar energy conversion efficiency (0.2-40 pA/cm^2 per monolayer with bias).

We have explored the plasmonic field enhancement of the proton current produced during the photosynthesis of bacteriorhodopsin (bR) by maximizing the blue light effect, where the influx of blue photons absorbed by the long-lived M intermediate drastically shortens the time scale of the bR photocycle, leading to current enhancement. To this end, we used three new approaches in our solution-based cell:

- We improved the charge carrier separation in solution.
- We maximized the plasmonic surface field effects by using modified cubic Ag nanoparticles.
- We optimized the degree of spectral overlap between the plasmonic optical band and the absorption of the photocycle intermediate that absorbs the blue light.

Theoretical models are used to explain experimental results, which show a photocurrent density of 0.21 $\mu A/cm^3$ in bR enhanced by 40 nm cuboidal silver nanoparticles sans bias. This value is 5,000 times larger than the published results for thin film bR electrochemical cells even with an applied bias.

Beating Nature in Capturing Solar Energy: Tailored Plasmonic Field Enhancement of the Current Produced from the Photosynthetic System of Bacteriorhodopsin

In our last year's abstract, we showed that we have achieved photocurrent densities as high as 25 nA/cm^3 in our wet electrochemical cell using porous membranes; however, these are not selective in the transport of cations and anions. This leads to an initial rapid flux of protons across the membrane followed by the flux of larger, bulkier anions, which neutralize some of the charges (**Figure 1B**). To minimize these ionic depolarization effects, we turned to Nafion membranes, common in proton exchange membrane fuel cells. These membranes are selective for cations and thereby limit the flux of anions across the membrane. This increases the overall charge carrier separation and allows for a more stable photocurrent.

Next, we further exploited the blue light effect, which occurs when the proper photocycle intermediate absorbs a blue photon (**Figure 1A**). This absorption almost instantly re-isomerizes the chromophore, shortening the photocycle by ~99.7%. This effect is rare in non-enhanced systems, so to encourage its occurrence, we exploited the properties of surface plasmons.

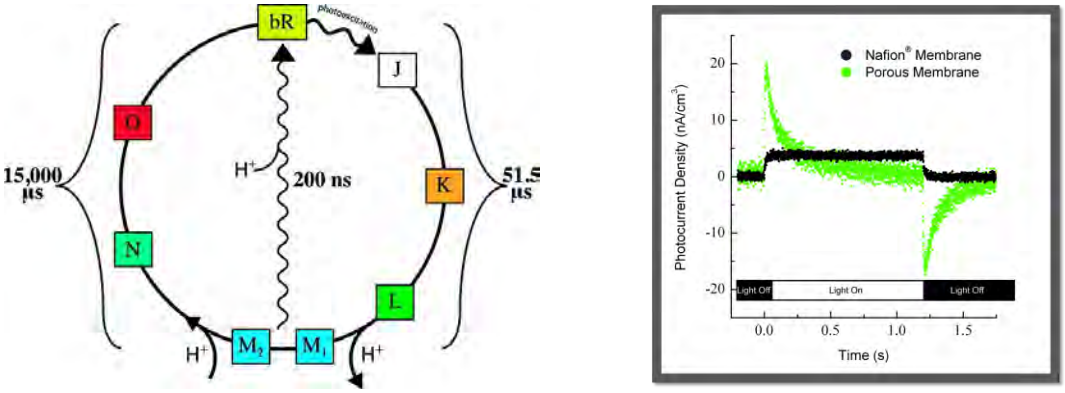

Figure 1. (**A**) Simplified bR photocycle. The M intermediate can either thermally relax to the bR ground state through a series of conformational changes in a time of 15 ms, or it can be photochemically converted back to the bR ground state in a time of 200 ns via absorption of blue light. The color of the box around each intermediate reflects its spectral absorbance wavelength in the visible region. (**B**) Photocurrent production of bR in our wet electrochemical cell using a porous (green) and Nafion (black) membrane. Nafion membranes provide higher stationary photocurrent without the initial spike seen using porous membranes via their proton selectivity.

Surface plasmon resonance is induced when an incident electromagnetic light wave couples with the conduction band electrons in a metal nanoparticle. We found that the plasmonic field of silver nanoparticles, which has excellent spectral overlap with the M intermediate absorption (**Figure 2A**), greatly enhances the local flux of blue photons. This leads to an enhancement in the rate of proton release and therefore an enhanced steady-state photocurrent.

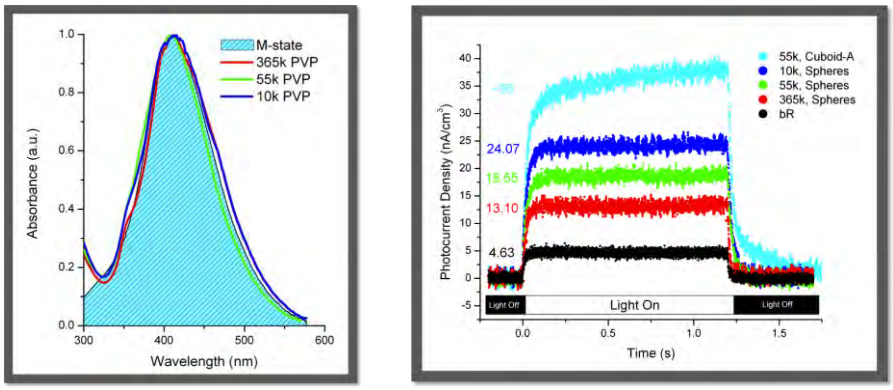

Figure 2. (**A**) Absorbance spectra of silver nanospheres capped with 10k (blue), 55k (green), and 365k (red) M.W. PVP showing spectral overlap with the M intermediate of bR (shaded cyan). (**B**) Bacteriorhodopsin native photocurrent generation (black), bR photocurrent generation under enhancement by 40 nm silver spheres capped with PVP of M.W. 10k (blue); 55k (green); and 365k (red); and initial, short-timescale observation of enhancement using 40 nm edge length silver cuboid-A capped with 55k M.W. PVP (cyan).

The relative field strength felt by each bR molecule is of great importance to the photocurrent enhancement. Capping agents are necessary for metal nanoparticle stability, however, in forming a protective barrier around the particles, the capping agent limits bR access to the surface of the particle, where the field is strongest. To prove this concept we examined capping shell thickness relation to photocurrent density (**Figure 2B**, red, green, blue). Stronger effective field intensity from thinner capping shells yields larger photocurrent enhancement for these particles with virtually the same spectral overlap with the M intermediate (**Figure 2A**); however, particle instability was noted with the thinnest capping shell.

The unique surface plasmon resonance of metal nanoparticles is highly sensitive to their local environment as well as their size, shape, and composition. The surface plasmon resonance of silver nanospheres has the best spectral overlap with the M intermediate absorption. However, metal nanoparticles with features such as corners and edges (e.g., prisms, cubes) exhibit larger plasmonic field intensities. Discrete Dipole Approximation (DDA) calculations for equally-sized spheres and cubes show the expected strongest field intensity at edges and corners of the cubic shape (**Figure 3A**).

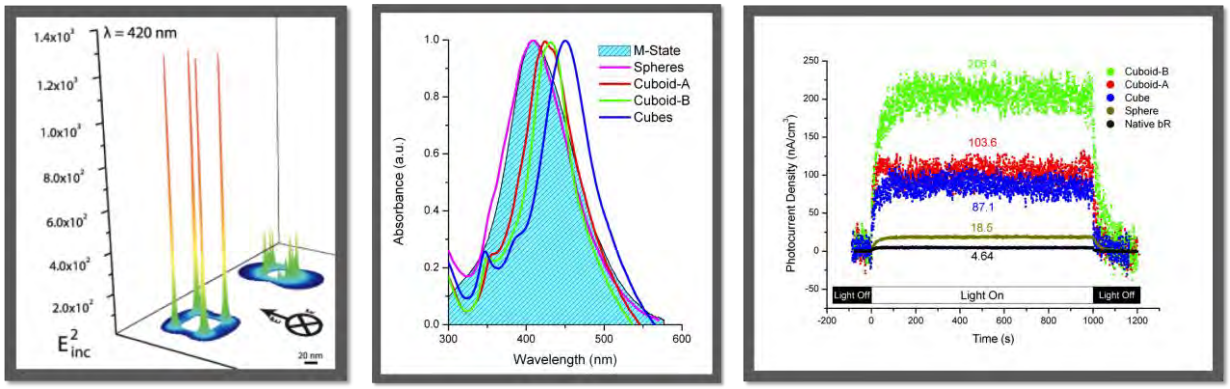

Figure 3. (**A**) 2D and 3D DDA electric field plots for 40 nm diameter silver sphere and 40 nm edge length silver cube, demonstrating stronger field intensities with sharper corners. (**B**) Absorbance spectra of 40 nm silver spheres, cuboids and cubes capped with 55k M.W. PVP showing decreasing spectral overlap with the M intermediate of bR (shaded cyan) with increasing sharpness of cube corners. (**C**) Bacteriorhodopsin photocurrent generation under blue light enhancement from 40 nm silver particles capped with 55k M.W. PVP. Illustrates photocurrent enhancement of native bR (black) using spheres (yellow); cuboid-A, with highly truncated corners (red); cuboid-B, with slightly truncated corners (green); and perfect cubes (blue).

The drawback of altering particle shape for this system lies in the fact that this shifts the absorption profile, decreasing spectral overlap with the M intermediate (**Figure 3B**). We examined a progression of shapes from spheres to cubes to find the best compromise between particle field strength and spectral overlap with the M intermediate.

Over the 1.2 s timescale (**Figure 2B**), the photocurrent density of Cuboid-A-enhanced bR is much higher than any sphere-enhanced photocurrent but shows an unfinished rise. The timescale was adjusted to 1000 s to investigate this. Over the course of this longer timescale experiment (**Figure 3C**), Cuboid-A, with highly rounded corners, reached a maximum of 103.6 nA/cm^3 after 100 s, a stark contrast to the ~36 nA/cm^3 photocurrent density observed over the 1.2 s timescale experiments.

Interestingly, perfect cubes, with the strongest field intensity, displayed less enhancement than did cuboid-B. The absorption profile (**Figure 3B**) explains why. The degree of spectral overlap with the M intermediate decreases significantly as the shape changes from cuboid-B to perfect cubes. These results are rendered visually in **Figure 4**, where the largest photocurrent density (0.2 μA/cm^3) is apparent for the particle that falls nearest the intersection of increasing field strength (corner integrity, green) and decreasing spectral overlap with the M intermediate (blue). This value is 50 times higher than pure bR in our wet electrochemical system (4.64 nA/cm^3) and 5,000 times larger than published results for thin film bR electrochemical cells. This high photocurrent density was stable for up to 6 consecutive hours of continuous irradiation, demonstrating the utility of specifically tailoring surface plasmons to the task at hand.

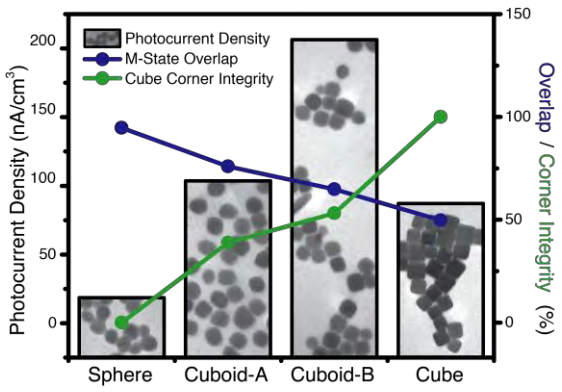

Figure 4. Photocurrent density of bR for each shape (bars), spectral overlap between the surface plasmon resonance band of the nanoparticle and the M intermediate absorption (blue), and the cube corner integrity (green) as an indicator of field strength. Relative overlap percentage was determined via integration of the normalized curves, and relative corner integrity was measured using the radius of curvature from TEM images (shown within the photocurrent bars). This figure illustrates that the largest enhancement in photocurrent density results from the particle has the best spectral overlap and field strength.

Future Plans

We will examine the dependence of bR photocurrent on the exciting wavelength throughout the visible spectrum both with and without nanoparticles. We will vary the energy of the plasmon resonance throughout the visible spectrum by using nanoparticles with a variety of sizes (spheres, cubes, rods, cages) and compositions (silver, gold, alloy) to ascertain the effect of plasmonic field enhancement on the many discrete-absorbing intermediates of the bR photocycle.

Publications During the Past Period

1. Szymanski, P.; El-Sayed, M. A., Some recent developments in photoelectrochemical water splitting using nanostructured TiO_2: a short review. *Theor. Chem. Acc.* **2012,** *131* (6).
2. Yen, C.-W.; Hayden, S. C.; Dreaden, E. C.; Szymanski, P.; El-Sayed, M. A., Tailoring Plasmonic and Electrostatic Field Effects To Maximize Solar Energy Conversion by Bacteriorhodopsin, the Other Natural Photosynthetic System. *Nano Lett.* **2011,** *11* (9), 3821-3826.
3. Allam, N. K.; Yen, C.-W.; Near, R. D.; El-Sayed, M. A., Bacteriorhodopsin/TiO_2 nanotube arrays hybrid system for enhanced photoelectrochemical water splitting. *Energy Environ. Sci.* **2011,** *4* (8), 2909-2914.
4. Allam, N. K.; Poncheri, A. J.; El-Sayed, M. A., Vertically Oriented Ti–Pd Mixed Oxynitride Nanotube Arrays for Enhanced Photoelectrochemical Water Splitting. *ACS Nano* **2011,** *5* (6), 5056-5066.
5. Hesabi, Z. R.; Allam, N. K.; Dahmen, K.; Garmestani, H.; A. El-Sayed, M., Self-Standing Crystalline TiO_2 Nanotubes/CNTs Heterojunction Membrane: Synthesis and Characterization. *ACS Appl. Mater. Interfaces* **2011,** *3* (4), 952-955.
6. Chu, L. K.; Yen, C. W.; El-Sayed, M. A., Bacteriorhodopsin-based photo-electrochemical cell. *Biosens. Bioelectron.* **2010,** *26* (2), 620-626.
7. Hayden, S. C.; Allam, N. K.; El-Sayed, M. A., TiO_2 Nanotube/CdS Hybrid Electrodes: Extraordinary Enhancement in the Inactivation of Escherichia coli. *J. Am. Chem. Soc.* **2010,** *132* (41), 14406-14408.
8. Allam, N. K.; Alamgir, F.; El-Sayed, M. A., Enhanced Photoassisted Water Electrolysis Using Vertically Oriented Anodically Fabricated Ti−Nb−Zr−O Mixed Oxide Nanotube Arrays. *ACS Nano* **2010,** *4* (10), 5819-5826.
9. Chu, L.-K.; Yen, C.-W.; El-Sayed, M. A., On the Mechanism of the Plasmonic Field Enhancement of the Solar-to-Electric Energy Conversion by the Other Photosynthetic System in Nature (Bacteriorhodopsin): Kinetic and Spectroscopic Study. *J. Phys. Chem. C* **2010,** *114* (36), 15358-15363.
10. Allam, N. K.; El-Sayed, M. A., Photoelectrochemical Water Oxidation Characteristics of Anodically Fabricated TiO_2 Nanotube Arrays: Structural and Optical Properties. *J. Phys. Chem. C* **2010,** *114* (27), 12024-12029.
11. Yen, C.-W.; Chu, L.-K.; El-Sayed, M. A., Plasmonic Field Enhancement of the Bacteriorhodopsin Photocurrent during Its Proton Pump Photocycle. *J. Am. Chem. Soc.* **2010,** *132* (21), 7250-7251.
12. Chu, L. K.; El-Sayed, M. A., Kinetics of the M-Intermediate in the Photocycle of Bacteriorhodopsin upon Chemical Modification with Surfactants. *Photochem. Photobio.* **2010,** *86* (2), 316-323.
13. Chu, L. K.; El-Sayed, M. A., Bacteriorhodopsin O-state Photocycle Kinetics: A Surfactant Study. *Photochem. Photobio.* **2010,** *86* (1), 70-76.

Statistical Mechanical and Multiscale Modeling of Catalytic Reactions

Jim Evans (PI) and Da-Jiang Liu
Ames Laboratory – USDOE and Department of Physics & Astronomy,
Iowa State University, Ames, IA 50011
evans@ameslab.gov

PROGRAM SCOPE:

The Chemical Physics and Computational & Theoretical Chemistry projects at Ames Laboratory pursue the modeling of **heterogeneous catalysis and other complex reaction phenomena** at surfaces and in mesoporous materials. This effort incorporates ***electronic structure analysis, non-equilibrium statistical mechanics, and coarse-graining or multi-scale modeling***. The *electronic structure* component includes DFT-VASP analysis of chemisorption and reaction energetics on metal surfaces, as well as application of QM/MM methods in collaboration with Mark Gordon (PI). The *non-equilibrium statistical mechanical and related studies* of reaction-diffusion phenomena include Kinetic Monte Carlo (KMC) simulation of atomistic models, coarse-graining, and heterogeneous multi-scale formulations. Topics of interest include: (i) anomalous transport and catalytic reaction in functionalized mesoporous materials; (ii) chemisorption and heterogeneous catalysis on metal surfaces, including both reactions on extended crystalline surfaces (connecting atomistic to mesoscale behavior) and nanoscale catalyst systems (exploring the role of fluctuations); (iii) general statistical mechanical models for reaction-diffusion processes exhibiting non-equilibrium phase transitions, metastability, critical phenomena, etc.. (iv) diffusion, self-organization, reaction,… on non-conducting surfaces

RECENT PROGRESS:

CATALYTIC REACTIONS IN FUNCTIONALIZED NANOPOROUS MATERIALS

Our basic goal is to elucidate the interplay between anomalous transport and catalytic reaction in surface functionalized nanoporous materials, particularly mesoporous silica. We have focused on the regime of narrow pores with effective diameter below 2 nm where inhibited passing of reactants and products can lead to single-file-diffusion. Initial studies focused on polymerization reactions. We performed KMC analysis of single-file diffusion-mediated polymerization ($A+A_n \rightarrow A_{n+1}$ as in PPB formation) where we elucidate pore-clogging seen in experiments as well as unusual growth kinetics and length distributions. The latter were explained within a non-Markovian CTRW formalism [8,12]. This analysis was extended to elucidate the observed surprising efficiency of the Sonagashira cross-coupling polymerization reaction mechanism $A+BAB\ldots \rightarrow ABAB\ldots$ [12]. Potential entry of monomers A and B into the pore in the "wrong" order for reaction (e.g., A ABAB B BAB) is shown not inhibit the formation of long polymers.

Recent work has considered basic conversion reactions $A \rightarrow B$ occurring inside linear nanopores where passing of reactants and products is strongly inhibited [11,12,19,21]. We are motivated by experiments at Ames Lab, e.g., conversion of PNB to an aldol compound. The reaction (and reactant) tend to be localized near the pore openings, with the interior exclusively populated by "trapped" product. There is a long history of analysis of such systems, mostly in the context of catalysis in zeolites. Despite this fact, there is a lack of understanding of such fundamental issues as the scaling of reactant penetration depth, and thus reactivity, with microscopic reaction rate, the form of the reactant concentration profile, etc. Some previous studies utilized mean-field reaction-diffusion treatments, but we find that these fail to describe

single-file diffusion and cannot capture above features. We developed a "hydrodynamic" reaction-diffusion theory which does better describe some aspects of behavior [11]. However, steady-state reaction near pore openings is controlled by fluctuations in adsorption-desorption and diffusion at the pore openings, a feature not included in hydrodynamic treatments. We thus developed a generalized hydrodynamic treatment (in the special case of comparable mobility of reactant and product species) capturing enhanced fluctuation-mediated transport near pore openings. This theory was shown to precisely capture reaction-diffusion behavior as confirmed by comparison with "exact" KMC simulation results [21]. Thus, the theory provides a powerful and efficient tool to analyze behavior as a function of the many experimental control parameters.

CHEMISORPTION AND HETEROGENEOUS CATALYSIS ON METAL SURFACES

Chemisorption and complexes on metal surfaces. Reliable description of chemisorption is key for modeling of catalytic reactions, e.g., to describe ordering in reactant adlayers, and possible restructuring and dynamics of the metal surface induced by chemisorbed reactants or other impurities. Sulfur (S) can act as a poison or promoter in catalysis, but also can induce metal substrate dynamics. Following our previous analysis of self-organized formation metal-S complexes and related enhanced decay of Ag nanoclusters on Ag(111), we have used DFT to analyze chemisorption and metal-S complex formation for S/Ag(100) [10]. For both S on Ag (111) and (100), enhanced destabilization of metal nanostructures is induced by metal-S complex formation. However, the kinetics are quite different for these systems and we continue analysis for the latter. We are exploring analogous behavior induced by adsorption of O and halogens.

Multi-site lattice-gas modeling of catalytic reactions. A long-standing goal for surface science has been to develop realistic atomistic models for "complete" catalytic reaction processes on metal surfaces. We have continued development and application of realistic multi-site lattice-gas (msLG) models and efficient KMC simulation algorithms to describe CO-oxidation on unreconstructed metal surfaces. Recently, we have performed extensive DFT analysis of adspecies interactions which control ordering in mixed reactant adlayers. In addition, reactive steady-states are impacted by dynamics, so we are also developing more realistic treatments for CO-adsorption subject to steering and funneling, and also for dissociative oxygen adsorption. Results will be incorporated into a comprehensive review on msLG modeling for Prog. Surf. Sci.

FUNDAMENTAL PHENOMENA IN FAR-FROM-EQUILIBRIUM REACTION SYSTEMS

An understanding of non-equilibrium 1^{st}-order phase transitions (such as catalytic poisoning transitions) and associated metastability and critical phenomena at a level comparable to that for equilibrium systems is one of the ***BESAC Science Grand Challenges*** goals *(Cardinal Principles of Behavior beyond Equilibrium)*. This requires advancing from traditional mean-field modeling to atomistic statistical mechanical modeling. We continue such studies for a version of Schloegl's second model for autocatalysis [13,17,18]. Despite the occurrence of "generic two-phase coexistence", metastablity and nucleation phenomena appear similar to thermodynamic systems. We are developing analytic and simulation tools for sophisticated analysis of this behavior.

DIFFUSION, SELF-ASSEMBLY, ETCHING, etc. ON NON-CONDUCTING SURFACES

We performed a QM/MM analysis with Gordon of Ga diffusion underlying the self-assembly of Ga rows via a "surface-polymerization reaction" during deposition on Si(100) [14]. We are developing efficient multiscale approaches (e-structure to atomistic to coarse-grained models) to describe evolution of imperfect stepped surfaces during reactive etching/growth processes [20].

FUTURE PLANS:

CATALYTIC REACTIONS IN FUNCTIONALIZED MESOPOROUS MATERIALS

We are working toward the development of more detailed system-specific models for catalytic conversion reactions in mesoporous silica (MSN). In particular, we wish to elucidate the observed dependence of reactivity on pore diameter for PNB conversion to an aldol compound (by Slowing, Pruski, et al.). This requires detailed assessment of the passing propensity for elongated reactants and products inside narrow pores, and incorporation of this behavior into coarse-grained models describing the interplay of inhibited transport and reaction. We are implementing stochastic Langevin dynamics to describe such passing phenomena. In addition, further development of our generalized hydrodynamic treatment is needed for these systems, e.g., to describe greatly differing differing reactant/product mobilities, etc.. Another issue (motivated by experiments) where we have already made progress is the analysis of the effects of multi-functionalization to expel one product from the pore (or at least to exclude its re-entry).

In addition, we are implementing a bond-switching MC algorithm for a Continuous Random Network (CRN) model to provide an atomistic-level description of amorphous catalyst materials.

CHEMISORPTION AND HETEROGENEOUS CATALYSIS ON METAL SURFACES

Atomistic msLG models of catalytic reactions on metal surfaces. We continue our core goal of developing realistic and predictive atomistic-level models and KMC simulation algorithms for catalytic reactions on various metal (111) and (100) surfaces. Of particular interest is enhanced fluctuations effects and more complex reaction kinetics (e.g., multistability) for higher pressures due to higher reactant coverages. There are also multiphysics and multiscale modeling challenges, e.g., mass-transport limited behavior at higher pressures requiring coupling of CFD treatments of reactor flow to our atomistic model using our HCLG multiscale modeling strategy.

Chemisorbed adlayer and metal surface dynamics. We are interested in exploring ordering and dynamics in chemisorbed layers, formation of metal complex and metal surface dynamics (observed by STM, PEEM, LEEM). Target systems are: halogens, chalcogens, H_2S and H_2O on on coinage metals (with Thiel); (CO+H)/Pd(111) (with Salmeron); diffusion in high-density O adlayers on Pt(111); the interplay between step structure and reaction processes (with Imbihl).

DIFFUSION AND REACTION ON NON-CONDUCTING SURFACES

We plan to continue and integrate high-level QM/MM analysis (with Gordon), atomistic KMC modeling, and potentially also computationally efficient and versatile coarse-grained step dynamics modeling of etching, oxidation, and other reactions on dynamic stepped surfaces. QM/MM can help address the limitations of DFT-based analysis of energetics in these systems.

FUNDAMENTAL PHENOMENA IN FAR-FROM-EQUILIBRIUM REACTION SYSTEMS

Analysis will continue of non-equilibrium phase transitions in a variety of statistical mechanical reaction-diffusion models. Issues of metastability and nucleation, and well as critical phenomena, are of fundamental interest for these non-equilibrium systems where the standard thermodynamic framework (i.e., involving a free energy) cannot be applied. We are extending these analyses to various ZGB-type surface reaction models, which although too simplistic to describe standard low-pressure reaction behavior, may provide a valuable paradigm for high-pressure high-coverage low-effective-surface-mobility fluctuation-dominated reaction systems.

PUBLICATIONS SUPPORTED BY USDOE CHEM. SCIENCES FOR 2010-PRESENT:

[1] *Diffusion of Atomic Oxygen on the Si(100) Surface*, P. Arora, W. Li, P. Piecuch, J.W. Evans, M. Albao, M.S. Gordon, J. Phys. Chem. C, **114**, 12649 (2010).

[2] *Shell structure and phase relations in electronic properties of metal nanowires from an electron-gas model*, Y. Han, D.-J. Liu, Phys. Rev. B, **82**, 125420 (2010).

[3] *Density functional analysis of key energetics in metal homoepitaxy: Quantum size effects in periodic slab calculations*, D.-J. Liu, Phys. Rev. B, **81**, 035415 (2010).

[4] *Interactions between Oxygen Atoms on Pt(100): Implications for Ordering during Chemisorption and Catalysis*, D.-J. Liu, J.W. Evans, ChemPhysChem, **11**, 2174 (2010).

[5] *Low-temperature adsorption of H_2S on Ag(111)*, S.M. Russell, D.-J. Liu, M. Kawai, Y. Kim, P.A. Thiel, J. Chem. Phys., **133**, 124705 (2010).

[6] *Adsorbate-enhanced transport of metals on metal surfaces: Oxygen and sulfur on coinage metals,* P.A. Thiel, M. Shen, D.-J. Liu, et al., J. Vac. Sci. Technol. A, **28** 1285-1298 (2010) (JVSTA Cover)

[7] *Metastability in Schloegl's second model for autocatalysis: Lattice-gas realization with particle diffusion*, X.F. Guo, Y. De Decker, J.W. Evans, Phys. Rev. E, **82**, 021121 (2010).

[8] *Polymer length distributions for catalytic polymerization within mesoporous materials: Non-Markovian behavior*, D.-J. Liu, H.T. Chen, V.S.Y. Lin, J.W. Evans, J. Chem. Phys. **132**, 154102 (2010).

[9] *Boundary conditions for Burton-Cabrera-Frank type step-flow models: coarse-graining of discrete deposition-diffusion equations*, D.M. Ackerman, J.W. Evans, SIAM Multiscale Model. Sim. **9**, 59 (2011)

[10] *Adsorption of sulfur on Ag(100)*, S.M. Russell, M.M. Shen, D.J. Liu, et al., Surf. Sci. **605**, 520 (2011).

[11] *Catalytic conversion reactions mediated by single-file diffusion in linear nanopores...,* D.M. Ackerman, J. Wang, J.H. Wendel, D.-J. Liu, M. Pruski, J.W. Evans, J. Chem. Phys. **134**, 114107 (2011).

[12] *Interplay between anomalous transport & catalytic reaction in single-file mesoporous systems*, D.-J. Liu, J. Wang, D. Ackerman, I. Slowing, M. Pruski, H. Chen, V. Lin, J.W. Evans, ACS Cat. **1**, 751 (2011).

[13] *Schloegl's second model for autocatalysis on a cubic lattice: Analysis via mean-field discrete reaction-diffusion equations*, C.-J. Wang, X. Guo, D.-J. Liu, J.W. Evans, J. Stat. Phys. **144**, 1308 (2011).

[14] *Adsorption and diffusion of Gallium Adatoms on the Si(100) -2x1 reconstructed surface: An MCSCF study using surface clusters*, L. Roskop, J.W. Evans, M.S. Gordon, J. Phys. Chem. C, **115**, 23488 (2011).

[15] *Comment on sulfur-induced reconstruction of Ag(111) surface studied by DFT*, M. Shen, D.-J. Liu, C.J. Jenks, P.A. Thiel, J. Phys. Chem. C **115**, 23651 (2011).

[16] *Destabilization of Ag nanoislands on Ag(100) by adsorbed sulfur*, M. Shen, S.M. Russel, D.-J. Liu, P.A. Thiel, J. Chem. Phys. **135**, 154701 (2011).

[17] *Tricriticality in generalized Schloegl models for autocatalysis: Lattice-gas realization with particle diffusion*, X. Guo, D.K. Unruh, D.-J. Liu, J.W. Evans, Physica A **391**, 633 (2012).

[18] *Schloegl's second model for autocatalysis on hypercubic lattices: Dimension-dependence of generic two-phase coexistence*, C.-J. Wang, D.-J. Liu, J.W. Evans, Phys. Rev. E, **85**, 041109 (2012).

[19] *Conversion reactions in surface-functionalized mesoporous materials*, J. Wang, D. Ackerman, K. Kandel, I.I. Slowing, M. Pruski, and J.W. Evans, MRS Proc. Symp. RR F11 (MRS, Pittsburgh, 2012).

[20] *Morphological evolution during growth and erosion on vicinal Si(100) surfaces: From electronic structure to atomistic and coarse-grained modeling*, D.-J. Liu, D.M. Ackerman, X. Guo, M.A. Albao, L. Roskop, M.S. Gordon, and J.W. Evans, MRS Proc. Symp. EE Fall 2011 (MRS, Pittsburgh, 2012).

[21] *Generalized hydrodynamic treatment of interplay between restricted transport & catalytic reactions in nanoporous materials*, D.M. Ackerman, J. Wang, J.W. Evans, Phys. Rev. Lett., **108**, 228301 (2012).

Confinement, Interfaces, and Ions: Dynamics and Interactions in Water, Proton Transfer, and Room Temperature Ionic Liquid Systems (DE-FG03-84ER13251)

Michael D. Fayer
Department of Chemistry, Stanford University, Stanford, CA 94305
fayer@stanford.edu

Surfaces and interfaces are the mediators of some of the most important reactions in chemistry, biology, and industry. In many cases, chemical moieties at surfaces are catalysts. The reactivity of the surface active atoms or molecules is strongly influenced by both local structure and dynamics on fast timescales. Despite a long-standing need, the tools to study structural dynamics of interfacial molecules under chemically relevant conditions have been lacking. We achieve the long standing goal of directly measuring the structural dynamics of a submonolayer of molecules bound to an interface. The dynamics and structure of a molecular catalyst were studied using ultrafast two dimensional infrared (2D IR) vibrational echo spectroscopy. (phenanthroline)$Re(CO)_3Cl$ ($RePhen(CO)_3Cl$), a CO_2 reduction photocatalyst, was bound to a planar silica interface with an eleven carbon chain using click chemistry. The combination of 2D IR vibrational echo spectroscopy and linear infrared spectroscopy performed on the metal carbonyl stretching modes under ambient pressure and temperature made possible the measurement of interfacial structural dynamics and the direct comparison of the monolayer/air and monolayer/liquid interfaces to the bulk solution. Linear IR spectroscopy experiments determined the orientation and surface concentration of the $RePhen(CO)_3Cl$ head group in the submonolayer. In addition, a new method, ultrafast IR heterodyne detected polarization selective transient gratings, was used to measure the vibrational population relaxation and anisotropy relaxation.

What makes these experiments a major advance is the very small number of molecules that are bound to the surface in the submonolayer. In a typical 2D IR vibrational echo experiment on a bulk liquid such as water, a few times 10^{14} molecules interact with the IR pulses used to perform the experiments. In the surface 2D IR experiments, a few times 10^{10} molecules participate in the experiments. Nonetheless, good data were obtained from the 2D IR experiments, and using the new transient grating method instead of the standard IR pump-probe experiment, made it possible to measure the population dynamics.

The net result is that it was possible to measure the spectral diffusion of the symmetric CO stretching mode of the $RePhen(CO)_3Cl$. Spectral diffusion is the frequency evolution of the vibration caused by structural evolution of the system. We studied the heterogeneous catalyst $RePhen(CO)_3Cl$ bound to the surface in air and in chloroform solvent. These results were compared to the just the head group ($RePhen(CO)_3Cl$ with no linker attaching it to the surface) in bulk chloroform solvent. The structural dynamics measure by spectral diffusion report on the time dependent environment of the $RePhen(CO)_3Cl$. Each $RePhen(CO)_3Cl$ is in a sea of surrounding chains linked to the surface. All of these are undergoing structural evolution. We found that the spectral diffusion time constants for the surface bound molecules are 76 ± 15 ps in air and 26 ± 4 ps in chloroform solvent. These values should be compared to the result for $RePhen(CO)_3Cl$ in bulk chloroform, which is 5 ±1 ps. In our initial report of this work (Science 334, 634-639 (2011)), we thought that a component of the spectral diffusion was caused by vibrational excitation transfer. Recent concentration dependent studies show that excitation transfer does not contribute to the observed spectral diffusion. Therefore, the numbers given above give the time dependence of solely structural evolution of the system. The results show that molecules linked to a surface undergo relatively rapid structural evolution, although it is substantially slower than dynamics in a bulk liquid.

Water exists in confined environments and at interfaces in a wide variety of important systems in chemistry, materials science, biology, geology, and technological applications. In chemistry, water plays an important role as a polar solvent often in contact with interfaces, for example, in ion exchange resin systems and chromatographic surfaces. Water in the nanoscopic channels of polyelectrolyte membranes is central to the operation of hydrogen and other fuel cells. In biology, water is found in crowded environments, such as cells, where it hydrates membranes and large biomolecules, as well as in pockets in proteins. In geology, interfacial water molecules can control ion adsorption and mineral dissolution. Embedded water molecules can change the structure of zeolites used as catalysts.

Water's unique properties can be traced to its formation of an extended hydrogen bonding network. Water molecules can make up to four hydrogen bonds in an approximately tetrahedral

arrangement. However, the hydrogen bonded network is not static. The network evolves constantly on a picosecond time scale by the concerted dissociation and formation of hydrogen bonds. This rapid evolution of water's hydrogen bond network enables processes ranging from proton diffusion to protein folding. While a great deal is known about the dynamics of bulk water, much less is known about the dynamics of water in nanoconfinement, at interfaces and when it is interacting with ionic species. The dynamics of water are changed a great deal when water is in nanoscopic environments, interacting with interfaces or ions. In addition, important processes such as proton transport, which is necessary in fuel cells, are dramatically changed when they do not occur in bulk pure water.

The infinite miscibility of dimethyl sulfoxide (DMSO) with water at room temperature makes water/DMSO solutions useful for gaining insight into changes in water hydrogen bond dynamics as water goes from a minor component to a major component of the solutions. While water is both a hydrogen bond donor and acceptor, DMSO is only a hydrogen bond acceptor. This difference gives rise to a variety of important properties of water/DMSO binary solutions. Solutions of water/DMSO form a eutectic in molar ratios of 2:1 and at low DMSO concentrations serves as a cryoprotectant with a depressed freezing point of 203 K. At mole fractions of 0.3-0.4 DMSO, water/DMSO solutions deviate strongly from ideality, with positive deviations in viscosity and density, and negative deviations in the heat of mixing. We have performed a comprehensive examination of the dynamics and interactions of water in mixtures of water and DMSO. Solutions were studied that range from very low water content to high water content. Five experimental observables were employed. The techniques, which were all applied as a function of water concentration, are infrared (IR) absorption spectra of the water hydroxyl stretch, IR pump-probe experiments that measure the hydroxyl stretch vibrational lifetimes, polarization selective IR pump-probe experiments that measure the water orientational relaxation times, two dimensional IR (2D IR) vibrational echo experiments that measure spectral diffusion of the hydroxyl stretch, and optical heterodyne detected optical Kerr effect (OHD-OKE) experiments that measure the orientational relaxation of DMSO. By combining the results of these methods, a detailed picture of the nature of water/DMSO dynamics and interactions was obtained, which in turn increased our understanding of how water behaves in complex environments.

Vibrational population relaxation of the hydroxyl stretch displayed two vibrational lifetimes even at very low water concentrations. The two lifetimes are associated with water-water and water-DMSO hydrogen bonds. The IR absorption spectra also showed characteristics of both water-DMSO and water-water hydrogen bonding. Although two populations were observed, water anisotropy decays (orientational relaxation) exhibited single ensemble behavior, indicative of concerted reorientation involving water and DMSO molecules. OHD-OKE experiments, which measure the orientational relaxation of DMSO, revealed that the DMSO orientational relaxation times are the same as orientational relaxation times found for water over a wide range of water concentrations within experimental error. The fact that the reorientation times of water and DMSO are basically the same shows that the reorientation of water is coupled to the reorientation of DMSO itself. These observations were described in terms of a jump reorientation model. Frequency-frequency correlation functions determined from the 2D IR experiments on the OD stretch show both fast and slow spectral diffusion. In analogy to bulk water, the fast component was assigned to very local hydrogen bond fluctuations. The slow component, which is similar to the slow water reorientation time at each water concentration, was associated with global hydrogen bond structural randomization.

Room temperature ionic liquids (RTIL) have been the object of extensive study in the past decade due to their unique properties including very low vapor pressure and non-flammability under ambient conditions, selective reaction medium, etc. One particular area of interest is the possible use of ionic liquids as alternative solvents in lithium ion batteries. The current generation of such batteries uses organic compounds as solvents. These solvents present safety issues due to properties such as volatility and high flammability. Thus RTILs could become greener and safer alternative.

Water dynamics are strongly influenced by their interactions with ions. RTILs are extremely hygroscopic. In practical applications, RTILs will always contain some water. We are studying water in RTILs using a variety of methods. RTILs provide a medium in which water can be studied at all concentrations. In normal salt solutions, such as NaBr, at high concentration the salt crystallizes out of the solution. Therefore, it is not possible to go to low enough water concentration to study the nature of water interacting with a sea of ions but not interacting with other water molecules. Therefore, RTILs

provides a medium for the study of water interacting with ions. Turning the problem around, we are also studying the influence of water on the dynamics and structure of RTILs.

Optical heterodyne-detected optical Kerr effect (OHD-OKE) measurements on a series of 1-alkyl-3-methylimidazolium tetrafluoroborate room-temperature ionic liquids (RTILs) as a function of chain length and water concentration were performed. The pure RTIL reorientational dynamics are identical in form to other molecular liquids studied previously by OHD-OKE (two power laws followed by a single exponential decay at long times), but are much slower at room temperature. In contrast, the addition of water to the longer alkyl chain RTILs caused the emergence of a long time bi-exponential orientational anisotropy decay. Such distinctly bi-exponential decays have not been seen previously in OHD-OKE experiments on any type of liquid and were analyzed using a wobbling-in-a-cone model. The slow component for the longer chain RTILs does not obey the Debye-Stokes-Einstein (DSE) equation across the range of solutions, and thus we attributed it to slow cation reorientational diffusion caused by a stiffening of cation alkyl tail-tail associations. The fast component of the decay was assigned to the motions (wobbling) of the tethered imidazolium head groups. The wobbling-in-a-cone analysis provided estimates of the range of angles sampled by the imidazolium head group prior to the long time scale complete orientational randomization. The heterogeneous dynamics and non-DSE behavior observed should have a significant effect on reaction rates in water/RTIL co-solvent mixtures.

We are continuing and extending our studies, a few of which are briefly outlined above. More information on our recent work is contained in the papers listed below. 2D IR vibrational echo experiments and IR polarization selective pump-probe experiments are being conducted on very dilute D_2O in the RTIL butylmethyl-ImidazoliumPF_6 at such low water concentration that the water is interacting with ions but not with other water molecules. These are the first experiments that can study the dynamics of isolated water molecules in an ionic solution. The results will provide information on the dynamics and structure of the RTIL and the nature of single water molecules interacting with ions. We are also conducting detailed 2D IR studies and pump-probe studies of water in salt solutions such as $MgSO_4$. We are comparing the influence mono and divalent cations and anions on water dynamics. Several types of experiments are being conducted on polyelectrolyte fuel cell membranes. These studies build on our earlier work on Nafion by extending the methods we developed to our membranes. IR pump-probe experiments on water in the membranes are being used to study the nature of water environments in the nanoscopic channels and water hydrogen bond dynamics. Orientational relaxation measures the time dependence of hydrogen bond reorganization. We will also use 2D IR vibrational echo experiments to investigate water dynamics in the membrane channels. In addition we are using photoacids in the membrane channels to study proton transport using time dependent fluorescence measurements including population dynamics and orientational relaxation. In both the IR experiments and the fluorescence experiments, the studies are being conducted as a function of the amount of water in the fuel cell membrane channels. We are also using fluorescence studies to investigate the influence of the addition of lithium ions to RTILs that can be useful in battery applications. The orientational relaxation of a probe chromophore, perylene, that locates in the hydrocarbon regions of the RTILS is used as a probe of structure and dynamics as a function of lithium ion concentration. We are also beginning studies of the dynamics and interactions of water in membranes made of carbon nanotubes and graphene oxide.

Publication from DOE Sponsored Research 2009 – present

(1) "Ion-Water Hydrogen Bond Switching Observed with 2D IR Vibrational Echo Chemical Exchange Spectroscopy," David E. Moilanen, Daryl Wong, Daniel E. Rosenfeld, Emily E. Fenn, and M. D. Fayer Proc. Nat. Acad. Sci. U.S.A. 106, 375-380 (2009).

(2) "Water Dynamics and Interactions in Water-Polyether Binary Mixtures," Emily E. Fenn, David E. Moilanen, Nancy E. Levinger, and Michael D. Fayer J. Am. Chem. Soc. 131, 5530-5539 (2009).

(3) "Water Dynamics at the Interface in AOT Reverse Micelles," David E. Moilanen, Emily E. Fenn, Daryl Wong and M.D. Fayer J. Phys. Chem. B 113, 8560–8568 (2009).

(4) "Geometry and Nanolength Scales vs. Interface Interactions: Water Dynamics in AOT Lamellar Structures and Reverse Micelles," David E. Moilanen, Emily E. Fenn, Daryl Wong, and M.D. Fayer J. Am. Chem. Soc. 131, 8318-8328 (2009).

(5) "Water Dynamics in Salt Solutions Studied with Ultrafast 2D IR Vibrational Echo Spectroscopy," M. D. Fayer, David E. Moilanen, Daryl Wong, Daniel E. Rosenfeld, Emily E. Fenn, and Sungnam Park Acc. of Chem. Res. 42, 1210-1219 (2009).
(6) "Water Dynamics in Large and Small Reverse Micelles: From Two Ensembles to Collective Behavior," David E. Moilanen, Emily E. Fenn, Daryl Wong, and Michael D. Fayer J. Chem. Phys. 131, 014704 (2009).
(7) "Water Dynamics at Neutral and Ionic Interfaces in Reverse Micelles," Emily E. Fenn, Daryl B. Wong, and M.D. Fayer Proc. Nat. Acad. Sci. U.S.A. 106, 15243-15248 (2009).
(8) "Solvent Control of the Soft Angular Potential in Hydroxyl-π Hydrogen Bonds: Inertial Orientational Dynamics," Daniel E. Rosenfeld, Zsolt Gengeliczki, and M. D. Fayer J. Phys. Chem. B 113, 13300-13307 (2009).
(9) "Proton Transfer and Proton Concentrations in Protonated Nafion Fuel Cell Membranes," D. B. Spry and M. D. Fayer J. Chem. Phys. B 113, 10210-10221 (2009).
(10) "Analysis of Water in Confined Geometries and at Interfaces," M. D. Fayer and Nancy E. Levinger Ann. Rev. Analytical Chem. 3, 89-107 (2010).
(11) "Room Temperature Ionic Liquids–Lithium Salts Mixtures: Optical Kerr Effect Dynamical Measurements," Bruno G. Nicolau, Adam Sturlaugson, Kendall Fruchey, Mauro C. C. Ribeiro, and M. D. Fayer J. Phys. Chem. B 114, 8350-8356 (2010).
(12) "Water Dynamics in Small AOT Reverse Micelles in Two Solvents: 2D IR Vibrational Echoes with 2D Background Subtraction," Emily E. Fenn, Daryl B. Wong, and M.D. Fayer J. Chem. Phys. 134, 054512 (2011).
(13) "Dynamics of Water Interacting with Interfaces, Molecules, and Ions," M. D. Fayer Acc. of Chem. Res. 45, 3-14 (2012).
(14) "Extracting 2D IR Frequency-Frequency Correlation Functions from Two Component Systems," Emily E. Fenn and M. D. Fayer J. Chem. Phys. 135, 07450 (2011).
(15) "Dynamics of Water at the Interface in Reverse Micelles: Measurements of Spectral Diffusion with 2D IR Vibrational Echoes," Emily E. Fenn, Daryl B. Wong, Chiara H. Giammanco, and M. D. Fayer J. Phys. Chem. B 115, 11658-11670 (2011).
(16) "Investigation of Nanostructure in Room Temperature Ionic Liquids using Electronic Excitation Transfer," Kendall Fruchey and M. D. Fayer J. Phys. Chem. B 116, 3054-3064 (2012).
(17) "Structural Dynamics of a Catalytic Monolayer Probed by Ultrafast 2D IR Vibrational Echoes," Daniel E. Rosenfeld, Zsolt Gengeliczki, Brian J. Smith, T. D. P. Stack, and M. D. Fayer Science 334, 634-639 (2011).
(18) "Water in a Crowd," M. D. Fayer Physiology 26, 381-392 (2011).
(19) "Orientational Dynamics of Room Temperature Ionic Liquid/Water Mixtures: Evidence for Water-Induced Structure and Anisotropic Cation Solvation," Adam L. Sturlaugson, Kendall S. Fruchey, and M. D. Fayer J. Phys. Chem. B 116, 1777-1787 (2012).
(20) "Water Dynamics in Water/DMSO Binary Mixtures," Daryl B. Wong, Kathleen P. Sokolowsky, Musa I. El-Barghouthi, Emily E. Fenn, Chiara H. Giammanco, Adam L. Sturlaugson, and Michael D. Fayer J. Phys. Chem. B 116, 5479-5490 (2012).

Chemical Kinetics and Dynamics at Interfaces

Fundamentals of Solvation under Extreme Conditions

John L. Fulton

Chemical and Materials Sciences Division
Pacific Northwest National Laboratory
902 Battelle Blvd., Mail Stop K2-57
Richland, WA 99354
john.fulton@pnl.gov

Collaborators: M. Baer, M. Balasubramanian, E. J. Bylaska, L. X. Dang, C. J. Mundy, T. Pham, G. K. Schenter, J. H. Weare

Program Scope

The primary objective of this project is to describe, on a molecular level, the solvent/solute structure and dynamics in fluids such as water under extremely non-ideal conditions. The scope of studies includes solute–solvent interactions, clustering, ion-pair formation, and hydrogen bonding occurring under extremes of temperature, concentration and pH. The effort entails the use of spectroscopic techniques such as x-ray absorption fine structure (XAFS) spectroscopy, high-energy x-ray scattering, coupled with theoretical methods such as molecular dynamics (MD-XAFS), and electronic structure calculations in order to test and refine structural models of these systems. In total, these methods allow for a comprehensive assessment of solvation and the chemical state of an ion or solute under any condition. The research is answering major scientific questions in areas related to energy-efficient separations, hydrogen storage and sustainable nuclear energy (aqueous ion chemistry and corrosion). This program provides the structural information that is the scientific basis for the chemical thermodynamic data and models in these systems under non-ideal conditions.

Recent Progress

The hydration of ions and the formation of contact ion pairs underlie processes in a large number of aqueous systems. Direct experimental measurement of ion-ion interactions decoupled from those of ion-water are limited. X-ray absorption fine structure (XAFS) spectroscopy, high-energy x-ray scattering (HEXS), and molecular dynamics (MD-XAFS) are being used to test and refine structural models of these systems.

Solvent-separated ion pair of $Ca^{2+}\bullet(H_2O)_n\bullet Cl^-$

Two types of ion-pair species occur in aqueous phases. There is the contact ion pair (CIP) wherein the anion directly adjoins the cation. As shown in Figure 1, there is also the solvent-separated ion pair (SSIP) wherein the cation and the anion are bridged by water molecules. This species is known from theory however a comprehensive characterization of its structure has not been reported. We applied a new method for the characterizing Ca^{2+}/Cl^- interaction. We simultaneously refine data from both x-ray absorption fine structure (XAFS) spectroscopy and

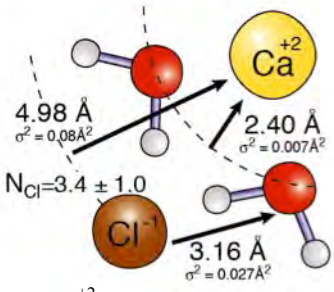

Figure 1. Ca^{+2} / Cl^- solvent separated ion pair in 6 m $CaCl_2$ from co-refinement of Ca- and Cl K-edge XAFS and HEXS scattering data. For clarity, only the bridging waters are shown.

from high- energy x-ray diffraction (HEXS) spectroscopy (X-ray Absorption/Diffraction Simultaneous Refinement (XADSR)). To our knowledge, spectra from these two diversely different experimental methods have not previously been simultaneously refined for disordered systems. XAFS has excellent sensitivity for a CIP structure whereas HEXS has the best sensitivity for the SSIP. Together they deliver a comprehensive picture of the cation and anion hydration and ion-paring structures. XADSR analysis shown in Figure 2, for 6.0 m aqueous $CaCl_2$, reveals that there are an insignificant number of Ca^{2+}-Cl^- CIP's, but there are approximately 3.4 SSIP's separated by about 4.98 Å. The results clearly illustrate how the strongly hydrated shell about the divalent Ca^{2+} hinders the formation of the CIP.

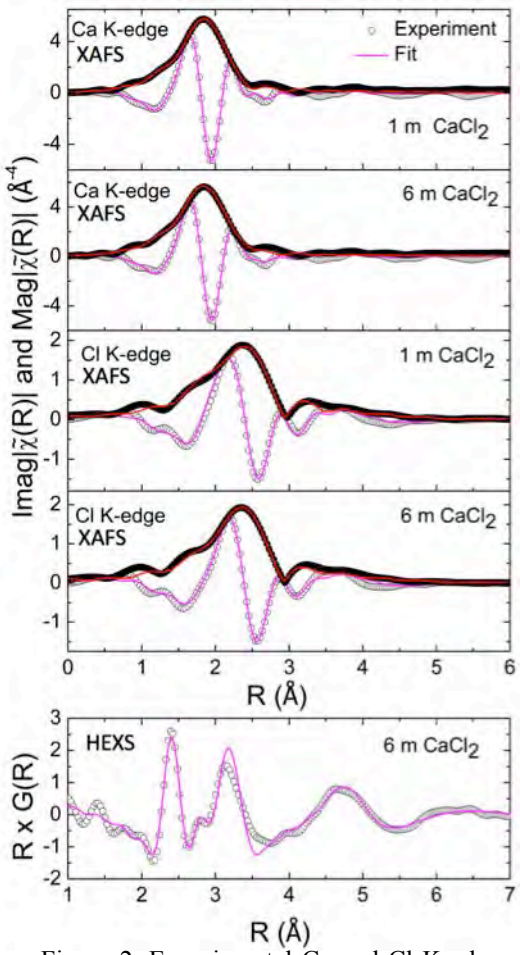

Figure 2. Experimental Ca and Cl K-edge XAFS and HEXS spectra and model fit for corefined structure of the Ca^{2+} / Cl^- solvent separated ion pair . The peak at 4.98 Å in the HEX spectra corresponds to the Ca^{2+} / Cl^- bond distance.

Hydronium Ion (H_3O^+) Pairing with Chloride (Cl^-). Experimental measurements of the structure of hydronium ion in water are scarce even though it is prevalent in a large number of biological, chemical, and geochemical systems. A recent effort using neutron diffraction (NDIS) attempts to decouple about 12 different pair distribution function. The advantage of XAFS is that it probes only the structure of the first peak in Cl-O pair distribution function comprising contributions from only Cl^-/H_2O and Cl^-/H_3O^+ interactions. These new XAFS measurements reveal that the structure of the Cl^-/H_3O^+ contact ion pair, as depicted in Fig. 3, is distinctly different from that of the H_2O structure about Cl^-. The Cl-O bond length (2.98 Å) for Cl^-/H_3O^+ is approximately 0.16 Å shorter than the Cl^-/H_2O bond. The bridging proton resides at an intermediate position between Cl and O at 1.60 Å from the Cl^- and approximately 1.37 Å from the O of the H_3O^+. The bridging-proton structure of this contact ion pair, (Cl-H-OH_2), is similar to the structure of the water Zundel ion, (H_2O-H-OH_2^+). In both cases there is a shortened Cl-O or O-O bond, and the intervening proton bond distances are substantially longer than for the covalent bonds of either HCl or H_2O. This XAFS study shows that, at lower concentrations (6 m HCl), the Cl^-/H_3O^+ ion pair is starting to form in appreciable amounts up to the point in the concentrated acid (16 m HCl) where all of the H_3O^+ species are paired with a Cl^-.

The Cl^-/H_3O^+ ion pair structure is difficult to reproduce in molecular dynamics simulations using classical intermolecular potentials. In fact, ab initio-based (DFT) molecular dynamics simulations capture some but not all of the measured local structure. Very recent results have

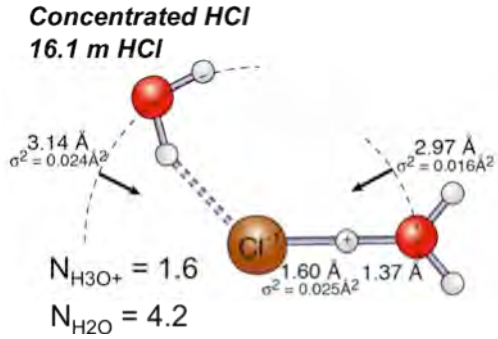

Figure 3. XAFS structural characterization of the Zundel-like H_3O^+/Cl^- ion pair. Only one of the waters hydrating the Cl^- is shown.

highlighted the role of nuclear quantum effects in the centering of the proton between the hydronium and chloride ions. Overall the XAFS results have provided key insights into this bulk aqueous structure.

First-row Transition Metal Hydration Structure: XAFS and ab initio MD Simulations. We completed a comprehensive study of many first-row transition metal ions. The water in the first hydration shell about these ions have a well-ordered octahedral structure giving rise to a series of strong multiple scattering signals (XAFS). We found that DFT-MD simulation (QM/MM, CPMD PBE96 , MM SPC/E) *quantitatively* reproduce these multiple scattering features. For instance, in the photoelectron multiple scattering region from 2 to 5.4 Å, the level of agreement is exceptional. The signal in this region is directly related to the photoelectron multiple scattering processes associated with both collinear 180° and triangular 90° O–ion–O paths. In order to achieve this level of agreement, the simulation must accurately predict the local pair distribution functions and angular distribution functions for these specific sets of O–ion–O atoms in the first shell structures. To our knowledge, this is the first time that any simulation has quantitatively modeled this series of multiple scattering features.

During this study we found that the default DFT pseudopotentials that are commonly used in electronic structure codes lead to metal-water distance errors of about 0.1 to 0.15Å. For the trivalent ions such as Cr^{3+} and Fe^{3+} this amounts to an error in the hydration enthalpy of about 400 kJ/mole from just the coulombic contribution alone. This distance error was corrected by adjusting the metal pseudopotentials by increasing the number of valence orbitals in the DFT calculation to include the 3s and 3p orbitals. Although these orbitals are not directly involved in bonding to the water, they are polarized by changes in the 3d bonding orbitals. The implications of these findings have far reaching consequences on how DFT-MD is deployed in describing aqueous ions in chemistry, interfaces and separations (e.g. lanthanide and actinides). Further this dramatic improvement in the simulation fidelity opens up the opportunity to quantitatively evaluate the XAFS higher order scattering features (> 4Å) that have mostly been ignored up to this point.

Future Plans

Cation-anion interactions in concentrated and high-temperature aqueous phase. The interaction of anions with cations in aqueous solutions underlies broad areas of biochemistry, geochemistry and atmospheric chemistry. To this day, there is an incomplete understanding of the interaction of simple salts such as Na^+ with Cl^- or of Li^+ with Cl^- dissolved in water. The electrostatic attractive interactions between counter ions are modulated by a delicate balance of different aqueous hydration effects that are not yet fully understood. We seek to define the relationship between the cation charge/size and the degree of chloride-cation interaction. Further, we seek to determine the precise nature of the cation-anion interaction potential in an aqueous system. We are exploring these systems with joint XAFS, HEXS, ND and MD analysis using both classical and DFT molecular dynamics methods. We are expanding this area of study by exploring the interaction of chloride with a series of monovalent and divalent cations in

concentrated aqueous solutions. The interaction of chloride (Cl-) with cations from the Group IA (Li^+, Na^+, K^+, Rb^+) and IIA (Be^{2+}, Mg^{2+}, Ca^{2+}, Sr^{2+}) elements is one of the primary interests since there are very few studies of these structures. The proposed study involves XAFS spectroscopy at the Cl K-edge using a new, low-Z cell that incorporates 200 nm thick Si_3N_4 windows (3 x 3 mm) . The same series of salts are being studied by both high energy x-ray diffraction (at APS) and by neutron diffraction (at SNS) to derive their longer range structure.

References to publications of DOE sponsored research (Oct. 1, 2009 - present)

1. J. L. Fulton, S. M. Kathmann, G. K. Schenter and M. Balasubramanian, "Hydrated Structure of Ag(I) Ion from Symmetry-Dependent, K- and L-Edge XAFS Multiple Scattering and Molecular Dynamics Simulations." **J. Phys. Chem. A** 113 (50), 13976-13984 (2009).
2. E. Cauet, S. Bogatko, J. H. Weare, J. L. Fulton, G. K. Schenter and E. J. Bylaska, "Structure and dynamics of the hydration shells of the Zn^{2+} ion from ab initio molecular dynamics and combined ab initio and classical molecular dynamics simulations." **J. Chem. Phys.** 132 (1), 194502 (2010).
3. G. S. Li, D. M. Camaioni, J. E. Amonette, Z. C. Zhang, T. J. Johnson and J. L. Fulton, "[CuCln](2-n) Ion-Pair Species in 1-Ethyl-3-methylimidazolium Chloride Ionic Liquid-Water Mixtures: Ultraviolet-Visible, X-ray Absorption Fine Structure, and Density Functional Theory Characterization." **J. Phys. Chem. B** 114 (39), 12614-12622 (2010).
4. J. L. Fulton, G. K. Schenter, M. D. Baer, C. J. Mundy, L. X. Dang and M. Balasubramanian, "Probing the Hydration Structure of Polarizable Halides: A Multiedge XAFS and Molecular Dynamics Study of the Iodide Anion." **J. Phys. Chem. B** 114 (40), 12926-12937 (2010).
5. J. L. Fulton and M. Balasubramanian, "Structure of Hydronium (H_3O^+)/Chloride (Cl^-) Contact Ion Pairs in Aqueous Hydrochloric Acid Solution: A Zundel-like Local Configuration." **J. Am. Chem. Soc.** 132 (36), 12597-12604 (2010).
6. Marcel Baer, Van-Thai Pham, John Fulton, Gregory Schenter, Mahalingam Balasubramanian, Christopher Mundy, "Is Iodate a Strongly Hydrated Cation?" **J. Phys. Chem. Letters**, 2, 2650–2654, (2011)
7. John L. Fulton, Eric J. Bylaska, Stuart Bogatko, Mahalingam Balasubramanian, Emilie Cauët, Gregory K. Schenter, John H. Weare, "Near quantitative agreement of model free DFT- MD predictions with XAFS observations of the hydration structure of highly charged transition metal ions." **J. Phys. Chem. Letters**, (2012, accepted)
8. Van-Thai Pham, John L. Fulton, "Ion-pairing in aqueous $CaCl_2$ and RbBr solutions: simultaneous structural refinement of XAFS and XRD data.", **J. Chem. Phys.**, (2012, accepted)

Ion Solvation in Nonuniform Aqueous Environments

Principal Investigator
Phillip L. Geissler
Faculty Scientist, Chemical Sciences, Physical Biosciences, and Materials Sciences Divisions

Mailing address of PI:
Lawrence Berkeley National Laboratory
1 Cyclotron Road
Mailstop: HILDEBRAND
Berkeley, CA 94720

Email: plgeissler@lbl.gov

Program Scope

Research in this program applies computational and theoretical tools to determine structural and dynamical features of aqueous salt solutions. It focuses specifically on heterogeneous environments, such as liquid-substrate interfaces and crystalline lattices, that figure prominently in the chemistry of energy conversion. In these situations conventional pictures of ion solvation, though quite accurate for predicting bulk behavior, appear to fail dramatically, e.g., for predicting the spatial distribution of ions near interfaces. We develop, simulate, and analyze reduced models to clarify the chemical physics underlying these anomalies. We also scrutinize the statistical mechanics of intramolecular vibrations in nonuniform aqueous systems, in order to draw concrete connections between spectroscopic observables and evolving intermolecular structure. Together with experimental collaborators we aim to make infrared and Raman spectroscopy a quantitative tool for probing molecular arrangements in these solutions.

Recent Progress

We have made significant recent progress in two major areas: (i) advancing the theory of nonlinear, surface-sensitive vibrational spectroscopy, and (ii) unraveling the thermodynamics of selective ion adsorption at the air-water interface. Our efforts in these two areas are distinct, but they are aimed towards the common purpose of understanding how small, charged solutes associate with a liquid's boundary.

Querying the structure and dynamics of macroscopic interfaces in the laboratory requires probes of a special nature. Measuring nonlinear susceptibilities of appropriate symmetry can, in effect, filter out signals from the bulk environment, which is centrosymmetric on average. The simplest vibrational version of these surface-sensitive probes, SFG, has become a popular method to characterize microscopic structure of aqueous interfaces in particular. In previous work we discovered a profound ambiguity common to all simulation-based approaches to computing SFG susceptibility. Obtaining a nonzero SFG signal from a liquid slab (the standard simulation geometry) requires artificially dividing the system into two opposing interfaces. The manner of this division (e.g., based on a

molecule's center of mass, or alternatively the oxygen atom, etc.) would appear to be an unimportant detail; in practice, however, predictions for SFG response are greatly sensitive to this convention. In recent work we have resolved this troubling ambiguity.

The traditional route to calculating spectroscopic observables begins with a multipole expansion of the molecular charge distribution. One typically focuses on the lowest-order non-vanishing terms in this expansion, often tantamount to considering a molecule as an electrical dipole that interacts with the radiation field at a single point. The standard formalism of SFG follows this prescription, employing the dipole approximation to express SFG subsceptibility χ_{SFG} in terms of averages over fluctuating molecular properties. It is the dipole-order susceptibility $\chi_{SFG}^{(D)}$ which we showed to suffer from the ambiguity described above: Seemingly equally valid ways to calculate $\chi_{SFG}^{(D)}$ yield very different results.

We have recently shown that this issue originates with a fundamental ambiguity in the molecular multipole expansion. Quadrupole-order response $\chi_{SFG}^{(Q)}$ is not forbidden in the centrosymmetric bulk environment; as a mathematical result, it (and all other even-order terms sharing this symmetry) becomes effectively one order higher in the multipole expansion. This conclusion places the theory of SFG on much firmer footing. In short, simulations cannot determine $\chi_{SFG}^{(D)}$ unambiguously because it is not a well-defined physical observable.

Our other major recent achievement has been to establish key microscopic factors that govern spatial distributions of dissolved salts in heterogeneous environments. Long-standing debates over the surface propensities of small ions were reinvigorated a decade ago by computer simulations demonstrating that charged model solutes can adsorb strongly to the air-water interface. From the perspective of classic theories of ion solvation in bulk polar solvents, this behavior is quite counterintuitive. Despite a significant amount of experimental and theoretical work in this area, a deep appreciation of the microscopic factors that distinguish interfacial solvation from bulk scenarios has remained outstanding.

In recent work, we have found that capillary waves are a key contributor to the thermodynamics of ion adsorption. This project proceeded in close collaboration with Rich Saykally's group, who measured interfacial SHG signals from simple inorganic ions as a function of concentration and temperature. These experiments revealed the enthalpy and entropy of adsorption to both be significantly negative, contrary to widespread assumptions based on conventional theories. Our accompanying computer simulations show this counterintuitive behavior to be quite revealing of microscopic mechanism.

The extremely favorable energy of solvating a small ion in a polar liquid is a consequence of induced polarization in their surroundings. As the solute approaches an interface, less solvent is available to polarize; energy is expected to increase considerably as a result. What ultimately counteracts this rise, we have shown, is a decrease in solvent-solvent interaction energy that is neglected in conventional applications of DCT. At the interface, volume excluded by a solute has an effect of reducing the area of contact

between liquid and vapor. Because this surface is energetically quite costly, the penalty of weakened dielectric response is offset. For an ion sufficiently large or weakly charged, the energetic benefit can substantially outweigh the dielectric cost. From this understanding we developed a simple but accurate local energy approximation, based on changes in solvent population in surface, bulk, and coordination regions.

Spatially local aspects of entropy, on the other hand, are unlikely to explain our measured and computed thermodynamic trends. As an ion sheds its coordination shell at the interface, orientational constraints on nearby solvent molecules are released, suggesting incorrectly a positive entropy of adsorption. Capillary waves, featuring nonlocal collective motions, respond to the solute's presence in a very different way. According to simulations, adsorbed ions suppress height fluctuations of the liquid's surface, even several molecular diameters away from the ion. Using a harmonic model in the spirit of capillary wave theory, we have used computed statistics of topographical fluctuations to estimate the accompanying loss of entropy. The sign and magnitude of this change are in accord with observed temperature dependence of ions' surface propensities.

Future Plans

A major goal for the next few years is to construct a predictive theory for ions' spatial distributions near a liquid-vapor interface. Our previous work has set the stage for this development, pointing to essential physical ingredients missing in previous approaches. With this knowledge we are poised to formulate a tractable mathematical description of this phenomenon, capable of predicting density profiles, thermodynamic driving forces, and key experimental control parameters.

The picture of capillary pinning we have advanced as a central aspect of ion adsorption can, by itself, be captured by a simple caricature of solvent density fluctuations near a liquid-vapor interface. An important first step towards a comprehensive theory for ions' surface propensities is thus to understand how the spectrum of capillary fluctuations in reduced models such as a lattice gas are sensitive to the forces exerted by small solutes. We have recently undertaken studies towards this end, using both theory and simulation. Preliminary results point to intuitive explanations of behavior we have observed in molecular systems.

A minimal model for ion adsorption should combine such descriptions of surface height fluctuations together with a representation of the polarization fluctuations that dominate ion solvation in bulk solution. Conventional applications of DCT miss important features of ion adsorption observed in computer simulations. One aim of our ongoing work is to adapt the DC description, so appealing in its simplicity and generality, to capture the dominant energetics of ion adsorption.

Our focus thus far has been on understanding properties of single ions in solution. In particular, we have aimed to predict free energy profiles in the microscopic vicinity of a liquid-vapor interface. While this quantity is well-defined at infinite dilution, many macroscopic properties require attention to correlations among ions. Energy applications often involve sufficiently high ionic strength that such correlations cannot be neglected.

Moreover, SHG studies by Saykally's group indicate that finite-concentration effects on adsorption appear at relatively low concentration. In previous theoretical work Debye-Hückel calculations have been performed in attempt to gauge these effects. As with conventional applications of DCT, however, this approach neglects many aspects of interfacial physics we now know to be important.

We aim to begin characterizing multi-ion correlations in the interfacial environment. The screening effects described by Debye-Hückel theory are of course an important component. But the adsorption mechanisms we have revealed suggest other, rather different consequences of ions' association. For example, the thermodynamics of interfacial pinning could favor clustering of two or more solutes, since one localized interfacial constraint is likely to be less costly than pinning at many dispersed sites. Similar mechanisms of solute aggregation have been discussed in the context of large molecules embedded in an elastic membrane. In addition, it is not clear how the energetics of excluding volume in the interfacial zone will depend upon solutes' spatial arrangement. We plan to explore these behaviors in computer simulations, both of detailed molecular models and of the reduced models we have described. Computing and parsing the reversible work required to separate an ion pair, as a function of their height, is an important first step in this direction.

Our resolution of ambiguities in calculating SFG susceptibility is formally reassuring, and serves to identify a well-defined observable quantity. As a practical matter, however, it indicates that estimating a true observable is substantially more difficult than was previously recognized. The machinery to calculate dipole-order susceptibility was developed in many stages, drawing from years of bulk vibrational studies. The basic perturbation theory for electric quadrupole contributions to SFG has been worked out, but many steps remain to make its calculation feasible. Furthermore, the quadrupole-order susceptibility $\chi_{SFG}^{(Q)}$ includes coupling of a molecule's magnetic dipole with the radiation field. One aspect of future work will be developing the complete formal theory we have presented into a workable computational scheme. Extending this theoretical treatment to the case of SHG would enable direct comparisons with Saykally's experiments.

Recent Publications

S.J. Byrnes, P.L. Geissler, and Y.R. Shen, "Ambiguities in Surface Nonlinear Spectroscopy Calculations," *Chem. Phys. Lett. Frontiers*, **516**, 115 (2011).

D. E. Otten, P. R. Shaffer, P. L. Geissler, and R. J. Saykally, "Elucidating the Mechanism of Selective Ion Adsorption to the Liquid Water Surface," *Proc. Natl. Acad. Sci.*, **109**, 701 (2012).

S. Vaikuntanathan, P. R. Shaffer, and P. L. Geissler, "Adsorption of solutes at liquid-vapor interfaces: insights from lattice gas models," to appear in *Faraday Discuss.*, **160** (2012).

P. L. Geissler, "Water interfaces, solvation, and spectroscopy," submitted to *Ann. Rev. Phys. Chem.* (2012).

Program Title: Theoretical Developments and Applications to Surface Science, Heterogeneous Catalysis, and Intermolecular Interactions

Principal Investigator: Mark S. Gordon, 201 Spedding Hall, Iowa Sate University and Ames Laboratory, Ames, IA 50011; mark@si.msg.chem.iastate.edu

Program Scope. Our research effort combines new theory and code developments with applications to a variety of problems in surface science and heterogeneous catalysis, as well as the investigation of intermolecular interactions, including solvent effects in ground and excited electronic states and the liquid-surface interface. Many of the surface science studies are in collaboration with Dr. James Evans. Much of the catalysis effort is in collaboration with Drs. Marek Pruski and Igor Slowing.

Recent Progress. Chemical processes on and with the Si(100) surface have been one research focus. The diffusion of Al on Si(100) was studied using an embedded cluster model and multi-reference electronic structure methods, including CASSCF explorations of the doublet and quartet potential energy surfaces and improved energies with multi-reference perturbation theory. The details of the potential energy surfaces depend critically on the presence of the bulk that is represented by molecular mechanics (MM). Only when edge effects are minimized by embedding the quantum mechanics (QM) region in a much larger MM region does a consistently realistic picture emerge. Similar results are obtained in the recent study of Ga on Si(100). It appears that both Al and Ga can form metal wires on the Si(100) surface. The etching and diffusion of O atoms on the Si(100) surface was also studied with the QM/MM model and both multi-reference methods and the cluster-in-molecule (CIM) CR-CC(2,3) coupled cluster method developed by the Piecuch group. The latter method combines a coupled cluster method, CR-CC(2,3), that is able break single bonds and account for the diradical character that is inherent in the Si(100) surface) with a novel method (CIM) for greatly speeding up accurate coupled cluster calculations. The CIM method enables the calculation of large clusters that can diminish the need for the MM part of the embedding scheme. Two complementary approaches for increasing the sizes of clusters that can be studied with accurate QM methods are the occupation restricted multiple active space (ORMAS) and the fragment molecular orbital (FMO) methods. The ORMAS method divides a large, intractable active space into chemically sensible subspaces, thereby making a very difficult calculation feasible. The utility of the ORMAS method has been demonstrated with Si(100) clusters of increasing size. The FMO method divides a large species into fragments to facilitate accurate QM calculations on very large systems. A fully analytic FMO/Hartree-Fock gradient has been derived and implemented in GAMESS, to enable geometry optimizations and molecular dynamics simulations. Mesoporous silica nanoparticles (MSN) have received increasing attention due to their catalytic capabilities. Because the MSN species are very complex, we have implemented the ReaxFF force field into GAMESS and are exploring the possibility of using this method to study catalytic processes in MSN species. A combined ReaxFF/NMR study, in collaboration with the Pruski group, demonstrated that the ReaxFF method can produce structural data that are consistent with the temperature-dependent NMR data.

The effective fragment potential (EFP) method that is designed to be a sophisticated model potential designed to accurately describe intermolecular interactions has been interfaced with the FMO method, so that low-cost explicit solvent effects can be incorporated into FMO studies. Both FMO-EFP energies and analytic gradients are now available. EFP interfaces have also been derived and implemented for configuration interaction with single excitations (CIS), multi-reference, multi-state perturbation theory, and equations-of-motion (EOM) coupled cluster theory. These interfaces provide an array of tools that are available to study solvent effects on electronic spectra and photochemistry. Initial studies have addressed the aqueous solvation of the n-π^* and π–π^* excitations in uracil. These are by far the most accurate calculations on this topic. The EFP method was also applied to the study of aqueous solvation of several anions, including bihalide ions and the nitrate ion. The latter study was particularly important, because it demonstrated that, contrary to predictions from simulations with (mostly inadequate) simple model potentials, only a modest number of water molecules are needed to force the anion to the interior. New advances in the EFP method include the development of a general approach to damping the various contributions to the potential and the development and implementation of the QM-EFP exchange repulsion.

Time-dependent density functional theory (TDDFT) is in principle a good compromise between accuracy and computational cost for studying electronic excited states. However, because DFT, and therefore TDDFT, is at it core a single determinant method, there are some phenomena that are very difficult to address with TDDFT. One very important phenomenon is the conical intersections that occur when two or more potential energy surfaces cross. Conical intersections are ubiquitous, and therefore very important, in photochemistry and photobiology. We have implemented the Krylov spin-flip approach with TDDFT and have demonstrated for ethylene, and most recently stilbene, that the new combined method can correctly describe conical intersections and the associated detailed structural information.

“Composite” methods refer to the use of multiple levels of theory to predict accurate thermodynamic properties of molecules. Most composite methods can predict very accurate thermochemistry, but are not reliable for the prediction of reaction mechanisms, barrier heights and (therefore) kinetics. We have recently developed a new composite method, called ccCA-CC(2,3), based on the Piecuch CR-CC(2,3) method, that can predict both thermodynamics and reaction mechanisms with very high accuracy.

Advances have also been made in high performance computational chemistry. An INCITE grant has enabled us to have access to the BlueGene /P at Argonne, where we have demonstrated that the FMO method allows essentially perfect scaling to the petascale (more than 131,000 processors).

Future Plans. The development of the FMO and CIM-CR-CC(2,3) methods will allow us to explore fully quantum studies of heterogeneous catalysis, in which we can minimize edge effects, because these methods will allow us to expand the size of the QM region in a computationally efficient manner. We are also developing a new embedded cluster method SIMOMM-Rx that replaces the Tinker force field with ReaxFF. Fully analytic

FMO/DFT gradients will be developed. The CIM-CR-C(2,3) method will be applied to studies of phenomena on the Si(100) surface, such as more extensive studies of diffusion of Ga and In. We will explore the use of ORMAS-PT2 for the adsorption of substrates on conducting metals, since QM/MM embedded cluster methods are not appropriate for such problems. Preliminary FMO studies have been performed on model MSN species at the Hartree-Fock level of theory with a minimal basis set. The agreement with the fully ab initio method is excellent, so we will now apply FMO with higher levels of theory and reliable basis sets. The EFP-QM exchange repulsion analytic gradients have been derived, and these will now be implemented so that any solvent can be studied. Related to this, we will work with the ReaxFF developers to obtain improved parameters for silica and silica-X, where X represents atoms in the important substrates. This will improve the ReaxFF capability to address heterogeneous catalysis on MSN species.

The spin-flip TDDFT method will be interfaced with the EFP method, so that one can explore photochemistry and photobiology, including conical intersections, in the presence of solvent. The SF-TDDFT method will also be interfaced with our non-adiabatic (vibronic) coupling matrix element code, so that one can study non-adiabatic interactions in solution.

References to publications of DOE sponsored research 2009-present

1. L. V. Slipchenko and M.S. Gordon, "Water-benzene interactions: An effective fragment potential and correlated quantum chemistry study", J. Phys. Chem A., 113, 2092 (2009).
2. L. Slipchenko and M.S. Gordon, "Damping functions in the effective fragment potential method", Mol. Phys., 107, 999 (2009).
3. D. Kina, P. Arora, A. Nakayama, T. Noro, M.S. Gordon, and T. Taketsugu, "QM/MM excited-state molecular dynamics study of coumarin 151 in water solution", Int. J. Quantum Chem., 109, 2308 (2009).
4. M.S. Gordon, J.M. Mullin, S.R. Pruitt, L.B. Roskop, L.V. Slipchenko and J.A. Boatz, "Accurate Methods for Large Molecular Systems", J. Phys. Chem. B (Invited Centennial Feature Article), 113, 9646 (2009).
5. T. Nagata, D. Fedorov, K. Kitaura, and M.S. Gordon, "A Combined Effective Fragment Potential - Fragment Molecular Orbital Method. I. The Energy Expression and Initial Applications", J. Chem. Phys., 131, 024101 (2009)
6. D.D. Zorn, M.A. Albao, J.W. Evans, and M.S. Gordon, "Binding and Diffusion of Al Adatoms and Dimers on the Si(100)-2x1 Reconstructed Surface: A Hybrid QM/MM Embedded Cluster Study", J. Phys. Chem. C, 113, 7277 (2009).
7. Y. Miller, J. Thomas, D.D. Kemp, B. Finlayson-Pitts, M.S. Gordon, D. Tobias, and R.B. Gerber, "Structure of Large Nitrate-Water Clusters at Ambient Temparatures: Simulations with Effective Fragment Potentials and Force Fields with Implications for Atmospheic Chemistry", J. Phys. Chem. A, 113, 12805 (2009).
8. N. Minezawa and M.S. Gordon, "Optimizing Conical Intersections by Spin-Flip Density Functional Theory: Application to Ethylene", J. Phys. Chem. A, 113, 12789 (2009).
9. D.D. Kemp and M.S. Gordon, "Aqueous Solvation of Bihalide Ions", J. Phys. Chem. A, 114, 1298 (2010).

10. D.D. Kemp, J. Rintelman, M.S. Gordon, and J.H. Jensen, "Exchange Repulsion between Effective Fragment Potentials and *Ab Initio* Molecules", Theor. Chem. Accts., 125, 481 (2010).
11. Y. Ge, M.S. Gordon, F. Battaglia, and R.O. Fox, "Theoretical Study of the Pyrolysis of Methyltrichlorosilane in the Gas Phase. 3. Reaction Rate Constants", J. Phys. Chem. A, 114, 2384 (2010).
12. A. Asadchev, V. Allada, J. Felder, B.M. Bode, T.L. Windus, and M.S. Gordon, "Uncontracted Rys Quadrature Implementation of up to g Functions on Graphical Processing Units", J. Comp. Theor. Chem., 6, 696 (2010).
13. P. Arora, L.V. Slipchenko, S.P. Webb, A. DeFusco, and M.S. Gordon, "Solvent-Induced Frequency Shifts: Configuration Interaction Singles combined with the Effective Fragment Potential Method, J. Phys. Chem. A, 114, 6742 (2010).
14. P. Arora, W. Li, P. Piecuch, J.W. Evans, M. Albao, and M.S. Gordon, "Diffusion of atomic oxygen on the Si(100) surface", J. Phys. Chem. C, 114, 12649 (2010).
15. D. Ghosh, D. Kosenko, V. Vanovschi, C.F. Williams, J.M. Herbert, M.S. Gordon, M.W. Schmidt, L.V. Slipchenko, and A.I. Krylov, "Non-covalent interactions in extended systems described by the Effective Fragment Potential method: Theory and application to nucleobase oligomers", J. Phys. Chem. A, 114, 12739 (2010).
16. T Nagata, D.G. Fedorov, K. Kitaura, and M.S. Gordon, "A combined effective fragment potential-fragment molecular orbital method. II. Analytic gradient and application to the geometry optimization of solvated tetraglycine and chignolin", J. Chem. Phys., 134, 034110 (2011).
17. T. Nagata, K. Brorsen, D.G. Fedorov, K. Kitaura, and M.S. Gordon, "Analytic energy gradient in the fragment molecular orbital method", J. Chem. Phys., 134, 124115 (2011).
18. A. DeFusco, J. Ivanic, M.W. Schmidt, and M.S. Gordon, "Solvent-Induced Shifts in the Electronic Spectra of Uracil", J. Phys. Chem. A, 115, 4574 (2011).
19. S. Nedd, C.-H. Tsai, I.I. Slowing, M. Pruski, and M.S. Gordon, "Using a Reactive Force Field to Correlate Mobilities Obtained from Solid-State ^{13}C NMR on MesoporousSilica Nanoparticle Systems", J. Phys. Chem. C, 115, 16333 (2011).
20. A. Devarajan, T.L. Windus, and M.S. Gordon, "Implementation of Dynamical Nucleation Theory Effective Fragment Potentials (DNTEFP) method for modeling aerosol chemistry", J. Phys. Chem. A, 115, 13987 (2011).
21. L. Roskop, J.W. Evans, and M.S. Gordon, "The adsorption and diffusion of gallium adatoms on the Si(100)-2x1 reconstructed surface: An MCSCF study utilizing molecular surface clusters", J. Phys. Chem. C, 115, 23488 (2011).
22. M.S. Gordon, D.G. Fedorov, S.R Pruitt, and L.V. Slipchenko, "Fragmentation Methods: A Route to Accurate Calculations on Large Systems", Chem. Rev, 112, 632 (2012) (INVITED).
23. G.D. Fletcher, D.G. Fedorov, S.R. Pruitt, T.L. Windus and M.S. Gordon, "Large-Scale MP2 Calculations on the Blue Gene Architecture Using the Fragment Molecular Orbital Method", J. Comp. Theor. Chem., 8, 75 (2012).
24. S. Nedd, N.J. DeYonker, A.K. Wilson, P. Piecuch, and M.S. Gordon, "Incorporating a Completely Renormalized Coupled Cluster Approach into a Composite Method for Thermodynamic Properties and Reaction Paths", J. Chem. Phys., 136, 144109 (2012).

Dynamics of Electrons at Interfaces on Ultrafast Timescales

Charles B. Harris P.I.
Chemical Sciences Division
Lawrence Berkeley National Lab
1 Cyclotron Road, Mail Stop Latimer
Berkeley, CA 94720
CBHarris@berkeley.edu

Program Scope:

The interface between two materials defines the behavior of electronic devices. In the case of photovoltaic cells, the interface between p-type and n-type materials drives charge separation. In the case of supercapacitors, charge is stored by molecular reorganization at the metal-solvent interface. The physical phenomena governing electronic properties at surfaces and interfaces are unique from the bulk solid; they are often poorly understood. Our research aims to explore the molecular mechanisms governing energy levels and dynamics of electrons at the metal-molecule interface. We use femtosecond time and angle resolved two-photon photoemission spectroscopy to probe the energy and momentum of electrons in thin film adlayers on a metal surface. Briefly, a pump pulse excites an electron from below the Fermi level of the substrate into a previously unoccupied state below the vacuum level. After a variable time delay, a probe pulse photoemits the electron into a time-of-flight detector. The low energy electrons generated in this process gives TPPE high surface sensitivity and high energy resolution. Angle resolved measurements allow TPPE to collect electronic spectra as a function of momentum. Momentum is conserved upon photoemission, and by changing the angle of the surface relative to the detector, momentum resolved band-structure can be determined. Localization can be determined by the curvature and intensity of the measured band structure. Our work has investigated several cases where delocalized electrons collapse into localized states on the femtosecond timescale.

Our recent work has primarily studied two classes of processes: electronic coupling within an ultrathin molecular layer and relaxation at solvent/metal electrode interfaces due to molecular reorganization within a film. In addition to these ongoing projects, we are continuing work that attempts to study the excitonic states of thin organic semiconductors relevant to organic photovoltaics. Finally, we are beginning work studying a series of unique self-assembled monolayer systems that aim to test theoretical predictions about how energy levels are aligned at metal/molecule interfaces.

Recent Progress:

Electron Solvation at the Ionic Liquid /Electrode Interface:

Room temperature ionic liquids are a new class of solvent consisting of charge separated ions. These materials do not need solute molecules to have ionic conductivity. As a result, they have attracted significant attention for uses in batteries, supercapacitors, photovoltaic Gratzel cells, catalysis, and electrochemical deposition. The high bulk viscosity of these materials is a kinetic barrier limiting bulk conductivity, and this has limited implementation. The slow solvent response of bulk ionic liquids has been measured by several spectroscopic techniques. We have studied the solvent response directly at the ionic liquid / metal electrode interface. We have found that the interfacial response occurs several orders of magnitude faster than the bulk. TPPE was used to measure the dynamic energy shifts associated with the solvent response, and spectroscopic results were used to identify and quantify molecular mechanisms. Finally, a

temperature dependent, equilibrium order-disorder transition was measured. This phase transition was observed by both the sample work function and the dynamic solvent response, providing further insight into the interface-specific mechanism of solvation.

Symmetry and Spatial Extent and of Image Electrons in Phthalocyanines/Ag(111):

Image state electrons typically exist within a few angstroms of a metal surface, and as a result, it is known that they are good probes of molecular adsorbates. The electron affinity and dielectric response of the molecule are known to modify the energetic position of the image state. The effects of spatial extent and symmetry of the image state wave function are less well known. Angle resolved two photon photoemission is used to measure the energy and local probability density of the image state as a function of the electronic momentum. Photoemission from high angles is able to probe the edge of the second Brilluoin zone. Using both quantum mechanical modeling and experimental measurements of photoemission, we show that the image state in a film of metal-phthalocyanines remains delocalized, but the wave function is modified significantly by interaction with the phthalocyanines surface. The image state takes on both the periodicity and the symmetry of the phthalocyanine surface crystal structure. Comparing model and experiment, we are able to estimate the potential energy corrugation across the surface that is experienced by an image state residing in an adsorbed molecular layer.

Explanation of the Anomalous Interfacial Capacitance of DMSO:

Charge injection from a metal to a solvent displays an interfacial capacitance as the molecular dipoles at the interface reorient. Dimethylsulfoxide (DMSO) is a common electrochemical solvent with an unusually low differential capacitance. TPPE is used to probe the solvent response to optical charge injection of a delocalized image state electron. TPPE is able to directly measure dynamic energy shifts resulting from solvation of the free electron. Angle resolved measurements observe the collapse of a free electron into a localized state. A single monolayer coverage shows a very small solvent response, whereas in a two monolayer coverage, the solvent solvates strongly. By comparisons with models for interfacial capacitance, we are able to determine mechanisms of capacitive response. We were able to experimentally prove proposed mechanisms in which strong binding to the metal electrode hinders dipole-reorientation in the first monolayer and results in a small interfacial capacitance.

Ongoing and Future Work:

Molecular Mechanisms of Solvation in Ionic Liquids:

Ionic liquids constitute a broad and poorly understood new class of solvents. In our previous work on charge solvation in ionic liquids, we were able to observe the ultrafast solvent response to charge injection at a metal electrode interface. The solvent response was found to differ from the bulk. Molecular mechanisms of this interface-specific charge solvation were quantified, using TPPE characterization of the electronic states and energies involved in charge injection. Further, temperature dependent measurements of the work function and reorganizational energy were able to identify an order-disorder transition. This proof-of-principle experiment opens up new questions and allows us to address several unanswered questions in the literature. Is the solvent response dominated by the cation or anion? Is the electron always found on the cation or can it sometime exist on the anion as has been proposed theoretically? Is the response different for a cation-dominated metal interface versus a mixed interface? We can directly answer these questions by examining solvent response as a function of chemical identity in a set of ionic liquids. These results will be able to extract general trends of chemical identity and solvation mechanisms.

Studying the Electronic Effects of Low Dimensional Phase Changes:

Molecular ordering in the first monolayer templates the ordering of subsequent layers and affects the performance molecular electronic devices. The intermolecular interactions that govern growth and ordering of molecular epitaxy are not fully understood. This is particularly important as the interactions in technologically relevant organic semiconductors are typically very weak and may be long ranged. Several groups have recently attempted to determine the intermolecular forces through both theoretical calculations and experimental determinations of phase diagrams. We use TPPE to measure a phase transition in submonolayer coverages of metallated phthalocyanines. Two phases are found to exist, a crystalline island phase and a diffusing 2D gas phase. These phases are found to coexist, and can be observed separately by taking advantage of a coverage-dependent image state energy. Temperature and coverage dependent measurements have found a non-equilibrium phase change as a function of coverage and temperature. Kinetic Monte Carlo simulations suggest that this is due to entropic effects and a weak intermolecular attraction. Our preliminary results and methods should be generally applicable to phase behavior in other molecular systems.

The Effects of Lattice Symmetry and Size on the Electronic States:

TPPE has evolved from studying model small molecules, such as pentanes and benzene, to larger, more device relevant molecules, such as those used in organic photovoltaic materials. These materials have lattice constants on the same lengths scale as low energy electrons at the surface meaning that the organization of the molecules at the interface can substantially effect the electronic structure of the image potential states. Previous work in our group studied the modification of the image state band structure using well-characterized and device relevant metallated phthalocyanine monolayers. Our future work plans to extend these studies in two directions. The first will use the three-fold symmetric subphthalocyanine molecule to study the effect of the lattice symmetry on the band-structure modification. The second will use the recently developed two-dimensional metal organic frameworks to study the effects of changing the lattice constant on the strength of the electron-lattice interaction. These studies will extend our understanding of the band-folding phenomenon and inform our future studies of device relevant molecules, allowing us to disentangle the effects of the lattice constant and symmetry of the system from the effects derived from molecular origins.

Excitations in Organic Semiconductors:

Organic semiconductors have emerged as large area of research due to their promising role in photovoltaics and electronic devices. Organic electronic devices have the advantage of being cheaper to produce, ease of fabrication, flexibility of devices, use of earth abundant materials, and greater absorption in the visible region. Unfortunately, current organic electronic devices exhibit poorer efficiencies than their inorganic counterparts. The loss in efficiency is believed to be due largely to difficulty in separating the exciton, an electron-hole pair, in the organic active material. Separation of the exciton requires an interface of differing organic materials, called the donor acceptor interface. The main criteria for separating the exciton into free charges is that the difference in LUMO energies between the differing materials be greater than binding energy of the exciton. With all the advances made in organic photovoltaics current efficiencies remain largely too low to be implementable on a large scale.

To date, there are few experimental studies accurately observing and quantifying charge separation at the organic donor-acceptor interface. Two photon-photoemission offers unique advantages for studying exciton and electron movement in organic photovoltaic systems. The technique provides the ability to create a well defined electronic donor/acceptor sample

mimicking real organic photovoltaic devices. The time and angle resolution of 2PPE will allow direct observation of the time scale of exciton separation and spatial extent. By studying these systems in a more fundamental and controlled manner, we can build the understanding of exciton separation and material properties that allow separation, and ultimately lead to better design and improved efficiency.

Fermi Level Pinning in Self-Assembled Monolayers:

Although crucial to most organic electronic devices, the energy level alignment at the organic/metal interface is not always well understood. Hybridization of the molecular and metals states combined with charge transfer and polarization effects make the prediction of the resulting electronic structure difficult. In order to better understand the interplay of these processes, many groups rely on quantum calculations performed at the plane wave or tight binding density function levels. Our research group has chosen to study a system predicted to have an unusual mechanism governing the energy level alignment.

The Fermi level pinning phenomenon is known to exist for some metal/organic interfaces. The 4-aminopyridine self-assembled monolayer has been predicted to have a delocalized unoccupied molecule-derived state at a binding energy greater than the work function of the Ag(111) surface. It is sometimes believed that this results in either partial or integer charge transfer and the partial filling of the molecular level. It has been proposed, however, that because of the large distance between the metal and the molecular state, the charge transfer is electrostatically disfavored. Instead a polarization is induced into the monolayer that moves the molecular state up in energy, allowing it to remain directly above the Fermi level. TPPE will be able to determine the occupancy of this molecular level and measure its coupling to the substrate which should make it possible to determine which Fermi level pinning mechanism is at work. Additional measurements on a related molecule, 4-methylpyridine, should allow us to further clarify the result because the molecular state in question resides on the amino group of the former molecule and is absent in the 4-methylpyridine.

Articles Supported by DOE Funding from 2010-2012 (1-4) and References:

[1] J.E. Johns, E.A. Muller, S.A. Garret-Roe, C.B. Harris. "Relaxation Dynamics in Image Potential States at Solid Interfaces", Dynamics at Solid State Surfaces and Interfaces: Volume 1: Current Developments (Book Chapter), Wiley-VCH, Weinheim, 75-97, (2010).

[2] E.A. Muller, B.W. Caplins, J.E. Johns, C.B. Harris. “Quantum Confinement and Anisotropy in Thin Film Molecular Semiconductors”, *Phys. Rev. B.*, 83(16), 165422-1 - 165422-5, (2011).

[3] E.A. Muller, M.L. Strader, J.E. Johns, A. Yang, B.W. Caplins, A.J. Shearer, D.E. Suich, C.B. Harris. “Femtosecond Solvation of Excess Electrons at the Ionic Liquid/Metal Electrode Interface”, *J. Am. Chem. Soc. (Submitted Aug. 2012)*

[4] Johns, J. Watching electrons transfer from metals to insulators using two photon photoemission, *LBNL Thesis* 2010, OSTI ID: 985947.

[5] Strader, M. Ultrafast electron dynamics of ultrathin films of electrochemical solvents adsorbed on an Ag(111) Substrate, *LBNL Thesis,* 2008, UMI:3331805.

[6] Strader, M. L.; Garrett-Roe, S.; Szymanski, P.; Shipman, S. T.; Johns, J. E.; Yang, A.; Muller, E.; Harris, C. B. “The ultrafast dynamics of image potential state electrons at the dimethylsulfoxide/Ag(111) interface”, *J. Phys. Chem. C* 2008, *112,* 6880.

[7] Yang, A.; Shipman, S. T.; Garrett-Roe, S.; Johns, J.; Strader, M.; Szymanski, P.; Muller, E.; Harris, C. B. “Two-photon photoemission of ultrathin film PTCA morphologies on Ag(111)”, *J. Phys. Chem. C* 2008, *112,* 2506.

Program Title: "SISGR: Single Molecule Chemical Imaging at Femtosecond Time Scales"
(DOE Grant Number: DE-SC0001785)

PI: Mark C. Hersam, Professor of Materials Science and Engineering, Chemistry, and Medicine; Northwestern University, 2220 Campus Drive, Evanston, IL 60208-3108;
Phone: 847-491-2696; Fax: 847-491-7820; E-mail: m-hersam@northwestern.edu;
WWW: http://www.hersam-group.northwestern.edu/

Co-PIs: Matthias Bode (Argonne National Lab), Jeffrey R. Guest (Argonne National Lab), Nathan P. Guisinger (Argonne National Lab), George C. Schatz (Northwestern University), Tamar Seideman (Northwestern University), Richard P. Van Duyne (Northwestern University)

1. Program Overview

Imaging molecular functionality with atomic spatial resolution and ultrafast temporal resolution will enable improved understanding of light-matter interactions and thus has the potential to impact the design of photovoltaic, photosynthetic, and photocatalytic materials and devices. While ultra-high vacuum (UHV) scanning tunneling microscopy (STM) can image and manipulate single molecules with atomic precision on surfaces, its temporal resolution is typically limited to the millisecond bandwidth of current preamplifiers. Furthermore, scanning tunneling spectroscopy (STS) only provides indirect chemical identification via measurements of the electronic density of states. On the other hand, pump-probe spectroscopy with ultrafast lasers can routinely achieve femtosecond temporal resolution. In addition, chemical fingerprinting can be achieved with vibrational spectroscopies such as surface-enhanced Raman spectroscopy (SERS). However, these optical techniques struggle to overcome the diffraction limit, which often implies spatial resolution at the micron scale. Our SISGR team seeks to overcome the respective limitations of UHV STM and laser spectroscopy by integrating these techniques into one experimental platform. Significant progress has made including the demonstration of surface-enhanced femtosecond stimulated Raman spectroscopy (SE-FSRS), single molecule tip-enhanced Raman spectroscopy (SM-TERS), and ultra-high vacuum tip-enhanced Raman spectroscopy (UHV-TERS). In parallel, new surface chemistries have been developed such as organic self-assembled monolayers stabilized via cooperative hydrogen bonding, surface photopolymerization, covalently modified graphene, and molecular *p-n* junctions based on pentacene and fullerenes. Since the systems and substrates chosen for this work are directly applicable to dye-sensitized solar cells, organic photovoltaics, and photocatalysis, this research program has provided insight into emerging energy technologies in addition to impacting the fundamental scientific goals outlined in the DOE Grand Challenges.

2. Recent Progress

2.1. Ultrafast Single-Molecule Raman Spectroscopy

A primary goal of this SISGR program is the development of tools and techniques that enable ultrafast Raman spectroscopy with single molecule sensitivity. Toward this end, progress has been made in several areas:

(1) *Surface-enhanced femtosecond stimulated Raman spectroscopy (SE-FSRS)*: A proof-of-principle experiment on SE-FSRS demonstrated a significant advance in combining the fields of plasmonics and ultrafast spectroscopy. Briefly, the plasmonic focusing of electromagnetic fields long used for surface-enhanced Raman spectroscopy (SERS) have been integrated with the ultrafast structural technique of femtosecond stimulated Raman spectroscopy (FSRS). Using a

100 kHz amplifier, SE-FSRS was successfully demonstrated on Au plasmonic nanoantennas with approximately 0.5 monolayers of *trans*-1,2-bis(4-pyridyl)ethylene (BPE) as the adsorbate.

(2) *Single molecule tip-enhanced Raman spectroscopy (SM-TERS)*: A second experimental advance is the application of the isotopologue proof for single molecule SERS (SM-SERS) to SM-TERS. Two isotopologues of Rhodamine 6G with unique vibrational signatures were used for this proof. A combination of experimental and theoretical studies provides a detailed view of the isotopic response of Rhodamine 6G–d_0 (R6G–d_0) and Rhodamine 6G–d_4 (R6G–d_4) in the 600 – 800 cm^{-1} region. The single molecule nature of the TERS experiment is confirmed through two lines of evidence. First, the vibrational signature of only one isotopologue was observed from multiple spectra. Second, spectral wandering of the peak location was observed, consistent with the observation of only a single molecule.

(3) *Ultra-high vacuum tip-enhanced Raman spectroscopy (UHV-TERS) integrated with molecular-resolution ultra-high vacuum scanning tunneling microscopy (UHV STM)*: The third experimental accomplishment is the acquisition of Raman spectra consisting of multiple vibrational modes using UHV-TERS. Using a plasmonic Ag tip and 633 nm continuous wave (CW) laser illumination of the UHV STM tip-sample junction, eight vibrational modes were resolved in the TER spectra for copper phthalocyanine (CuPc) adlayers on Ag (111). Concurrently, sub-nanometer molecular resolution STM images were obtained, revealing subtle features in the CuPc adlayer, including the orientation and boundaries between ordered molecular domains. Furthermore, density-functional theory (DFT) calculations were carried out that allow quantitative identification of eight different vibrational modes in the TER spectra

2.2. Molecular-Resolution Characterization and Manipulation of Surface Chemistry

This SISGR program is actively exploring UHV STM methods for characterizing and manipulating chemical reactions at the molecular scale. For example, electron-driven and photon-driven chemistries are being studied on the surfaces of electronic materials such as silicon and graphene. Specific accomplishments include:

(1) *Characterization and manipulation of organic molecules on epitaxial graphene*: Organic adlayers of 3,4,9,10-perylene-tetracarboxylic acid dianhydride (PTCDA), N,N′-dioctyl-3,4,9,10-perylenedicarboximide (PTCDI-C8), 10,12 pentacosadiynoic acid (PCA), 4-nitrophenyl diazonium (4-NPD) tetrafluoroborate, and C_{60} have been assembled and characterized at the molecular scale with UHV STM and STS on epitaxial graphene on SiC(0001). In particular, FCL has been employed to form heteromolecular nanostructures of PTCDA and PTCDI-C8, while graphene nanoribbons have been nanopatterned by FCL on 4-NPD functionalized surfaces. In addition, ultraviolet photopolymerization has been characterized at the molecular scale for one-dimensionally ordered PCA monolayers. For C_{60} adsorbed to epitaxial graphene, the molecular adlayer was found to be decoupled/shielded from any significant charge transfer from the underlying SiC(0001) surface states.

(2) *Characterization and manipulation of inorganic atomic adsorbates on epitaxial graphene*: In this work, epitaxial graphene on SiC(0001) is oxidized at room temperature in UHV using atomic oxygen. Atomic resolution characterization with STM is quantitatively compared to density functional theory, showing that UHV oxidization results in uniform epoxy functionalization. Furthermore, this oxidation is shown to be fully reversible at temperatures as low as 260ºC. Similar results have also been obtained for atomic hydrogen on graphene.

(3) *Preparation and characterization of chemical vapor deposition (CVD) graphene on copper*: In this work, graphene is grown via chemical vapor deposition on copper. In particular, graphene grown on Cu foil via *ex situ* CVD was studied at the atomic scale. In addition, a

method for synthesizing graphene on single crystal Cu(111) in UHV was demonstrated. These results have helped reveal the role of grain boundaries in charge transport measurement for CVD graphene on Cu.

2.3. Rectification in Monolayer Molecular *p-n* Junctions

The interfaces in bulk heterojunction organic photovoltaics are critical to their operation; however, characterization of these interfaces is non-trivial since they are buried in device-scale structures. In order to gain insight into correlations between structure and function, model *p-n* junctions with a prototypical acceptor-donor system – C_{60} and pentacene (Pn) – have been fabricated and characterized with STM. Specific accomplishments include:

(1) The structure of the first and second layer of Pn self-assembled on Cu(111) has been observed. For the bilayer, Pn is electronically decoupled from the Cu(111) substrate.

(2) By sequentially depositing monolayers of C_{60} and Pn on a Cu(111) surface, a molecular rectifier has been demonstrated at the single molecular layer level. *I-V* curves acquired on C_{60} alone show symmetric behavior for positive or negative bias, while the *I-V* curves acquired on Pn/C_{60} show a significant suppression of current under positive sample bias.

(3) By concurrently depositing both Pn and C_{60} on a Cu(111) surface, these molecules can also form co-planar heterostructured domains that are not only well-ordered, but also chiral. Introducing chirality into acceptor-donor heterojunctions suggests the potential to combine charge separation with spin separation or optical polarization sensitivity.

3. Future Plans

In future work, we intend to utilize the knowledge and momentum gained from the aforementioned accomplishments to advance the following project objectives:

(1) *Advancing the spatial and temporal resolution of UHV-TERS*: (a) Small-ensemble/single-molecule surface chemistry will be studied by spatially resolved continuous wave UHV-TERS; (b) Ultrafast charge transfer dynamics of surface-mounted chromophoric molecules will be characterized by ultrafast SERS/SE-FSRS/TERS; (c) Constrained density functional theory (CDFT) will be employed for structural and TERS modeling, while a time-dependent perturbation theory approach will determine the rate of photoinduced electron transfer; (d) Tip-enhanced FSRS will be modeled including electrodynamics effects associated with the tip and charge transfer dynamics that are initiated by the actinic pulse.

(2) *Development of plasmonic substrates for UHV-TERS/STM*: (a) Recognizing the need to decouple adsorbates from the de-excitation pathways presented by plasmonically active surfaces, a variety of buffer layers will be developed including chemical vapor deposition of graphene and seeded growth of ultrathin, conformal dielectrics by atomic layer deposition; (b) In addition to thin films, methods for *in situ* oxide nanoparticle growth will be developed due to the importance of supported oxide nanoparticles in catalysis and dye-sensitized solar cells. (c) Configuration-biased Monte Carlo methods in combination with DFT or tight-binding theory with periodic boundary conditions will be used to study buffer layer growth methods and the resulting substrate electronic structure.

(3) *Preparation and characterization of optically active adsorbates and monolayers*: (a) In an effort to probe photosynthetic processes at the single molecule limit, chlorophyll and carotenoids will be isolated on the aforementioned plasmonic substrates; (b) Single molecule manipulation techniques will be employed to study molecular charge transfer complexes as a function of intermolecular spacing; (c) The fundamental limit of organic

photovoltaics will be explored via stacked molecular heterostructures consisting of alternating monolayers of donor and acceptor molecules.

4. Publications

[1] M.A. Walsh, M.C. Hersam, *Chem. Comm.*, **46**, 1153 (2010).
[2] M.A. Walsh, S.R. Walter, K.H. Bevan, F.M. Geiger, M.C. Hersam, *J. Am. Chem. Soc.*, **132**, 3013 (2010).
[3] N.L. Yoder, R. Jorn, C.-C. Kaun, T. Seideman, M.C. Hersam, *Current-Driven Phenomena in Nanoelectronics*, T. Seideman, Ed.; Pan Stanford Publishing, 2011, Ch. 7.
[4] Md.Z. Hossain, M.A. Walsh, M.C. Hersam, *J. Am. Chem. Soc.*, **132**, 15399 (2010).
[5] Q.H. Wang, M.C. Hersam, *Nano Lett.*, **11**, 589 (2011).
[6] Q.H. Wang, M.C. Hersam, *ECS Trans.*, **28**, 95 (2010).
[7] Q.H. Wang, M.C. Hersam, *MRS Bulletin*, **36**, 532 (2011).
[8] J.D. Emery, Q.H. Wang, M. Zarrouati, P. Fenter, M.C. Hersam, M.J. Bedzyk, *Surf. Sci.*, **605**, 1685 (2011).
[9] Md.Z. Hossain, J.E. Johns, K.H. Bevan, H.J. Karmel, Y.T. Liang, S. Yoshimoto, K. Mukai, T. Koitaya, J. Yoshinobu, M. Kawai, A.M. Lear, L.L. Kesmodel, S.L. Tait, M.C. Hersam, *Nature Chemistry*, **4**, 305 (2012).
[10] N. Jiang, E.T. Foley, J.M. Klingsporn, M.D. Sonntag, N.A. Valley, J.A. Dieringer, T. Seideman, G.C. Schatz, M.C. Hersam, R.P. Van Duyne, *Nano Lett.*, in press, DOI: 10.1021/nl2039925 (2012).
[11] L. Gao, J.R. Guest, N.P. Guisinger, *Nano Lett.*, **10**, 3512 (2010).
[12] J. Cho, L. Gao, J. Tian, H. Cao, W. Wu, Q. Yu, J.R. Guest, Y.P. Chen, N.P. Guisinger, *ACS Nano*, **5**, 3607 (2011).
[13] J.A. Smerdon, M. Bode, N.P. Guisinger, J.R. Guest, *Phys. Rev. B*, **84**, 165436 (2011).
[14] J. Cho, J. Smerdon, L. Gao, Ö. Süzer, J.R. Guest, N.P. Guisinger, *Nano Lett.*, **12**, 3018 (2012).
[15] J. Tian, H. Cao, W. Wu, Q. Yu, N.P. Guisinger, Y.P. Chen, *Nano Lett.*, in press, DOI: 10.1021/nl3002974 (2012).
[16] Y. Qinkai, L. A. Jauregui, W. Wu, R. Colby, J. Tian, Z. Su, H. Cao, Z. Liu, D. Pandey, D. Wei, T.F. Chung, P. Peng, N.P. Guisinger, E.A. Stach, J. Bao, S.-S. Pei, Y.P. Chen, *Nature Materials*, **10**, 443 (2011).
[17] J.M. Mullin, J. Autschbach, G.C. Schatz, *Comp. Theor. Chem.,* **987**, 32 (2012).
[18] J.M. Mullin, G.C. Schatz, *J. Phys. Chem. A*, **116**, 1931 (2012).
[19] J.M. McMahon, S.K. Gray, G.C. Schatz, *J. Phys. Chem. C*, **114**, 15903 (2012).
[20] N. Harris, L.K. Ausman, J.M. McMahon, D.J. Masiello, G.C. Schatz, *Computational Nanoscience*; E. Bichoutskaia, Ed.; 2011; Vol. 4; pp 148-79.
[21] R.R. Frontiera, A.-I. Henry, N.L. Gruenke, R.P. Van Duyne, *J. Phys. Chem. Lett.*, **2**, 1199 (2011).
[22] M.G. Blaber, A.-I. Henry, J.M. Bingham, G.C. Schatz, R.P. Van Duyne, *J. Phys. Chem. C*, **116**, 393 (2012).
[23] M.D. Sonntag, J.M. Klingsporn, L.K. Garibay, J.M. Roberts, J.M. Dieringer, T. Seideman, K. Scheidt, L. Jensen, G.C. Schatz, R.P. Van Duyne, *J. Phys. Chem. C*, **116**, 478 (2012).
[24] M.G. Reuter, M.C. Hersam, T. Seideman, M.A. Ratner, *Nano Lett.*, **12**, 2243 (2012).
[25] A. Salomon, R.J. Gordon, Y. Prior, T. Seideman, M. Sukharev, *Phys. Rev. Lett.*, in press (2012).
[26] M. Reuter, M.A. Ratner, T. Seideman, *Phys. Rev. B*, in press (2012).

Chemical Kinetics and Dynamics at Interfaces

Laser induced reactions in solids and at surfaces

Wayne P. Hess (PI), Alan G. Joly and Kenneth M. Beck

Chemical and Materials Sciences Division
Pacific Northwest National Laboratory
P.O. Box 999, Mail Stop K8-88,
Richland, WA 99352, USA
wayne.hess@pnnl.gov

Additional collaborators include A.L. Shluger, P.V. Sushko
J.T. Dickinson, W.D. Wei and S.J. Peppernick

Program Scope

The chemistry and physics of electronically excited solids and surfaces is relevant to the fields of photocatalysis, radiation chemistry, and solar energy conversion. Irradiation of solid surfaces by UV, or higher energy photons, produces energetic species such as core holes and free electrons, that relax to form electron-hole pairs, excitons, and other transient species capable of driving surface and bulk reactions. The interaction between light and nanoscale oxide materials is fundamentally important in catalysis, microelectronics, sensor technology, and materials processing. Photostimulated desorption studies, of atoms or molecules, provide a direct window into these important processes and are particularly indicative of electronic excited state dynamics. Greater understanding is gained using a combined experiment/theory approach. We therefore collaborate with leading solid-state theorists who use *ab initio* calculations to model results from our laser desorption and photoemission experiments. The interaction between light and metal nano objects can lead to intense field enhancement and strong optical absorption through excitation of surface plasmon polaritons. Such plasmon excitation can be used for a variety of purposes such as ultrasensitive chemical detection, solar energy generation, or to drive chemical reactions. Large field enhancements can be localized at particular sites by careful design of nanoscale structures. Similar to near field optics, field localization below the diffraction limit can be obtained. The dynamics of plasmonics excitations is complex and we use finite difference time domain calculations to model field enhancements and optical properties of complex structures including substrate couplings or interactions with dielectric materials.

Approach:

In photodesorption studies, photon energies are chosen to excite specific surface structural features that lead to particular desorption reactions. The photon energy selective approach takes advantage of energetic differences between surface and bulk exciton states and probes the surface exciton directly. We measure velocities and state distributions of desorbed atoms or molecules from ionic crystals using resonance enhanced multiphoton ionization and time-of-flight mass spectrometry. Application of this approach to controlling the yield and state distributions of desorbed species requires detailed knowledge of the atomic structure, optical properties, and electronic structure. To date we have thoroughly demonstrated surface-selective excitation and reaction on alkali halides. However, technological applications of alkali halides are limited compared to oxide materials. Oxides serve as dielectrics in microelectronics and form the basis for exotic semi- and super-conducting materials. Although the electronic structure of oxides differs considerably from alkali halides, it now appears possible to generalize the exciton model

for laser surface reactions to these interesting and diverse materials. Our recent studies have explored nanostructured samples grown by chemical vapor deposition or thin films grown by reactive ballistic deposition (RBD) in addition to cleaved single-crystal surfaces. We have demonstrated that desorbed atom product states can be selected by careful choice of laser wavelength, pulse duration, and delay between laser pulses. Recently, we have applied the technique of photoemission electron microscopy (PEEM) to these efforts. In particular, we are developing a combined PEEM two-photon photoemission approach to probe spatially-resolved excited electronic state dynamics in nanostructured materials.

Recent Progress

Since hyperthermal desorption is typically observed following surface excitation, we surmise that the hyperthermal O-atom desorption, from metal oxides, is due to electronic state dynamics induced by *surface specific* excitation. In contrast, *bulk* excitation of these oxides at higher photon energies (7.9 eV) has always led to lower kinetic energy (thermal) O-atom emission. Similar results were obtained in irradiation studies of alkali halides. Recently we observed a new highly-hyperthermal O-atom desorption from nanostructured CaO using 6.4 eV photons, which strongly excite the bulk material. The resulting O-atom kinetic energy distribution peaks near 0.7 eV, more than four times that observed previously for either CaO or MgO following surface specific excitation. Irradiation of a nanostructured CaO sample with 6.4 eV photons charges the surface and creates surface hole species. Further absorption of 6.4 eV photons in the bulk induces indirect $\Gamma - X$ transitions and produces bulk excitons, in which the electrons occupy 3*d* states of Ca ions. These bulk excitons can diffuse at room temperature towards the surface and subsequently tunnel to the surface layer or undergo Förster resonance energy transfer to surface trapped hole sites to form a trapped hole + exciton complex. We suggest that some amount of this excess exciton energy is transferred into the kinetic energy of desorbing O-atoms making them highly-hyperthermal.

Very intense photoelectron emission has been observed from localized points on nanostructured metal surfaces following UV femtosecond (fs) laser excitation. The regions of intense emission, dubbed ‘hot spots’, are due to collective charge oscillations, termed localized surface plasmons (LSPs). The intensity of the incident electric field can be amplified several orders of magnitude when resonantly coupled with the LSP mode of the nanostructure. The electromagnetic (EM) field amplification is largely responsible for non-linear phenomena such as surface enhanced Raman scattering (SERS) although SERS intensities are a convolution of both electronic and chemical Raman enhancement factors. While the EM contribution is believed to dominate the overall SERS signal, obtaining a quantitative measure of individual chemical and EM contributions, from a single molecule or hot spot, has proved challenging.

It is possible to measure the field enhancement due to a nanoparticle LSP using PEEM. By applying a two-photon excitation scheme, using fs laser pulses, isolated EM enhancements can be examined and photoemission yields can be correlated with detailed structural images from complementary microscopic techniques such as scanning electron microscopy (SEM). Polystyrene spherical nanoparticles (average diameter ~ 465 nm) were deposited on an atomically flat mica substrate and covered with a 50 nm Ag thin film. This sample geometry provides a clear distinction between two fundamental shapes, *i.e.* a flat surface and a semi-shell nanoparticle. Since both particle and substrate are coated with the same 50 nm thick Ag film, intense nanoparticle photoemission can be attributed to field enhancement derived from the LSP. We determined the EM enhancement factors for over 100 nanoparticles. The distribution is asymmetric with a median value of roughly 16 but with some particles yielding enhancement factors between 100 and 375. We then correlated the photoemission yields with detailed structures of the individual particles and were able to associate particular anomalous structures

with the most intense electron emission. Similar studies of solid metal nanoparticles using a range of sizes (20 to 120 nm in diameter) are underway.

PEEM is a charged particle (photoelectrons) imaging technique and has therefore been applied almost exclusively to conducting materials and in particular metals. We have found, however, that wide-gap semiconductors and even insulating materials, in some cases, yield high quality PEEM images. We have imaged 3 μm diameter polystyrene spheres supported on a thin metal substrate illuminated by 400 nm (~ 3.1 eV) and 800 nm (~ 1.5 eV) femtosecond (fs) laser pulses. Intense photoemission is generated by microspheres even though polystyrene is an insulator and its ionization threshold is well above the photon energies employed. We observe the most intense photoemission from the far side (the side opposite the incident light) of the illuminated microsphere that is attributed to light focusing within the microsphere. The light focused though the microsphere then propagates to the thin film surface where photoemission from the metal substrate can be imaged. For the case of p-polarized, 800 nm fs laser pulses, we observe photoemission exclusively from the far side of the microsphere and additionally resolve sub-50 nm hot spots in the supporting Pt/Pd thin film that are located only within the focal region of the microsphere. We find that the fs PEEM images at both 400 and 800 nm can be modeled using finite difference time domain (FDTD) electrodynamic simulations. The FDTD simulations predict light focusing in the optically transparent microsphere and subsequent focusing of the transmitted field on the supporting metal surface. The ability to obtain high resolution and high contrast PEEM image from an insulator is attributed to photoinduced conductivity of the polystyrene microspheres.

Future Directions

If exciton-based desorption can be generalized from alkali halides to metal oxides then selective excitation of specific surface sites could lead to controllable surface modification, on an atomic scale, for a general class of technologically important materials. While exciton-based desorption is plausible for MgO and CaO, we note that the higher valence requires a more complex mechanism. With the aid of DFT calculations we have developed such a hyperthermal desorption mechanism that relies on the combination of a surface exciton with a three-coordinated surface-trapped hole, a so-called “hole plus exciton” mechanism. In every instance we have studied, a hyperthermal O-atom KE distribution can be linked to an electronic surface excited state desorption mechanism. In contrast, a thermal O-atom KE distribution clearly indicates a bulk derived origin for desorption. In analogy to alkali halide thermal desorption, we have considered a bulk-based thermal desorption mechanism involving trapping of two holes at a three-coordinated site (a “two-hole localization” mechanism). Our calculations, however, do not indicate that two-hole localization is likely without invoking a dynamical trapping process. Since extensive calculations have not yielded an enduring theoretical model for thermal desorption we are exploring possible nonthermal mechanisms that yield low kinetic energy particle desorption in the “thermal energy” range. Initial experiments on CsBr thin films suggest intriguing possibilities of near-thermal desorption from surface molecular anion centers (H centers). We will therefore study low energy desorption from thin films of CsBr, CsI, and perhaps RbI grown on insulators and metals. We also plan to grow and study other oxide surfaces in the near term such as ZrO_2, BaO, and ZnO.

PEEM combined with interferometric time-resolved two-photon photoemission is an experimental method which offers both nanometer spatial and fs time resolution. Using these techniques it should be possible to time-resolve PEEM images of localized surface plasmons for various plasmonics nanostructures such as wires, spheres or particle aggregates. Using PEEM we have directly recorded plasmonic enhancement factors, of core-shell particles, without the presence of a molecular emitter as required using surface enhanced Raman scattering (SERS).

This is a significant advantage of PEEM in characterizing novel plasmonic substrates. By adding a time-resolved capability to our PEEM experiments (a Mach-Zhender interferometer is currently under construction) the way opens to a whole new array of applications such as correlating the enhancement factors and dynamics of spatially resolved hotspots formed in the nano-gaps of particle aggregates or in gaps between nanowires.

Future plans include femtosecond PEEM to study plasmon resonant photoemission from noble metal nanostructures and pulse-pair PEEM to probe dynamics of oxide nanostructures on surfaces. We will interrogate such metal-insulator systems using a variety of advanced techniques including: x-ray and ultraviolet photoelectron spectroscopy (XPS, UPS) femtosecond 2PPE, PEEM, atomic force microscopy (AFM) and laser desorption. Femtosecond time-resolved PEEM can reveal spatially resolved ultrafast dynamics and is a powerful tool for studying the near-surface electronic states of nanostructures or plasmonic devices. We will explore the formation of interfacial polarons on a sample of nanoscale insulator (either alkali halides or metal oxides) islands on Cu (111) and possibly other metal substrates. Our goal is to resolve the temporal and spatial evolution of electron emission and the dynamics of small interfacial polarons using the combined PEEM and 2PPE approach. We are also presently developing capabilities to perform energy-resolved two-photon photoemission using a hemispherical analyzer XPS instrument. In combination we expect these two techniques will provide *spatially-resolved* electronic state dynamics of nanostructured metal-insulator materials.

References to publications of DOE BES sponsored research (2009 to present)

1. K.M. Beck, A.G. Joly, and W.P. Hess, “Two-color laser desorption of nanostructured MgO thin films,” *Appl. Surf. Sci.* **255**, 9562 (2009).

2. A.G. Joly, K.M. Beck, and W.P. Hess, “Photodesorption of excited iodine atoms from KI (100),” *J. Chem. Phys.* **131**, 144509 (2009).

3. K.M. Beck, A.G. Joly, and W.P. Hess, "Effect of Surface Charge on Laser-induced Neutral Atom Desorption." *Appl. Phys. A*, **101**, 61 (2010).

4. G. Xiong, R. Shao, S.J. Peppernick, A.G. Joly, K.M. Beck, W.P. Hess, M. Cai, J Duchene, J.Y. Wang W.D. Wei “Materials Applications of Photoelectron Emission Microscopy,” *J. Metals*, **62**, 90 (2010).

5. S.J. Peppernick, A.G. Joly, K.M. Beck, W.P. Hess “Plasmonic Field Enhancement of Individual Nanoparticles by Correlated Scanning and Photoemission Electron Microscopy” *J. Chem. Phys.* **134**, 034507 (2011).

6. P.V. Sushko, A.L. Shluger A.G. Joly, K.M. Beck, and W.P. Hess, “Exciton-driven highly-hyperthermal O-atom desorption from nanostructured CaO” *J. Phys. Chem. C*. **115**, 692 (2011) Cover.

7. S.J. Peppernick, A.G. Joly, K.M. Beck, and W.P. Hess “Near-Field Focused Photoemission from Polystyrene Microspheres Studied with Photoemission Electron Microscopy”, *J. Chem. Phys.* **137**, 014202 (2012).

8. S.J. Peppernick, A.G. Joly, K.M. Beck and W.P. Hess, J. Wang, Y.C. Wang and W.D. Wei, “Two-Photon Photoemission Microscopy of a Plasmonic Silver Nanoparticle Trimer,” *Appl. Phys. A* (in press).

Spectroscopic Imaging Toward Space-Time Limit

Wilson Ho

Department of Physics & Astronomy and Department of Chemistry
University of California, Irvine
Irvine, CA 92697-4575 USA

wilsonho@uci.edu

Program Scope:

This project is concerned with the experimental challenge of reaching single molecule sensitivity with sub-molecular spatial resolution in optical spectroscopy and photochemistry. These experiments would lead to an understanding of the inner machinery of single molecules that are not possible with other approaches. Results from these studies will provide the scientific basis for understanding the unusual properties, processes, and phenomena in chemical and physical systems at the nanoscale. The experiments rely on the combination of the unique properties of lasers and scanning tunneling microscopes (STM). By using a low temperature scanning tunneling microscope (STM) and optics in the nano-junction, it has become possible to probe optical phenomena with sub-atomic resolution. Specific examples of such capabilities include the spatial dependence of multi-electron induced light emission and photo-induced desorption of single molecules, and the primary steps of electron transfer to a single molecule. In the conversion of sun light to energy and in optoelectronics, a promising scheme involves the use of nanoscale objects as the active media. The investigation of the fundamental mechanisms of how light can be efficiently coupled to molecules and nanostructures not only can lead to new scientific phenomena but also form the basis for new technology.

Recent Progress:

Bond-selective chemistry, which involves selectively breaking and forming specific bonds, is one of the ultimate goals of chemistry. Achieving bond-selectivity in a complex functionalized molecule is particularly important for advancing the molecule-based technologies, such as molecular electronics, organic solar cells, and nanomachines. However, due to the rich internal degrees of freedom and the intramolecular energy redistribution in functionalized molecules, bond-selective control has so far been difficult to realize. We succeeded to induce a sequence of target-selective bond dissociation (Fig. 1) and formation (Fig. 2) steps in a single thiol-based π-conjugated molecule adsorbed on a NiAl(110) surface, using a scanning tunneling microscope (STM). By locally injecting the energy-tunable tunneling electrons into the resonant states derived from the functional groups in the molecule, we were able to selectively abstract different functional groups from the molecule step by step and monitor the evolution of the molecular electronic structure both in energy and real space at each reaction step. Furthermore, the bond-selective dissociations allowed us to activate the sulfur functional groups and form different types of Au-S bonds by manipulating and attaching a single gold atom to the sulfur atom at each end of the molecule. The microscopic geometry of the Au-S bond at the single molecule level and its influence on the electronic structure of the molecule were determined by

the STM, which might underlie the understanding of electron transport in the widely used thiol-based molecular junction. This work not only opens up the possibility of submolecular control of the bond-selective chemistry in a single functionalized molecule, but also reveals the changes in the molecular electronic structure associated with bond dissociation and formation, which are crucial evidences for orbital hybridization in chemical transformation.

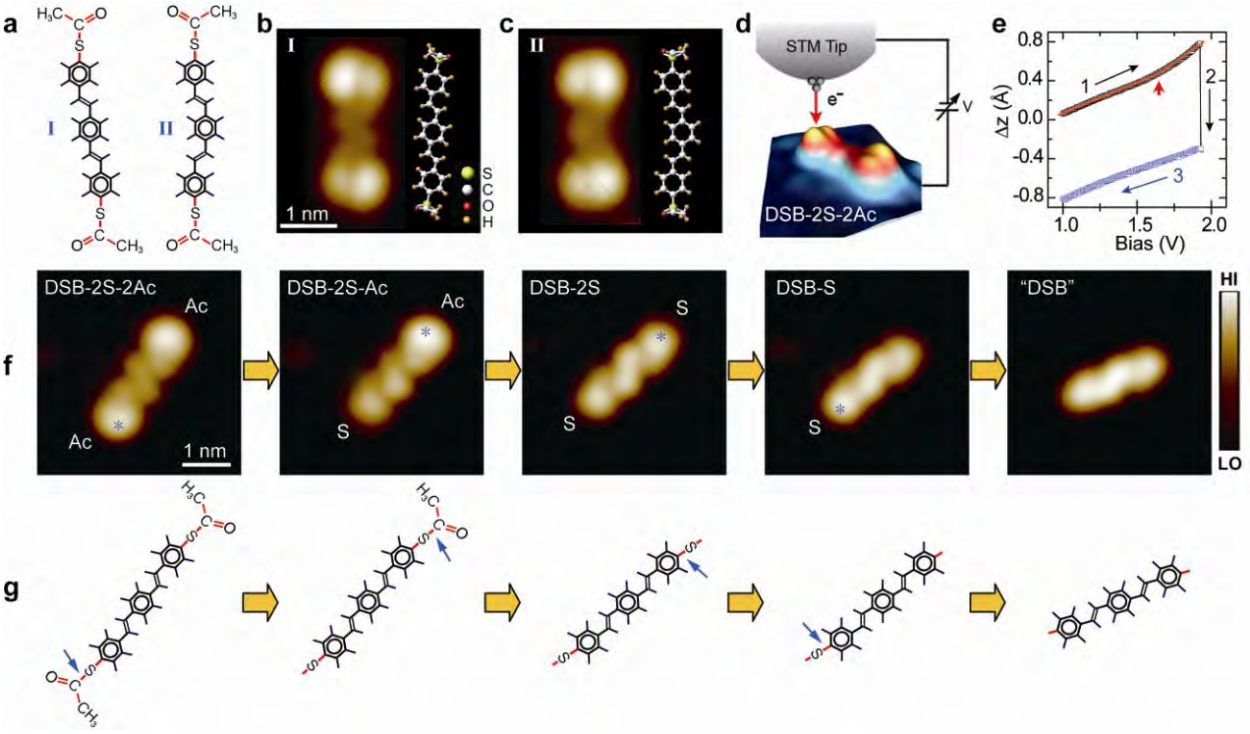

Figure 1. Stepwise dissociation sequence of the DSB-2S-2Ac molecule (Ac denotes acetyl group). a, Schematic models for two rotational isomers of the DSB-2S-2Ac molecules, noted as I and II. **b** and **c**, STM topographies of the DSB-2S-2Ac (I) and (II), respectively. Set point: V=2.2 V and I=50 pA. Ball-and-stick models for the two isomers, which are scaled (×1.5) to the size of the molecules, are inserted into **b** and **c** for comparison. **d**, Schematic drawing of the selective dissociation of different functional groups by injecting electrons at precise locations of the molecule. **e**, The typical Δz-V characteristics in the dissociation event of a DSB-2S-2Ac molecule. The red arrow indicates the bias at which the slope of the curve starts to increase because of the emergence of Ac-derived states. Step 1: the sample bias is ramped up from 1 V at constant current 1nA; step 2: tip height encounters a sudden jump upon dissociation of the acetyl group; step 3: the bias is immediately ramped down to 1 V. **f** and **g**, Topographies and corresponding schematics scaled (×1.8) for clarity of the different products in the dissociation sequence. Set point: V=1.6 V and I=50 pA. The asterisks in **f** indicate the locations for injecting electrons by the STM tip. The small arrows (blue) in **g** denote the bonds to be broken in the different steps for the dissociation sequence.

Nonlinear optical processes have become ubiquitous ever since the first demonstration of second harmonic generation in 1961 by Franken *et al.* following the first successful operation of the laser by Maiman in 1960. Following these historical development, the emergence of new spectroscopic methods has led to advances in our basic understanding of the different states of

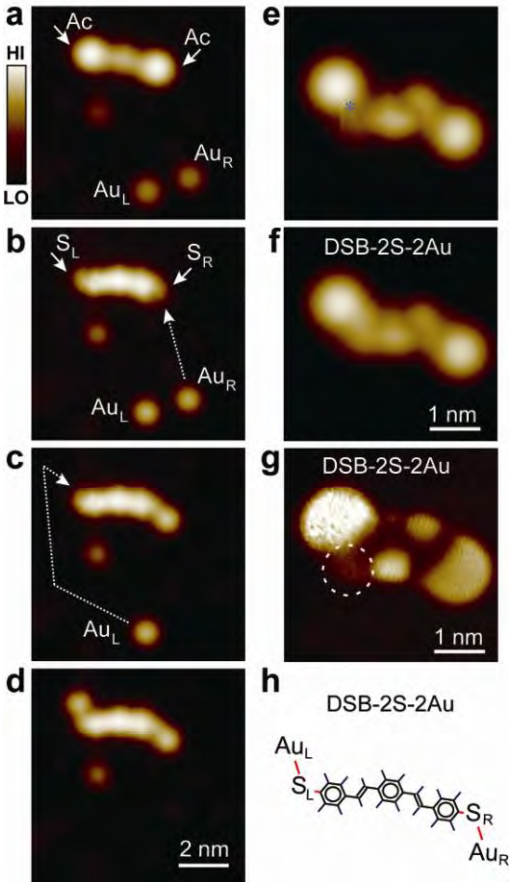

Figure 2. Formation sequence of the DSB-2S-2Au complex. a-d, Manipulation sequence of attaching two gold atoms to a DSB-2S (II) molecule. The arrows in **a** indicate the acetyl groups and in **b** the sulfur atoms. The dotted lines in **b** and **c** depict the trajectories along which the Au atoms were manipulated to the proximity of the molecule. The round protrusion below the molecule in **a-d** corresponds to an unknown impurity on the surface and can move around during the scanning. It does not interact with the adjacent molecule and the Au atoms. Set point for topographies: V=1.0 V, I=50 pA. **e** and **f**, Zoom-in STM topographies before and after the formation of the Au-S_L covalent bond, respectively. The asterisk in **e** indicates the location where 2.2-eV electrons were injected by STM tip to form the Au-S_L covalent bond ("nano-welding"). The fuzzy feature below the asterisk in **e** arises from the instability of the molecule under the perturbation of the tip before formation of the covalent bond. Set point for topographies: V=2.0 V, I=50 pA. **g**, dI/dV image of the DSB-2S-2Au complex. Imaging conditions: V=1.6 V, I=50 pA. The dotted circle highlights the shared orbital structure in the Au_L-S_L covalent bond between the Au atom and the molecule. **h**, Schematic model of the DSB-2S-2Au complex.

matter in biology, chemistry, materials, and physics. These nonlinear experiments are enabled by the high power of pulsed lasers. Due to space charge effects in an electron beam, nonlinear processes induced by electrons are limited. However, by confining the electron flow to nanoscale dimensions, the electron flux can be made to be sufficiently high that processes induced by multiple electron excitations can be observed. Such spatial confinement is present in the STM where atomic scale processes depend nonlinearly on the tunneling current, for example, the transfer of a single atom between the surface and the tip, and the dissociation and rotation of a single molecule.

Tunneling electrons have been shown to lead to light emission by coupling to plasmons in the nanocavity of the STM. By increasing the tunneling current, emission of light at twice and three times the energy of the tunneling electrons have been measured, as shown in Fig. 3. In contrast to second and third harmonics generation by a pulsed laser, the emitted light has a continuous distribution up to the energy corresponding to twice and three times the voltage bias between the tip and the sample and with spectral peaks associated with the nano-plasmonic modes of the metallic tip and the substrate. The observation of plasmonic emissions with multiple electron excitations raises the question regarding collective electronic modes associated with the metallic nanocavity of the STM junction. The strength of the emission depends on the lifetime of the plasmons and the magnitude of the tunneling current, i.e. on the excitation and decay rates. The available data are expected to stimulate theoretical analysis.

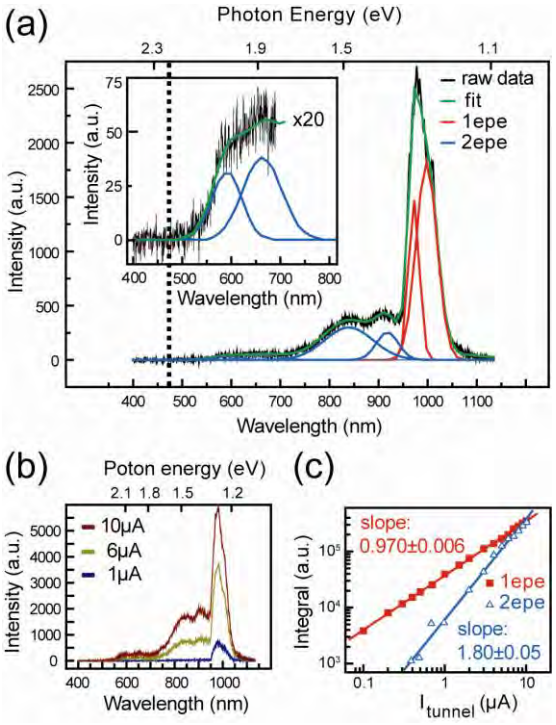

Figure 3. One and two electron induced light emission from STM junction consisting of a Ag tip and NiAl(110). (a) Emission spectra comprising both one electron photoemission (1epe) and 2epe data simultaneously (U_{bias}=*1.3V*, I_t=*4 μA*). The data are well fitted (green line) by multiple Gaussian profiles. The inset shows a zoom-in of the high energy part, clarifying the fitting with two peaks. Four peaks are attributed to the 2epe (blue) while two peaks are used to fit the 1epe. (b) Current dependence of the simultaneously measured 1epe and 2epe. (c) Integrated intensity of 1epe (squares) and 2epe peaks (triangles) as a function of tunneling current in a double logarithmic plot. A slope of 0.97 is determined for 1epe and a slope of 1.8 for 2epe.

Future Plans:

The ability to probe changes in real time with sub-Ångström spatial resolution would open a new window for viewing the inner machinery of matter. The plan for the future aims at pushing spectroscopic imaging toward the simultaneous limits of sub-Ångström and <30 femtoseconds. We have initiated the investigation of laser induced desorption of molecular hydrogen from Au(110) surface. The weakly adsorbed molecular hydrogen allowed inelastic electron tunneling spectroscopy (STM-IETS) of the rotational mode. In addition, we have initiated the monitoring of the changes in the rotational and vibrational energies of a single hydrogen molecule as the tunneling gap is decreased. We will obtain the spectroscopy for different isotopes (H_2, D_2, HD) and measure the time scale for photodesoption of individual molecules. This work will be extended to other molecules and substrates to probe spatially resolved excited state lifetimes. Another goal is to continue the measurement of multi-electron induced light emission from different systems. These experiments are expected to provide a fundamental understanding of matter by revealing them in previously unattainable regimes of space and time. Furthermore, knowledge of the coupling of light to nanoscale objects bring us one step closer toward the realization of efficient conversion of sun light to energy, a broad range of optoelectronics and plasmonics, and economically competitive photocatalysis.

References to Publications of DOE Sponsored Research:

[1] "Submolecular control, spectroscopy, and imaging of bond-selective chemistry in single functionalized molecules", Ying Jiang, Qing Huan, Laura Fabris, Guillermo C. Bazan and Wilson Ho, Nature Chemistry, in press (2012).

[2] **"**Two-Electron Induced Light Emission from a Tunneling Junction", Christian A. Bobisch, Chi Chen, Ying Jiang and Wilson Ho, Phys. Rev. Lett., submitted (2012).

THEORY OF THE REACTION DYNAMICS OF SMALL MOLECULES ON METAL SURFACES

Bret E. Jackson

Department of Chemistry
104 LGRT
710 North Pleasant Street
University of Massachusetts
Amherst, MA 01003
jackson@chem.umass.edu

Program Scope

Our objective is to develop realistic theoretical models for molecule-metal interactions important in catalysis and other surface processes. The dissociative adsorption of molecules on metals, Eley-Rideal and Langmuir-Hinshelwood reactions, recombinative desorption and sticking are all of interest. To help elucidate the experiments that study these processes, we examine how they depend upon the nature of the molecule-metal interaction, and experimental variables such as substrate temperature, beam energy, angle of impact, and the internal states of the molecules. Electronic structure methods based on Density Functional Theory (DFT) are used to compute the molecule-metal potential energy surfaces. Both time-dependent quantum scattering techniques and quasi-classical methods are used to examine the reaction dynamics. Effort is directed towards developing improved quantum methods that can accurately describe reactions, as well as include the effects of temperature (lattice vibration) and electronic excitations.

Recent Progress

The dissociative chemisorption of methane on a Ni catalyst is the rate-limiting step in the chief industrial process for H_2 production. However, even on this catalyst the reaction probability is very small under typical conditions, and the dynamics are not fully understood. Most of our recent efforts have focused on the dissociative chemisorption of methane on metals, in an attempt to understand how methane reactivity varies with the temperature of the metal, the translational and vibrational energy in the molecule, and the properties of the metal surface. Initial studies of methane dissociation on Ni(111) used DFT to compute the barrier height and explore the potential energy surface (PES) for this reaction, with an emphasis on how it changes due to lattice motion. At the transition state for dissociation, we found that if the metal lattice is allowed to relax, the Ni atom over which the molecule dissociates puckers out of the surface by a few tenths of an Å. Put another way, thermal motion of this Ni atom causes the barrier to dissociation to change, which should lead to a strong variation in the reactivity with temperature. High dimensional quantum scattering calculations which allowed for the inclusion of several key methane degrees of freedom (DOF), as well as the motion of the metal atom over which the reaction occurs, found that the reaction probability was significantly larger than for a static lattice, and strongly increased with temperature.

In an attempt to better understand the role of lattice motion on methane dissociation, we implemented a variety of mixed quantum-classical models [1,3]. The best approach was to treat both the lattice motion and the molecular center of mass motion classically, and the remaining molecular DOF quantum mechanically. While this lost some tunneling contributions from motion normal to the surface, it allowed us to directly observe the motion of the lattice at a given collision energy. The majority of the reaction probability came from collisions between a

methane molecule and a lattice atom that was at or near its outer turning point, where the barrier is lowest, at the time of impact. Moreover, most of the reactions occurred for lattice atoms that were on the high-energy tail of the Boltzmann distribution, and there was only minor recoil of the metal atom. This led to the development of a sudden model, where quantum calculations were implemented for several frozen lattice configurations, Monte Carlo sampled at the substrate temperature. Because the heavy metal atom was not explicitly included in the evolution, this required two orders of magnitude less computer time, and reproduced the results of earlier fully quantum studies on Ni(111) reasonably well [1]. More detailed studies led to a further improvement of this model, including the change in both the energy and the location of the barrier to dissociation with lattice motion. This was shown to give excellent agreement with the quantum studies of methane dissociation on both Ni(111) and Pt(111) [3].

We spent over two years using DFT to examine the energetics of methane dissociation on Ni(100), Ni(111), Pt(100), Pt(111) and the stepped Pt(110)-(1x2) surface. The data we collected was compared, contrasted and published in a single rather large paper [2]. For all 5 surfaces we examined product binding energies at all high-symmetry sites, and then mapped out the lowest energy transition states (24 in all). These various pathways to reaction were compared with each other and with experiment. We also examined how the heights and the locations of these barriers changed with lattice motion; i.e., the lattice (phonon) coupling. While these metals share many characteristics, there are interesting surface-to-surface variations in both the barrier height and the phonon coupling. A simple model was developed for a temperature-dependent "activation energy", using only data from our DFT studies of the transition state [2]. This activation energy can be several tenths of an eV lower than the static surface barrier height, and its variation with substrate temperature has been observed in recent experiments on Pt(110)-(1x2).

Exciting the vibrational modes of methane can increase the reaction probability. This increase, relative to that from putting the same amount of energy into translational motion, the so-called efficacy, is different for different vibrational modes, as well as for the same mode on different metal surfaces. We have made significant progress in understanding this mode-selective chemistry, using a formulation based on the Reaction Path Hamiltonian (RPH). Assuming only that the PES is harmonic for displacements away from the reaction (or minimum energy) path, one can use DFT to compute a reasonably accurate PES that includes all 15 molecular DOF. We computed the RPH for methane dissociation on Ni(100), and then derived close-coupled equations by expanding the wavefunction in the adiabatic vibrational states of the molecule. Time-dependent quantum dynamics showed that the ν_1 mode (symmetric stretch), which significantly softens at the transition state, is strongly coupled to the reaction coordinate. As a result there is a large vibrational efficacy for this mode, as observed by two experimental groups. We demonstrated how the efficacies for vibrational enhancement are related to transitions from higher to lower energy vibrationally adiabatic states, or to the ground state, with the excess energy going into motion along the reaction path, increasing the reaction probability [4]. We extended our RPH approach to compute full 15-dimensional reaction probabilities for methane dissociation on metal surfaces [6]. The surface impact sites are correctly averaged over, and the effects of lattice motion are included using our sudden model [1,3]. These were the first calculations, based entirely on *ab intio* data, which could be compared directly with experimental studies of methane dissociative adsorption. For methane dissociation on Ni(100), agreement with experiment was good, in terms of both the magnitude of the reactivity over a broad range of incident energy, and the efficacies of the different vibrational modes for promoting reaction [6]. More importantly, it is now possible to follow the flow of energy within the molecule as it dissociates, providing a detailed understanding of how translational, vibrational and lattice energy contribute to reactivity.

In recent years we have studied H-graphite reactions, important in the formation of molecular Hydrogen on graphitic dust grains in space, the etching of graphite walls in fusion reactors, and the modification of the electronic properties of graphene. Two recent studies examined the physisorption of H. We have developed a powerful approach to these types of problems based on the reduced density matrix, which allows us to evolve a quantum system weakly coupled to a bath over relatively long times. Thus, we can not only compute, quantum mechanically, the scattering into free and bound states, we can observe the relaxation and/or desorption from these states over long times. In a study of H physisorption on graphite, we showed that sticking is enhanced at low energies by diffraction mediated trapping states, and examined the adsorption and subsequent desorption of H on graphite in great detail. We compared our reduced density approach with more traditional wavefunction-based approaches, and demonstrated the utility and accuracy of these various methods [5]. More recently, these wavefunction-based close coupling approaches were used to examine H sticking on single-layer graphene at very low energies. We showed that support of graphene on a substrate, or suspension of graphene over a hole in a substrate modifies the dispersion properties of the lattice vibrations, stabilizing the two-dimensional structure. This in turn modifies the H-graphene phonon coupling, leading to anomalously large sticking probabilities at very low temperatures [7].

A collaboration with the Kroes group (Leiden) used AIMD, *ab initio* molecular dynamics, to study H_2 dissociation on Cu(111). In AIMD, one computes the instantaneous forces on the particles "on the fly", using DFT in our case. This eliminates the need to construct approximate many-dimensional PESs, which is extremely difficult when lattice motion is involved. Our studies showed that lattice motion and temperature could effect some aspects of H_2-Cu(111) scattering, particularly the quadrupole alignment parameter [8]. A book chapter discussing the effects of lattice motion on gas-surface reactions is in press [9]. The primary focus is on our methane studies, where the molecule-phonon coupling is unusually strong.

Two major projects are near completion, both applying our full-dimensional RPH approach to methane reactions on metals. Studies on Ni(111) were motivated by experiments from the Utz group (Tufts), where they were able to measure dissociative sticking probabilities over a wide range of surface temperatures. This was the first real test of the model we developed for including lattice motion effects in these reactions [1,3]. Not only did our *ab initio* methods accurately reproduce the observed variation with temperature, they were able to explain why the variation in reactivity with temperature was strong for certain energies and weak for others. In addition, we were able to model and explain the variation in reactivity with nozzle temperature in terms of contributions to sticking from vibrationally excited molecules. Another set of studies focused on Pt(110)-(1x2), where the missing-row reconstruction leads to a very large surface corrugation, making this an excellent model for real (rough) catalysts. Our focus was on comparing the reactivity and the molecule-phonon coupling at the step edges with that on the terrace sites of smooth Pt(111) and Pt(100) surfaces, as well as comparing with experimental work from the Beck group (EPFL). We found that the edge sites were more reactive, as expected, but that the effects of lattice motion were not any larger than on smoother surfaces, even though the phonon coupling was far more complicated, involving the motion of several lattice atoms. This coupling increases the dissociative sticking probability by about an order of magnitude when the surface temperature increases from 400 K to 600 K, in agreement with the experiments.

Future Plans

Two on-going projects involve methane chemisorption on Pt(111), which we compared with Ni(111) in an early low-dimensional study. While we found the Pt surface to be more

reactive than the Ni, experiment suggests that the difference is even larger than our study found. On both metals, the transition state is over the top site. However, on Ni, the methyl group moves towards a hollow site during the reaction, while on Pt the methyl remains at the top site. This behavior, if included in the model, should lead to a further lowering of the reactivity for Ni relative to Pt, as the heavy methyl group does not tunnel as effectively as the H. This motion is included in our full 15-dimensional RPH study of Ni(111), and we plan to do a similar study on Pt(111). However, this has been put on hold by some recent (unpublished) experimental results from the Beck group that suggest that the barrier to dissociation varies with product coverage on the surface. This suggests that our DFT barrier heights may also vary with the size of our model system. We are currently trying to sort this all out, as well as to elucidate the Beck experiments

Another study uses a purely classical RPH to examine methane reactions on Ni(100). We are interested in how well classical mechanics works for this reaction, and will test various perturbative and sudden approximations made in the quantum formulation. We are also examining H-Ag scattering, subsurface penetration and thermal desorption, motivated by experiments in the Wodtke group. A collaboration with the Kroes group will use AIMD to examine CD_3H reactions on Pt(111), in connection with on-going experiments in the Beck group. We also continue to explore ways to extend our more "standard" quantum scattering approaches. In particular, we are looking at ways to average over impact sites and better describe vibrational motion. We are constructing a PES for CD_3H chemisorption on Ni(111), treating the molecule as a pseudo-diatomic by having the (unreactive) CD_3 group evolve adiabatically, but correctly including the zero point energy effects in the 6-dimensional Hamiltonian. Finally, we have derived a fully quantum model for the time evolution of a scattering molecule coupled to the electronic excitations of a metal substrate, using reduced density matrix methodologies. We have yet to compute the electronically non-adiabatic couplings, and hope to initially examine the case of H-metal scattering and sticking.

References

[1]. A. K. Tiwari, S. Nave and B. Jackson," Methane dissociation on Ni(111): A new understanding of the lattice effect," Phys. Rev. Lett. 103, 253201 (2009).
[2]. S. Nave, A. K. Tiwari and B. Jackson," Methane dissociation on Ni(111), Pt(111), Ni(100), Pt(100) and Pt(110)-(1x2): Energetic study," J. Chem. Phys. 132, 054705 (2010).
[3]. A. K. Tiwari, S. Nave and B. Jackson," The temperature dependence of methane dissociation on Ni(111) and Pt(111): Mixed quantum-classical studies of the lattice response," J. Chem. Phys. 132, 134702 (2010).
[4]. S. Nave and B. Jackson," Vibrational mode-selective chemistry: Methane dissociation on Ni(100)" Phys. Rev. B 81, 233408 (2010).
[5]. B. Lepetit, D. Lemoine, Z. Medina, and B. Jackson, "Sticking and desorption of hydrogen on graphite: a comparative study of different models," J. Chem. Phys. 134, 114705 (2011).
[6] B. Jackson and S. Nave, "The dissociative chemisorption of methane on Ni(100): Reaction path description of mode-selective chemistry" J. Chem. Phys. 135, 114701 (2011).
[7] B. Lepetit and B. Jackson, "Sticking of hydrogen on supported and suspended graphene at low temperature," Phys. Rev. Lett. 107, 236102 (2011).
[8] Effect of surface motion on the rotational quadrupole alignment parameter of D_2 reacting on Cu(111), F. Nattino, C. Díaz, B. Jackson, and G.J. Kroes, Phys. Rev. Lett. 108, 236104 (2012).
[9] B. Jackson, "The effects of lattice motion on gas-surface reactions", in *Dynamics of Gas-Surface Interactions: Atomic-level understanding of scattering processes at surfaces*, Springer Series in Surface Sciences, R. D. Muiño and H. F. Busnengo, eds., (accepted).

DE-FG02-07ER15889: **Probing catalytic activity in defect sites in transition metal oxides and sulfides using cluster models: A combined experimental and theoretical approach**

Caroline Chick Jarrold and Krishnan Raghavachari
Indiana University, Department of Chemistry, 800 East Kirkwood Ave.
Bloomington, IN 47405
cjarrold@indiana.edu, kraghava@indiana.edu

I. Program Scope

Our research program combines experimental and computational methods to study well-defined cluster models of heterogeneous catalytic materials. The focus of our studies has been transition metal oxide and sulfide clusters in non-traditional oxidation states (surface defect models) and their chemical and physical interactions with water and CO_2. The applications that are being modeled are H_2 production from photocatalyic decomposition of water, and photocatalytic CO_2 reduction using Group 6 (Mo and W) oxides and sulfides. The experiments and calculations are designed to probe fundamental, cluster-substrate molecular-scale interactions that are governed by charge state, peculiar oxidation states, and unique physical structures.

The general strategy of our studies continues to be as follows: (1) Determine how the molecular and electronic structures of transition metal suboxide and subsulfide clusters evolve as a function of oxidation state by reconciling anion photoelectron spectra of the bare clusters with high-level DFT calculations. Anions are of particular interest because of the propensity of metal oxide and sulfides to accumulate electrons in applied systems. (2) Measure and analyze the kinetics of cluster reactivity with water or CO_2. (3) Dissect possible reaction mechanisms computationally, to determine whether catalytically relevant interactions are involved. (4) Verify these challenging computational studies by spectroscopic investigation of observed reactive intermediates. (5) Probe the effect of local electronic excitation on bare clusters and cluster complexes, to evaluate photocatalytic processes. The overarching goal of this project is to identify particular defect structures that balance structural stability with electronic activity, both of which are necessary for a site to be simultaneously robust and catalytically active, and to find trends and patterns in activity that can lead to improvement of existing applied catalytic systems, or the discovery of new systems.

II. Recent Progress

A. Toward a new understanding of structural and electronic properties of transition metal suboxide systems

The general approach taken in our studies has become fairly commonplace for determining small cluster structures. However, attempts to determine the structures of transition metal suboxide clusters tend to be complicated by an abundance of energetically competitive structural isomers and spin states. The complex electronic structure arises from partial occupation of metal-local *d*-orbitals by a number of electrons determined by the extent to which the cluster is reduced. The range of accessible electronic structures in these clusters is further expanded by the presence of bridging oxo groups, which are well known to antiferromagnetically couple two metal centers via a superexchange mechanism. Treating these electronically complex systems with low-cost DFT methods is generally not effective, and attempts to develop new computational approaches for doing so are ongoing. However, several chemically important structural and electronic trends of the suboxide systems have been determined by comparing results on different metal oxides, which we summarize here. [Ref. 1]

First, the highest occupied orbitals on metal suboxide clusters (including the orbital of the cluster anions involved in all detachment processes) are localized on nearly degenerate metal-local *nd* orbitals, facilitating the stability of exotic spin states. This feature echoes the nature of oxygen vacancies on bulk transition metal oxide surfaces. Second, charge state has significant impact on cluster structure: Terminal bonds are relatively more stable compared to *M*-O-*M* bridge bonds in anions than in neutrals. This

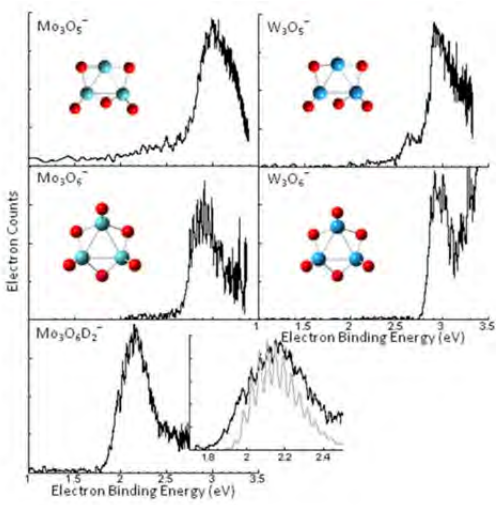

Fig. 1. PE spectra of $M_3O_y^-$ (M = Mo, W; y = 5,6) and $Mo_3O_6D_2^-$; no $W_3O_6D_2^-$ was observed under identical conditions.

suggests that charge transfer from a vacancy to a substrate on an O-vacancy results in "spring-loading" M=O bonds. A consequence of this is that structures with a higher bridge bond to terminal bond ratio have lower electron affinities, which allows us to assign the general structure of a cluster based on observed electron affinity. Third, asymmetric distribution of O-atoms is expected for many suboxide systems, which sets up the proximity of metal centers in disparate oxidation states. Finally, in all of our calculations, multiple structural isomers are predicted to be energetically competitive. Spin contamination and antiferromagnetic coupling are common features in computational results on lower oxides, which has spurred further efforts on developing new ways of treating these systems with DFT methods.

B. New computational results on $M_xO_y^-$ (M =Mo/W, x=1-4, $y < 3x$) + H_2O reactions

In our quest to develop more efficient materials for H_2 production from water decomposition, we had previously studied H_2 production from $M_xO_y^-$ (M =Mo/W, x= 1 - 4, $y < 3x$) + H_2O reactions, in which sequential oxidation coupled with H_2 production was observed.[Refs. 2, 7, 10, 13-15] In a series of experimental studies on the $M_3O_y^-$ + H_2O (or D_2O) reaction, interesting differences in the $Mo_3O_y^-$ and $W_3O_y^-$ product distributions were observed, in spite of the striking similarity between the structures of the molybdenum and tungsten oxide cluster anions. Kinetically trapped $M_xO_{y+1}H_2^-$ complexes were formed at different values of y for Mo and W. Figure 1 shows the PE spectra obtained for the bare and structurally identical $M_3O_y^-$ (y = 5 and 6) clusters, and the vibrationally resolved PE spectrum of the peculiar trapped intermediate formed in the $Mo_3O_5^-$ + H_2O reaction that is NOT observed in the $W_3O_5^-$ + H_2O reaction.

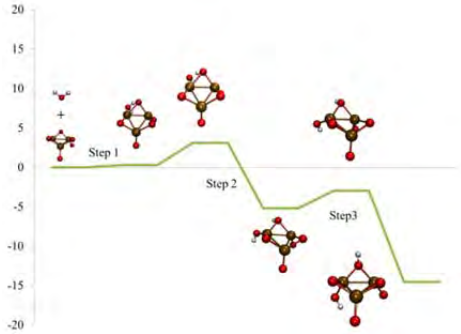

Figure 2. The reaction energy pathway (Y axis is in terms of free-energies) for the formation of the kinetic-trap formation in the reaction of $Mo_3O_5^-$ with water.

Computational studies were useful in identifying some of the reactive sites in small clusters that lead to a pathway conducive to H_2 production. However the roles played by a plethora of significant factors such as the different catalytic properties of oxygen vacancies on different metal-oxide surfaces, the differing metal-oxygen bond strengths, the initial electrostatic complex formed, the geometric factors involved in the liberation of H_2 and the effect of using bigger clusters to better mimic the bulk metal oxide surface in catalytic H_2 production from water remain poorly understood. Our current work provides new insights on all of these crucial aspects. Using the chemical reactions of $W_3O_5^-$ and $Mo_3O_5^-$ clusters with H_2O, we experimentally as well as computationally explain how and why the molybdenum-oxide in its reaction with water prefers to form a kinetic-trap whereas the tungsten-oxide shows a propensity to generate H_2 (Figures 2 and 3). The kinetic-trap formed in the reaction of $Mo_3O_5^-$ with water can potentially lead to several

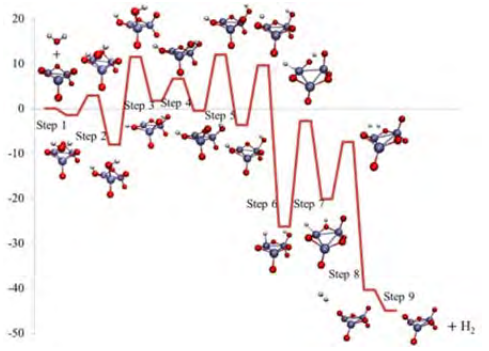

Figure 3. The reaction energy pathway (Y axis is in terms of free-energies) for H_2 liberation in the reaction of $W_3O_5^-$ with water

different kinds of structures. Our study confirms that only one out of several possible structures is obtained. In the case of $W_3O_5^-$ getting oxidized to $W_3O_6^-$ and releasing H_2, our novel observation is that the geometry of the $W_3O_6^-$ obtained after oxidation is considerably different from the geometry of the lowest-energy isomer of $W_3O_6^-$. Our recent mechanistic discovery of the reactivity-induced fluxionality in transition metal oxide clusters [Refs 2, 7] has been invaluable to unearth these significant results.

C. Computational studies of molybdenum sulfide versus molybdenum oxide clusters

Molybdenum and tungsten sulfides have been proved to be efficient hydrogenation and desulfurization catalysis. Several instances can be found in the literature where chemical processes of hydrogen evolution are significantly improved by the use of Mo or W sulfides as catalysts [Zong, X.; Yan, H. J.; Wu, G. P.; Ma, G. J.; Wen, F.Y.; Wang, L.; Li, C. *J. Am. Chem. Soc*. **2008**, 130, 7176]. To understand the role of sulfides and to compare/contrast them with oxides, we have conducted a detailed computational investigation on the water reactivity of $M_2S_4^-$ and $M_2S_5^-$ clusters (M = Mo, W). Prior to studying reactivity, we first investigated all possible geometric and electronic structures of $M_2S_n^-$ (n=2-6). We determined that all the metal sulfides have doublet electronic states in their lowest energy isomer except for $M_2S_4^-$, which have quartet ground states. The lowest energy isomers for Mo and W sulfides typically have more bridging sulfide bonds than the corresponding number of bridging oxide bonds in the oxides, a consequence of the *M-S-M* bonds being less strained than *M-O-M* bonds.

Study of chemical reactivity of metal sulfides with water has been initiated with $M_2S_4^-$ and $M_2S_5^-$ clusters. We propose several competitive energetically favorable reaction pathways which lead to the evolution of hydrogen. Selectivity in initial water addition and subsequent proton movement are found to be the key steps in all the proposed reaction channels. Initial adsorption of water is most favored involving terminal sulfur atom in $M_2S_5^-$ isomers whereas the most preferred orientation of water addition involves bridging sulfur atom in case of $M_2S_4^-$ isomers. In all the H_2 elimination steps, the interacting hydrogen atoms involve a metal hydride and a metal hydroxide (or thiol) group. H_2 elimination step involving a thiol and a hydroxyl group has a higher barrier. For all the reaction pathways, $Mo_2S_n^-$ always has a relatively higher barrier than the W analogue. Reactions of $M_2S_4^-$ and $M_2S_5^-$ clusters with water are exothermic and can undergo reactions with water to liberate H_2 with low barriers.

D. Reactions between transition metal oxide cluster anions and simple alcohols

An important outcome of the computationally determined $M_xO_y^-$ + H_2O reaction pathways was the role of H-mobility. One of the ways to test these reaction pathways is to perform reactivity studies between the transition metal oxide clusters and alcohols, which, in addition to adding two additional distinct chemical bonds, present the limited mobility of the alkoxy moiety. Furthermore, there are economic motives for finding non-precious metallic catalysts for use to treat fuel alcohol emissions.

Preliminary studies on the $^{186}W_xO_y^-$ + MeOH and $^{186}W_xO_y^-$ + EtOH reactions have been completed, with representative results shown in Figure 4. While the kinetic analysis is in the early stages, dialkoxy products are the most significant products observed, which most likely accompany H_2 production with the addition of two alcohols.

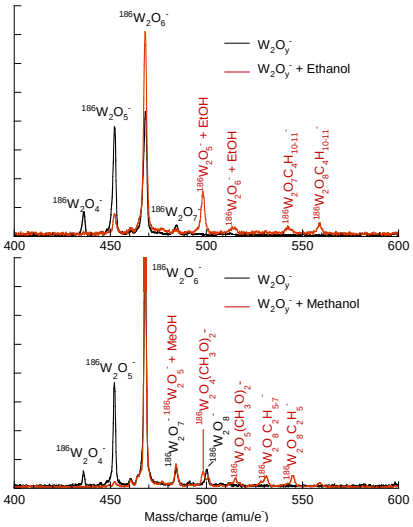

Figure 4. Mass spectra of ditungsten oxo clusters prior to (black trace) and after exposure to an alcohol.

III. Future Plans

A strength of the research program is the synergistic interplay between theory and experiment. Our target is to achieve a generalized description of the chemical reactivity of the transition metal oxides resulting in H_2 liberation. Work towards this end involves studying the feasibility of H_2 liberation from

each of the intermediates obtained in the fluxionality pathway of the clusters in the reactions of ammonia, water, and hydrogen sulfide. Other newer directions include the study of alcohol reactivity with the Mo/W oxide clusters with the view of better understanding the energetically relevant process of alcohol oxidation.

Temperature-dependence studies of reaction kinetics, which will allow a direct benchmarking of calculated reaction barriers, are planned to commence in Fall, 2012. Metal sulfide cluster structure and reactivity studies will also be initiated. Independently controlled two-reagent reactivity studies (e.g., $Mo_xO_y^- + CO_2 + H_2$) will be done in an effort to model full-cycle processes. Further, with the recent approval of a supplemental equipment grant, the resonant two-photon detachment technique will be applied to clusters and complexes to probe the role of photoexcitation in reactivity.

IV. References to publications of DOE sponsored research that have appeared in 2009–present or that have been accepted for publication

1. "Properties of Metal Oxide Clusters in non-Traditional Oxidation States," J. E. Mann, N. J. Mayhall and C. C. Jarrold, Chem. Phys. Lett. **525-6**, 1-12 (2012).
2. "Fluxionality in the Reactions of Transition-Metal Oxide Clusters: The Role of Metal, Spin-state and the Reacting Small Molecule," R. O. Ramabhadran, E. L. Becher, III, A. Chowdhury, and K. Raghavachari, J. Phys. Chem. A **116**, 7189-7196 (2012).
3. "Study of Nb_2O_y (y = 2-5) anion and neutral clusters using photoelectron spectroscopy and DFT calculations," J. E. Mann, S.E. Waller, D.W. Rothgeb and C. C. Jarrold, J. Chem. Phys. **135**, 104317 (2011).
4. "Structures of trimetallic molybdenum and tungsten suboxide cluster anions," D. W. Rothgeb, J. E. Mann, S. E. Waller and C. C. Jarrold, J. Chem. Phys. **135**, 104312 (2011).
5. "Molybdenum Oxides versus Molybdenum Sulfides: Geometric and Electronic Structures of $Mo_3X_y^-$ (X = O, S and y = 6, 9) Clusters," N.J. Mayhall, E.L. Becher, A. Chowdhury, and K. Raghavachari, J. Phys. Chem A, **115**, 2291-2296 (2011).
6. "Resonant two-photon detachment of WO_2^-," J.E. Mann, S.E. Waller, D.W. Rothgeb and C.C. Jarrold, Chem. Phys. Lett. **506**, 31-36 (2011).
7. "Proton Hop Paving the Way for Hydroxyl Migration: Theoretical Elucidation of Fluxionality in Transition-Metal Oxide Clusters," R.O. Ramabhadran, N.J. Mayhall, and K. Raghavachari, J. Phys. Chem. Lett. **1,** 3066-3071 (2010).
8. "Electrochemistry of Substituted Salen Complexes of Nickel(II):Nickel(I)-catalyzed Reduction of Alkyl and Acetylenic Halides," M. P. Foley, P. Du, K. J. Griffith, J. A. Karty, M. S. Mubarak, K. Raghavachari, and D. G. Peters, J. Electroanal. Chem. **647**, 194-203 (2010).
9. "Electrochemical Reduction of 5-Chloro-2-(2,4-Dichlorophenoxy)Phenol (Triclosan) in Dimethylformamide," K. N. Knust, M. P. Foley, M. S. Mubarak, S. Skljarevski, K. Raghavachari, and D. G. Peters, J. Electroanal. Chem. **638**, 100-108 (2010).
10. "H_2 production from reactions between water and small molybdenum suboxide cluster anions," D.W. Rothgeb, J.E. Mann, and C.C. Jarrold, J. Chem. Phys. **133**, Article 054305 (2010).
11. "CO_2 reduction by group 6 transition metal suboxide cluster anions," E. Hossain, D.W. Rothgeb, and C.C. Jarrold, J. Chem. Phys. **133**, Article 024305 (2010).
12. "Electronic structure of coordinatively unsaturated molybdenum and molybdenum oxide carbonyls," E. Hossain and C. C. Jarrold, J. Chem. Phys. **130**, 064301 (2009).
13. "Unusual products observed in gas-phase $W_xO_y^- + H_2O$ and D_2O reactions," D. W. Rothgeb, E. Hossain, A. T. Kuo, J. L. Troyer, C. C. Jarrold, N. J. Mayhall, and K. Raghavachari, J. Chem. Phys. **130**, 124314 (2009).
14. "Water reactivity with tungsten oxides: H_2 production and kinetic traps," N. J. Mayhall, D.W. Rothgeb, E. Hossain, C. C. Jarrold and K. Raghavachari, J. Chem. Phys. **131**, Article 144302 (2009).
15. "Termination of the $W_2O_y^- + H_2O/D_2O \rightarrow W_2O_{y+1}^- + H_2/D_2$ reaction: Kinetic versus thermodynamic effects," D. W. Rothgeb, E. Hossain, N. J. Mayhall, K. Raghavachari, and C. C. Jarrold, J. Chem. Phys. **131**, Article 144306 (2009).

Critical evaluation of theoretical models for aqueous chemistry and CO_2 activation in the temperature-controlled cluster regime

DE-FG02-00ER15066 and DE-FG02-06ER15800

K. D. Jordan (jordan@pitt.edu), Dept. of Chemistry, University of Pittsburgh, Pittsburgh, PA 15260

M. A. Johnson (mark.johnson@yale.edu), Dept. of Chemistry, Yale University, New Haven, CT 06520

Program Scope

Our joint program integrates experimental and theoretical methods to exploit the unique properties of isolated cluster ions as media in which to quantify the molecular-level interactions underlying the cooperative behavior of solvent networks such as that found in liquid water. This endeavor has traditionally been concerned with structural identification of reaction intermediates found in radiation chemistry, including the hydrated electron as well as the free radicals that arise from it in radiation-damaged systems.

Recent Progress

An excellent example where several years of theoretical and methodological advances resulted in a comprehensive picture of a complex chemical event is illustrated by our very recent paper describing the dynamics of photo-initiated, water network-mediated intracluster capture of excess electrons. The overall scheme is outlined in Fig. 1 and described in Ref. [8]. In that study, Ar-mediated condensation was used to capture the highly unstable entrance channel reactant consisting of a neutral CO_2 molecule attached to a hydrated electron cluster. Vibrational excitation then triggered the electron scavenging process generating the hydrated CO_2 radical anion, where vibrational and photoelectron spectroscopies were combined to characterize both the reactant and product species. The lack of mode-specific excitation of the intracluster reaction (i.e., independent of whether excitation occurs directly to the excess electron or to vibrational modes on either the water network or CO_2 reactant) established that the reaction occurred via statistical passage over a transition state. This allowed us to theoretically explore (using direct dynamics) the role of a solvent promoting reaction over a barrier in

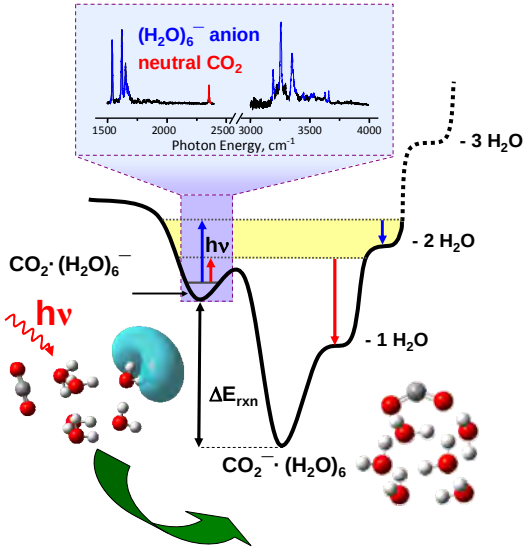

Figure 1. The potential energy landscape describing photochemical activation of a metastable reactant complex to initiate an intra-cluster electron capture reaction.

a regime where each solvent molecule is involved in the reaction. Specific structural motifs were identified as key features of the transition state, including a partial H-bond to the incipient CO_2^- moiety prior to electron transfer.

We are now extending the cluster work to explore electron capture onto other electron scavengers (such as nitromethane) as well as to characterize free radicals generated by electron attachment to multidentate H-bond bridges such as those found in double-stranded DNA. Regarding the latter, our first complete work on the archetypal formic acid dimer anion is described in Ref. [9]. The important structural motifs of this particular system were uncovered by following the spectral evolution with extensive isotope labeling and carrying out theoretical analyses of the various anharmonic effects. Another aspect of electron induced aqueous chemistry is the nature of the interaction between a diffuse electron and its associated water network, and we have recently completed our analysis of the distorted "Fano" lineshapes arising from interaction of vibrational levels of the supporting water network with the electron cloud. That work was carried out with Yale colleague and fellow CPIMS PI John Tully, and reported in Ref. [8].

The CO_2 work mentioned above was strategically chosen as a part of a transition in program emphasis designed to capitalize on our expertise in understanding solvent-mediated electron attachment and direct it toward resolving key obstacles encountered in the catalytic transformation of CO_2 into transportable fuels. First, we established the molecular structure of the critical carbamate intermediate in the pyridine-based photoelectrocatalysis scheme pioneered by the Bocarsly group, again relying on theoretical analysis of the vibrational spectra, with details presented in Ref. [6]. Next, we uncovered the origin of the remarkably large solvatochromic shift of the C-H stretching vibration in the surprisingly complex formate ion, HCO_2^-. This species is often generated early in reductive activation of CO_2, and in Ref. [7] we trace the effect to a large intramolecular charge redistribution along the C-H bond-breaking coordinate.

In an important recent experimental advance, we dramatically broadened the scope of chemistry that we can study to include non-aqueous systems by incorporating ion sources that not only provide universal access to both aqueous and non-aqueous species, but do so in a temperature-controlled fashion. This was carried out in close consultation with Profs. L.-S. Wang and X. Wang using methods they developed at PNNL and first reported at a CPIMS meeting. We are particularly interested in the structures of species invoked to explain the advantages of ionic liquids [IL] as media for CO_2 chemistry. ILs have attracted considerable attention because of their large Henry's law constants for CO_2 uptake, their being considered green solvents (in part due to the low vapor pressures), and their favorable catalytic activity in electrochemical reduction of CO_2. In imidazolium-based ILs [such as those based on 1-ethyl-3-methyl imidizolium (emim) cations], it has been reported that the CO_2 activity is mostly correlated with the chemical nature of the anionic component (e.g, BF_4^-, $N(CN)_2^-$, PF_6^-, acetate, etc.), prompting many theoretical efforts to reveal the intermolecular CO_2 interactions with various anionic partners. We are addressing the important molecular-level questions involving the specific interactions of CO_2 with the anionic components of the ionic liquids that trap and lower the overpotential in electrochemical processing of CO_2. Specifically, one of the important characteristics associated with strong CO_2 uptake into solution is the generation of

partially bent CO_2 groups in the adducts. It is highly likely that this motif contributes to lowering of the overpotential in electrochemical (and photoelectrochemical) reduction of CO_2, which is, in turn, the goal of the catalyst design. On the theoretical side, one of the most intriguing and not widely appreciated aspects of CO_2 chemistry is that bent CO_2 structures can occur either with or without delocalization of an excess electron onto the CO_2. The traditional view is that the bent structures necessarily are accompanied by electron delocalization onto the CO_2, but recent theoretical work on the binding of CO_2 to the TiO_2 anatase surface identified bent structures without delocalization of the electron onto the CO_2. This suggests that some of these structures actually can be viewed as having an electronic structure more consistent with an electronically excited CO_2 molecule.

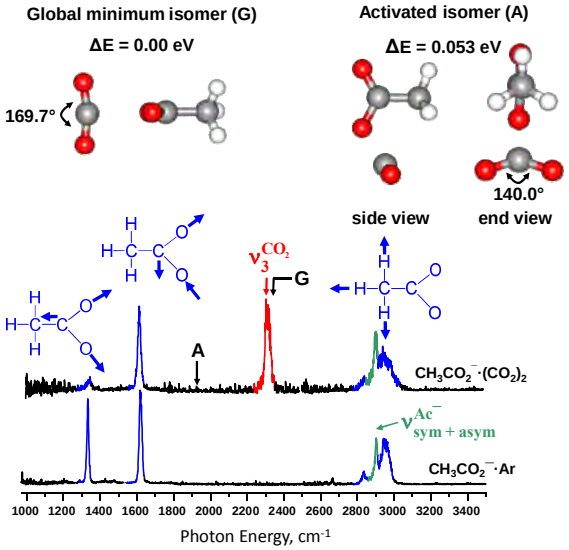

Fig. 2. Vibrational spectra of $CH_3CO_2^-\cdot(CO_2)_2$ cluster ion (top) along with the Ar-tagged spectrum of $CH_3CO_2^-$ (bottom). Transitions due to the acetate anion are highlighted in blue, while the asymmetric stretch of neutral CO_2 is shown in red. The breadth of the CO_2 feature suggests the presence of different binding sites, but the feature is indicative of a linear CO_2 molecule (isomer G). The activated isomer (A) is calculated to have a much lower energy CO_2 asymmetric stretch (arrow labeled A in upper trace).

We will present vibrational spectra of CO_2 adducts with the acetate ion, a species that has been reported to show high CO_2 solubility when present in an IL. In the case of the acetate-CO_2 adducts, two isomers are predicted to occur. One of these sequesters a primarily neutral CO_2 molecule between the oxygen atoms of the $CH_3CO_2^-$ ion, while the other features attachment of one of the carboxylate oxygen atoms to the central carbon atom of CO_2. The latter motif is calculated to occur 0.053 eV higher in energy, but has the bent geometry that is desirable for catalysis. Our goal is to provide critical experimental benchmarks that can be used to establish the level of theory required to describe the intermolecular distortions of CO_2 adducts. The spectrum of the acetate-CO_2 cluster is presented in Fig. 2, where the CO_2 molecule is clearly present as a linear species. To access the predicted higher energy activated configuration, we will next exploit our Ar-mediated approach to quench collision complexes into both the ground state and activated isomers. The two isomeric components will then be isolated using our pump-probe scheme developed in the previous grant period.

Future Plans

Looking to the future, we will increasingly rely on direct injection of reaction mixtures into our cryogenic spectrometers which now allow temperature control prior to spectroscopic interrogation. One of the most attractive first systems to engage with this new technology will be investigation of spectral diffusion of size-selected water clusters at a well-defined temperature. Specific targets include the onset of site-to-site migration and surface melting,

observables that arise from subtle features of the potential landscape. We will thus provide spectroscopic benchmarks that will challenge and lead to refinement of theoretical models describing flexible water.

Papers since October 1, 2009 under CPIMS DOE support

1. **"Survey of Ar-tagged predissociation and vibrationally mediated photodetachment spectroscopies of the vinylidene anion, $C_2H_2^-$",** Helen K. Gerardi, Kristin J. Breen, Timothy L. Guasco, Gary H. Weddle, George H. Gardenier, Jenny E. Laaser, and Mark A. Johnson, *J. Phys. Chem. A*, **114**, 1592-1601, 2010.

2. **"Isolating the spectral signatures of individual sites in water networks using vibrational double-resonance spectroscopy of cluster isotopomers",** Timothy L. Guasco, Ben M. Elliott, Mark A. Johnson, Jing Ding, and Kenneth D. Jordan, *J. Phys. Chem. Lett.*, **1**, 2396-2401, 2010.

3**. "Downsizing the hydrated electron's lair,"** Kenneth D. Jordan and Mark A. Johnson, *Science,* **329**, 42-43, 2010.

4. **"Vibrational Predissociation Spectrum of the Carbamate Radical Anion, $C_5H_5N\text{-}CO_2^-$, Generated by Reaction of Pyridine with $(CO_2)_m^-$,"** Michael Z. Kamrath, Rachael A. Relph, and Mark A. Johnson, *J. Am. Chem. Soc*., **132**, 15508-15511, 2010.

5. **"Unraveling the Anomalous Solvatochromic Response of the Formate Ion Vibrational Spectrum: An Infrared, Ar-Tagging Study of the HCO_2^-, DCO_2^-, and $HCO_2^-\cdot H_2O$ Ions,"** Helen K. Gerardi, Andrew F. DeBlase, Xiaoge Su, Kenneth D. Jordan, Anne B. McCoy, and Mark A. Johnson," *J. Phys. Chem. Lett.*, **2**, 2437-2441, 2011.

6. **"Vibrational Fano resonances in dipole-bound anions,"** Stephen T. Edwards, Mark A. Johnson, and John C. Tully*, J. Chem. Phys*., **136**, 15305, 2012.

7. **"Structural characterization of electron-induced proton transfer in the formic acid dimer anion, $(HCOOH)_2^-$, with vibrational and photoelectron spectroscopies,"** Helen K. Gerardi, Andrew F. DeBlase, Christopher M. Leavitt, Xiaoge Su, Kenneth D. Jordan, Anne B. McCoy, and Mark A. Johnson, *J. Chem. Phys.*, **136**, 134318, 2012.

8. **"Bottom-up view of water network-mediated CO_2 reduction using cryogenic cluster ion spectroscopy and direct dynamics simulations,"** Kristin J. Breen, Andrew F. DeBlase, Timothy L. Guasco, Vamsee K. Voora, Kenneth D. Jordan, Takashi Nagata, and Mark A. Johnson*, J. Phys. Chem. A*, **116**, 903-912, 2012.(Cover article)

Nucleation Chemical Physics

Shawn M. Kathmann
Chemical and Material Sciences Division
Pacific Northwest National Laboratory
902 Battelle Blvd.
Mail Stop K1-83
Richland, WA 99352
shawn.kathmann@pnl.gov

Program Scope

The objective of this work is to develop an understanding of the chemical physics governing nucleation. The thermodynamics and kinetics of the embryos of the nucleating phase are important because they have a strong dependence on size, shape and composition and differ significantly from bulk or isolated molecules. The technological need in these areas is to control chemical transformations to produce specific atomic or molecular products without generating undesired byproducts, or nanoparticles with specific properties. Computing reaction barriers and understanding condensed phase mechanisms is much more complicated than those in the gas phase because the reactants are surrounded by solvent molecules and the configurations, energy flow, and ground and excited state electronic structure of the entire statistical assembly must be considered.

Recent Progress and Future Directions

Better Descriptors for Heterogeneous Ice Nucleation

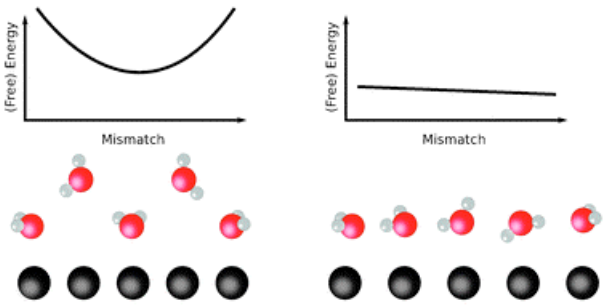

It has long been known that ice nucleation usually proceeds heterogeneously on a favorable surface of a foreign body. However, little is know at the microscopic level about which properties of a material determine its propensity to be an effective nucleating agent. The subtle chemical and epitaxial characteristics for a favorable ice nucleating agent, as has been described by Turnbull and Vonnegut [1] as a simple crystallographic disregistry parameter. This is in stark contrast to explanations encompassing the specific detailed electronic/chemical/structural effects. Using grand canonical Monte Carlo simulations we find that this tradition view does not account for the array of structures in the first water overlayer on a model heterogeneous interface. We find that, in order to describe the water structures formed, a good match between the substrate and the nearest neighbor oxygen-oxygen distance is a better descriptor than the bulk ice lattice constant. Current and future work will understand the role of surface chemistry, reconstruction, defects, as well as the near and far-field interfacial electric effects.

To this end we have begun to explore the nucleation of ice on polar kaolinite. A recent experimental study [2] found that ice preferentially nucleates on a positively charged pyroelectric (lithium tantalate $LiTaO_3$) surface versus a negatively charged surface giving rise to an E ~ 0.03 V/Å. Others [3-4] have found that electric fields greater than ~ 0.01 V/Å are required to nucleate ice. The common belief is that the field favorably influences the orientation of water molecules, however, the underlying mechanism is still a mystery. Here we focus our attention towards understanding and quantifying how this electrical nucleation catalysis occurs from both classical and quantum mechanical descriptions of spatial charge distributions. Using 192 TIP4P/2005 water molecules and a model polar kaolinite surface (with 204 atoms) we performed over 500 ns of NVT dynamics at 220K to observe ice formation. The profiles of the electric potentials over the slab as well as the resulting time dependent distributions are shown in the Figure below. By using point charges, one can separate out the water and kaolinite contributions to the

total potentials. One can see from the potential profile decomposition (left) that the kaolinite surface is polar setting up an electric field ~ 0.05 V/Å across the slab of water consistent with other theory and experimental studies. Furthermore, the time-dependent distributions of the electric potentials (right) can be used as an order parameter to characterize ice nucleation.

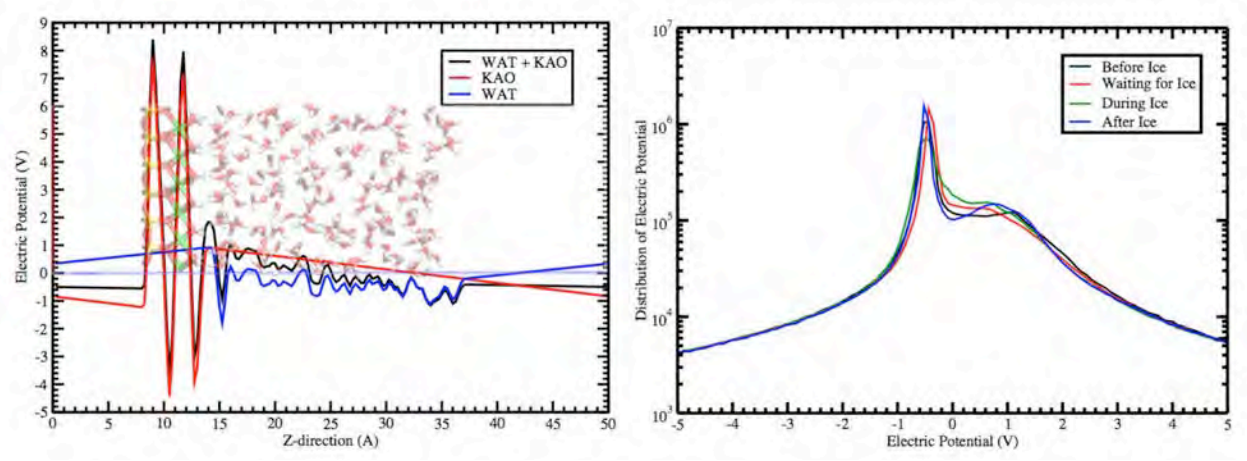

Photoelectron Spectroscopy of Cationic Interactions with Dicarboxylate Dianions

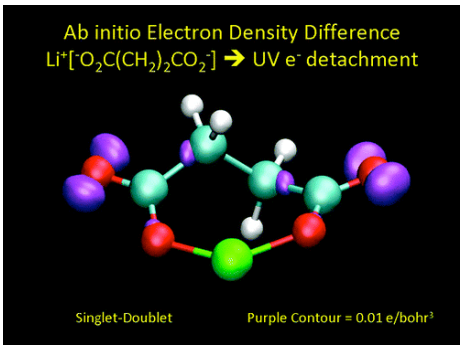

Alkali metal cations often show pronounced ion-specific interactions and selectivity with macromolecules in biological processes, colloids, and interfacial sciences, but a fundamental understanding about the underlying microscopic mechanism is still very limited. Here we report a direct probe of interactions between alkali metal cations (M^+) and dicarboxylate dianions, $^-O_2C(CH_2)nCO_2^-$ (Dn^{2-}) in the gas phase by combined photoelectron spectroscopy (PES) and ab initio electronic structure calculations on nine M^+–Dn^{2-} complexes (M = Li, Na, K; n = 2,4,6). PES spectra show that the electron binding energy (EBE) decreases from Li^+ to Na^+ to K^+ for complexes of M^+–D_2^{2-}, whereas the order is $Li^+ < Na^+ \sim K^+$ when M^+ interacts with a more flexible D_6^{2-} dianion. Quantum chemical calculations suggest that M^+ prefers to interact with both ends of the carboxylate $-COO^-$ groups by bending the flexible aliphatic backbone, and the local binding environments are found to depend upon backbone length n, carboxylate orientation, and the specific cation M^+. The observed variance of EBEs reflects how well each specific dicarboxylate dianion accommodates each M^+. This work demonstrates the delicate interplay among several factors (electrostatic interaction, size matching, and strain energy) that play critical roles in determining the structures and energetics of gaseous clusters as well as ion specificity and selectivity.

Crystalloluminescence, Concentration Effects, and Charge Transfer

Conventional wisdom supposes that when NaCl crystallizes from a supersaturated solution, the solvated Na^+ and Cl^- ions simply relocate from their tight hydration spheres to their most stable positions in the crystal lattice. However, observations over 200 years ago reported the emission of long-lived light resulting from the crystallization of certain salts (e.g., NaCl, KCl, etc.) – *crystalloluminescence*. We propose a mechanism where the ions, in the metastable configurations sampled during the crystallization event, transform into radicals and then radiatively decay – luminesce – back into ions again while forming the crystal. Luminescence is typically defined in terms of the conditions under which it is observed as opposed the exact underlying nuclear and electronic configurations that comprise the entire mechanism.

Said differently, non-adiabatic dynamics play a role in the dynamic heterogeneities underlying the thermodynamics and kinetics of crystallization from glasslike supersaturated aqueous electrolytes.

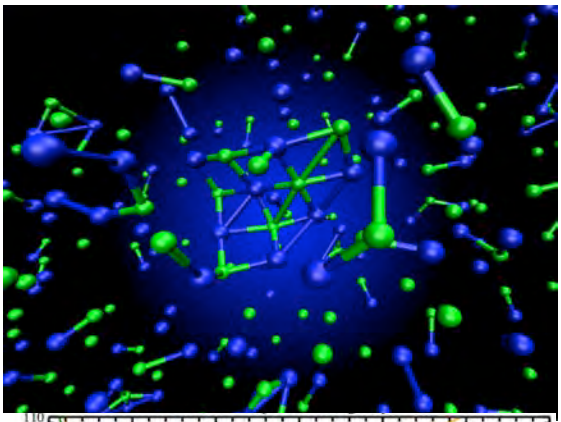

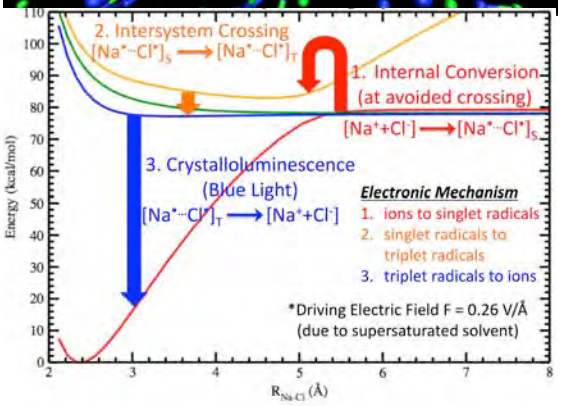

To understand and accurately quantify the mechanisms underlying crystallization several challenging aspects of condensed phase chemical physics must be confronted: concentration effects, charge transfer, and electronic transitions. Concentrated aqueous solutions have strong electric fields at the ion positions due to the hydrating waters, glasslike behavior, as well as multiple relaxation times as NMR, Optical Kerr, and Dielectric Relaxation spectroscopies [5]. Since it has been observed that during crystallization of NaCl salts from solution a burst of long-lived blue-violet light is emitted, we propose that this is only possible if some of the ions transform into radicals and then luminesce back into ions while forming the crystal. The this end, MRCI/aug-cc-pvtz calculations (using MOLPRO) on the NaCl dimer with zero and non-zero applied electric fields have shown that the avoided crossing (~9 Å at zero field) moves inward (to ~5.4 Å) with an applied biasing field of 0.26 V/Å and the excited triplet π state is stabilized with a vertical phosphorescence of ~2.8 eV (blue-violet light).

As a next step, we are investigating the influence of 2nd Na^+ ion on the excited state manifold of NaCl. In order to scan the potential energy landscape a grid was constructed by fixing a NaCl molecule in the coordinate system in such a way that the vector pointing from Cl to Na is parallel to the y-axis and the middle between the two atoms coincides with the origin. A second Sodium atom was placed at different displacements in the xy plane varying the angle with the y-axis (θ) and the distance from the origin (r). The calculations on $[Na_2Cl]^+$ were performed (using COLUMBUS) at the MCSCF level using C_s symmetry. A first inspection of the results shows that the ground state is lowest when the Na atom is close to the Cl atom with all three atoms being in a colinear $[Na\text{-}Cl\text{-}Na]^+$ arrangement (θ=180°). By rotating the Na atom up to the other possible linear arrangement (θ=0°, $[Cl\text{-}Na\text{-}Na]^+$) the ground state is destabilized and the first few excited states are lowered in energy. This stabilization of the excited states when the two Sodium atoms are brought close together is attributed to the fact that the excitation goes to a larger/more delocalized orbital that is a superposition of the two Na 3s orbitals rather than a single Sodium 3s.

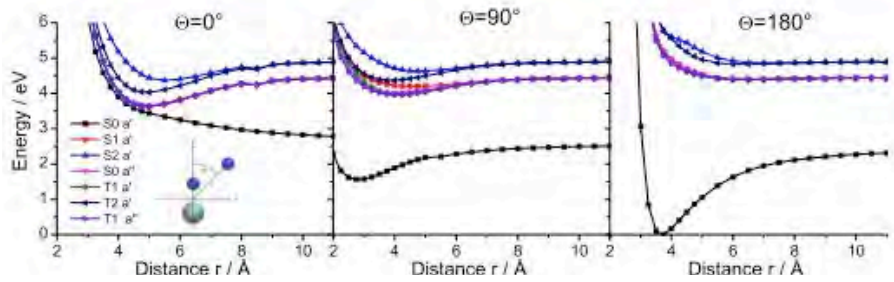

Some additional calculations (shown at right) at the CCSD(T)/aug-cc-pvdz showed that the optimized radical triplet state of a single cube of salt $[Na_4Cl_4]$ lies ~2.8 eV above the heterolytic singlet state.

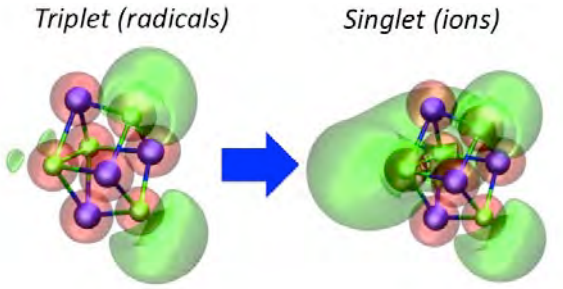

Our calculations have shown that charge transfer occurs as a function of concentration via *ab initio* re-sampling the classical trajectories and using Bader analysis to partition the electronic density into charges. For the configurations sampled, the Cl^- and H_2O charges show the greatest changes. Furthermore, this analysis helps to understand and quantify the limitations of modeling atoms in condensed phases with partial point charges.

Some ongoing work includes: (1) performing *ab initio* MD instead of simply using *ab initio* methods to resample the classical potential to study charge transfer, (2) using QM/MM hydrid DFT functionals to obtain distributions of excited (singlet and triplet) states to ground state singlet photon energies as well as spin-orbit interactions and oscillator strengths for the concentrated electrolytes, (3) use the Hartree potential analysis to compute the surface potentials of various aqueous electrolytes as functions of concentration as well as investigate the electrical properties of the crystal-aqueous phase interfaces to compare with available experiments, and (4) computing potentials of mean force for ions in solutions from the *ab initio* MD to use in accelerated dynamics to model crystallization kinetics.

Direct collaborators on this project include G.K. Schenter, C.J. Mundy, Marat Valiev, Xuebin Wang, John Fulton, and Postdoctoral Fellows Bernhard Sellner and Marcel Baer. Outside collaborations with the University College London include Stephen Cox and Angelos Michaelides on ice nucleation (Chemistry), and Jake Stinson and Ian Ford on sulfuric acid-water nucleation (Physics).

Acknowledgement: This research was performed in part using the Molecular Science Computing Facility in the Environmental Molecular Sciences Laboratory located at PNNL and the BES NERSC facility. Battelle operates PNNL for DOE.

References:

1. D. Turnbull and B. Vonnegut, "Nucleation Catalysis", *Industrial and Engineering Chemistry*, **44**(6), 1292 (1952).
2. D. Ehre, E. Lavert, M. Lahav, I. Lubomirsky, "Water Freezes Differently on Positively and Negatively Charged Surfaces of Pyroelectric Materials", *Science*, **327**, 672 (2010).
3. J.Y. Yan and G.N. Patey, "Heterogeneous Ice Nucleation Induced by Electric Fields", *Physical Chemistry Letters*, **2**, 2555 (2011).
4. C.A. Stan, S.K.Y. Tang, K.J.M. Bishop, and G.M. Whitesides, "Externally Applied Electric Fields up to 1.6×10^5 V/m Do Not Affect the Homogeneous Nucleation of Ice in Supercooled Water", *Journal of Physical Chemistry B*, **115**, 1089 (2011).
5. D.A. Turton, J. Hunger, G. Hefter, R. Buchner, and K. Wynne, "Glasslike Behavior in Aqueous Electrolyte Solutions", *Journal of Chemical Physics*, **128**, 161102 (2008).

Publications of DOE Sponsored Research (2010-present)

Invited Cover Article – S.M. Kathmann, GK Schenter, BC Garrett, B Chen, and JI Siepmann, "Thermodynamics and kinetics of nanoclusters controlling gas-to-particle nucleation." *Journal of Physical Chemistry C* **113**, 10354-10370 (2009).

Invited - C.J. Mundy, S. M. Kathmann, R. Rousseau, G. K. Schenter, J. Vande Vondele, and J. Hutter, "Scalable Molecular Simulation: Toward and Understanding of Complex Chemical Systems," *SciDAC Review*, 17, 10, (2010).

Cover Article – S.M. Kathmann, I-FW. Kuo, C.J. Mundy, and G.K. Schenter, "Understanding the Surface Potential of Water." *Journal of Physical Chemistry B*, **115**, 4369 (2011).

G. Murdachaew, M. Valiev, S.M. Kathmann, and X. Wang, "Study of Ion Specific Interactions of Alkali Cations with Dicarboxylate Dianions", *Journal of Physical Chemistry A*, **116**, 2055 (2012).

Communication – S.J. Cox, S.M. Kathmann, J.A. Purton, M.J. Gillan, and A. Michaelides, "Non-hexagonal ice at hexagonal surfaces: the role of lattice mismatch", *Physical Chemistry Chemical Physics*, **14**, 7944 (2012).

Chemical Kinetics and Dynamics at Interfaces

Structure and Reactivity of Ices, Oxides, and Amorphous Materials

Bruce D. Kay (PI), R. Scott Smith, and Zdenek Dohnálek
Chemical and Materials Sciences Division
Pacific Northwest National Laboratory
P.O. Box 999, Mail Stop K8-88
Richland, Washington 99352
bruce.kay@pnnl.gov

Additional collaborators include P. Ayotte, P. J. Feibelman, G. A. Kimmel, J. Knox, J. Matthiesen, R. A. May, G. S. Parkinson, and N. G. Petrik

Program Scope

The objective of this program is to examine physiochemical phenomena occurring at the surface and within the bulk of ices, oxides, and amorphous materials. The microscopic details of physisorption, chemisorption, and reactivity of these materials are important to unravel the kinetics and dynamic mechanisms involved in heterogeneous (i.e., gas/liquid) processes. This fundamental research is relevant to solvation and liquid solutions, glasses and deeply supercooled liquids, heterogeneous catalysis, environmental chemistry, and astrochemistry. Our research provides a quantitative understanding of elementary kinetic processes in these complex systems. For example, the reactivity and solvation of polar molecules on ice surfaces play an important role in complicated reaction processes that occur in the environment. These same molecular processes are germane to understanding dissolution, precipitation, and crystallization kinetics in multiphase, multicomponent, complex systems. Amorphous solid water (ASW) is of special importance for many reasons, including the open question over its applicability as a model for liquid water, and fundamental interest in the properties of glassy materials. In addition to the properties of ASW itself, understanding the intermolecular interactions between ASW and an adsorbate is important in such diverse areas as solvation in aqueous solutions, cryobiology, and desorption phenomena in cometary and interstellar ices. Metal oxides are often used as catalysts or as supports for catalysts, making the interaction of adsorbates with their surfaces of much interest. Additionally, oxide interfaces are important in the subsurface environment; specifically, molecular-level interactions at mineral surfaces are responsible for the transport and reactivity of subsurface contaminants. Thus, detailed molecular-level studies are germane to DOE programs in environmental restoration, waste processing, and contaminant fate and transport.

Our approach is to use molecular beams to synthesize "chemically tailored" nanoscale films as model systems to study ices, amorphous materials, supercooled liquids, and metal oxides. In addition to their utility as a synthetic tool, molecular beams are ideally suited for investigating the heterogeneous chemical properties of these novel films. Modulated molecular beam techniques enable us to determine the adsorption, diffusion, sequestration, reaction, and desorption kinetics in real-time. In support of the experimental studies, kinetic modeling and simulation techniques are used to analyze and interpret the experimental data.

Recent Progress and Future Directions

Probing the interaction of amorphous solid water on a hydrophobic surface: dewetting and crystallization kinetics of ASW on carbon tetrachloride The interaction of water with a hydrophobic surface is important for understanding many industrial and biological processes. The canonical wisdom is that water on a hydrophobic surface clusters to form structures that maximize the number of hydrogen bonds, thus lowering the overall energy of the system. While exact determination of the energetics of ASW interaction with CCl_4 is difficult, the formation of water clusters is expected because bulk water has a surface energy approximately three times that of CCl_4. There have been several recent theoretical and experimental investigations that have focused on the molecular level structure at the liquid water/hydrophobic substrate interface. Despite this work, more experimental work is needed to further

our understanding of structure and energetics of water on hydrophobic surfaces.

In a recent study we used temperature programmed desorption (TPD) and reflection absorption infrared spectroscopy (RAIRS) to probe the structure and crystallization kinetics of water deposited on CCl_4 layers. The desorption of carbon tetrachloride from beneath an ASWoverlayer provides information about the dewetting and crystallization of ASW. When not covered by an ASW overlayer, a 5 monolayer (ML) thick CCl_4 film heated at 0.6 K/s has a desorption peak at ~140 K. However, when an ASW film is deposited on top, and wets the CCl_4 film, no desorption below 140 K is observed. Instead desorption of the CCl_4 underlayer is delayed until crystallization induced cracking of the ASW overlayer opens an escape path to the surface. The subsequent rapid episodic release of CCl_4 has been termed the "molecular volcano". Infrared spectroscopy confirmed that the eruption of the "volcano" is directly correlated to the crystallization of the ASW overlayer and that the crystallization kinetics are dependent upon the ASW thickness and deposition temperature.

Thus, two distinct desorption regions are observed: one occurring at high temperatures commensurate with crystallization of the ASW overlayer (molecular volcano) and a second associated with a lower temperature mechanism which is an attenuated version of unhindered CCl_4 desorption. The appearance of a free (unhindered) CCl_4 desorption pathway at higher deposition temperatures indicates that the H_2O overlayer is not completely wetting the hydrophobic CCl_4 surface. The extent of dewetting was studied as a function deposition temperature and overlayer thickness. At all deposition temperatures (25 to 125 K) the covered fraction increases with ASW coverage albeit with different coverage dependencies. Also observed was that with increasing deposition temperature the amount of water required to completely cover the CCl_4 increases. For example at 25 K, CCl_4 is completely covered by 5 ML, whereas at 125 K this same amount of water is sufficient to cover only ~17% of the surface. In fact, at 125 K the low temperature (<140 K) CCl_4 desorption is not quenched until 50 ML of water are deposited.

These results indicate that the interaction of ASW with the hydrophobic CCl_4 surface depends on both the amount of ASW deposited and the deposition temperature. At low deposition temperatures ASW can kinetically "wet" the hydrophobic CCl_4 layer. However, as the deposition temperature is increased adsorbing water molecules become more mobile and are able to adopt a lower-energy dewetted structure. The lower energy configuration involves the formation of an increased number of hydrogen bonds, ultimately exposing portions of the lower surface energy CCl_4 substrate. The structure of the first few layers of water on both hydrophilic and hydrophobic substrates is an area of great scientific interest and ongoing research. Ongoing and future work in our laboratory will focus on determining the structure, kinetics, and energetics of nanoscale water films on CCl_4 and other hydrophobic surfaces.

Determination of crack propagation and distribution during the crystallization of nanoscale amorphous solid water films Amorphous solid water is a disordered version of ice created by vapor deposition onto a cold substrate (typically less than 130 K). It has a higher free energy than the crystalline phase of ice, and when heated above its glass transition temperature, it transforms into a metastable supercooled liquid. This unusual form of water exists on earth only in laboratories, after preparation with highly specialized equipment. It is thus fair to ask why there is any interest in studying such an esoteric material. Much of the scientific interest results from the ability to use ASW as a model system for exploring the physical and reactive properties of liquid water and aqueous solutions. ASW is also thought to be the predominant form of water in the extremely cold temperatures of many interstellar and planetary environments. In addition, ASW is a convenient model system for studying the stability of amorphous and glassy materials as well as the properties of highly porous materials. A fundamental understanding of such properties is invaluable in a diverse range of applications, including cryobiology, food science, pharmaceuticals, astrophysics, and nuclear waste storage, among others.

Crystallization of ASW can result in structural changes in the film. As mentioned briefly above, when an inert gas (CCl_4, Ar, CO_2, Kr , Xe, CO, N_2, O_2, and others) is deposited underneath an ASW overlayer (deposited at low temperature) the inert gas desorption is delayed until crystallization induced cracking of the ASW releases the trapped underlayer. We have termed the episodic release of trapped gases from ASW the "molecular volcano". The observed abrupt desorption is likely due to the formation

of cracks, fissures, or grain boundaries that accompany the crystallization kinetics and form a connected release pathway.

In some recent work we used the molecular volcano desorption peak of O_2 to explore the mechanism of crack formation. Composite films were created by depositing 1 ML of O_2 and then capping it with various overlayer thicknesses of ASW. The films were heated and the desorption of the underlayer was monitored with a mass spectrometer. At low overlayer thicknesses (< 100 ML) nearly all of the inert gas underlayer desorbs in a molecular volcano event. However as the overlayer thickness is increased, an increasing fraction of the inert gas does not desorb in a volcano event but instead desorbs at higher temperature when the ASW film itself desorbs. We refer to the desorption at higher temperature as the "trapped" fraction. A plot of the "trapped" faction versus the ASW overlayer coverage yields a sigmoidal-like curve that plateaus at near 600 ML. Below 200 ML, the trapped fraction increases slowly, implying that most of the crystallization-induced cracks span the entire overlayer thickness, opening a path for all of the O_2 to desorb. Above 200 ML, the trapped fraction increases rapidly until all the O_2 is trapped at thicknesses above 600 ML. The rapid increase in trapped fraction indicates that increasing numbers of cracks are unable to span the thicker ASW films, thus increasing the amount of trapped O_2. The vertical length distribution of crystallization-induced cracks through ASW is determined by taking the derivative of the trapped faction versus overlayer thickness curve. We find that ASW induced crack distribution is peaked ~340 ML (50 ML FWHM).

The infrared spectra obtained concomitantly with the desorption experiments revealed that for all film thicknesses (25 to 600 ML) the onset of crystallization occurred at the same temperature but the temperature for the volcano desorption increased with overlayer thickness. These results suggested that that cracks propagate on the time scale of the experiment, i.e., cracks do not "instantaneously" span the ASW. Further it showed that cracks do not initiate from random evenly dispersed nuclei, because if they did, the onset of the molecular volcano would be thickness independent. These results led us to create films where O_2 and Kr were selectively placed at various positions in the ASW overlayer. We found that the closer to the top of the film, the earlier in temperature the volcano desorption peak occurred. Through a series of experiments we were able to show conclusively that the direction of crack formation begins at the ASW/vacuum interface and moves downward into the film. Future work will focus on the kinetics of crystallization induced crack formation.

Probing the mobility of supercooled liquid 3-methyl pentane at temperatures near the glass transition using rare gas permeation Supercooled liquids are thermodynamically metastable with respect to their corresponding lower free energy crystalline phases. As a supercooled liquid is cooled below its melting temperature, molecular motion slows and the time it takes for the system to sample the available energy landscape increases. If crystallization is avoided, at some temperature this time increases to the point where the system cannot sample the available energy space on the laboratory timescale (e.g. ~100 s) and the system is said to be out of thermal equilibrium and non-ergodic. The behavior of a supercooled liquid, as it either crystallizes or becomes a glass, is of great interest in a number of technological and fundamental disciplines. We have recently explored the diffusivity of supercooled liquids using the permeation of inert gases through vapor deposited amorphous solid overlayers. The main idea of the technique is that when the amorphous solid is heated above its T_g it transforms into a supercooled liquid and the underlying inert gas can begin to diffuse through the overlayer. We have previously used this approach to measure the diffusivity of methanol, ethanol, and their mixtures at temperatures near T_g and shown that inert gas permeation rate is directly correlated to the diffusivity of the supercooled liquid itself.

In more recent work we studied the diffusivity of supercooled three-methyl pentane (3MP) using the inert gas permeation technique. Three-methyl pentane is a good glass former and is notoriously difficult to crystallize and as such viscosity data are available at temperatures down to its T_g of 77 K. We find that the permeation rate of the inert gas probes (Ar, Kr, Xe) all have a non Arrhenius temperature dependence that is well-described by a Vogel-Fulcher-Tamman (VFT) equation indicating fragile behavior. The results also show that the Stokes-Einstein (SE) equation, that predicts that the diffusivity, *D*, and the

viscosity, η, are inversely related, $D \propto T/\eta$, breaks down at temperatures approaching T_g. The fractional Stokes-Einstein equation, $D \propto (T/\eta)^n$, does fit the permeation data, albeit with different values of n for each gas. There is qualitative agreement with the SE equation in that the permeation rate decreases with increasing radius of the rare gas probe, but the small differences in radii significantly underestimate the observed differences in the permeation rates. Instead the permeation rates are better correlated with the rare gas-3MP interaction energy than with the atomic gas radius. This work demonstrates that the permeation technique can be applied to more complex molecules than our prior work on relatively small alcohols (methanol, ethanol). Future work using the inert gas permeation technique will focus on understanding the diffusion mechanism in other low temperature supercooled liquids.

References to Publications of DOE sponsored Research (October 2009- present)

1. J. Matthiesen, R. S. Smith, and B. D. Kay, *"Using Rare Gas Permeation to Probe Methanol Diffusion near the Glass Transition Temnperature",* Physical Review Letters **103**, 245902 (2009).
2. R. S. Smith, J. Matthiesen, and B. D. Kay, *"Measuring diffusivity in supercooled liquid nanoscale films using inert gas permeation. I. Kinetic model and scaling methods"*, Journal of Chemical Physics **133**, 174504 (2010).
3. J. Matthiesen, R. S. Smith, and B. D. Kay, *"Measuring diffusivity in supercooled liquid nanoscale films using inert gas permeation. II. Diffusion of Ar, Kr, Xe, and CH_4 through Methanol"*, Journal of Chemical Physics **133**, 174505 (2010).
4. G. S. Parkinson, Z. Dohnalek, R. S. Smith, and B. D. Kay, *"Reactivity of Fe^0 Atoms with Mixed CCl_4 and D_2O Films over FeO(111)"*, Journal of Physical Chemistry C **114**, 17136 (2010).
5. R. S. Smith, J. Matthiesen, and B. D. Kay, *"Breaking through the glass ceiling: The correlation between the self-diffusivity in and krypton permeation through deeply supercooled liquid nanoscale methanol films"*, Journal of Chemical Physics **132**, 124502 (2010).
6. P. Ayotte, P. Marchand, J. L. Daschbach, R. S. Smith, and B. D. Kay, *"HCl Adsorption and Ionization on Amorphous and Crystalline H_2O Films below 50 K"*, Journal of Physical Chemistry A **115**, 6002 (2011).
7. P. J. Feibelman, G. A. Kimmel, R. S. Smith, N. G. Petrik, T. Zubkov, and B. D. Kay, *"A unique vibrational signature of rotated water monolayers on Pt(111): Predicted and observed"*, Journal of Chemical Physics **134**, 204702 (2011).
8. J. Matthiesen, R. S. Smith, and B. D. Kay, *"Mixing It Up: Measuring Diffusion in Supercooled Liquid Solutions of Methanol and Ethanol at Temperatures near the Glass Transition"*, Journal of Physical Chemistry Letters **2**, 557 (2011).
9. R. A. May, R. S. Smith, and B. D. Kay, *"Probing the interaction of amorphous solid water on a hydrophobic surface: dewetting and crystallization kinetics of ASW on carbon tetrachloride"*, Physical Chemistry Chemical Physics **13**, 19848 (2011).
10. R. S. Smith, J. Matthiesen, J. Knox, and B. D. Kay, *"Crystallization Kinetics and Excess Free Energy of H_2O and D_2O Nanoscale Films of Amorphous Solid Water"*, Journal of Physical Chemistry A **115**, 5908 (2011).
11. D. W. Flaherty, N. T. Hahn, R. A. May, S. P. Berglund, Y. M. Lin, K. J. Stevenson, Z. Dohnalek, B. D. Kay, and C. B. Mullins, *"Reactive Ballistic Deposition of Nanostructured Model Materials for Electrochemical Energy Conversion and Storage"*, Accounts of Chemical Research **45**, 434 (2012).
12. R. A. May, R. S. Smith, and B. D. Kay, *"The Molecular Volcano Revisited: Determination of Crack Propagation and Distribution During the Crystallization of Nanoscale Amorphous Solid Water Films"*, Journal of Physical Chemistry Letters **3**, 327 (2012).
13. R. S. Smith and B. D. Kay, *"Breaking Through the Glass Ceiling: Recent Experimental Approaches to Probe the Properties of Supercooled Liquids near the Glass Transition"*, Journal of Physical Chemistry Letters **3**, 725 (2012).
14. R. S. Smith, N. G. Petrik, G. A. Kimmel, and B. D. Kay, *"Thermal and Nonthermal Physiochemical Processes in Nanoscale Films of Amorphous Solid Water"*, Accounts of Chemical Research **45**, 33 (2012).

Correlating electronic and nuclear motions during photoinduced charge transfer processes using multidimensional femtosecond spectroscopies and ultrafast x-ray absorption spectroscopy

Munira Khalil
University of Washington, Department of Chemistry, Box 351700, Seattle, WA 98195
Email: mkhalil@chem.washington.edu

The goal of this research program is to measure coupled electronic and nuclear motions during photoinduced charge transfer processes in transition metal complexes by developing and using novel femtosecond spectroscopies. In this program, we will use a unique two-pronged experimental approach to relate commonly measured kinetic parameters in transient photochemical experiments to the time-evolving distributions of molecular and electronic structures of the reactants and products and their interactions with the solvent bath. One part of the research program will focus on the development of novel three-dimensional visible-infrared experiments employing a sequence of visible and infrared fields to directly correlate electronic and vibrational motion during ultrafast photochemical reactions. These experiments will measure time-dependent anharmonic vibrational couplings of the high-frequency solute vibrations with the low-frequency solvent and solute degrees of freedom, time-dependent vibronic couplings, and elucidate the role of incoherent and coherent vibrational relaxation and transfer pathways during and following electron transfer.

Our work has focused on the following areas: (i) understanding photoinduced linkage isomerism in Fe(II) complexes[1] (ii) 2D IR spectroscopy of mixed valence complexes to measure vibrational couplings between terminal and bridging cyanide ligands[2] (iii) Elucidating the role of high frequency vibrations during ultrafast back electron transfer[3] (iv) Developing fifth-order spectroscopies to measure the non-equilibrium vibrational relaxation dynamics during a photoinduced charge transfer process[4,5] (v) Using DFT based methods to model Fe K-edge and N Kedge transient x-ray experiments probing ultrafast photoinduced spin crossover in Fe(II) complexes[6] and (vi) Using transient Ru L-edge x-ray absorption spectroscopy as a probe of electronic changes during intramolecular charge transfer processes.[7]

Photoinduced linkage isomerism in metal – nitrosyl compounds is a rich field of study in which irradiation of the sample by light causes the nitrosyl ligand to bond to the metal center in multiple ways. We studied photoinduced metal – nitrosyl linkage isomerism in sodium nitroprusside ($Na_2[Fe^{II}(CN)_5NO]\cdot 2H_2O$, SNP) dissolved in methanol using picosecond transient infrared (IR) spectroscopy. The high sensitivity of this technique allowed the simultaneous observation of two known metastable (MS) iron – nitrosyl linkage isomers of SNP, $[Fe^{II}(CN)_5(\eta^1\text{-ON})]^{2-}$ (MS1) and $[Fe^{II}(CN)_5(\eta^2\text{-NO})]^{2-}$ (MS2) at room temperature. The transient population of free nitrosyl radicals (NO·) is also measured in the sample solution. These three transient species are detected using their distinct nitrosyl stretching frequencies at 1794 cm^{-1} (MS1), 1652 cm^{-1} (MS2) and 1851 cm^{-1} (NO·). The metastable isomers and NO· are formed on a sub-picosecond time scale and have lifetimes greater than 100 ns. A UV (400 nm)−pump power dependence study reveals that MS1 can be formed with one photon, while MS2 requires two photons to be populated at room temperature in solution. We developed a photochemical kinetic scheme to model our data and the analysis revealed that photoisomerization and

photodissociation of the metal – NO moiety are competing photochemical pathways for SNP dissolved in methanol at room temperature.

Obtaining a detailed description of photochemical reactions in solution requires measuring time-evolving structural dynamics of transient chemical species on ultrafast time scales. Time-resolved vibrational spectroscopies are sensitive probes of molecular structure and dynamics in solution. We developed doubly resonant fifth-order nonlinear visible−infrared spectroscopies to probe non-equilibrium vibrational dynamics among coupled high-frequency vibrations during an ultrafast charge transfer process using a heterodyne detection scheme. The method enables the simultaneous collection of third- and fifth-order signals, which respectively measure vibrational dynamics occurring on electronic ground and excited states on a femtosecond time scale. Our data collection and analysis strategy allows transient dispersed vibrational echo (t-DVE) and dispersed pump−probe (t-DPP) spectra to be extracted as a function of electronic and vibrational population periods with high signal-to-noise ratios (S/N > 25). These fifth-order experiments can measure (i) time-dependent anharmonic vibrational couplings, (ii) nonequilibrium frequency−frequency correlation functions, (iii) incoherent and coherent vibrational relaxation and transfer dynamics, and (iv) coherent vibrational and electronic (vibronic) coupling as a function of a photochemical reaction.

To decipher the role of vibrational phase and energy relaxation in ultrafast photoinduced charge transfer processes, we have performed several experiments on a trinuclear cyano-bridged mixed valence complex of the form $[(CN)_5Fe^{II}–CN–Pt^{IV}(NH_3)_4–NC–Fe^{II}(CN)_5]^{4–}$ (herein denoted as $Fe^{II}Pt^{IV}Fe^{II}$) in aqueous solution. $Fe^{II}Pt^{IV}Fe^{II}$ has a high-energy metal-to-metal charge transfer band arising from charge transfer from Fe(II) to Pt(IV) over the cyanide bridging ligand. We have assigned and subsequently used the four cyanide stretching (ν_{CN}) vibrations – ν_{bridge} (2116 cm^{-1}), ν_{axial} (2074 cm^{-1}), ν_{trans} (2060 cm^{-1}), and ν_{radial} (2050 cm^{-1}) – as a multidimensional probe of vibrational excitation, redistribution, and relaxation dynamics as ultrafast back-electron transfer (BET) from the Pt to Fe atom occurs. First, femtosecond transient IR spectroscopy was used to monitor electronic dynamics, such as the rate of BET and subsequent vibrational relaxation dynamics. Our data allowed us to determine that BET to the electronic ground state occurs in 110 ± 10 fs, during which greater than 6 quanta (n) of vibrational energy are directed into the ν_{bridge} mode (n_{bridge} > 6). Intramolecular vibrational energy redistribution from the ν_{bridge} mode excites the solvent-accessible ν_{trans} mode on a 630 ± 50 fs time scale. Vibrational cooling to n = 1 and vibrational relaxation ensue on time scales of 1.3 ± 0.1 and 15–20 ps, respectively. These results highlight the important role played by a coupled network of high-frequency vibrations in ultrafast charge transfer processes in solution.

We used t-HDVE spectroscopy to perform a multiple-population-period (one electronic and one vibrational) experiment to probe coherent and incoherent vibrational relaxation energy dynamics among the highly excited CN stretching modes indirectly populated by BET in $Fe^{II}Pt^{IV}Fe^{II}$ dissolved in D_2O. Our results provide experimental evidence that the nuclear motions of the molecule are both coherently and incoherently coupled to the electronic charge transfer process. We observe that intramolecular vibrational relaxation dynamics among the highly excited ν_{CN} modes change significantly en route to equilibrium. The experiment also measures a 7 cm^{-1} shift in the frequency of

a ~57 cm^{-1} oscillation reflecting a modulation of the coupling between the probed high-frequency ν_{CN} modes for $\tau_{vis} < 500$ fs.

Our group is using and developing transient X-ray absorption spectroscopy (XAS) to understand changes in the electronic structure of molecules following light absorption. In particular, we have been studying photoinduced charge transfer processes in ruthenium and iron complexes possessing applications in molecular switching and solar energy technology. Following excitation of a metal-to-ligand charge transfer (MLCT) transition by visible light many transition metal complexes form metastable excited states with properties that differ greatly from their ground states. Transition metal XANES provides a detailed local probe of electronic structure surrounding the metal atoms that is sensitive to oxidation state, spin configuration, and metal—ligand interactions. Our research involves a mixed experimental and computational approach.

We have investigated the photoinduced spin crossover event in the Fe(II) complex $[Fe(tren(py)_3]^{2+}$ using density functional methods. Previous experimental work has demonstrated that excitation of this Fe complex dissolved in solution with 400 nm light converts the low-spin (LS) singlet ground state into a high-spin (HS) quintet species. The transition to high-spin is accompanied by a large geometric change that is indicated by the transient X-ray absorption spectrum. We have subsequently focused on identifying signatures of the changing electronic structure in these spectra. Our work has extended the transition potential (TP) DFT method that has been widely used for first row elements to simulate the k-edge X-ray absorption near edge spectra of iron. Our results show that one can use the TP methodology to simulate a 40 eV range of the X-ray spectrum. We have also used time-dependent (TD) DFT calculations to simulate the pre-edge features in the XAS spectrum. Analysis of the pre-edge features has allowed us to map out the 3d orbitals of the low- and high-spin moieties. From this analysis, we have extracted ligand field parameters and information about excited state electron distributions. In a related study we are investigating the SCO process in $[Fe^{II}(bpy)_3]^{2+}$ by TDDFT and nitrogen K-edge XAS. We have performed TDDFT calculations to simulate the transient X-ray absorption spectra of the HS and LS species at N K-edge. Our results are in good agreement with experiment predicting a –0.3 eV shift in the $1s \rightarrow \pi^*$ transition energy. These results show that N K-edge spectra of ligating nitrogen atoms can be used to track changes in metal—ligand bonding following photochemical events.

Our next study focused on the ground and excited state electronic structure of $Ru(dcbpy)_2(NCS)_2$ (termed N3), a widely used dye molecule in dye sensitized solar cells (DSSCs). Many studies focusing on the design of DSSCs have shown that the electronic structure of the dye molecule is important for efficient charge-carrier creation and dye regeneration. We have applied transient Ru L-edge XAS to study the rearrangement of electron density following photoexcitation of $N3^{4-}$. Excitation of the MLCT transition from the $^1A_1$ ground state of the $N3^{4-}$ dye leads to the formation of a ^{3}MLCT state with a ~59 ns lifetime. Ru L_3-edge XAS shows that the $^1A_1$ spectrum exhibits two features labeled B and C, and the ^{3}MLCT spectrum contains three features labeled A', B', and C'. The appearance of the A' feature in the ^{3}MLCT spectrum arises from a hole in the Ru 4d orbitals created by the MLCT excitation. Moreover, energetic shifts of +1.0 eV from B to B' and +0.9 eV from C to C' are observed.

TDDFT simulations of the Ru L_3-edge allow us to assignment of these features observed in the XA spectra of $N3^{4-}$. We find that the A' feature arise from a transition

from a Ru $2p_{3/2}$ orbital to an orbital of mixed Ru 4d and NCS π character. Features B and B' arise from transitions to states that are mostly Ru 4d orbitals of e_g character, and features C and C' are probes of the NCS π* orbitals. After accounting for a 2 eV stabilization of the Ru $2p_{3/2}$ orbitals in the ^{3}MLCT state, we conclude that the Ru e_g orbitals stabilize by 1.0 eV and the NCS π* orbitals stabilize by 0.6 eV. The MLCT transition in $N3^{4-}$ moves an electron an orbital of mixed Ru 4d and NCS π * character to one of the dcbpy ligands. This results in a decrease in electron density at the Ru center and on the NCS ligands. Consequently, we can identify shifts in the B and C features as markers of a decrease in electron density at the Ru atom and on the NCS ligands, respectively. The transient XAS results have an important design implication. In a DSSC the dye is oxidized following an MLCT transition to create charge carriers. Following oxidation the dye must be regenerated by a solution phase redox couple. Dye molecules containing NCS ligands have shown superior regeneration efficiency. Our experiment shows that the initial MLCT transition modifies the electronic structure on the NCS ligands and could provide a driving force for the regeneration process.

DOE Supported Publications (Oct 2009 - Present)

(1) Lynch, M. S.; Cheng, M.; Van Kuiken, B. E.; Khalil, M. Probing the Photoinduced Metal-Nitrosyl Linkage Isomerism of Sodium Nitroprusside in Solution Using Transient Infrared Spectroscopy. *J. Am. Chem. Soc.* **2011**, *133*, 5255.
(2) *Uncovering Coherent and Incoherent Vibrational Interactions in a Transition Metal Mixed Valence Complex Using Femtosecond Two-Dimensional Infrared Spectroscopy* by Lynch, M. S.; Van Kuiken, B. E.; Cheng, M.; Daifuku, S.; Khalil, M., in Ultrafast Phenomena XVII, Oxford University Press, 2011, pp 346.
(3) Lynch, M. S.; Van Kuiken, B. E.; Daifuku, S. L.; Khalil, M. On the Role of High-Frequency Intramolecular Vibrations in Ultrafast Back-Electron Transfer Reactions. *J. Phys. Chem. Lett.* **2011**, *2*, 2252.
(4) Lynch, M. S.; Slenkamp, K. M.; Cheng, M.; Khalil, M. Coherent Fifth-Order Visible–Infrared Spectroscopies: Ultrafast Nonequilibrium Vibrational Dynamics in Solution. *J. Phys. Chem. A* **2012**, *116*, 7023.
(5) Lynch, M. S.; Slenkamp, K. M.; Khalil, M. Communication: Probing Non-Equilibrium Vibrational Relaxation Pathways of Highly Excited C≡N Stretching Modes Following Ultrafast Back-Electron Transfer. *J. Chem. Phys.* **2012**, *136*, 241101.
(6) Van Kuiken, B. E.; Khalil, M. Simulating Picosecond Iron K-Edge X-Ray Absorption Spectra by Ab Initio Methods to Study Photoinduced Changes in the Electronic Structure of Fe(II) Spin Crossover Complexes. *J. Phys. Chem. A* **2011**, *115*, 10749.
(7) Van Kuiken, B. E.; Huse, N.; Cho, H.; Strader, M. L.; Lynch, M. S.; Schoenlein, R. W.; Khalil, M. Probing the Electronic Structure of a Photoexcited Solar Cell Dye with Transient X-Ray Absorption Spectroscopy. *J. Phys. Chem. Lett.* **2012**, *3*, 1695.

Chemical Kinetics and Dynamics at Interfaces

Non-Thermal Reactions at Surfaces and Interfaces

Greg A. Kimmel (PI) and Nikolay G. Petrik

Chemical and Materials Sciences Division
Pacific Northwest National Laboratory
P.O. Box 999, Mail Stop K8-88
Richland, WA 99352
gregory.kimmel@pnnl.gov

Program Scope

The objectives of this program are to investigate 1) the thermal and non-thermal reactions at surfaces and interfaces, and 2) the structure of thin adsorbate films and how this influences the thermal and non-thermal chemistry. Energetic processes at surfaces and interfaces are important in fields such as photocatalysis, radiation chemistry, radiation biology, waste processing, and advanced materials synthesis. Low-energy excitations (e.g. excitons, electrons, and holes) frequently play a dominant role in these energetic processes. For example, in radiation-induced processes, the high energy primary particles produce numerous, chemically active, secondary electrons with energies that are typically less than ~100 eV. In photocatalysis, non-thermal reactions are often initiated by holes or (conduction band) electrons produced by the absorption of visible and/or UV photons in the substrate. In addition, the presence of surfaces or interfaces modifies the physics and chemistry compared to what occurs in the bulk.

We use quadrupole mass spectroscopy, infrared reflection-absorption spectroscopy (IRAS), and other ultra-high vacuum (UHV) surface science techniques to investigate thermal, electron-stimulated, and photon-stimulated reactions at surfaces and interfaces, in nanoscale materials, and in thin molecular solids. Since the structure of water near interface plays a crucial role in the thermal and non-thermal chemistry occurring there, a significant component of our work involves investigating the structure of aqueous interfaces. A key element of our approach is the use of well-characterized model systems to unravel the complex non-thermal chemistry occurring at surfaces and interfaces. This work addresses several important issues, including understanding how the various types of low-energy excitations initiate reactions at interfaces, the relationship between the water structure near an interface and the non-thermal reactions, energy transfer at surfaces and interfaces, and new reaction pathways at surfaces.

Recent Progress

Oxygen Photochemistry on TiO_2(110): Recyclable, Photoactive Oxygen Produced by Annealing Adsorbed O_2

The thermal and photochemistry of oxygen adsorbed on TiO_2(110) are areas of active research. The interest is driven by both practical and scientific considerations. For example, titanium dioxide photocatalysts are used for removing organic pollutants from water and as thin film coatings on self-cleaning surfaces, and could potentially be used for photocatalytic splitting of water into H_2 and O_2. We have investigated the photochemistry of oxygen adsorbed on TiO_2(110) at 30 K and annealed up to 600 K.[4] UV irradiation results in exchange of atoms between chemisorbed and physisorbed oxygen. Annealing chemisorbed oxygen to 350 K maximizes these exchange reactions, while such reactions are not observed for oxygen that is dissociatively adsorbed on TiO_2(110) at 300 K. The chemisorbed species is stable under multiple cycles of UV irradiation. Atoms in the chemisorbed species can be changed from ^{18}O to ^{16}O and then back to ^{18}O via the exchange reactions. The results show that annealing oxygen on TiO_2(110) to ~350 K produces a stable chemical species with novel photochemical properties.

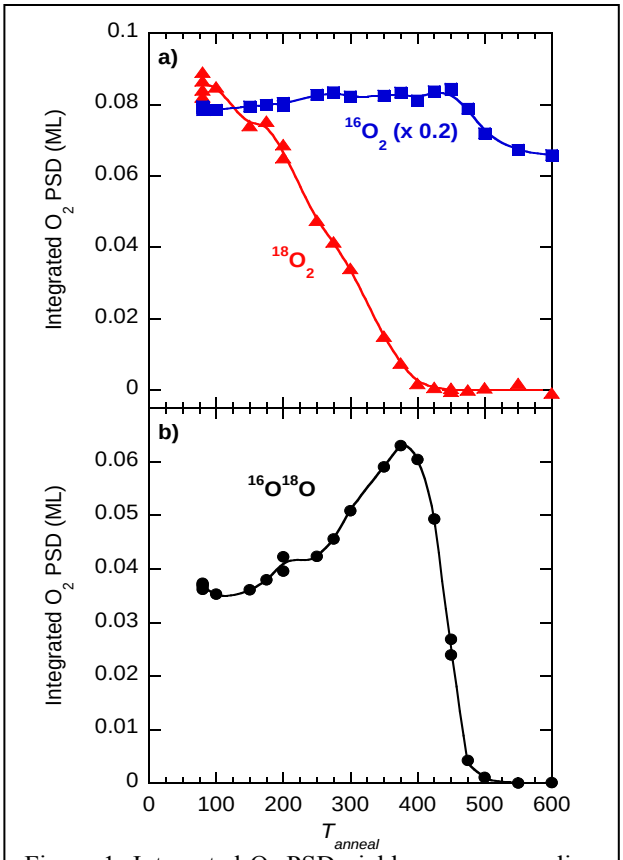

Figure 1: Integrated O_2 PSD yields versus annealing temperature, T_{anneal}. $^{18}O_2$ was deposited at 30 K and annealed. Then physisorbed $^{16}O_2$ was deposited and the system was irradiated with UV light while the desorption of the O_2 isotopes was monitored with a mass spectrometer.

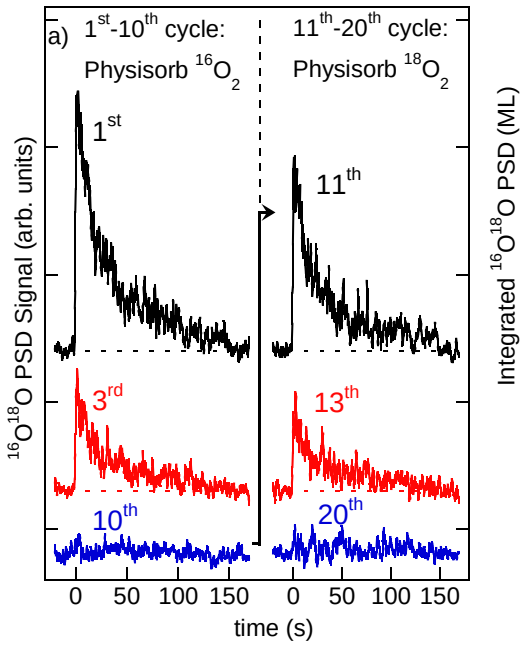

Figure 2: $^{16}O^{18}O$ PSD signals versus time for repeated UV irradiations. See text for details.

Figure 1 shows the time-integrated $^{16}O_2$, $^{18}O_2$, and $^{16}O^{18}O$ photon-stimulated desorption (PSD) yields versus annealing temperature, T_{anneal}, of chemisorbed oxygen. $^{18}O_2$ was adsorbed at 30 K and annealed at T_{anneal} for 240 s. Then 0.4 ML $^{16}O_2$ was adsorbed and the sample was irradiated (both at 30 K). The $^{16}O^{18}O$ PSD signal results from photon-stimulated reactions involving the exchange of atoms between the chemisorbed oxygen and physisorbed O_2. The $^{18}O_2$ PSD yield decreases approximately monotonically as T_{anneal} increases and is essentially zero above 400 K (Fig. 1a, red triangles). The $^{16}O_2$ PSD yield is nearly independent of T_{anneal} (Fig. 1a, blue squares). In contrast, the $^{16}O^{18}O$ PSD yield initially increases with increasing annealing temperature, goes through a maximum at T_{anneal} ~ 375 K, and then rapidly drops to zero for high temperatures (Fig. 1b, black circles). Annealing above ~400 K brings Ti interstitials to the surface that react with the adsorbed oxygen to form TiO_x islands, resulting in the observed decrease in the $^{16}O_2$ and $^{16}O^{18}O$ PSD yields. The results in Figure 1 suggest that annealing TiO_2(110) with adsorbed oxygen leads to the creation of a distinct, stable species on the surface, and changes in the angular distribution of the desorbing oxygen versus T_{anneal} support this hypothesis (data not shown).

Remarkably, the chemisorbed oxygen species responsible for the photon-stimulated exchange reactions is not destroyed by repeated cycles of UV irradiation. Figure 2 shows the $^{16}O^{18}O$ PSD signals versus time for an experiment with repeated UV irradiations. For this experiment, $^{18}O_2$ was annealed at 350 K. The sample was subsequently dosed with physisorbed $^{16}O_2$ at 30 K and irradiated with UV light. The black trace in the upper left corner of Figure 2 (labeled "1st") shows the $^{16}O^{18}O$ PSD versus time for the first irradiation. This was followed by nine more cycles where the sample was heated to 100 K (to desorb any remaining physisorbed O_2), dosed with $^{16}O_2$ and UV irradiated. The red and blue traces on the left side of Figure 2 show the $^{16}O^{18}O$ PSD signals for the third and tenth irradiation cycles, respectively. By the tenth irradiation cycle, the $^{16}O^{18}O$ PSD is essentially zero. Following the first ten UV irradiation

cycles, another ten irradiation cycles were performed, however the oxygen physisorbed on the sample was switched to $^{18}O_2$. For the eleventh irradiation cycle, the $^{16}O^{18}O$ PSD signal reappears (Fig. 2 - upper right, black line). For irradiation cycles 12 – 20, $^{16}O^{18}O$ PSD signal decreases again. The results presented here suggest that oxygen adsorbed on reduced TiO_2(110) and then annealed to temperatures above 100 K forms a distinct chemical species with interesting photochemical properties. At present, the chemical state of the oxygen that reacts with physisorbed O_2 and many of the details of that reaction are not known. More research is needed to determine the detailed state of the reactive, chemisorbed oxygen. However, two likely candidates are O_2 adsorbed in a bridging oxygen vacancy and tetraoxygen. These results show that the photochemistry of O_2 on TiO_2(110) is more complicated than previously appreciated.

Polarization- and azimuth-resolved infrared spectroscopy of water on TiO_2(110): Anisotropy and the hydrogen-bonding network

The structure of water at interfaces influences the physical, chemical and biological processes relevant to a large number of natural and man-made systems. As a result, the structure of water at surfaces has been extensively studied. Still, even the simplest and arguably most experimentally accessible issue – the ground-state arrangement of the first water layer on a solid surface – has been hard to resolve. In collaboration with Marcel Baer, Chris Mundy, Roger Rousseau, and Joost VandeVondele, we have investigated the structure and dynamics of thin water films on TiO_2(110) using polarization- and azimuthal-resolved IRAS and density functional theory (DFT).[6] The IRAS spectra indicate strong anisotropy in the water films. The vibrational densities of states predicted by the *ab-initio* molecular dynamics (AIMD) simulations for 1 and 2 monolayer coverages agree well with the observations. The results provide new insight into the structure of water on TiO_2(110) and resolve a long-standing puzzle regarding the hydrogen-bonding between molecules in the first and second monolayer on this surface. More generally, the results also demonstrate the capabilities of polarization- and azimuthally-resolved IRAS for investigating the structure and dynamics of adsorbates on dielectric substrates.

Figure 3 shows IRAS and AIMD results for 1 ML D_2O films on TiO_2(110). IRAS spectra for s- and p-polarized light incident along the [001] and [1$\bar{1}$0] azimuths (Fig. 3d) indicate significant

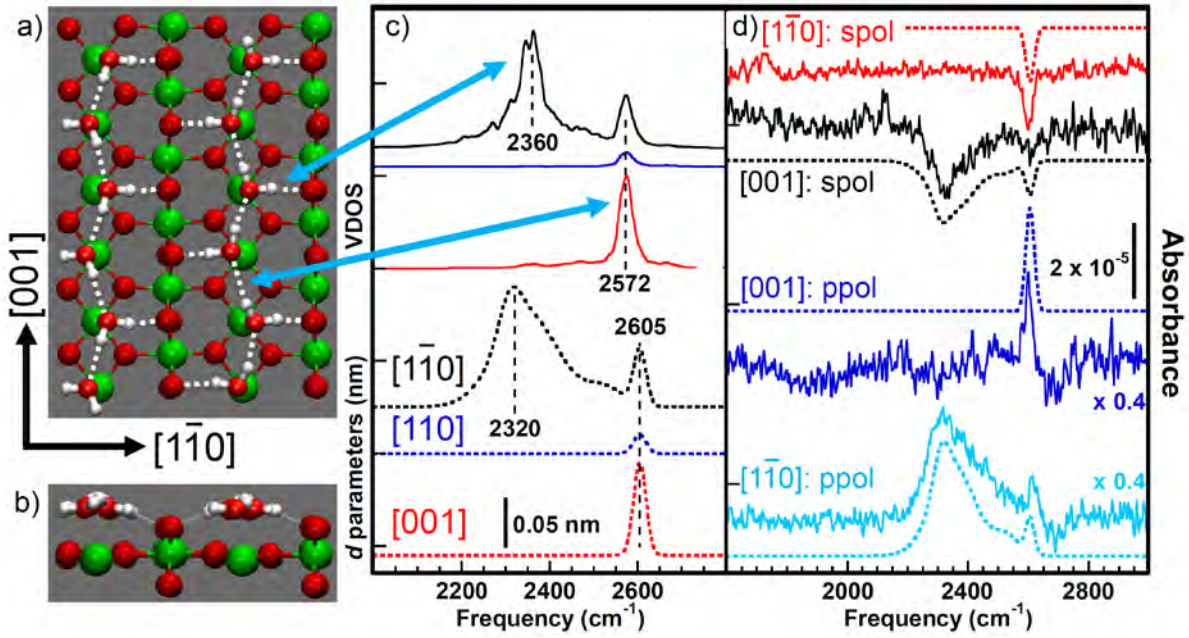

Figure 3. Structure and dynamics for θ = 1 ML D_2O on TiO_2(110). a) top view and b) side view of the calculated structure using *ab-initio* molecular dynamics. c) Calculated VDOS (solid lines) and $d(\omega)$ parameters (dashed lines) versus frequency. The same colors are used for each direction for both the VDOS and *d* parameters. d) IRAS spectra for s- and p-polarized light along both azimuths (solid lines) and simulated spectra (dashed lines) using d-parameter theory.

anisotropy in the structure of the water film. The AIMD simulations provide a simple interpretation of the IRAS spectra. For θ = 1 ML on a defect-free surface, every molecule is nearly equivalent. Thus there are two types of H-bonds, and one IR band associated with each. Once the projections of each bond along the different directions are included, the bands associated with the two bonds can be clearly identified. The first band, due to H-bonds between adjacent D_2O_{Ti}'s (see Fig. 3a and 3b), are primarily parallel to the BBO rows and are responsible for the narrow peak at 2605 cm^{-1} in the experiments and at 2572 cm^{-1} in the VDOS (Fig 3c, red lines). Since these bonds are not completely parallel to the BBO rows, the same peak is also evident in the other directions. The second H-bond, between D_2O_{Ti} and BBO, is primarily along $[1\,\bar{1}\,0]$ and leading to the peak at 2320 cm^{-1} in IRAS and 2360 cm^{-1} in theory (Fig. 3c, black lines).

For 2 ML D_2O films on TiO_2(110), the water films are also strongly anisotropic due the influence of the substrate (data not shown). However as the coverage increases, the influence of the substrate on subsequent water layers is reduced and the films become more isotropic. These results provide new insight into the binding of water on TiO_2(110).

Future Directions:

Important questions remain concerning the factors that determine the structure of thin water films on various substrates. We plan to continue investigating the structure of thin water films on non-metal surfaces, such as oxides, and on metals where the first layer of water does not wet the substrate. For the non-thermal reactions in water films, we will use IRAS to characterize the electron-stimulated reaction products and precursors. We will also continue our investigations into the photochemistry of small molecules on TiO_2(110).

References to publications of DOE sponsored research (FY 2010 – present)

[1] Nikolay G. Petrik and Greg A. Kimmel, "Photoinduced Dissociation of O_2 on Rutile TiO_2(110)," *J. Phys. Chem. Lett.* **1**, 1758 (2010).

[2] Nikolay G. Petrik and Greg A. Kimmel, "Electron- and hole-mediated reactions in UV-irradiated O_2 adsorbed on reduced rutile TiO_2(110)," *J. Phys. Chem. (C)*, **115**, 152 (2011).

[3] Peter J. Feibelman, Greg A. Kimmel, R. Scott Smith, Nikolay G. Petrik, Tykhon Zubkov, and Bruce D. Kay, "A unique vibrational signature of rotated water monolayers on Pt(111): Predicted and observed," *J. Chem. Phys.,* **134**, 204702 (2011).

[4] Nikolay G. Petrik and Greg A. Kimmel, "Oxygen Photochemistry on TiO_2(110): Recyclable, Photoactive Oxygen Produced by Annealing Adsorbed O_2," *J. Phys. Chem. Lett,* **2**, 2790 (2011)**.**

[5] R. Scott Smith, Nikolay G. Petrik, Greg A. Kimmel, and Bruce D. Kay, "Thermal and non-thermal physiochemical processes in nanoscale films of amorphous solid water," *Accounts of Chemical Research*, **45,** 33 (2012).

[6] G. A. Kimmel, M. Baer, N. G. Petrik, J. VandeVondele, R. Rousseau, and C. J. Mundy, "Polarization- and azimuth-resolved infrared spectroscopy of water on TiO_2(110): Anisotropy and the hydrogen-bonding network, " *J. Phys. Chem. Lett,* **3**, 778 (2012).

Radiation Chemistry Underpinning Nuclear Power Generation

Jay A. LaVerne, David M. Bartels Daniel M. Chipman, Sylwia Ptasinska
Notre Dame Radiation Laboratory, University of Notre Dame, Notre Dame, IN 46556
laverne.1@nd.edu, bartels.5@nd.edu, chipman.1@nd.edu, ptasinska.1@nd.edu

Program Scope

The focus of this work is on understanding the fundamental chemistry of the radiation effects underlying applications in the field of nuclear energy. The project builds on NDRL strengths developed over many years in addressing fundamental radiation chemical topics by examining in detail a few specific challenges found in the field of nuclear power generation. The project addresses the three broad areas: reactor chemistry, fuel and waste processing, and waste storage that are linked by the common factor of the influence of interfaces. The focus of much of the research is water and aqueous media because of its ubiquitous nature throughout the nuclear industry. Important questions being answered include how the radiolysis of water either modifies or is modified by a nearby interface. In reactor chemistry, specific topics being addressed are radiation enhanced corrosion, rates of radical reactions at high temperature and the production and destruction of aqueous H_2O_2 at interfaces. The knowledge obtained aids in the management of existing reactors and in the development of next generation reactors. Specific topics investigated in separation systems include an examination of the stable products in the radiolysis of water at extreme pH and the effects of added ceramic oxides. Gas production in the radiolysis of resins, especially when associated with water, is being explored to aid in the management and development of waste separation streams. The third area of research focuses on the radiation chemistry associated with waste storage. This part examines the effects of water radiolysis on interfaces and the radiolysis of polymers used in waste storage. Both topics address the production of hazardous gases, which are especially important in the storage and transportation of waste in sealed containers.

Recent Progress and Future Plans

The oxidation of FeO and Fe_2O_3 is important in the radiolytic aging of steels and other components in nuclear reactors. Diffuse reflectance infrared Fourier transform studies of the water on the surfaces of these oxides have been combined with newly acquired temperature programmed desorption studies to show that two types of chemisorbed water appear to be on the surface of nanoparticles of FeO and Fe_2O_3. This water is strongly bound with energies of 1 to 2 eV. The nature of this bound water is not known, but there is obviously strong bonding of the chemisorbed water with surface OH groups. Irradiation of these oxides leads to very little production of molecular hydrogen compared to that found with zirconia, which suggests that the transport of energy through the bulk solid or the reactive sites on the surface is much different than observed with zirconia. X-ray Photoelectron Spectroscopy, XPS, examination of FeO following irradiation shows no noticeable oxidation of the Fe sites on the surface. Similar results are observed with Fe_2O_3. These materials seem to be surprisingly inert with respect to the radiolysis of water at their surface. An XPS examination of the variation of the oxygen atom environment may provide additional information on the radiolytic oxidation of the surface. Oxidation reactions with added hydrogen peroxide will be performed to gain more information on the ability to oxidize the surface.

XPS studies have been performed on semiconductor heterostructures, i.e., systems composed of ultrathin layers (a few atomic monolayers) of different compounds. The following samples have been characterized by XPS: thin layers of Fe on GaAs, GaAs nanowires on a GaAs (111B) substrate, ZnTe nanowires on a GaAs (111B) substrate and GaAs core /Fe shell nanowires on a GaAs (111B) substrate. Materials studied in this project were fabricated by molecular beam epitaxy in the laboratory of Prof. J. Furdyna and M. Dobrowolska at Notre Dame. In the case of samples with a thin layer of Fe on GaAs, the oxidation layer has been detected. The XPS analysis of Fe2p, Fe3p and O1s peaks has been performed in order to estimate oxidation states on the surface. Figure 1 presents the XPS Fe2p spectrum for one of the analyzed samples of a thin layer of Fe on GaAs. The XPS spectra were fitted using the literature values for various iron oxides. From the Fe peaks it was found that the ratio of Fe^{3+} to Fe^{2+} was roughly three and the ratio of Fe^{3+} to Fe^{0+} was roughly six. Similar analysis was done for other iron samples deposited on GaAs semiconductors.

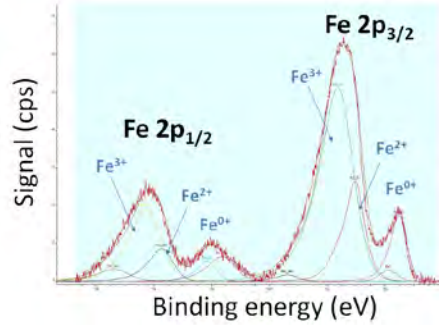

Figure 1. XPS spectrum of iron oxide.

Hydrogen is added to reactor cooling loops to prevent radiolysis and maintain a low corrosion potential, but the amount of hydrogen actually required has not been established. A "benchmark" experiment was performed at Atomic Energy of Canada Limited (AECL) nearly twenty years ago, which has been discussed at nearly every reactor chemistry meeting since. In collaboration with workers at National Nuclear Laboratory, Harwell, UK, we have made extensive progress in modeling this experiment in the past year. In the AECL experiments the reactor test loop was operated at a fixed hydrogen concentration for a period of time and then oxygen was "titrated" into the loop at a relatively constant rate to remove hydrogen by recombination in the radiation field. The concentration of hydrogen steadily decreases as oxygen is titrated in until a "critical hydrogen concentration" (CHC) of ~0.5 scc/kg (scc = standard cubic centimeters, i.e., about 20 micromolal) is reached. At this point both hydrogen and oxygen concentrations increase sharply as net radiolysis occurs, and $[H_2]$ eventually reaches 2.5 scc/kg in the limit of zero "excess reducing equivalents" (ERE=$[H_2]$-$[H_2O_2]$-2 $[O_2]$, in units of $[H_2]$). The AECL loop experiment was simulated using the 2009 Elliot/Bartels reaction rate and yield database. The base calculation CHC in Figure 2 is an order of magnitude too low, and the calculation grossly fails to predict the steady state $[H_2]$ at zero ERE. A comprehensive sensitivity study was carried out. The forward and reverse rate constants for equilibrium (R32) (numbering scheme from Elliot and Bartels)

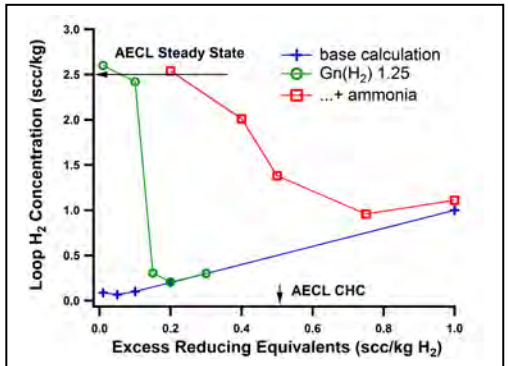

Figure 2. Addition of 10mM ammonia and reactions R35-R38 to the previous calculation with $G_n(H_2) = 1.25$, finally demonstrates a CHC behavior similar to the AECL experiment, using plausible rate constants

$$H + H_2O \leftrightarrows OH + H_2 \qquad (R32)$$

can have a large effect on the CHC and the steady state concentrations. A similarly large effect is obtained from changing the ratio of yields of molecular products H_2 and H_2O_2 to that for radicals. No other parameters of the model can change the result significantly. We measured the backward rate R32b to within 10% ten years ago. This year, we measured steady state [H_2] in water using electron radiolysis from a Van de Graaff accelerator. This measurement gives the forward rate R32f to within a factor of two, in good agreement with the previous estimate. Consequently, reaction rates can be excluded as the reason for the base model failure.

A classical force field has been determined to describe the interaction between a hydrogen molecule and water by fitting an analytic potential energy surface to high-level electronic structure calculations. This potential surface is qualitatively similar to that determined recently for an H atom with water, although differing in quantitative detail. Molecular dynamics simulations using the potential have been initiated to describe the properties of molecular hydrogen in water from ambient up to supercritical conditions, for use in calculations of important reaction rates

Tabulated high temperature escape yields for neutron radiolysis are only estimated from scavenger experiments. In order to obtain the observed steady state [H_2], it proves necessary to postulate no radicals and molecular yields of $G_n(H_2) = G_n(H_2O_2) = 1.25$ molecules/100eV from the (recoil ion) neutron radiolysis. The result is the green curve of Figure 2. However, the observed value of CHC is impossible to model with pure water chemistry. AECL workers reported that some ammonia impurity was also present in the loop at about 10 micromolar concentration. We postulate the following reactions are important near the CHC threshold:

$$NH_3 + OH \rightarrow NH_2 + H_2O \quad \text{(R35)}$$

$$NH_2 + H \rightarrow NH_3 \quad \text{(R36)}$$

$$NH_2 + OH \rightarrow NH_2OH \quad \text{(R37)}$$

$$NH_2OH + e^-_{aq} \rightarrow NH_2 + OH^-_{aq} \quad \text{(R38)}$$

With reasonable rate constant estimates, we are able to calculate the red curve of Figure 2, if we also use the modified neutron *G*-values. We conclude that a fully quantitative model of the AECL benchmark experiment requires accurate high temperature rate constants for nitrogen species and especially the neutron *G*-values.

Polyvinyl chloride has been used extensively to bag radioactive waste materials and a variety of silicones have been suggested as matrices for encapsulating waste materials. Our studies with both of these compounds initially focused on the production of gaseous compounds, especially molecular hydrogen. More recent work in this period has focused on examination of the main molecular compounds using a variety of spectroscopic techniques. The radiolysis of aerated samples results in the production of C-O compounds as identified by FTIR. These compounds are probably peroxides formed by the addition of oxygen to parent radicals. EPR studies of the polyvinyl chloride have also identified peroxides in addition to other radicals. Some of the radicals formed in polyvinyl chloride persist for more than six months, while most of the radical species decay within about 24 hours. Chemistry over extended periods of time was also observed in the production of chloride anion in the radiolysis of aqueous suspensions of polyvinyl chloride. Current studies are examining the radiolysis of these polymers with various amounts of water containing scavengers of the precursor to molecular hydrogen.

Publications with BES support since 2010

Dziewinska K.M.; Peters A.M.; LaVerne J.A.; Martinez P.; Dziewinski J.J.; Pugmire D.L.; Flores H.G.; Trujillo S.M.; Rajesh P. *IOP Conf. Ser. Mater. Sci. Eng.* **2010**, **9**, 012932 Selection and evaluation of a new Pu density measurement fluid.

Haygarth K.; Bartels D.M. *J. Phys. Chem. A* **2010**, **114**, 7479-84 Neutron and beta/gamma radiolysis of water up to supercritical conditions. II. SF_6 as a scavenger for hydrated electron.

LaVerne J.A.; Roth O.; Pimblott S.M. 2010 "pH Dependence of H_2O_2 in the radiolysis of water"; Nuclear Plant Chemistry Conference, Quebec City, Canada.

Lefticariu L.; Pratt L.M.; LaVerne J.A.; Schimmelmann A. *Earth and Planet. Sci. Lett.* **2010**, **292**, 57-67 Anoxic pyrite oxidation by water radiolysis products - a potential source of biosustaining energy.

Merga G.; Saucedo N.; Cass L.C.; Puthussery J.; Meisel D. *J. Phys. Chem. C* **2010**, **114**, 14811-8 "Naked" gold nanoparticles: Synthesis, characterization, catalytic hydrogen evolution, and SERS.

Schmitt C.; LaVerne J.A.; Robertson D.; Bowers M.; Lu W.; Collon P. *Nucl. Inst. Meth. Phys. Res. A* **2010**, **268**, 1551-7 Equilibrium charge state distributions for boron and carbon ions emerging from carbon and aluminium targets.

Balcerzyk A.; LaVerne J.A.; Mostafavi M. *J. Phys. Chem. A* **2011**, **115**, 4326-33 Direct and indirect radiolytic effects in highly concentrated aqueous solutions of bromide.

LaVerne J.A. Radiation chemistry of water with ceramic oxides. In *Charged Particle and Photon Interactions with Matter: Recent Advances, Applications, and Interfaces*; Hatano, Y., Katsumura, Y., Mozumder, A., Eds.; CRC Press, Taylor & Francis Group: Boca Raton, FL, 2011; pp 425-44.

Roth O.; Hiroki A.; LaVerne J.A. *J. Phys. Chem. C* **2011**, **115**, 8144-9 Effect of Al_2O_3 nanoparticles on radiolytic H_2O_2 production in water.

Roth O.; LaVerne J.A. *J. Phys. Chem. A* **2011**, **115**, 700-8 Effect of pH on H_2O_2 production in the radiolysis of water.

Schmitt C.; LaVerne J.A.; Robertson D.; Bowers M.; Lu W.T.; Collon P. *Nucl. Instrum. Methods Phys. Res., Sect. A* **2011**, **269**, 721-8 Target dependence for low-Z ion charge state fractions.

Sims H.E.; Henshaw J.; Bartels D.M. *Radiat. Phys. Chem.* (*submitted*)
Modeling the critical hydrogen concentration in the AECL test reactor.

Bartels D.M.; Wu W.; Kanjana K.; Sims H.E.; Henshaw J. *NPC 2012 Proceedings* "Laboratory and modeling studies in search of the critical hydrogen concentration".

Groenewold G.S.; Elias G.; Mincher B.J.; Mezyk S.P.; LaVerne J.A. *Talanta* In press. Characterization of CMPO and its radiolysis products by direct infusion ESI-MS.

Kanjana K.; Haygarth K.S.; Wu W.; Bartels D.M. *Radiat. Phys. Chem.* (*submitted*) Laboratory Studies in search of the critical hydrogen concentration.

Roth O.; Dahlgren B.; LaVerne J. *J. Phys. Chem. C* In press. Radiolysis of water on ZrO_2 nanoparticles.

Single-Molecule Interfacial Electron Transfer

H. Peter Lu
Bowling Green State University
Department of Chemistry and Center for Photochemical Sciences
Bowling Green, OH 43403
hplu@bgsu.edu

Program Scope

Our research is focused on the use of single-molecule high spatial and temporal resolved techniques to understand molecular dynamics in condensed phase and at interfaces, especially, the complex reaction dynamics associated with electron and energy transfer rate processes. The complexity and inhomogeneity of the interfacial ET dynamics often present a major challenge for a molecular level comprehension of the intrinsically complex systems, which calls for both higher spatial and temporal resolutions at ultimate single-molecule and single-particle sensitivities. Single-molecule approaches are unique for heterogeneous and complex systems because the static and dynamic inhomogeneities can be identified, characterized, and/or removed by studying one molecule at a time. Single-molecule spectroscopy reveals statistical distributions correlated with microscopic parameters and their fluctuations, which are often hidden in ensemble-averaged measurements. Single molecules are observed in real time as they traverse a range of energy states, and the effect of this ever-changing "system configuration" on chemical reactions and other dynamical processes can be mapped. The goal of our project is to integrate and apply these techniques to measure the energy flow and electron flow between molecules and substrate surfaces as a function of surface site geometry and molecular structure. We have been primarily focusing on studying electron transfer under ambient condition and electrolyte solution involving both single crystal and colloidal TiO_2 and related substrates. The resulting molecular level understanding of the fundamental interfacial electron transfer processes will be important for developing efficient light harvesting systems and broadly applicable to problems in interface chemistry and physics.

Recent Progress

Studies of Interfacial Electron Transfer (ET) Dynamics by Combined Single-Molecule Photon-Stamping Spectroscopy and Femtosecond Transient Absorption Spectroscopy. Single-molecule spectroscopy and ensemble-averaged transient absorption measurements provide powerful "zoom-in" and "zoom-out" views of the interfacial ET dynamics of the PF/TiO_2 system (9-phenyl-2,3,7-trihydroxy-6-fluorone: PF). The ultrafast ET processes deduced from the ensemble transient femtosecond absorption spectroscopy are precisely projected to a wide time window revealed by our single-molecule lifetime measurements. In the PF/TiO_2 system, the ET rate is dominated by the electronic coupling between PF and TiO_2, and the ultrafast FET corresponding to the strong coupling can be observed from ensemble transient absorption dynamics (Figure 1), and the relatively slower FET corresponding to the relatively weaker coupling can be demonstrated by single molecule fluorescence photon-stamping measurements.

Based on the biexponential characteristics of the BET dynamics and the deduced two typical charge recombination processes (Figures 1), we propose a model consisting of two different interfacial ET channels to characterize the FET and BET reactions in the ET dynamics of the PF/TiO_2 system. Figure 2 shows the schematic diagrams of the interfacial ET in PF/TiO_2 system for two typical interactions, strong coupling and weak coupling. In the strong coupled state, under photon excitation, the electron state of PF-TiO_2 is directly transferred into $PF^{\delta+}$-$TiO_2^{\delta-}$ charge separation state within 0.4 ps, which is similar to the intra-molecular forward electron transfer such as a charge separation in

MLCT (metal to ligand charge transfer) processes. The charge transfer process can be monitored by the formation of charge separation state at 540 nm in the transient absorption measurements. The 3.0 ps charge recombination time was obtained from the recovery of ground state bleaching and the decay of charge separation state. At single molecule level, the location of charge transfer state, charge transfer rate and charge recombination rate are inhomogeneous. In the weak coupled PF/TiO_2 system, the electron of PF is injected into the conduction band or energetically accessible surface state via its excited singlet state of PF (Figure 2B). This forward electron injection takes picoseconds to nanoseconds time scale, depending upon the interaction of individual PF/TiO_2 events in which the excited state of PF is shown as electron transfer singlet states in Figure 2B. After injection, the electron presumably undergoes trapping and de-trapping, and non-Brownian motions or scattering in TiO_2 NP and then recombines with the cation $PF^{\delta+}$. The BET process takes tens of nanoseconds or up to sub-microseconds, which is demonstrated by our transient absorption spectroscopy.

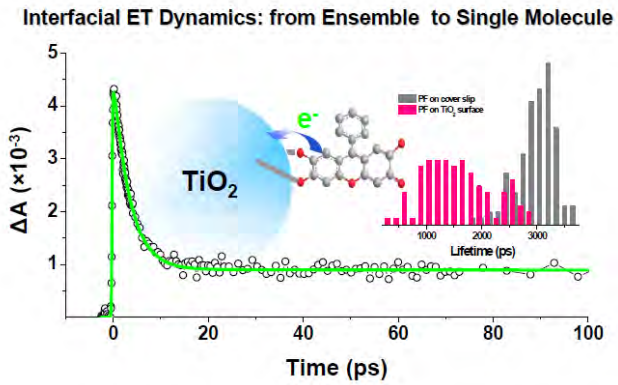

Figure 1. Transient spectral traces of ensemble-averaged ultrafast spectroscopy measurements on interfacial electron transfer dynamics of PF/TiO_2 NP system. **(Inset)** Fluorescence lifetime distribution of PF on a cover glass surface (gray) and on a TiO_2 NPs coated surface (pink).

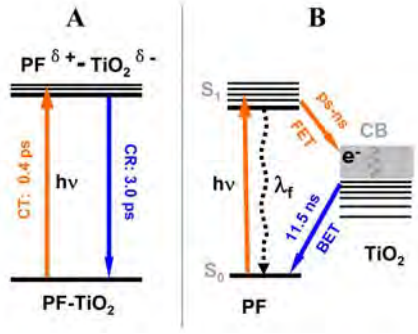

Figure 2. Schematic diagrams showing two typical electronic couplings and two typical interfacial electron transfer cases in PF/TiO_2 system. **(A)** Strong electronic coupling channel. PF-TiO_2 and $PF^{\delta+}$-$TiO_2^{\delta-}$ are the ground state and the charge transfer state, respectively. CT: charge transfer, CR: charge recombination. **(B)** Weak electronic coupling channel. S_0 and S_1 are the ground state and excited state of PF in TiO_2 colloids solution, respectively. CB: conduction band, FET: forward electron transfer, BET: backward electron transfer.

Characterize the Surface States in Interfacial Electron Transfer Dynamics. Surface states have been demonstrated to play important roles in interfacial electron transfer process. Their density and energy distributions are the possible parameters that affect the charge transfer pathways. We have used TiO_2/alizarin, a typical model system with strong electronic coupling, to probe these parameters. In this experiment, we used confocal and tip-enhanced high-resolution near-field luminescence and Raman imaging spectroscopy to analyze the interfacial charge transfer energetics down to the single site and single-molecule level, well beyond the spatial resolution of the optical diffraction limit.

Surfaces states on rutile TiO_2 (110) surface have been investigated and visualized by traditional approaches such as scanning tunneling microscopy. We suggest that the single surface states revealed by our nanoscale imaging are originated from the bridging oxygen vacancies, which can be deduced from the donut-shape optical patterns under radial polarized mode laser excitation because only for quantum systems with a two dimensional transition dipole moment can give circular optical patterns. On the basis of a quantum-chemical calculation, O-vacancy formation in rutile Ti(110)

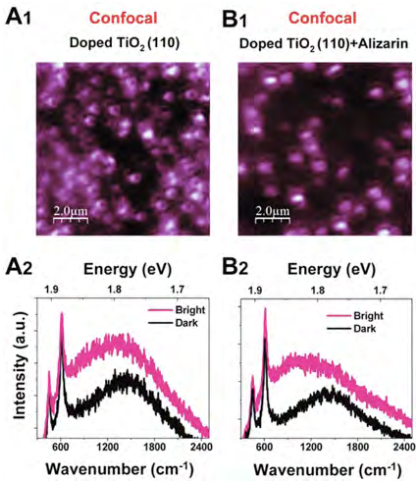

surface results in two excess electrons occupying 3d orbitals on Ti atoms neighboring the vacancy. With laser excitation, electrons at the valence band can be excited to higher energy states, for example, trap states below the conduction band.

Figure 3. Optical response of the abundant surface states of the Nb-doped rutile TiO_2 (110) surface. **(A1)** Confocal imaging and **(A2)** Raman/luminescence spectra of TiO_2 (110) surface. **(B1)** Confocal imaging and **(B2)** Raman/luminescence spectra of TiO_2 (110) surface with alizarin (1 μM).

Probing Single-Electron Self-Exchange Dynamics Across a Molecule-Metal Interface. For a redox reaction, the key processes are the electron transfer between the reductant and oxidant and subsequently produce the reduced states or oxidized states of chemical species. Therefore, electron transfer dynamics is the core of the redox reaction dynamics. The probability for the molecule to stay in the oxidized state is high when the gate voltage is far greater than the formal redox potential. For a metal-molecule-metal junction, current-induced metal-atom motions, molecular conformation changes, and chemical bond fluctuations have been suggested to be the chemical and mechanical reasons of the fluctuations. On the other hand, the fluctuation of the conductance in a single molecule-metal junction is coincident with the fluctuation and inhomogeneity of the single molecule dynamics.

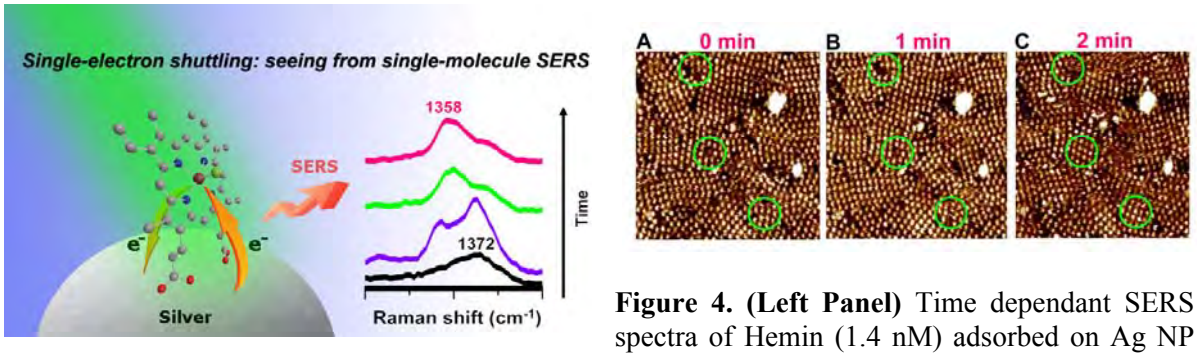

Figure 4. (Left Panel) Time dependant SERS spectra of Hemin (1.4 nM) adsorbed on Ag NP surfaces. Typical vibrational modes, ν_4, ν_3, ν_2, and ν_{10}, are prominent but show strong fluctuation at the single molecule level. Four consecutive spectra, which show the evolution of ν_4 from the oxidized state to the reduced state, are shown as a zoom-in view. **(Right Panel)** The thermally driven redox reaction of single Co(II)Pc molecules at the Au (111) surface with a reduction potential of 0.1 V vs. SCE at **(A)** 0 min **(B)** 1 min **(C)** 2 min. The fluctuation of the brightness of a single molecule indicates the oxidation states changes.

The ground-state single-electron charge transfer dynamics at the Hemin/Ag NP interface hasbeen investigated by using SMSERS and spectroelectrochemistry. The electron transfer at the Hemin/Ag interface is evidenced by the prominent shift of a specific Raman mode ν_4, which is a typical marker of the oxidation state of the Iron center in Hemin. The fluctuation dynamics of the Raman spectra has been quantitatively investigated by the autocorrelation and crosscorrelation function analysis. On the basis of the data analysis and combined with the single-molecule spectroelectochemistry control measurements, we suggest that the single molecule redox reaction at the Hemin/Ag interface is primarily driven by thermal fluctuation. The ground-state single-electron charge transfer events at the Hemin/Ag NP interface naturally exist, and it is different from the charge-transfer enhancement factor in SERS. This work reveals a real-time picture of the charge transfer dynamics at the

molecule-metal interface without a strong electric field. Our new information is relevant for a further understanding, design, and manipulation of the charge transfer processes at the molecule-metal interfaces or metal-molecule-metal junctions, which are fundamental elements in single-molecule electronics, catalysis, and solar energy conversion.

Future Research Plans

Interfacial ET dynamics strongly involves with and regulated by molecule-surface interactions. To decipher the underlying mechanism of the complex and inhomogeneous interfacial electron transfer dynamics, we plan to study interfacial electron transfer on single crystal TiO_2 surfaces by using pump-probe ultrafast single-molecule spectroscopy and near-field scanning microscopy. Our study will focus on understanding the interfacial electron transfer dynamics at specific crystal sites (kinks, planes, lattices, and corners) with high-spatially and temporally resolved topographic/spectroscopic characterization at individual molecule basis, characterizing single-molecule rate processes, reaction driving force, and molecule-substrate electronic coupling. Our effort will also be focused on understanding the TiO_2 electron trap centers and surface states.

Publications of DOE sponsored research (FY2009-2012)

1. Desheng Zheng, Leonora Kaldaras, H. Peter Lu, "Total Internal Reflection Fluorescence Microscopy Imaging-Guided Confocal Single-Molecule Fluorescence Spectroscopy," *Review of Scientific Instruments*, **83**, 013110 (2012).

2. X. Wang, D. Zhang, Y. Wang, P. Sevinc, H. Peter, Lu, A. J. Meixner, "Interfacial Electron Transfer Energetics Studied by High Spatial Resolution Tip-Enhanced Raman Spectroscopic Imaging," *Angewandte Chemie International Edition* **50***,* (2011) A25-A29.

3. Yuanmin Wang, Papatya C. Sevinc, Yufan He, H. Peter Lu, "Probing Ground-State Single-Electron Self-Exchange Across a Molecule-Metal Interface," *J. Am. Chem. Soc.,* **133**, 6989-6996 (2011).

4. Sevinc, Papatya; Wang, Xiao; Wang, Yuanmin; Zhang, Dai; Meixner, Alfred; Lu, H. Peter, "Simultaneous Spectroscopic and Topographic Near-Field Imaging of TiO_2 Single Surface States and Interfacial Electronic Coupling," *Nano Letter*, **11**, 1490-1494 (2011).

5. H. Peter Lu, "Acquiring a Nano-View of Single Molecules in Actions," *Nano Reviews* **1**, 6-7 (2010).

6. Guo, Lijun; Wang, Yuanmin; Lu, H. Peter, "Combined Single-Molecule Photon-Stamping Spectroscopy and Femtosecond Transient Absorption Spectroscopy Studies of Interfacial Electron Transfer Dynamics," *J. Am. Chem. Soc.* **132**, 1999-2004 (2010) (Cover page).

7. Yufan He, Xiaohua Zeng, Saptarshi Mukherjee, Suneth Rajapaksha, Samuel Kaplan, H. Peter Lu, "Revealing Linear Aggregates of Light Harvesting Antenna Proteins in Photosynthetic Membranes," *Langmuir* **26**, 307-313 (2010) (Cover page).

8. Yuanmin Wang, Xuefei Wang, and H. Peter Lu, "Probing single-molecule interfacial geminate electron-cation recombination dynamics," *J. Am. Chem. Soc.* **131**, 9020–9025 (2009).

9. Yuanmin Wang, Xuefei Wang, Sujit Kumar Ghosh, H. Peter Lu, "Probing single-molecule interfacial electron transfer dynamics of porphyrin on TiO_2 nanoparticles," *J. Am. Chem. Soc*. **131**, 1479-1487 (2009).

Solution Reactivity and Mechanisms through Pulse Radiolysis

Sergei V. Lymar
Chemistry Department, Brookhaven National Laboratory, Upton, NY 11973-5000
e-mail: lymar@bnl.gov

Program Scope

This program applies pulse radiolysis for investigating reactive intermediates and inorganic reaction mechanisms. The specific systems are selected based on their fundamental significance or importance in energy and environmental problems.

The first project investigates physical chemistry of nitrogen oxides and their congeneric oxoacids and oxoanions. They play an essential role in environmental chemistry, particularly in the terrestrial nitrogen cycle, pollution, bioremediation, and ozone depletion. Nitrogen-oxygen intermediates are also central to the radiation-induced reactions that occur in nuclear fuel processing and within attendant nuclear waste. Redox and radical chemistry of the nitrate/nitrite system mediates the most of radiation-induced transformations in these environments. Equally important are the biological roles of nitrogen oxides. This research program applies time-resolved techniques for elucidation of the prospective reactions in terms of their thermodynamics, rates and mechanisms, focusing on the positive nitrogen oxidation states, whose chemistry is of the greatest current interest.

The goal of the second project is to gain mechanistic insight into water oxidation catalysis through characterization of the catalyst transients involved in the catalytic cycle. Development of catalysts to carry out the four-electron water oxidation remains the greatest challenge in the solar energy utilization. Of all catalysts that have been examined, the dimeric oxo-bridged ruthenium ion ($[(bpy)_2(H_2O)Ru\text{-}O\text{-}Ru(OH_2)(bpy)_2]^{4+}$, known as the "blue dimer") has been the most extensively studied, but the reaction mechanisms remain to be established. The major impediment has been the difficulties in identification and characterization of the reaction intermediates. In this project, we use radiolysis techniques to generate and characterize the redox states of the catalyst involved in water oxidation by the "blue dimer" and by an all-inorganic catalyst based on cobalt hydrous oxide immobilized on silica nanoparticles that we have recently developed.

Collaborators on these projects include M. Valiev (PNNL),[1] Shafirovich (NYU),[2] J. Hurst (WSU),[3] and H. Schwarz (BNL, emeritus).[4]

Recent Progress.

The nitrate radical ion ($NO_3^{\bullet 2-}$). This is a major species that mediates the radiation-induced transformations in nuclear fuel processing and in Hanford nuclear wastes. However, properties and reactivity of $NO_3^{\bullet 2-}$ are not understood. With pulse radiolysis, the radical can be generated through the rapid $e^-_{aq} + NO_3^-$ reaction but decays rapidly via hydrolysis: $NO_3^{\bullet 2-} + H_2O \leftrightarrow NO_2^{\bullet} + 2OH^-$ (data to the left). The lowest of the literature reduction potentials $E^0(NO_3^-/NO_3^{\bullet 2-}) = -0.89$ V[5] predicts the hydrolysis equilibrium constant $K_{hydr} \approx 0.02$ M^2; that is, the equilibrium favors $NO_3^{\bullet 2-}$ even at modest alkalinities. However, we do not

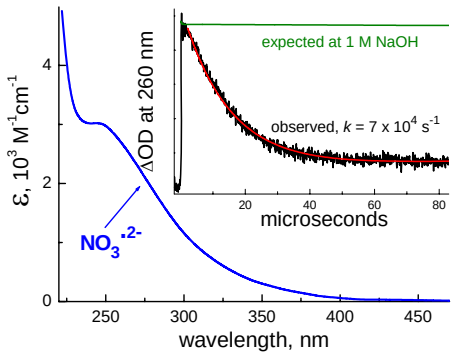

observe the predicted effects, which indicates that K_{hydr} >50 M^2 and sets the *upper* limit $E^0(NO_3^-/NO_3^{\bullet 2-})$ < -1.1 V; that is, the potential is more negative than all literature values. We observe both a primary kinetic isotope effect and large negative kinetic salt effect on the $NO_3^{\bullet 2-}$ radical decay. Both effects are consistent with late, product-like hydrolysis transition state (shown to the right) of charge less than -2 and involving a proton transfer.

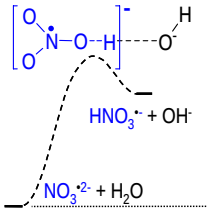

Hydrogen atom abstraction from tert-butyl alcohol.[4] Tertiary butyl alcohol (*tert*-BuOH) holds a special place in radiation chemistry; it is widely used to convert a highly reactive major primary water radiolysis product, $OH^\bullet$ radical, into a much less reactive $^\bullet CH_2C(CH_3)_2OH$ radical. Many hydrogen atom reactions with various compounds were investigated under these conditions. As with $OH^\bullet$, $H^\bullet$ abstracts an H atom from *tert*-BuOH; that is, $(CH_3)_3COH + H^\bullet \rightarrow {}^\bullet CH_2C(CH_3)_2OH + H_2$. However, the rate constant literature values for this reaction varied greatly and, considering its importance, the situation was untenable.

Through a combination of pulse radiolysis, purification, and analysis techniques, the rate constant for the $H^\bullet + (CH_3)_3COH$ reaction in aqueous solution is for the first time definitively determined to be $(1.0 \pm 0.15) \times 10^5$ M^{-1} s^{-1}, which is about half of the tabulated value and ten times lower than the more recently suggested revision.[6] Our result fits on the Polanyi-type, rate-enthalpy linear correlation (shown to the left) that we found for the analogous reactions of other aliphatic alcohols. The existence of such a correlation and its large slope are interpreted as an indication of the mechanistic similarity of the H atom abstraction from α- and β-carbon atoms in alcohols occurring through the late, product-like transition state. *tert*-Butyl alcohol is commonly contaminated by much more reactive secondary and primary alcohols, whose content can be sufficient for nearly quantitative scavenging of the H atoms, skewing the H atom reactivity pattern, and explaining the disparity of the literature data. The ubiquitous use of *tert*-butanol in pulse radiolysis and the results of this work suggest that many other previously reported rate constants for the H atom, particularly the smaller ones, may be in jeopardy.

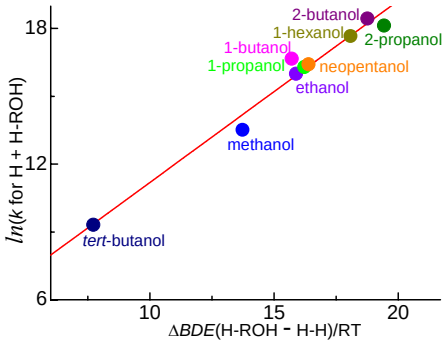

Intermediates in water oxidation catalysis. Research from several laboratories, have established that water oxidation catalysis by the *cis,cis*-$[(bpy)_2(H_2O)Ru\text{-}O\text{-}Ru(OH_2)(bpy)_2]^{4+}$ (known as the *blue dimer* **{3,3}**, structure to the left) involves its progressive oxidation with the attendant loss of protons to the ruthenyl **{5,5}** dimer.[7] However, the properties of the unstable oxidation states higher than **{3,4}** and catalysis mechanism remain in dispute. We found that persulfate stoichiometrically oxidizes **{3,3}** to **{3,4}**. This unusual reaction provides a clean way to generate **{3,4}** over a large pH range, which has made possible assessment of the **{3,4}** reactivity toward oxidizing radicals and obtaining and characterization of the **{4,4}** state.[3] The slow hydroxide ion attack on the catalyst's aromatic ligands often result in the formation of OH-adduct.[8] As shown to the right, the same species are obtained by the rapid $OH^\bullet$ attack, which makes pulse radiolysis the best method for investigating these adducts, whose importance arises because they: (1) may

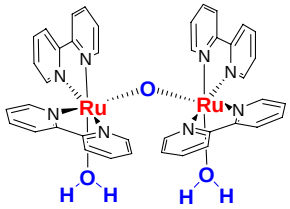

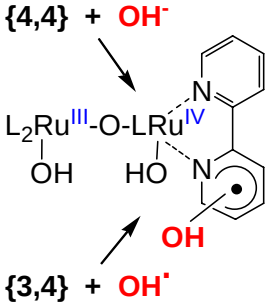

lead to ligand hydroxylation and eventually to catalyst oxidative degradation,[8b] and (2) have been invoked to explain oxygen evolution with both oxygen atoms derived from bulk water.[9] Our pulse radiolysis data show that the $OH^{\bullet}$ radical does very rapidly forms adducts with both **{3,3}** and **{3,4}**. Within a 100 μs, the **{3,3}-OH** adduct expels OH^- and the net result is oxidation of **{3,3}** to **{3,4}**. In contrast and counter intuitively, the net result of the $OH^{\bullet}$ + **{3,4}** reaction in *reduction* of **{3,4}** to **{3,3}**, strongly indicating that the catalyst in **{4,4}** and higher states are susceptible to nucleophilic attack by H_2O or OH^-. The reduction process is complex; it occurs on timescales from microseconds to seconds, is not yet understood, and will be studied in the future work.

Recently, in our search for purely inorganic, inexpensive, and efficient water oxidation catalysts we have introduced a catalyst based on Co hydroxide immobilized on the silica nanoparticles.[2] In TEM, the catalyst appears as ~1 nm $Co(OH)_2$ "blobs" on ~10 nm particle surfaces. With $Ru(bpy)_3^{3+}$ as a one-electron oxidant, stoichiometric oxygen evolution is obtained: $4Ru(bpy)_3^{3+} + 2H_2O \xrightarrow{-[Co/SiO_2]} O_2 + 4H^+ + 4\ Ru(bpy)_3^{2+}$. The *lower limit* for the catalyst turnover frequency in oxygen evolution of ~300 s^{-1} per cobalt atom is estimated, which attests to a very high catalytic activity. The role of silica is to stabilize insoluble cobalt hydroxide against precipitation. This catalyst is optically transparent in the entire UV-vis range and is thus suitable for mechanistic investigations by time-resolved spectroscopic techniques.

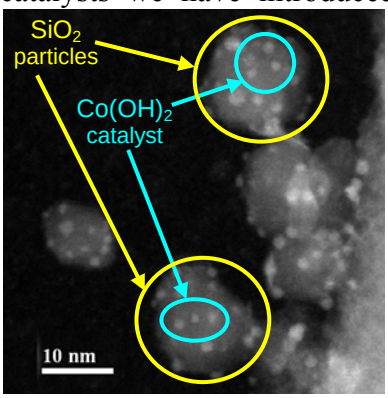

Future Plans

Pathways and energetics of NO reduction will be investigated with the purposes to develop new methods of generating nitroxyl species ($^1HNO/^3NO^-$) and to establish their thermochemistry.

Spin-forbidden bond breaking/making reactions involving nitroxyl will be investigated. The first is protonation of $^3NO^-$ by Brønsted acids. The second spin-forbidden reaction of interest is the addition of $^3O_2$ to ^1HNO, which could directly lead to peroxynitrite, $ONOO^-$, and is potentially very significant because it replaces mildly reducing HNO by strongly oxidizing $ONOO^-$.

Energetics of $NO_3^{\bullet 2-}$ radical will be studied from equilibrating $NO_3^-/NO_3^{\bullet 2-}$ couple with the reference redox couples.

The nature of catalyst transients formed during water oxidation will be further clarified: (1) we will continue characterization of the **{4,4}** and **{4,5}** states of "blue dimer" focusing on identification of its protonation state and understanding the decomposition pathways. For the Co/SiO_2 catalyst, time-resolved spectroscopic techniques will be applied to address the following major questions: (1) Is the catalysis two-electron or truly four-electron; *e.g.*, H_2O_2 *vs.* O_2 as the immediate product? (2) What metal oxidation states are involved? (3) What are the rate determining and the highest reduction potential steps in the catalytic cycle?

References (DOE sponsored publications in 2009-present are marked with asterisk)

(1*) Valiev, M.; Lymar, S. V. *J. Phys. Chem. A* **2011**, *115*, 12004-12010.
(2*) Tomer, Z.; Lihua, Z.; Vladimir, S.; Lymar, S. V. *J. Am. Chem. Soc.* **2012**, in press.
(3*) Cape, J. L.; Lymar, S. V.; Lightbody, T.; Hurst, J. K. *Inorg. Chem.* **2009**, *48*, 4400-4410.

(4*) Lymar, S. V.; Schwarz, H. A. *J. Phys. Chem. A* **2012**, *116*, 1383-11389.
(5) Cook, A. R.; Dimitrijevic, N.; Dreyfus, B. W.; Meisel, D.; Curtiss, L. A.; Camaioni, D. M. *J. Phys. Chem. A* **2001**, *105*, 3658-3666.
(6) Wojnárovits, L.; Takács, E.; Dajka, K.; Emmi, S. S.; Russo, M.; D'Angelantonio, M. *Radiat. Phys. Chem.* **2004**, *69*, 217-219.
(7) (a) Meyer, T. J.; Huynh, M. H. V. *Inorg. Chem.* **2003**, *42*, 8140-8160. (b) Hurst, J. K. *Coord. Chem. Rev.* **2005**, *249*, 313-328. (c) Liu, F.; Concepcion, J. J.; Jurss, J. W.; Cardolaccia, T.; Templeton, J. L.; Meyer, T. J. *Inorg. Chem.* **2008**, *47*, 1727-1752.
(8) (a) Nord, G.; Wernberg, O. *J. Chem. Soc. Dalton Trans.* **1975**, 845-849. (b) Ghosh, P. K.; Brunschwig, B. S.; Chou, M.; Creutz, C.; Sutin, N. *J. Am. Chem. Soc.* **1984**, *106*, 4772-4783.
(9) (a)Yamada, H.; Siems, W. F.; Koike, T.; Hurst, J. K. *J. Am. Chem. Soc.* **2004**, *126*, 9786-9795. (b) Ozkanlar, A.; Cape, J. L.; Hurst, J. K.; Clark, A. E. *Inorg. Chem.* **2011**, *50*, 8177-8187.

Spectroscopy of Organometallic Radicals

Michael D. Morse
Department of Chemistry
University of Utah
315 S. 1400 East, Room 2020
Salt Lake City, UT 84112-0850
morse@chem.utah.edu

I. Program Scope:

In this project, we seek to obtain fundamental physical information about unsaturated, highly reactive organometallic radicals containing open *d* subshell transition metal atoms. Gas phase electronic spectroscopy of jet-cooled transition metal (TM) molecules is used to obtain fundamental information about ground and excited electronic states of such species as the transition metal carbides, nitrides, and halides, and of organometallic radicals such as CrCCH, and CuCCH. Spectroscopic studies of actinide species such as UN and ThO_2 are also being pursued with the goal of understanding the electronic structure and chemical bonding in these species, which present severe challenges for computational chemistry. Ionic species will become available for investigation when the construction of a new ion trap spectrometer is complete.

II. Recent Progress:

A. Optical spectroscopy of CrC, TaC, ZrF, ZrCl, OsN, CuCCH, VC, VN, and UN

During 2009-2012, we published papers on the resonant two-photon ionization spectroscopy of CrC, TaC, ZrF and ZrCl, and OsN. The work on CrC and TaC were the first spectroscopic investigations of any kind for these molecules, and led to the determination of the ground electronic state symmetry and bond length. The studies of ZrF were likewise the first investigations of this molecule ever reported, providing an accurate determination of the ground state symmetry, bond length, and vibrational frequency. Our studies on ZrCl supplemented previous work on this molecule and identified a number of new spectroscopic transitions. Finally, our work on OsN greatly increased our knowledge of the excited states of this molecule, leading to the identification of seven excited electronic states arising from the $1\sigma^2\ 2\sigma^2\ 1\pi^4\ 1\delta^3\ 3\sigma^1\ 2\pi^1$ and $1\sigma^2\ 2\sigma^2\ 1\pi^4\ 1\delta^2\ 3\sigma^2\ 2\pi^1$ electronic configurations. Because these studies have been published and have been described in previous abstracts, they will not be discussed further here.

More recently, we have worked on the spectroscopy of CuCCH. This molecule is not an organometallic radical, *per se*, since it has a closed shell $^1\Sigma^+$ ground state. However, it is quite reactive and is important in organic synthesis, where copper acetylides form the basis of the Sonogashira cross-coupling reaction. Our studies of CuCCH have identified three electronic band systems in the visible region. The lowest energy system, identified as the $\tilde{a}1 \leftarrow \tilde{X}\ ^1\Sigma^+$ system, is a spin-forbidden system with an upper state lifetime greater than 100 μs. Nevertheless, we have succeeded in recording the spectrum and rotationally resolving the origin band at 20249 cm^{-1}. It is likely that the upper state is a $^3\Pi_1$ state, but this can only be determined through comparisons with *ab initio* calculations that are in progress. Further to the blue (23130 cm^{-1}) we have located a strongly allowed $\tilde{A}\ ^1\Sigma^+ \leftarrow \tilde{X}\ ^1\Sigma^+$ band system with an upper state lifetime of 450 ns. Finally, a third strongly allowed band system is observed at 24673 cm^{-1}

($\tau \approx 820$ ns), but we have not been able to rotationally resolve this system, so the symmetry of its upper state is not yet known.

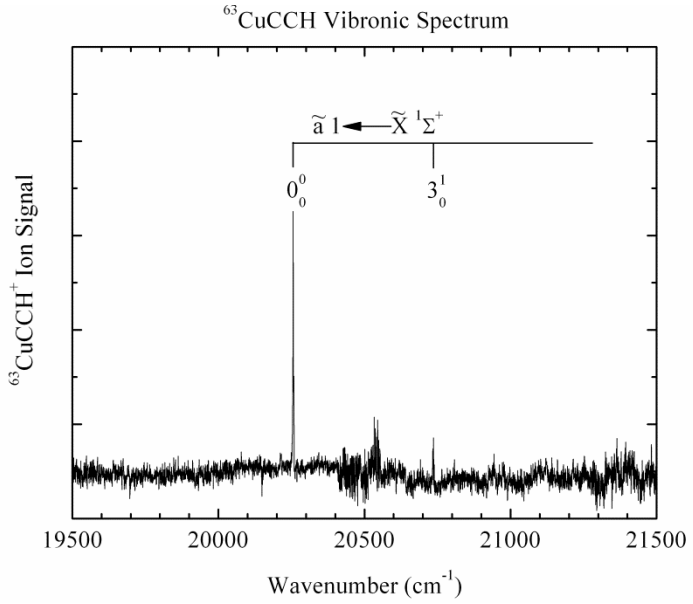

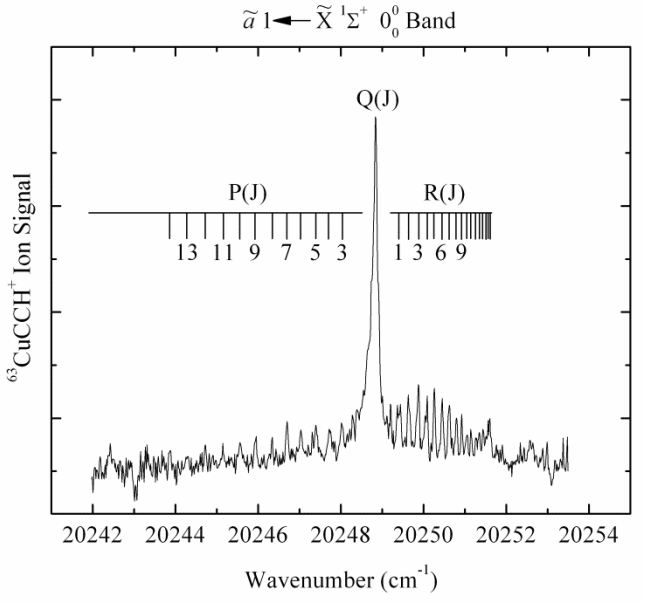

Figures 1 and 2. Low resolution spectrum of the $\tilde{a}1 \leftarrow \tilde{X}\ ^1\Sigma^+$ band system of CuCCH, and high resolution spectrum of its origin band.

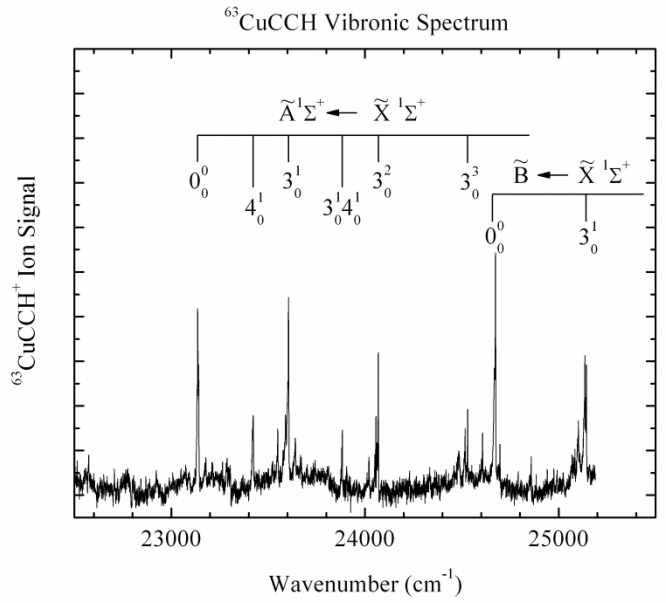

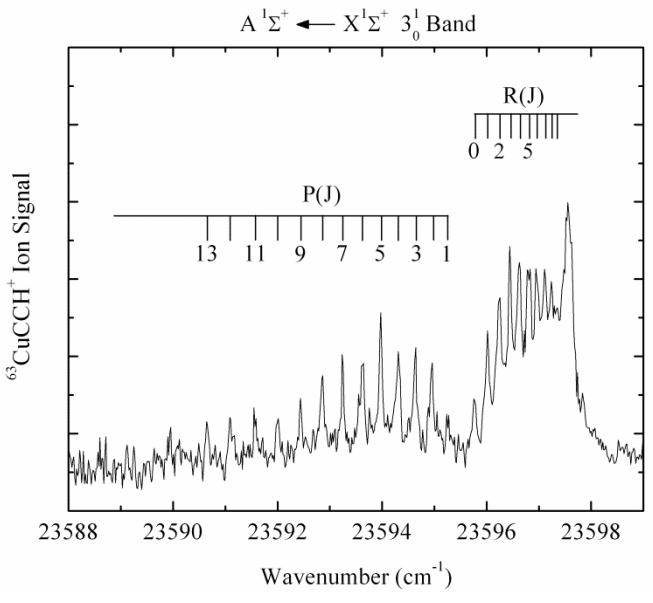

Figures 3 and 4. Low resolution spectrum of the $\tilde{A}\ ^1\Sigma^+ \leftarrow \tilde{X}\ ^1\Sigma^+$ band system of CuCCH, and high resolution spectrum of its 3_0^1 band.

We have also continued our studies of the transition metal carbides, and have very recently had success on the difficult molecule, VC. The molecule has been calculated to have a triply bound, $1\sigma^2\ 2\sigma^2\ 1\pi^4\ 1\delta^1$, $^2\Delta_{3/2}$ ground state with an exceptionally large dipole moment

(about 7.3 D). Our studies have provided the first gas-phase spectra of any kind for this molecule and show that it does indeed have an $\Omega''=3/2$ ground state, consistent with the calculated $^2\Delta_{3/2}$ ground state. Our rotationally resolved studies also provide $r_0'' = 1.6180(3)$ Å, in reasonable agreement with the calculated value of $r_e''=1.636$ Å. We plan to pursue a collaboration with Prof. Tim Steimle at Arizona State University to measure the dipole moment of this unusual molecule, to see if the unusually large calculated value is correct.

While investigating the spectra of VC, we also observed spectroscopic transitions in the VN molecule, which was probably formed due to residual NH_3 in the instrument from a previous experiment on UN. Although this molecule has been well-studied, we nevertheless found several transitions that have not previously been observed. We anticipate that this will permit one or more new excited states of this molecule to be identified.

We have also begun work to collect and analyze the spectrum of UN. As expected, the molecule has a complicated vibronic spectrum due to the large number of possible arrangements of electrons in the 5*f*, 6*d*, and 7*s* orbitals. Preliminary rotationally resolved studies suggest that the ground state of the molecule may have $\Omega= 3.5$ with a bond length of approximately 1.76 Å, but further work is in progress to obtain a definitive result.

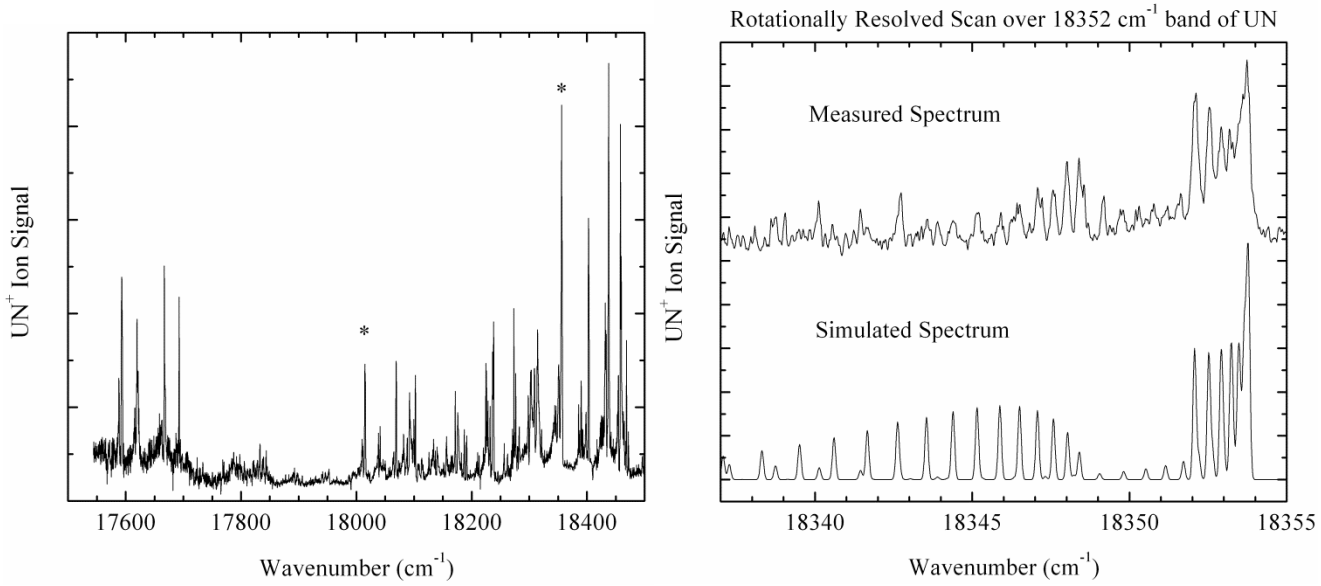

Figure 5 and 6. Low resolution spectrum of UN, showing complicated vibronic structure, and high resolution spectrum of the 18352 cm^{-1} band.

III. Future Plans

A. R2PI and DF spectroscopy of transition metal carbides and radicals

Projects for the upcoming year include: (1) Completion of the analysis of the spectra of VC, VN, CuCCH, and CrCCH, and publication of the results; (2) Additional scans of the spectra of UN to find bands that are clean and unperturbed, for a determination of the ground state symmetry and bond length; (3) Dispersed fluorescence of UN to locate low-lying excited electronic states; (4) Search for the electronic spectrum of ThO_2; (5) Search for electronic spectra of ThC and UC; (6) Collaboration with Prof. Steimle on the electric dipole moments of VC and UN.

B. Photodissociation spectroscopy of cold, trapped ions

With DOE funding, we have been building a new ion photodissociation spectrometer that is designed to record photodissociation action spectra of cryogenically cooled transition metal ion complexes. The method will generate transition metal ion complexes that will be mass-selected, cooled in a cryogenic trap, irradiated, and photofragmented. The fragment ions will be selectively detected and the spectrum of the cold ion will be recorded by measuring the fragment ion signal as a function of the laser wavenumber. After a great deal of painstaking design and construction, the instrument is now nearly complete. The electron impact ionization source is finished, along the first quadrupole mass filter, and the turning quadrupole. These devices have been tested and work well. The ion trap has been constructed and is in place, but has not yet been tested. The second turning quadrupole is mounted and ready to use, and the machine shop is now building a mount for our second mass-selective quadrupole, which will be tuned to transmit fragment ions. The Daly detector is ready to use as well, and has been used to record mass spectra using the electron impact source, first quadrupole mass filter, and turning quadrupole combination.

Among the first species we will investigate are the transition metal carbonyl cations $FeCO^+$, $CoCO^+$, $NiCO^+$, $CrCO^+$, and related species with larger numbers of ligands.

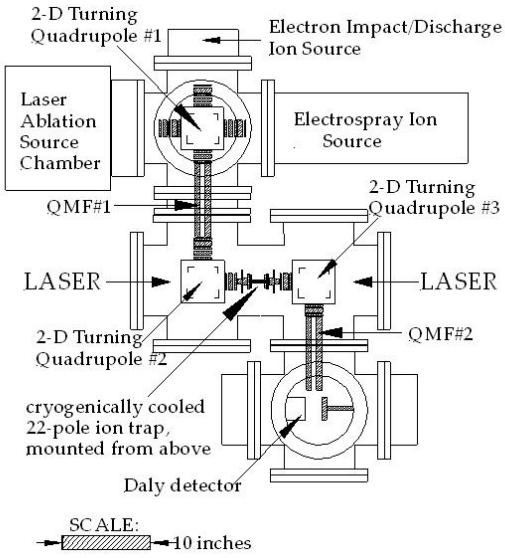

Figure 7. Design plan for the Utah ion trap photodissociation spectrometer.

IV. Publications from DOE Sponsored Research October 1, 2009-present:

1. D. J. Brugh, M. D. Morse, A. Kalemos and A. Mavridis, "Electronic spectroscopy and electronic structure of diatomic CrC," J. Chem. Phys. **133**, 034303/1-034303/8 (2010).
2. O. Krechkivska and M. D. Morse, "Resonant two-photon ionization spectroscopy of jet-cooled tantalum carbide, TaC," J. Chem. Phys. **133**, 054309/1-054309/8 (2010).
3. A. Martinez and M. D. Morse, "Spectroscopy of diatomic ZrF and ZrCl: 760 - 555 nm," J. Chem. Phys. **135**, 024308/1-024308/10 (2011).
4. M. A. Garcia and M. D. Morse, "Resonant two-photon ionization spectroscopy of jet-cooled OsN: 520-418 nm," J. Chem. Phys. **135**, 114304/1-12 (2011).

Ab initio approach to interfacial processes in hydrogen bonded fluids

Christopher J. Mundy
Chemical and Materials Sciences Division
Pacific Northwest National Laboratory
902 Battelle Blvd, Mail Stop K1-83
Richland, WA 99352
chris.mundy@pnnl.gov

Program Scope

The long-term objective of this research is to develop a fundamental understanding of processes, such as transport mechanisms and chemical transformations, at interfaces of hydrogen-bonded liquids. Liquid surfaces and interfaces play a central role in many chemical, physical, and biological processes. Many important processes occur at the interface between water and a hydrophobic liquid. Separation techniques are possible because of the hydrophobic/hydrophilic properties of liquid/liquid interfaces. Reactions that proceed at interfaces are also highly dependent on the interactions between the interfacial solvent and solute molecules. The interfacial structure and properties of molecules at interfaces are generally very different from those in the bulk liquid. Therefore, an understanding of the chemical and physical properties of these systems is dependent on an understanding of the interfacial molecular structure. The adsorption and distribution of ions at aqueous liquid interfaces are fundamental processes encountered in a wide range of physical systems. In particular, the manner in which solvent molecules solvate ions at the interface is relevant to problems in a variety of areas. Another major focus lies in the development of models of molecular interaction of water and ions that can be parameterized from high-level first principles electronic structure calculations and benchmarked by experimental measurements. *The aforementioned studies are performed using novel algorithms based in density functional theory (DFT) in conjunction with high performance computing through a* ***2008-2012 INCITE award****.* These models will be used with appropriate simulation techniques for sampling statistical mechanical ensembles to obtain the desired properties.

Progress Report

Elucidating structure and reactivity ions in bulk and at the air-water interface: Although DFT holds tremendous promise as an efficient electronic structure theory; applications of DFT to aqueous systems have produced mixed results when attempting to reproduce experimentally determined benchmarks. Although there is no molecular model that can reproduce the full phase diagram of water, the shortcomings of popular exchange-correlation functionals based on the generalized gradient approximation (GGA), *e.g.* BLYP and PBE, are known to underestimate the liquid density and yield a more structured liquid then classical empirical potentials. Notwithstanding that there could be many reasons for these deficiencies in DFT, one major shortcoming is the lack of dispersion interactions in current implementations. Correcting the liquid density at ambient conditions has far reaching implications for use of DFT in studying systems with open boundary conditions, such as liquid-vapor interfaces. To this end we have we have established new benchmarks on the role of dispersion on the equilibrium properties of water [7] using the correction due to Grimme [*Journal of Computational Chemistry 25*, 1463 (2004)] that amounts to an empirical damped dispersion interaction that is parameterized to used with

both BLYP and PBE. Our results have shown that the addition of the empirical correction due to Grimme yields the correct density for liquid water at ambient conditions and significantly better structural and dynamic properties utilizing BLYP. We have also extended this work to the calculation of liquid-vapor coexistence curves for methanol and methane where the majority of the cohesive interactions are known to come from dispersion interactions [6].

Recent literature has pointed to the specific ion effect as being a *local* effect, as opposed to an ions long-range effect on water's structure. Recently we have compared the first solvation shell of simple (I^-) and complex ions (IO_3^-) using the extended x-ray absorption fine structure (EXAFS) technique in conjunction with molecular dynamics (MD)[5,14]. In a head-to-head comparison of empirical polarizable models with DFT based interaction potentials it was found that DFT was able to account for subtle experimental features in EXAFS spectra leading to a picture of the solvation shell of I- that is less structured than that obtained with empirical polarizable interaction potentials [5]. This over structuring of the empirical polarizable potential can be traced to a larger induced dipole moment of iodide, namely 2.6 Debye compared to the DFT value of 1.2 Debye [5]. Moreover, in the case of IO_3^- DFT has provided unprecedented agreement with XAFS data supporting the surprising picture of IO_3^- as being a strong kosmotrope [14].

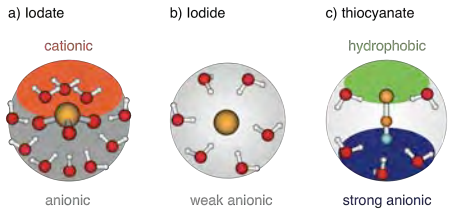

Figure 1: Schematic representations of the solvation of iodate, iodide, and thiocyanate. Iodate shows strong cationic and ionic solvation producing it's kosmostropic nature [1,5]. Iodide has a more flexible anionic solvation shell making it a weak chaotrope [1,10,14]. Thiocyanate depicts both a hydrophobic end (S) and a strong anionic part (N) giving it directionality in the vicinity of a broken symmetry and it's strong chaotropic behavior [1].

Our results suggest that the first solvation shell structure will likely be sensitive to the near-field charge density of the ions and surrounding water molecules. The ability of DFT to provide a faithful representation of the underlying charge density is not a surprise. We can further push this concept and consider the role of the first solvation shell in determining interfacial propensity. To this end, we investigated three ions with similar polarizabilities but significantly different categorization with respect to the Hofmeister series. Specifically, we have studied IO_3^- (a strong kosmotrope), I^-, and SCN^- (a strong chaotrope) and examined the hydration structure under both bulk and interfacial conditions. Our results suggest that it is indeed the characterization of the hydration structure rather than the underlying polarizablility that is a strong indicator of surface propensity [1] **(see Figure 1).**

<u>Understanding the relationship between dielectric continuum theory and molecular simulation:</u>

Although there is now a consensus that large polarizable halides can be present at the air-water interface, there is no agreement on the specific nature of the molecular interaction that gives rise to surface propensity. Although early studies implicate polarization and more recent studies have found they can explain the underlying thermodynamic driving forces using simple point charge models of the molecular interaction [Otten et al, *Proceedings of the National Acadamy of Sciences 109*, 701 (2012)]. Netz and co-workers [*Annual Reviews of Physical Chemistry 63*, 401 (2012)] have used molecular simulation using point charges in conjunction with dielectric

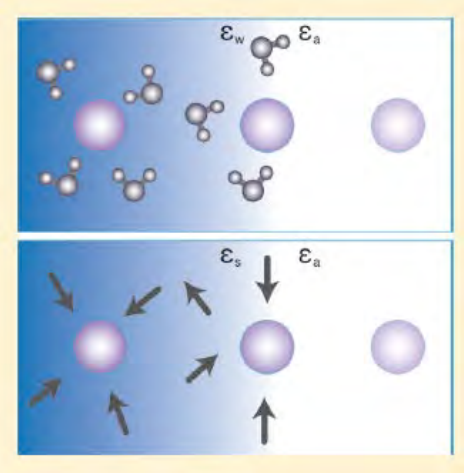

Figure 2: Schematic on the effects of two different solvents on the surface adsorption of hard-sphere ions. Our results indicate that the driving force of ions to interfaces is model dependent [2].

continuum theory to explain the surface tension of the halide salts. Levin and co-workers [*Physical Review Letters 103*, 257802 (2009)] have used a *polarizable ion* dielectric continuum theory to also explain the surface tension data of halide salts. Interestingly, the single ion potential of mean force (PMF) for iodide agrees quite well (regarding the depth of the shallow local minimum at the interface) with these two very different approaches. Our Recent DFT calculations that intrinsically include polarization also show good agreement with the aforementioned PMFs for iodide [10]. The question regarding the role of polarization and the connection of molecular simulation to dielectric continuum theory still remains. To this end, we constructed molecular simulations of charged hard-spheres (HS) in model solvents (SPC/E and Stockmayer fluid) where the separation of cavitation and dielectric response is clear (see **Figure 2**). We proposed a dielectric theory that contains the free energy of cavitation (proportional to volume of HS), and charging (proportional to square of the charge) where the dielectric constants and volume scaling was determined by molecular simulation [2]. Our results indicate that the underlying physics of anion adsorption is dependent on the nature of the solvent (*e.g.* SPC/E or Stockmayer). The symmetric nature of the Stockmayer fluid precludes the existence of a surface potential and it is only cavitation that determines surface activity. SPC/E water has a surface potential due to the broken symmetry of both the cavity and interface. It was shown in our study [2] and a recent independent study [Arslagarin and Beck, *Journal of Chemical Physics 136*, 104503 (2012)] that this notional "surface potential" provides an *additional* crucial driving force that allows point-charge models in SPC/E to give rise to surface adsorption.

Future directions

The role of this notional "surface potential" is currently being explored in the context of DFT and the use of inherently polarizable models for the solute and solvent (with G.K. Schenter). Future research will be extended to elucidation of the solvation and surface properties of more complex anions such as the oxyanions (with G.K. Schenter and J. Fulton) such as ClO_3^- and BrO_3^- where both exhibit very interesting behavior in the context of the Hofmeister series. We are currently investigating the role of hydrophobic solvation with John D. Weeks. We are using multiple representations of the molecular interaction for water (*e.g.* TIP5P, SPC/E, flavors of DFT) to understand the structural response to a model hydrophobe and the signatures of volume to area scaling.

Acknowledgements. This work was performed with Yan Levin (Brazil) John D. Weeks (U. Maryland), D.J. Tobias (UC-I), Ilja Siepmann (U. Minn.), and I.-F.W. Kuo (LLNL), Greg Schenter (PNNL), Liem Dang (PNNL), Marcel D. Baer (PNNL), Abe Stern (UC-I), Joost VandeVondele (U. Zurich), Greg Kimmel (PNNL), John Fulton (PNNL), Roger Rousseau (PNNL) and Shawn M. Kathmann (PNNL).

Publications from BES support (2010- present)

1. Baer, MD and **Mundy, CJ**, "An *ab initio* approach to understanding the specific ion effect," *Faraday Discussions*, (accepted)
2. Baer, MD; Stern, AC; Levin, Y; Tobias, DJ; **Mundy, CJ**, "Electrochemical Surface Potential Due to Classical Point Charge Models Drives Anion Adsorption to the Air-Water Interface," *Journal of Physical Chemistry Letters* **3**, 1948-7185 (2012)
3. Kimmel, GA; Baer, M; Petrik, NG; VandeVondele, J; Rousseau, R; **Mundy, CJ**, "Polarization and Azimuth-Resolved Infrared Spectroscopy of Water on TiO_2(110): Anisotropy and the Hydrogen-Bonding Network," *Journal of Physical Chemistry Letters* **3,** 1948-7185 (2012)
4. Lewis, T; Winter, B; Stern, AC; Baer, MD; **Mundy, CJ**; Tobias, DJ; Hemminger, JC, "Does Nitric Acid Dissociate at the Aqueous Solution Surface?," *Journal of Physical Chemistry C* **115,** 21183 (2011)
5. Baer, MD; Pham, VT; Fulton, JL; Schenter, GK; Balasubramanian, M; **Mundy, CJ**, "Is Iodate a Strongly Hydrated Cation?," *Journal of Physical Chemistry Letters* **2**, 2650-2654 (2011)
6. McGrath, MJ; Kuo, IFW; Ghogomu, JN; **Mundy, CJ**; Siepmann, JI, "Vapor-Liquid Coexistence Curves for Methanol and Methane Using Dispersion-Corrected Density Functional Theory," *Journal of Physical Chemistry B* **115**, 11688-11692 (2011)
7. Baer, MD; **Mundy, CJ**; McGrath, MJ; Kuo, IFW; Siepmann, JI; Tobias, DJ, "Re-examining the properties of the aqueous vapor-liquid interface using dispersion corrected density functional theory," *Journal of Chemical Physics* **135,** 124712 (2011)
8. Lewis, T; Winter, B; Stern, AC; Baer, MD; **Mundy, CJ**; Tobias, DJ; Hemminger, JC, "Dissociation of Strong Acid Revisited: X-ray Photoelectron Spectroscopy and Molecular Dynamics Simulations of HNO_3 in Water*," Journal of Physical Chemistry B* **115**, 9445 (2011)
9. Murdachaew, G; **Mundy, CJ**; Schenter, GK; Laino, T; Hutter, J, "Semiempirical Self-Consistent Polarization Description of Bulk Water, the Liquid-Vapor Interface, and Cubic Ice," *Journal of Physical Chemistry A* **115**, 6046-6053 (2011)
10. Baer, MD; **Mundy, CJ**, "Toward an Understanding of the Specific Ion Effect Using Density Functional Theory," *Journal of Physical Chemistry Letters* **2**, 1088-1093 (2011)
11. Kathmann, SM; Kuo, IFW; **Mundy, CJ**; Schenter, GK, "Understanding the Surface Potential of Water," *Journal of Physical Chemistry B* **115**, 4369-4377 (2011)
12. Murdachaew G, **Mundy CJ**, Schenter GK, "Improving the density functional theory description of water with self-consistent polarization," *Journal of Chemical Physics* **132,** 164102 (2010)
13. McGrath MJ, Ghogomu JN**, Mundy CJ**, et al. "First principles Monte Carlo simulations of aggregation in the vapor phase of hydrogen fluoride," *Physical Chemistry Chemical Physics* 12, 7678 (2010)
14. Fulton JL, Schenter GK, Baer MD, et al. "Probing the Hydration Structure of Polarizable Halides: A Multiedge XAFS and Molecular Dynamics Study of the Iodide Anion," *Journal of Physical Chemistry B* **114,** 12926 (2010)
15. Baer M, **Mundy CJ**, Chang TM, et al, "Interpreting Vibrational Sum-Frequency Spectra of Sulfur Dioxide at the Air/Water Interface: A Comprehensive Molecular Dynamics Study," *Journal of Physical Chemistry B* **114**, 7245 (2010)
16. **Mundy CJ**, KA Maerzke, MJ McGrath, IFW Kuo, G. Tabbachi, and JI Siepmann, "Vapor-liquid phase equilibria of water modelled by a Kim-Gordon potential." *Chemical Physics Letters* **479**, 60-64 (2010)

DYNAMIC STUDIES OF PHOTO- AND ELECTRON-INDUCED REACTIONS ON NANOSTRUCTURED SURFACES

Richard Osgood, Center for Integrated Science and Engineering, Columbia University, New York, NY 10027, Osgood@columbia.edu

Program Scope or Definition:

Our current research program examines the photon- and electron-initiated reaction mechanisms, half-collision dynamics, and other nonequilibrium-excited dynamics effects, occurring with excitation of adsorbates on well-characterized metal-oxide and nanocrystal surfaces. In order to explore these dynamics, we have first developed new synthesis methods for uncapped nanocrystals *with specific reconstructions and orientation* in a UHV STM instrument. We have used tunneling from the tip of our STM (and will use an *in situ* flood UV lamp) to excite adsorbate molecules at specific sites of these nanocrystals. The resulting chemistry and surface dynamics are then investigated via imaging of reaction fragments in the vicinity of the reaction sites. Additional research tools are time-of-flight detection, XPS, standard UHV probes, *in situ* TPD, and molecular computational tools. Our initial experiments have been directed toward electronic-tunneling reactions in a series of linear aromatics on rutile TiO_2(110) surfaces, as well as the determination of the conditions needed to form uncapped TiO_2 nanocrystals with a known atomic structure. Our adsorbate molecules have been chosen to have sufficient binding energy to examine reactions at temperatures of > 100K.

From the perspective of DOE energy needs, photoexcitation is of continuing interest for its importance in photocatalytic destruction of environmental pollutants, in several methods of solar-energy conversion, and in a variety of applications of nanotechnology. Our recent work in this program has yielded several new research findings regarding the preparation of nanocrystals and their reactive properties, the structure of adsorbed aromatics on TiO_2 surfaces, and the observation of tip-induced-electron bond cleavage within these molecules.

Recent Progress:

The methodology of our research program is to progress from measurements on a planar single-crystal sample of TiO_2(110) surface to comparable experiments on a nanocrystal surface. The nanocrystals are prepared using surface-alloy growth, which is a synthesis method pioneered in our group; thus characterization of this method forms an important component of our research. In our talk here, we will focus on both the nanocrystals, thermal-induced reactions and molecular orientation, and on our recent research on tip induced reactions of adsorbate molecules on a single-crystal TiO_2 surface. Our central tool for this research is our instrumented STM system.

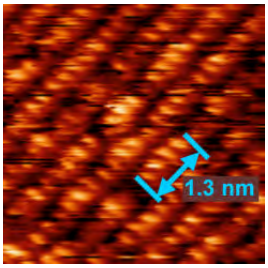

Fig. 1: 5 nm × 5 nm STM image of 4-bromobiphen-yl-exposed TiO_2 (110) surface at T=300K. Bright ellipse-like features are due to Ti sites in TiO_2 substrate.

Adsorption Geometry of Reaction Target Molecules on a Reconstructed Surface: Planar Aromatics on Single-Crystal, Rutile TiO_2(110)

Molecular orientation plays a key role in many surface or interfacial applications involving self-assembly, catalysis, and charge transfer. STM in conjunction with a pristine surface is a powerful tool that allows direct observation of the geometric orientation of adsorbed molecules and hence can further our

understanding of factors that control orientation. Surprisingly there are only limited direct scanning-probe observations of the adsorption geometry of organic molecules on TiO_2. We have now used STM to examine the adsorbate geometries from 0 ~ 1 ML coverage of relatively large aromatic molecules, *viz* anthracene and its halogenated derivative chloroanthracene, and the related molecule 4-bromobiphenyl.

Our imaging experiments at low temperatures demonstrated that our apparatus could image a single adsorbed molecule and that our surface adsorbates have anisotropic, temperature-dependent mobilities for diffusion across our surface. STM images taken at room temperature show that at high coverage both of molecular species assemble into periodic patterns on the TiO_2 surface with individual molecules aligned along the $Ti^{(5)}$ atom row of the substrate. Individual molecules of the organic adsorbates were found to be mobile on the surface in the direction parallel to the Ti atomic lattice. The observed lateral alignment suggests attractive interactions for anthracene and 2-chloroanthracene and repulsive interactions for 4-bromobiphenyl.

In the case of the 4-bromobiphenyl layers, the *mutual* arrangement of the molecules in neighboring rows (**Fig. 1)** differs strikingly from the arrangement of anthracene on the same substrate. Such an arrangement can be readily explained through the polarity of 4-bromobiphenyl; the presence of the halogen atom at the extremity of the molecule creates a significant electric-dipole moment. This polarity leads to the negatively charged bromine atom being electrostatically attracted to the positively charged aromatic rings of a neighboring molecule. In analyzing images, it is important to take into account the lattice structure; the lattice is seen in the repeating patterning of protrusions or bright ellipse-like dots with a spacing of ~0.3 nm due to the surface lattice spacing for $Ti^{(5)}$ atoms.

Thermal Reactions on Nanocrystal Surfaces and Their Catalytic Properties

Understanding of electron-induced reactions requires first that we have a clear grasp of the thermal reactions, which are present on the nanocrystals prepared as described above. Of course nanometer-scale catalytically important materials are of research interest in their own right due to the possibility of nano-scale size effects. Thus in this talk we will describe our studies of the reactivity of TiO_2 nanocrystals, prepared by the surface alloy-assisted method, with 2-propanol, chosen as our chemical probe molecule. Temperature programmed desorption (TPD) was used as a primary tool for reaction product analysis and scanning tunneling microscopy (STM) was used to monitor the morphology of the titania crystallites. **Figure 2** shows an STM image of a typical surface preparation used in the study. The nanocrystals had an average height of 1 nm and width of 15 nm with a dominantly hexagonal morphology. Our analysis of desorption products from propanol-exposed nano-TiO_2/Au(111) surface was based on monitoring multiple ion masses during TPD experiments and on comparison of the results with the TPD spectra obtained from two other reference surfaces: pristine Au(111) and TiO_2 rutile(110) surface. The desorption of propanol and propanol-derived products from the TiO_2 nanocrystal surfaces was observed in the 270 – 570 K temperature range and could be distinguished from desorption of propanol from the Au(111) surface below 270 K. Only three desorption products were detected: unreacted 2-propanol, propene, and acetone, as shown in **Fig. 3**. With

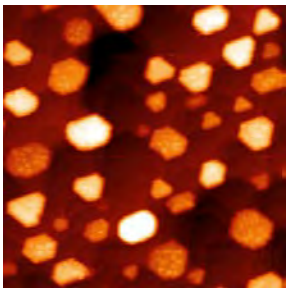

Fig. 2. 200 × 200 nm STM image of Au(111) surface with TiO_2 nanocrystals.

increasing propanol coverage, the TiO_2-related TPD peaks were occupied before the appearance of any Au(111)-related peaks, which indicate sufficient mobility of 2-propanol molecules on both Au(111) and nano-TiO_2 surfaces below 270 K. Our calculations and experimental measurements showed that in comparison with rutile(110), the nano-TiO_2/Au(111) surface shows higher reactivity both in terms of the fraction of reactive sites and in terms of lower reaction barrier. Also the desorption temperatures of products from supported TiO_2 nanocrystals were shown to depend strongly on the morphology of the nanocrystals.

The experimental observations made as a result of our work are as follows: (1) propanol completely fills adsorption sites on TiO_2 nanocrystals before filling Au(111) sites; the local adsorption site density of the nanocrystals is 0.4 ML; (2) almost ½ of propanol molecules adsorbed on TiO_2 nanocrystals desorb at ~310 K, exhibiting behavior, which is identical to propanol adsorbed on the $Ti^{(5)}$ atoms of rutile(110) surface; (3) more than ¼ of propanol molecules undergo chemical reactions either of dehydration to form propene or, in smaller part, dehydrogenation to form acetone. Some sites on TiO_2 nanocrystals show almost 40 kJ/mol reduction in the reaction barrier for propene formation compared to BBOv on rutile(110), while acetone is not produced on rutile(110). Thus, in comparison with rutile(110), the nano-TiO_2/Au(111) surface shows higher reactivity both in terms of the fraction of reactive sites and of reaction barrier.

STM Tip-Induced Dissociation Dynamics on Surfaces.

Scanning tunneling microscopy offers a unique approach to exploration of molecular dissociation dynamics at an atomic scale. Namely, as shown by the W. Ho Group, an STM allows injection of an electron or electrons with a specified energy into a selected molecule in a specific adsorption configuration. Initial studies of this approach have been carried out in the Palmer and Polanyi Groups for reactions on semiconductor surfaces and shown to yield dynamical information on the charge-transfer threshold electron energy for a specific reaction, the identity of adsorbate states suitable for dissociation, fragment trajectories across the surface following bond scission, and the nature and sensitivity to the adsorption geometry of the products. Note that for photocatalysis, the electron-induced reaction similarly involves charge transfer from the bulk of a substrate to an adsorbed molecule followed by bond cleavage. Such a study thus tries to answer the same fundamental chemical physics questions as in gas phase reaction dynamics except that on a surface determine the role of the surface perturbation on the half-collision event and fragments.

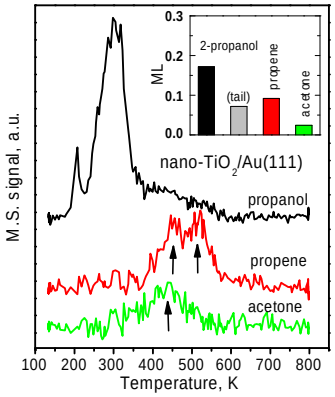

Fig. 3. TPD spectrum from a nano-TiO_2/Au(111) surface having 0.1 ML of 2-propanol coverage. The inserts show the calculated distribution of the desorption products.

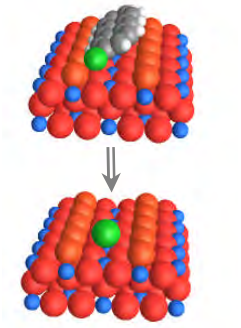

Fig. 4: Cartoon showing the change in 2-chloroanthracene following tip-induced *e* reaction. The green atom is the remaining Cl.

Our talk will discussion our initial studies of the dynamics of STM tip-induced reactions on single-crystal TiO_2(110). The experiments use 2-chloro-anthracene since this halogenated species is labile to electron bond cleavage after electron attachment. The orientation of this molecule is known from our imaging studies. To investigate tip-induced reactions, individual molecules were imaged before and after a voltage was applied to the tip placed within tunneling distance to the molecule. It was found that above a threshold tip voltage, e.g. 3V, the reaction was seen as the disappearance of the molecule and appearance of a new fragment, chlorine. **Figures 4** and **5** show such a dissociation event; after dissociation an adatom of Cl is located above a titanium atom in a Ti$^{(5)}$ row. Our studies have shown the pattern of fragmentation of this molecule is reproducible and that the electron-energy threshold is related to the alignment of the molecular orbital energies with the substrate.

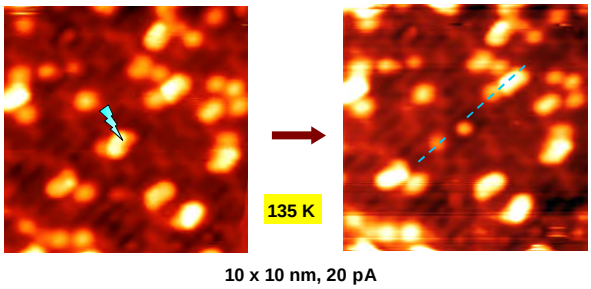

Fig. 5: STM images showing a surface prior to and after tip injection of an electron in an adsorbate molecule.

Future Plans

In summary, our work will focus on dynamical phenomena uncovered via the STM imaging of the spatial distribution of molecular fragments from tip-induced reactions with precise control of current and energy of the tunneling electrons. Our intent is to understand the methods and physics of the tip induced reaction process, first on well prepared single-crystal metal-oxides and, subsequently, on nanocrystals of these same materials. For each type of nanoparticle our research will have the following elements: a) formation and characterization of the nanoparticles; b) determination of adsorbed state, c) investigation of any thermal surface chemistry; and, c) measurement of dynamics following either tip- or UV-induced fragmentation. These experiments have involved establishing new experimental methods and instrumentation in our STM chamber, including a precise evaporator, UV source, and XPS instrumentation.

Recent DOE-Sponsored Publications

1. D. Potapenko, J. Hrbek, and R.M. Osgood, Jr., "Scanning Tunneling Microscopy Study of Titanium Oxide Nanocrystals Prepared on Au(111) by Reactive-Layer-Assisted Deposition." ACS Nano 2, 7, 1353-1362 (2008)
2. T.-L. Chen, M.B. Yilmaz, D. Potapenko, A. Kou, N. Stojilovic, R.M. Osgood, Jr., "Chemisorption of Tert-Butanol on Si(100)." Surf. Sci. 602, 21, 3432-3437 (2008)
3. D. Potapenko and R.M. Osgood, Jr., "Preparation of TiO_2 nanocrystallites by oxidation of Ti-Au(111) surface alloy." Nano Lett. 9, 6, 2378-2383 (2009)
4. L. Cao, N.-C. Panoiu, and R.M. Osgood, Jr., "Surface Second Harmonic Generation from Scattering of Surface Plasmon Polaritons by Radially Symmetric Nanostructures" Phys. Rev. B, 79, 235416 (2009)
5. D. Potapenko, N. Choi, and R.M. Osgood, Jr., "Adsorption Geometry of Anthracene and 4-Bromobiphenyl on TiO_2(110) Surfaces." J. Phys. Chem. 114, 19419 (2010)
6. D.V. Potapenko, Z. Li, and R.M. Osgood, Jr., "Dissociation of Single 2-Chloroanthracene Molecules by STM-Tip Electron Injection." J. Phys. Chem. C, 116, 7, 4679-4685 (2012)

Studies of surface adsorbate electronic structure and femtochemistry at the fundamental length and time scales

Hrvoje Petek
Department of Physics and Astronomy and Chemistry
University of Pittsburgh
Pittsburgh, PA 15260

Our research focuses on the electronic structure and dynamics of solids, surfaces, and molecule covered surfaces. We are interested in the surface electronic excitation and the subsequent dynamics leading to charge transfer or photochemistry. The correct description of surface electronic structure, photoexcitation, interfacial charge transfer, energy and momentum relaxation of carriers, and femtochemistry are essential for the intellectual framework for applications of photoinduced phenomena at interfaces, such as the photovoltaic and photocatalytic solar energy conversion. In this abstract we introduce examples of our femtosecond time-resolved multi-photon photoemission (TR-MPP) and low-temperature STM studies of electronic surfaces and interfaces.

Transient exciton formation in metals. When light interacts with a solid it creates a coherent polarization field, i.e., an exciton-polariton, which has both particle and field properties. An exciton can lose coherence through scattering to absorb a photon, or decay coherently by electron-hole (*e-h*) pair recombination to emit a photon. Excitons have never been found in metals because Coulomb interaction is fully screened by charge density fluctuations. The screening response takes time, but is thought to occur on the sub-femtosecond time scale in typical metals. An exception may be silver, which has a sharp bulk plasmon resonance at ~3.8 eV. Sudden introduction of a charge in Ag creates surface plasmon oscillation with ~1 fs period, which dephases on a few femtosecond time scale. When the screening response occurs on a time scale comparable to the laser pulse duration, it may be possible to observe a correlated *e-h* pair state, i.e. a transient exciton, in an MPP measurement.

We have investigated MPP spectra of Cu(111) and Ag(111) surfaces focusing on the near-resonant and resonant two photon transition from the occupied Shockley surface (SS) state to the unoccupied image potential (IP) penultimate intermediate state before emission of electron into vacuum (Fig. 1). IP states of metals are not features of the static electronic structure. Rather, they form as a consequence of the many-body screening of an external charge. In other words, they are the asymptotic states after the screening has become fully established.

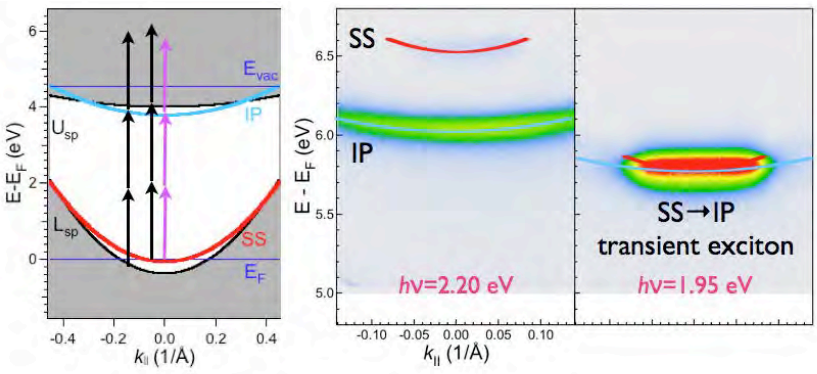

Figure 1. *The projected band structure of Ag(111) surface showing the resonant (purple) and nonresonant (black) excitation pathways for the SS and IP states, and 3PP spectra (final state energy vs. parallel momentum) under nonresonant (2.20 eV) and resonant (1.95 eV) conditions.*

Figure 1 shows the band structure of Ag(111) and 3PP spectra for resonant and near-resonant excitation conditions. For the near-resonant condition, the energy-momentum image of photoemitted electrons shows dispersive SS and IP states indicated by red and blue curves. At the resonant condition, however, the dispersive surface bands collapse into a non-dispersive feature. Such non-dispersive spectra are expected for photoemission from excitonic states, because in a correlated *e-h* pair, the electron can take on any momentum spanned by the occupied part of the hole band, as long as the exciton momentum is conserved. Similar experiments on Cu(111) surface do not show the non-dispersive feature, consistent with faster screening suppressing the *e-h* correlation.

The spectra in Fig. 1 show that MPP spectra can probe the fundamental many-body response of metals in response to perturbation by an external field. Because excitonic states are the primary manifestation of interaction between light and-solid state materials, the ability to follow the formation and decay of excitons is fundamental to solar energy conversion processes.

2D superatom states. In the spatial domain, we have investigated the formation of a molecular quantum-well with single-molecule resolution. Several years ago 2PP spectroscopy provided the evidence that a monolayer of flat lying C_6F_6 molecules on Cu(111) surface forms a molecular quantum well with an effective mass of $2m_e$ for its LUMO state of σ* character. How flat lying π-conjugated molecules can hybridize into a delocalized band has been until now a mystery.

We have performed low temperature STM measurements on C_6F_6 on Cu and Au surfaces from single molecule to multilayer coverages. By dz/dV spectroscopy we could measure the σ* state energy as a function of the number of nearest neighbors, and found that the energy is stabilized consistent with an intermolecular hopping integral β=0.026 eV. This behavior could be reproduced nearly quantitatively by a DFT calculation of the electronic structure of unsupported C_6F_6 from a single molecule to a monolayer film. The calculations show that the band formation is an intrinsic property of C_6F_6 molecules, which raises the question of the origin of the intermolecular interactions that enable the dispersive band formation.

We have therefore investigated the electronic properties of the σ* state by low temperature STM and theory. As required for the strong intermolecular interaction, the σ* state has a diffuse wave function with a long tail extending past the F atom periphery (Fig. 2). This behavior is reminiscent of the superatom molecular orbitals (SAMOs) of hollow molecules, which we discovered in C_{60} and related materials. SAMOs of hollow molecules are bound to the hollow

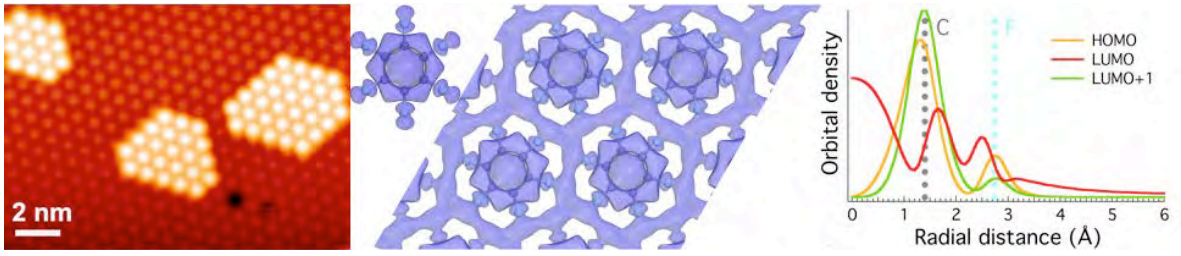

Figure 2. *STM image of C_6F_6 monolayer and second monolayer islands on Cu(111) surface. The calculated probability density of the σ* state for a single molecule and σ* band for a monolayer quantum well. The density projecting beyond F atoms forms the delocalized state. The radial wave function cross sections for the π HOMO, σ* LUMO, and π* LUMO+1 orbitals. The SAMO characteristics of σ*, i.e. the nonnuclear density in the molecular center and beyond the F atom periphery, enable strong wave function hybridization into a delocalized band.*

core rather than the ions of the cage. Examining the probability density of the σ* state, we find that it is distributed in nonnuclear regions with the maximum density within the hollow benzene ring. This leads us to the conclusion that the σ* state is in fact a 2D superatom state, and suggests a new paradigm for designing molecular semiconducting materials with nearly-free electron band transport. Such electronic orbitals should exist in other flat molecules, and we are exploring by theory the factors that control the energies of SAMOs, in order to discover materials with superior charge transport properties.

Molecular chemisorption on 1D substrates. By low temperature STM we discovered highly unusual chemisorption behavior of CO molecules on Cu(110)-O (2x1) surface. The substrate consists of 1D Cu-O- chains, where Cu atoms forming the chains have weak interaction with the Cu substrate. The chemisorption of CO through the usual π donation and σ back donation mechanism results in formation of Cu-C bond. The d-orbitals of Cu atom that have the correct symmetry for the π interaction are engaged in Cu-O bonds. Therefore, in order to form Cu-C bond, CO molecules pull Cu atoms out by 1 Å from the Cu-O- chains causing a rehybridization of the Cu-O bonds. Moreover, the entire OC-Cu structure tilts by 45° from the surface normal in one of two equivalent configurations, in order to optimize the dipole-image dipole interaction with the surface. As a consequence of CO existing in two equivalent tilted structures with a low intercomversion barrier, the STM images (Fig. 3a) of single CO molecules at low coverages and 77K surface temperature appear as two spots separated by 5Å. Cooling the sample to 4K freezes the molecule in one of the tilted structures.

At higher coverages, the tilted OC-Cu units experience attractive dipole-dipole interaction leading to formation of long, single CO molecule wide rows running perpendicular to the surface Cu-O- chains, with a minimum separation between rows of 8 substrate unit cells. Our theoretical modeling indicates that the CO rows repel each other through the strain introduced by lifting of Cu atoms from Cu-O- chains.

The strongly anisotropic interactions between CO molecules on Cu(110)-O (2x1) surface are

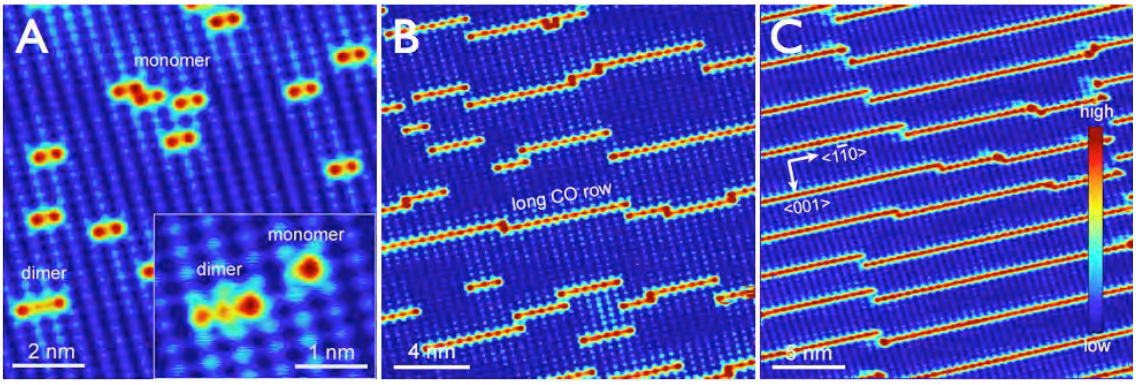

Figure 3. *The structure of CO chemisorption on Cu(110)-(2x1)-O surface. a) Low coverage structure at 77 K, where to the metronome tilting motion of Cu-CO unit causes single CO monomers to appear as a pair of bright spots. The inset shows the frozen tilted structures of a monomer and dimer at 4K. b) At intermediate coverages CO molecules have the propensity to aggregate into linear structures. The bright contrast of the substrate emanating from CO lines reflects the chemisorption induced substrate distortion. c) CO monolayer coverage where CO molecules assemble in a grating structure with 8-9 substrate unit cells between CO lines.*

likely to also occur in low coordination sites on catalytic surfaces. Therefore we believe that the present surface is an exemplary model of interactions that may be important in catalysis. We are exploring other anisotropic surfaces and chemisorbates that may exhibit similar chemical properties to CO/Cu(110)-O surface. Moreover, by STM tip it is possible to switch CO molecules between two 45° tilted configurations. We are exploring the chemical interactions that enable such switching as a model of a simple single molecule switch.

DOE Basic Energy Sciences Sponsored Publications 2009-2012

1. Achilli, S., Trioni, M.I., Chulkov, E.V., Echenique, P.M., Sametoglu, V., Pontius, N., Winkelmann, A., Kubo, A., Zhao, J., & Petek, H., "Spectral properties of Cs and Ba on Cu(111) at very low coverage: Two-photon photoemission spectroscopy and electronic structure theory." *Phys. Rev. B* **80**, 245419 (2009).
2. Huang, T., Zhao, J., Feng, M., Petek, H., Yang, S., & Dunsch, L., "Superatom orbitals of $Sc_3N@C_{80}$ and their intermolecular hybridization on Cu(110)-(2x1)-O surface." *Phys. Rev. B* **81**, 085434 (2010).
3. Hu, S., Zhao, J., Jin, Y., Yang, J., Petek, H., & Hou, J.G., "Nearly Free Electron Superatom States of Carbon and Boron Nitride Nanotubes." *Nano Lett.* **10**, 4830 (2010).
4. Feng, M., Zhao, J., Huang, T., Zhu, X., & Petek, H., "The Electronic Properties of Superatom States of Hollow Molecules." *Acc. Chem. Res.* **44**, 360 (2011).
5. Wang, L.-M., Sametoglu, V., Winkelmann, A., Zhao, J., & Petek, H., "Two-Photon Photoemission Study of the Coverage-Dependent Electronic Structure of Chemisorbed Alkali Atoms on a Ag(111) Surface." *J. Phys. Chem. A* **115**, 9479 (2011).
6. Feng, M., Cabrera-Sanfelix, P., Lin, C., Arnau, A., Sánchez-Portal, D., Zhao, J., Echenique, P.M., & Petek, H., "Orthogonal Interactions of CO Molecules on a One-Dimensional Substrate." *ACS Nano* **5**, 8877 (2011).
7. Huang, T., Zhao, J., Feng, M., Popov, A.A., Yang, S., Dunsch, L., & Petek, H., "A Molecular Switch Based on Current-Driven Rotation of an Encapsulated Cluster within a Fullerene Cage." *Nano Lett.* **11**, 5327 (2011).
8. Feng, M., Lin, C., Zhao, J., & Petek, H., "Orthogonal Intermolecular Interactions of CO Molecules on a One-Dimensional Substrate." *Annu. Rev. Phys. Chem.* **63**, 201 (2012).
9. Lin, C., Feng, M., Zhao, J., Cabrera-Sanfelix, P., Arnau, A., Sánchez-Portal, D., & Petek, H., "Theory of orthogonal interactions of CO molecules on a one-dimensional substrate." *Phys. Rev. B* 85, 125426 (2012).
10. Petek, H., Feng, M., & Zhao, J., The Electronic Structure of Metal–Molecule Interfaces in *Current-driven phenomena in nanoelectronics*, T. Seideman ed. (World Scientific 2010).
11. Winkelmann, A., Chiang, C.-T., Tusche, C., Ünal, A.A., Kubo, A., Wang, L., & Petek, H., Ultrafast multiphoton photoemission microscopy of solid surfaces in the real and reciprocal space in *Dynamics of interfacial electron and excitation transfer in solar energy conversion: theory and experiment*, P. Piotrowiak ed. (Royal Society of Chemistry, London, 2012).
12. Bovensiepen, U., Petek, H., & Wolf, M. eds., Dynamics at Solid State Surfaces and Interfaces, Vol. 1: Current Developments, 1 ed. (Wiley-VCH Verlag Gmbh & Co., Weinheim, 2010).
13. Bovensiepen, U., Petek, H., & Wolf, M. eds., Dynamics at Solid State Surfaces and Interfaces, Vol. 2: Fundementals, 1 ed. (Wiley-VCH Verlag Gmbh & Co., Weinheim, 2012).

Ultrafast electron transport across nanogaps in nanowire circuits

Eric O. Potma

Department of Chemistry
University of California, Irvine
Irvine, CA 92697
e-mail: epotma@uci.edu

Program Scope

In this Program we aim for a closer look at electron transfer through single molecules. To achieve this, we use ultrafast laser pulses to time stamp an electron tunneling event in a molecule that is connected between two metallic electrodes, while reading out the electron current. A key aspect of this project is the use of metallic substrates with plasmonic activity to efficiently manipulate the tunneling probability. The first part of this program is concerned with developing highly sensitive tools for the ultrafast optical manipulation of tethered molecules through the evanescent surface field of plasmonic substrates. The second part of the program aims to use these tools for exercising control over the electron tunneling probability.

Recent Progress

In order to use pulsed surface fields for the manipulation of tethered molecules, we first developed several strategies for efficiently coupling femtosecond light fields into two-dimensional metallic substrates. We have used the process of four-wave mixing (FWM) as a probe to test the nonlinear activity of the surface fields.

Using different excitation geometries, we have shown that femtosecond surface fields can efficiently drive nonlinear polarizations in nanoscopic structures on the surface.[1, 2] A counter-propagating excitation geometry is shown in Figure 1. We demonstrated that background-free, surface-sensitive $\chi^{(3)}$ signals can be generated from surface-bound structures and molecules in a controlled fashion.[3] We have also found that the surface plasmon fields enhance the $\chi^{(3)}$ response from such structures by at least 100 times, relative to regular excitation conditions on a bare glass surface.

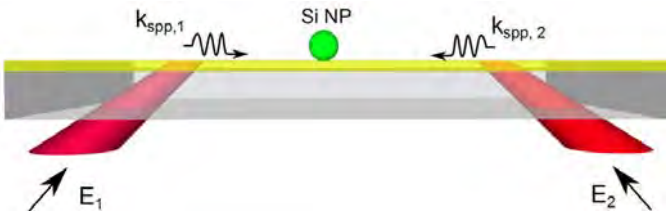

Figure 1: A scheme for the testing the ability of pulsed surface waves to generate optical nonlinearities in surface-bound objects. In this counter-propagating scheme, two femtosecond pulses are coupled into a 40 nm thick gold film at the Kretschman angle, generating two counter-propagating surface plasmon polariton waves. These pulsed surface waves can drive a nonlinear polarization in a probe particle (silicon nanoparticle). Strong, background-free FWM signals from the Si nanoparticle were observed.

These results are promising indicators that pulsed surface fields can be employed as actors in optical experiments of tethered molecules. However, the surface fields in these early experiments exhibited poor lateral confinement. Better control over the spatial properties of the pulsed plasmon waves is required to efficiently couple them into nanoscopic electrodes. Our first step in this direction is to focus the plasmon wave to a sub-micrometer spot, which improves the coupling efficiency into sub-wavelength waveguides. This approach can be compared, for instance, with focusing a freely propagating field into an optical fiber. For the purpose of plasmon focusing, we have fabricated Fresnel lenses in 40 nm gold surfaces. In order to test the ability of the focused surface fields to elicit nonlinear excitations, we have designed a dual Fresnel lens that yields two overlapping focal fields, which conveniently enables the generation of FWM signals.[4] An example is shown in Fig 2.

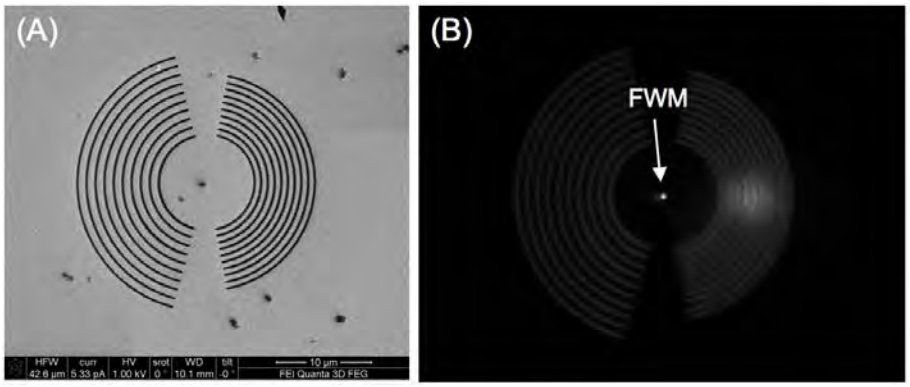

Figure 2: (A) SEM image of a dual Fresnel lens for plasmonic focusing. The lens consists of two halves with different periodic spacings of the grooves. The left half supports focusing of 820 nm light, while the right half support focusing of 720 nm light. A silicon nanoparticle is placed in the focal region for probing the ability of the focused surface waves to generate optical nonlinearities. (B) CCD image showing FWM of a Si nanoparticle upon focusing two femtosecond plasmon waves to the same sub-micrometer sized spot. A high FWM excitation efficiency is observed.

Future Plans

After having established that femtosecond plasmon waves can be controlled in a precise manner, our next steps will focus on optimizing the surface chemistry of target molecules and the fabrication of nanoscopic electrodes in our surface assay. As a first testbed, we have fabricated a sub-micron sized probing compartment which is positioned in the focal plane of the Fresnel lenses, as shown in Figure 3. This compartment services as a reservoir for molecules immersed onto the surface. The focal fields will excite a local plasmon mode of the groove, enabling local probing of molecules in the reservoir. Reducing the size of the reservoir will help us determine the capability of the plasmon waves to communicate with fewer and fewer molecules. Using focused ion beam techniques, grooves with a width down to 10 nm can be fabricated.

The next step is to replace the reservoir by fabricated nanowires that span a micrometer-wide gap. Nanogaps with a width in the 2 to 5 nm range will be engineered in the wires through controlled electron migration techniques. In a subsequent step we will bridge the gap with molecular substrates. We plan to use electric field controlled techniques for enhancing the alignment of long-chain molecules such as DNA across the gap. Once successful, we will prepare for a series of plasmon induced tunneling experiments.

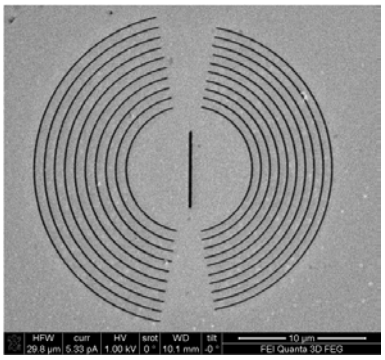

Figure 3: Testbed device for probing molecules with plasmonic waves in a well-defined reservoir. The plasmon mode of the central groove can be excited very efficiently and locally by the focused fields, enabling nonlinear probing of molecules in a controlled atto-liter volume.

Publications with acknowledged DOE support:

[1] Y. Wang, X. Liu, D. Whitmore, W. Xing, and E. O. Potma, "Remote multi-color excitation using femtosecond propagating surface plasmon polaritons in gold films," *Opt. Express* **19**, 13454–13463 (2011).

[2] X. Liu, Y. Wang, and E. O. Potma, "Surface-mediated four-wave mixing of nanostructures with counterpropagating surface plasmon polaritons," *Opt. Lett.* **36**, 2348–2350 (2011).

[3] Y. Wang, X. Liu, A. R. Halpern, K. Cho, R. M. Corn, and E. O. Potma, "Wide field, surface-sensitive four-wave mixing microscopy of nanostructures," *Appl. Opt.*, **51** 3305–3312 (2012).

[4] X. Liu, Y. Wang, and E. O. Potma, "A dual-color plasmonic focus for surface-selective four-wave mixing," *Appl. Phys. Lett.*, *in press* (2012).

This page is intentionally left blank

Richard J. Saykally; Department of Chemistry, University of California *and*
Chemical Sciences Division, Lawrence Berkeley National Laboratory
Berkeley, CA 94720-1460
saykally@berkeley.edu *http://www.cchem.berkeley.edu/rjsgrp/index.html*

Project I. Soft X-ray Spectroscopy of Liquids and Solutions

Program Scope or Definition

The goal of this project is to explore, develop, and apply novel methodologies for atom-specific characterization of volatile liquids, solutions, and and their surfaces, employing combinations of liquid microjet technology with synchrotron X-ray and Raman spectroscopies and close connection with state-of-the-art theory.

Recent Progress

Towards a Complete Understanding of CO_2 – Carbonate Equilibria [1]

The dissolution of carbon dioxide in water and the ensuing hydrolysis reactions are of profound importance for understanding the behavior and control of carbon in the terrestrial environment. Using liquid microjet technology, the first X-ray absorption spectra of aqueous carbonate have been measured as a function of pH to characterize the evolution of electronic structure of carbonate, bicarbonate, carbonic acid and dissolved CO2. The corresponding carbon K-edge core-level spectra were calculated using a first-principles electronic structure approach which samples molecular dynamics trajectories. Measured and calculated spectra are in excellent agreement. Each species exhibits similar, but distinct, spectral features which are interpreted in terms of the relative C–O bond strengths, molecular configuration, and hydration strength. This work provides benchmarks for future studies of this system.

Electronic Structure of Aqueous Borohydride: A Potential Hydrogen Storage Medium [2,3]

With large weight percent hydrogen capacity, stable reactants, and benign reaction products, borohydride salts have been considered as good prospects for transportable hydrogen storage materials, with molecular hydrogen released via hydrolysis. We examine details of the hydration of sodium borohydride by the combination of X-ray absorption spectroscopy of liquid microjets and first principles' theory. Compared to solid sodium borohydride, the aqueous sample exhibits an uncharacteristically narrow absorption feature that is shifted to lower energy, and ascribed to the formation of dihydrogen bonds between borohydride and water that weaken the boron–hydrogen covalent bonds. Water also acts to localize the highly excited molecular orbitals of borohydride, causing transitions to excited states with p character to become more intense and a sharp feature, uncharacteristic of tetrahedral molecules, to emerge. The simulations indicate that water preferentially associates with borohydride on the tetrahedral corners and edges.

Towards a Predictive Theory of Core-Level Molecular Spectra [4,5, 11-12]

The development of near edge X-ray absorption fine structure spectroscopy (NEXAFS) of liquid microjets has provided a useful new tool for characterizing the details of solvation for increasingly complex systems. NEXAFS probes the unoccupied molecular orbitals, which are highly sensitive to intermolecular interactions. This new approach to the study of liquids is yielding important insights into the behavior of aqueous systems, but the chemical information that can be extracted from the measurements is currently limited by the reliability of available theoretical methods for computing core-level spectra. The accurate description of an absorption event of several hundreds of eV of energy is an ongoing challenge in theoretical chemistry. In collaboration with LBL scientist David Prendergast, we are using the excited core hole (XCH)

method recently developed by Prendergast and Galli to compute the NEXAFS spectra of prototype systems, such as pyrrole[12] –an archtypical aromatic molecule-and compare the results with experimental spectra measured at the ALS. Near edge X-ray absorption fine structure (NEXAFS) spectra of pyrrole measured at the carbon and nitrogen K-edges both in the gas phase and when solvated in water, are compared with spectra simulated using a combination of classical molecular dynamics and first principles density functional theory in the excited state core hole approximation. The excellent agreement enabled detailed spectral assignments. Pyrrole is highly reactive in water and reaction products formed by the autopolymerization of pyrrole in water are identified. The solvated spectra measured at two different temperatures, indicate that the final states remain largely unaffected by both hydration and temperature. This is somewhat unexpected, as the nitrogen in pyrrole can donate a hydrogen bond to water. This study provides a good demonstration of the ability of the XCH method to describe core-level spectra of highly delocalized bonding systems, which are problematic for the methods now commonly used.

Towards a Systematic Atom-Specific Spectroscopic Method for the Study of Hydration in Small Biomolecules(6,7,10)

Using liquid microjets to avoid the often incapacitating problem of radiation damage to fragile solutes has enabled the measurement of pH-dependent NEXAFS spectra of amino acids, including glycine, proline, lysine, and the tripeptide triglycine[7], as well as ATP[6] and peptoid molecules[10]. This, in turn, has permitted the study of the effets of selected salts on polypeptide conformations[7,9], with the aim of elucidating the origins of Hofmeister effects in biology.

Future Plans

1. Develop a microfluidics-based mixing system for generating short lived species, e.g. carbonic acid, in liquid microjets for study by X-ray spectroscopy. Apply this technology to the study of hydration and hydrolysis of carbon dioxide, nitrogen oxides, and sulfur oxides.
2. Complete the XAS study of ionic perturbation of local water structure, such that the entire Hofmeister series is ultimately addressed. We seek a comprehensive picture of the effects of both cations and anions on the local structure of water. Raman spectroscopy measurements will also be performed on these systems, the data from which provide complementary insights and aid in the theoretical modeling.
3. Extend our studies of amino acid hydration vs. pH to include all natural amino acids. Use the same approach to continue the study of hydration of the peptide bonds in small polypeptides, nucleotide bases, nucleosides, and nucleotides, as well as the novel “peptoid” molecules.

References (DOE supported papers: 2009-present) – 12 total

[available at http://www.cchem.berkeley.edu/rjsgrp/opening/pubs.htm]

1. *A. H. England, A. M. Duffin, C. P. Schwartz, J. S. Uejio, D. Prendergast, and R. J. Saykally "On the Hydration and Hydrolysis of Carbon Dioxide," *Chem. Phys. Letters* **514,** 187(2011)*Cover Article.

2. *A. M. Duffin, A. H. England, C. P. Schwartz, J. S. Uejio, G. C. Dallinger, O. Shih, D. Prendergast, and R. J. Saykally "Electronic Structure of Aqueous Borohydride: A Potential Hydrogen Storage Medium" *Phys. Chem. Chem. Phys.,* **13**, 17077 (2011) *Cover Article.

3. A. Duffin, C. Schwartz, A. England, J. Uejio, D. Prendergast, and R.J. Saykally, "pH-Dependent X-ray Absorption Spectra of Aqueous Boron Hydrides," *J. Chem. Phys.* **134**, 154503 (2011).
4. C.P. Schwartz, S. Fatehi, R.J. Saykally, and D. Prendergast, "The importance of electronic relaxation for intercoulombic decay in aqueous systems," *Phys. Rev. Lett.* **105,** 198102 (2010).
5. C.P. Schwartz, R.J. Saykally, and D. Prendergast, "An analysis of the NEXAFS spectra of molecular crystal: α-glycine," *J. Chem. Phys.* **133,** 044507 (2010).
6. D. Kelly, C.P. Schwartz, J.S. Uejio, A.M. Duffin, A.H. England, and R.J. Saykally, "Near edge x-ray absorption fine structure spectroscopy of aqueous adenosine triphosphate at the carbon and nitrogen K-edges," *J. Chem. Phys.* **133,** 101103-101106 (2010).
7. C.P. Schwartz, J.S. Uejio, A.M. Duffin, A.H. England, D. Kelly, D. Prendergast, and R.J. Saykally, "Investigation of Protein Conformation and Interactions with Salts via X-ray Absorption Sectroscopy," *PNAS* **107,** 14008-14013 (2010).
8. G.N.I. Clark, C.D. Cappa, J.D. Smith, R.J. Saykally, and T. Head-Gordon "The Structure of Ambient Water," *Mol. Phys.* **108,** 1415-1433 (2010).
9. C.P. Schwartz, J.S. Uejio, A.M. Duffin, W.S. Drisdell, J.D. Smith, and R.J. Saykally, "Soft X-ray Absorption spectra of aqueous salt solutions with highly charged cations in liquid microjets," *Chem. Phys. Lett.* **493,** 94-96 (2010). LBNL-3897E
10. J.S. Uejio, C.P. Schwartz, A.M. Duffin, A.H. England, D. Prendergast, And R.J. Saykally, "Monopeptide versus Monopeptoid: Insights on Structure and Hydration of Aqueous Alanine and Sarcosine via X-ray Absorption Spectroscopy," *J. Phys. Chem. B* **114,** 4702(2010). LBNL-3896E
11. S. Fatehi, C.P. Schwartz, R.J. Saykally, and D. Prendergast, "Nuclear quantum effects in the structure and lineshapes of the N_2 NEXAFS spectrum," *J. Chem. Phys.* **132,** 094302-094309 (2010). LBNL-3895E
12. C.P. Schwartz, J.S. Uejio, A.M. Duffin, A.H. England, D. Prendergast, and R.J. Saykally, "Auto-oligomerization and hydration of pyrrole revealed by x-ray absorption spectroscopy," *J. Chem. Phys.* **131,** 114509-114516 (2009). LBNL-2651E

Project II. Characterization of Liquid Electrolyte Interfaces

Program Scope or Definition

The goal of this project is to apply nonlinear optical spectroscopies in close connection with state-of-the-art theory for characterization of electrolyte interfaces, seeking to establish the general principles that govern surface properties and reactivities of liquid-vapor and solid-liquid interfaces and fundamental processes such as evaporation.

Recent Progress

Towards a Complete Molecular Mechanism of Ion Adsorption to Aqueous Interfaces [1,2]

As a route to clarifying the mechanism that selectively drives ions to and away from the air/water interface, we have measured the temperature dependence of the adsorption free energy of the thiocyanate ion by UV resonant SHG spectroscopy. Adsorption of aqueous thiocyanate ions from bulk solution to the liquid/vapor interface was measured as a function of temperature . The resulting adsorption enthalpy and entropy changes of this prototypical chaotrope were both determined to be negative. This surprising result is supported by molecular simulations, which clarify the microscopic origins of observed thermodynamic changes. Calculations reveal energetic influences of adsorbed ions on their surroundings to be remarkably local. Negative adsorption enthalpies thus reflect a simple repartitioning of solvent density among surface, bulk,

and coordination regions. A different, and much less spatially local, mechanism underlies the concomitant loss of entropy. Simulations indicate that ions at the interface can significantly bias surface height fluctuations even several molecular diameters away, imposing restrictions consistent with the scale of measured and computed adsorption entropies. Based on these results, we expect an ion's position in the Hofmeister lyotropic series to be determined by a combination of driving forces associated with the pinning of capillary waves and with a competition between ion hydration energy and the neat liquid's surface tension.

Towards a Predictive Theory of Water Evaporation [3,4]

Liquid microjet technology affords the opportunity to study the details of water evaporation, free from the obfuscating effects of condensation that have plagued previous studies. Studying small (diameter < 5 μm) jets with Raman thermometry, we find compelling evidence for the existence of a small but significant energetic barrier to evaporation, in contrast to most current models. Studies of heavy water indicate a similar evaporation coefficient, and thus an energetic barrier similar to that of normal water[. A transition state model developed for this process provides a plausible mechanism for evaporation in which variations in libration and translational frequencies account for the small observed isotope effects. The most important practical result of this work is the quantification of the water evaporation coefficient (0.6), which has been highly controversial, and is a critical parameter in models of climate and cloud dynamics. A molecular-level description of the mechanism for water evaporation has been developed by the Chandler group using their TPS methodology for simulating such rare events, and a paper is in preparation.

We have measured the effects of ionic solutes on water evaporation rates. Ammonium sulfate, the most common ionic solute in atmospheric aerosols, was shown to have no statistically significant effect on the rate[3], whereas sodium perchlorate effected a 25% reduction[4].

Future Plans

1. Temperature dependences for surface adsorption of some other prototype salts will be measured, as we work with the Geissler group to develop a general understanding and predictive theory of the forces that drive some ions to the surface and repel others.
2. Extension of these measurements to solid/liquid interfaces will be explored.
3. Continue investigations and characterization of the evaporation of liquid water by Raman thermometry and mass spectrometry, seeking to quantify the effects of salts and surfactants on the evaporation process. Work with Chandler group on developng a predictive theory of this process.

References (DOE supported papers: 2009-present) – 4 total

[available at http://www.cchem.berkeley.edu/rjsgrp/opening/pubs.htm]

1. D.E. Otten, R. Onorato, R. Michaels, J. Goodknight, R. J. Saykally "Strong Surface Adsorption of Aqueous Sodium Nitrite as an Ion Pair," *Chem. Phys. Lett.* **519-520**, 45-48 (2012).

2. *D.E. Otten, P. Shaffer, P. Geissler, R.J. Saykally "Elucidating the Mechanism of Selective Ion Adsorption to the Liguid Water Surface," PNAS **109** (3), 701-705 (2012). *featured in Editor's Choice *Science* **335,** 505(2012), "Sacrifices at the Surface".

3. W.S. Drisdell, R.J. Saykally, and R.C. Cohen, "Effect of Surface Active Ions on the Rate of Water Evaporation," *J. Phys. Chem.C* **114,** 11880-11885 (2010).

4. W.S. Drisdell, R.J. Saykally, and R.C. Cohen, "On the evaporation of ammonium sulfate solution," *PNAS* **106,** 18897-18901 (2009). LBNL-2972E

Molecular Theory & Modeling

Development of Statistical Mechanical Techniques for Complex Condensed-Phase Systems

Gregory K. Schenter
Chemical & Materials Sciences Division
Pacific Northwest National Laboratory
902 Battelle Blvd.
Mail Stop K1-83
Richland, WA 99352
greg.schenter@pnnl.gov

The long-term objective of this project is to advance the development of molecular simulation techniques to better understand the relation between the details of molecular interaction and the prediction and characterization of macroscopic collective properties. This involves the investigation of representations of molecular interaction as well as statistical mechanical sampling techniques. Molecular simulation has the promise to provide insight and predictive capability of complex physical and chemical processes in condensed phases and interfaces. For example, the transport and reactivity of species in aqueous solutions, at designed surfaces, in clusters and in nanostructured materials play significant roles in a wide variety of problems important to the Department of Energy. This includes the design, control and characterization of catalytic systems for energy storage and conversion.

Throughout our studies we struggle with finding the balance between efficiency and accuracy in the description of molecular interaction. We search for the appropriate amount of explicit treatment of electronic structure that allows for efficient sampling of a statistical mechanical ensemble of a system of interest. Including this detail provides a more accurate and robust description of the multipole structure of the charge density of molecules and their polarization and charge transfer response. In comparison, we explore the extent that empirical potentials can be modified to take these effects into account, through point polarizability or flexibility. We have also been exploring empirical corrections to semi-empirical (NDDO) theory [a,9] and DFT [b,5] that make these approaches both accurate and tractable. A significant scientific challenge is to understand the extent that these effects must be taken into account as the homogeneous symmetry of a uniform bulk system is broken. The symmetry of the bulk aqueous system can be broken by ion solvation. This often takes the form of the introduction of a hydrophobic cavity as well as a charge inhomogeneity. The water network will respond to the ion. If the water structure is enhanced, the ion is a Kosmotrope (structure maker); if the water structure is broken, the ion is a Chaotrope (structure breaker). We are also interested in understanding how the description of molecular interaction must be modified in order to describe concentrated electrolytes. Another source of broken symmetry occurs at vacuum/liquid, liquid/solid, and liquid/liquid interfaces.

Recently, we have discovered that a Density Functional Theory (DFT) description of molecular interaction provides a quantitative representation of the short-range interaction and structure when compared to Extended X-ray Absorption Fine Structure (EXAFS) measurements. To do this it is essential to develop a simulation protocol that places you in the correct region of the bulk phase diagram. You need good densities. We have established that a BLYP DFT simulation of 100's of H_2O's at 300K, with Grimme's D2 dispersion correction, and a MOLOPT DZ basis set effectively does this. [c] Recently we have compared and contrasted the solvation of

two ions I^- [3] and IO_3^- [7]. One is a Chaotrope while the other is a Kosmotrope, respectively. This is substantiated by the Jones-Dole B coefficient: B= -0.073 for Iodide, B= +0.140 for Iodate. In these studies we generated a statistical ensemble of configurations using the CP2K electronic structure/statistical mechanics package [d]. From this ensemble, a series of electron multiple scattering calculations are performed using the FEFF9 code [e] to generate a configuration average EXAFS spectra to compare to experimental measurement.

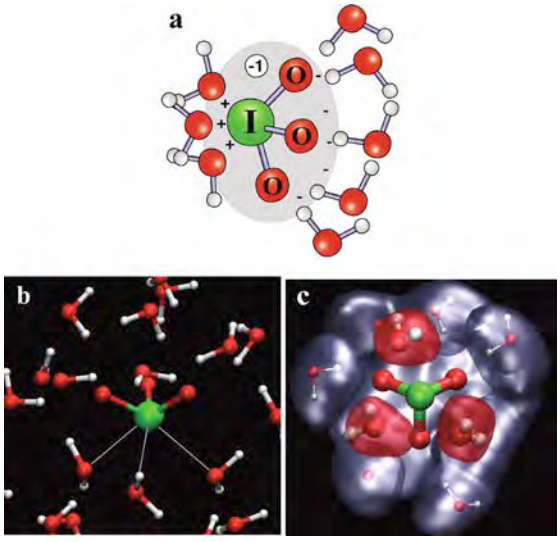

Figure 1. a) Schematic of waters hydrating IO_3^-, b) typical configuration, c) average density of O's(red) and 2nd shell water H's (blue).

From our simulation, we find three waters that are strongly bound to the iodate with water oxygens pointing towards the iodide, consistent with it carrying a net positive charge. [See Figure 1.] These three waters form a symmetrical structure that is only present in the condensed phase.

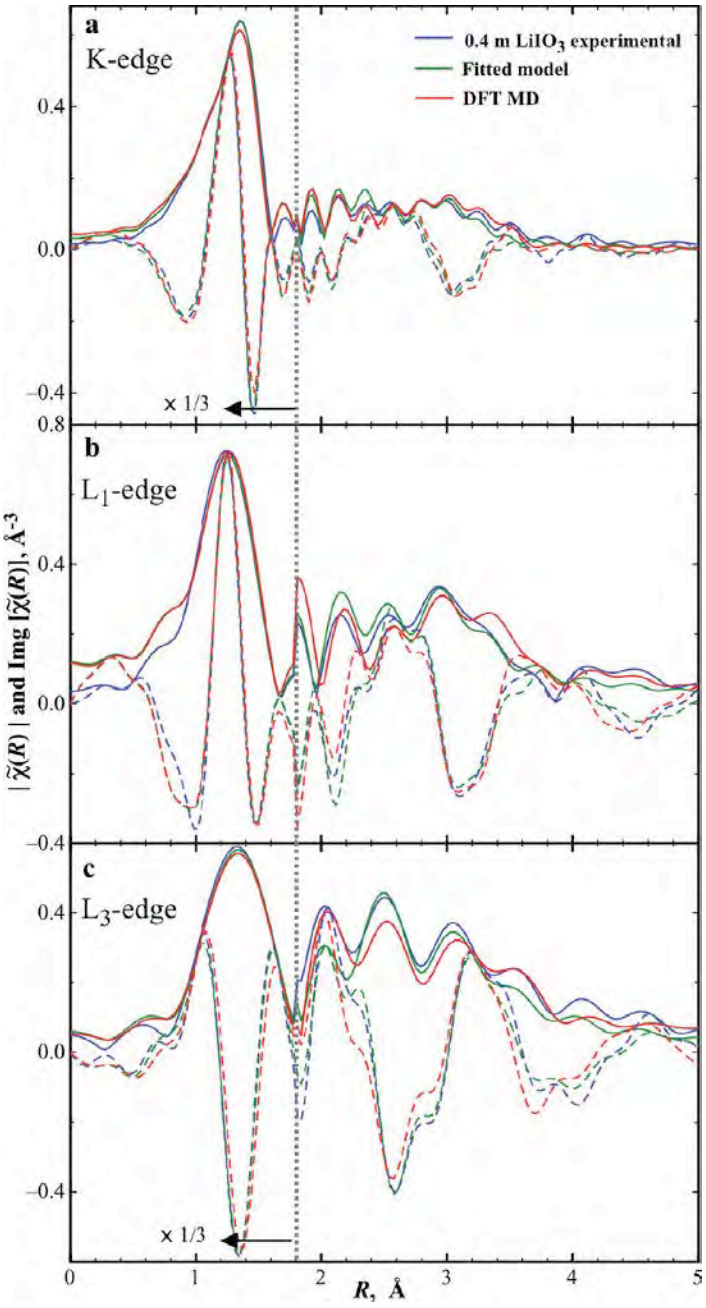

Figure 2. Comparison of the K- (a), L1- (b) and L3-edge (c) XAFS spectra for the 0.4 m $LiIO_3$ solution (blue) with model fit (green) and MD-XAFS (red) spectra generated from the DFT simulation. Both k^2- weighted magnitude, $|\tilde{\chi}(R)|$ (solid) and imaginary, $\mathrm{Im}\,\tilde{\chi}(R)$ (dashed) components.

Figure 2 shows the XAFS k^2-weighted $|\tilde{\chi}(R)|$ and $\mathrm{Im}\,\tilde{\chi}(R)$ plots for the 0.4 m $LiIO_3$ solution. The figure also shows two additional spectra in which one is the result of a model fit, and the other is the MD-EXAFS spectrum from the ensemble generated from the DFT simulation. For all spectra, the primary peak at 1.4 Å is due to scattering from the bonded O of IO_3^- (1.8 Å). The scattering signal between 1.6 and 5 Å is due to scattering (i) from H_2O's hydrating the I of IO_3^-, (ii) from H_2O's hydrating the O's of IO_3^-, and (iii) from three different

intramolecular multiple scattering processes for IO_3^- (triangular (three legs), double return (four legs) one O, and double return (four legs) two O's). The decoupling of these paths is made possible through the evaluation of three different X-ray edges and employing the property of multiple-edge, symmetry-dependent multiple scattering in which the XAFS phase-shift responses for the L1- and L3- edge spectra are strongly dependent on the local symmetry. This method allows one to efficiently decouple the overlapping single scattering H_2O and the multiple scattering IO_3^- signals.

In the future we will extend these studies to concentrated electrolytes and more complex ions such as the oxyanion series: IO_3^-, BrO_3^-, ClO_3^-, and ClO^-. We are also exploring the relation of EXAFS analysis to neutron and X-ray diffraction measurements.

Acknowledgements: Direct collaborators on this project include C. J. Mundy, M. Baer and J. Fulton. Interactions with S. S. Xantheas, L. X. Dang and S. M. Kathmann have significantly influenced the course of this work.

This research was performed in part using the computational resources in the National Energy Research Supercomputing Center (NERSC) at Lawrence Livermore National Laboratory. Battelle operates Pacific Northwest National Laboratory for the US Department of Energy.

References

a. D. T. Chang, G. K. Schenter, and B. C. Garrett "Self-consistent polarization neglect of diatomic differential overlap: Application to water clusters," J. Chem. Phys. **128** (16), 164111 (2008).
b. K. A. Maerzke, G. Murdachaew, C. J. Mundy, G. K. Schenter, and J. I. Siepmann, "Self-Consistent Polarization Density Functional Theory: Application to Argon," J. Phys. Chem. A **113** (10), 2075-2085 (2009).
c. M. D. Baer, C. J. Mundy, M. J. McGrath, I. F. W. Kuo, J. I. Siepmann, and D. J. Tobias. "Re-Examining the Properties of the Aqueous Vapor-Liquid Interface Using Dispersion Corrected Density Functional Theory." J. Chem. Phys. **135** (12), 124712 (2011).
d. The CP2K developers group, http://cp2k.berlios.de/ (2008) J. VandeVondele, M. Krack, F. Mohamed, M. Parrinello, T. Chassaing and J. Hutter, Comp. Phys. Comm. **167**, 103 (2005).
e. J. J. Rehr, R. C. Albers, S. I. Zabinsky, Phys. Rev. Lett. **69**, 3397 (1992); M. Newville, B. Ravel, D. Haskel, J. J. Rehr, E. A. Stern, and Y. Yacoby, Physica B, **208-209**, 154 (1995); A. L. Ankudinov, C. Bouldin, J. J. Rehr, H. Sims, and H. Hung, Phys Rev. B **65**, 104107 (2002).

References to publications of DOE sponsored research (2010-present)

1. E. Cauet, S. Bogatko, J. H. Weare, J. L. Fulton, G. K. Schenter, and E. J. Bylaska, "Structure and dynamics of the hydration shells of the Zn^{2+} ion from ab initio molecular dynamics and combined ab initio and classical molecular dynamics simulations," J. Chem. Phys. **132** (19), 194502 (2010).
2. J. L. Fulton, S. M. Kathmann, G. K. Schenter, E. J. Bylaska, S. A. Bogatko, and J. H. Weare, "XAFS spectroscopy and molecular dynamics: Aqueous ions and ion pairs under non-ideal conditions," Geochim. Cosmochim. Acta **74** (12), A311-A311 (2010).
3. J. L. Fulton, G. K. Schenter, M. D. Baer, C. J. Mundy, L. X. Dang, and M. Balasubramanian,

"Probing the Hydration Structure of Polarizable Halides: A Multiedge XAFS and Molecular Dynamics Study of the Iodide Anion," J. Phys. Chem. B **114** (40), 12926-12937 (2010).
4. C. J. Mundy, S. M. Kathmann, R. Rousseau, G. K. Schenter, J. Vande Vondele, and J. Hutter, "Scalable Molecular Simulation: Toward an Understanding of Complex Chemical Systems," SciDAC Review **17**, 10 (2010).
5. G. Murdachaew, C. J. Mundy, and G. K. Schenter, "Improving the density functional theory description of water with self-consistent polarization," J. Chem. Phys. **132** (16), 164102 (2010).
6. R. Atta-Fynn, E. J. Bylaska, G. K. Schenter, and W. A. de Jong, "Hydration Shell Structure and Dynamics of Curium(III) in Aqueous Solution: First Principles and Empirical Studies," J. Phys. Chem. A **115** (18), 4665-4677 (2011).
7. M. D. Baer, V. T. Pham, J. L. Fulton, G. K. Schenter, M. Balasubramanian, and C. J. Mundy, "Is Iodate a Strongly Hydrated Cation?," J. Phys. Chem. Lett. **2** (20), 2650-2654 (2011).
8. S. M. Kathmann, I. F. W. Kuo, C. J. Mundy, and G. K. Schenter, "Understanding the Surface Potential of Water," J. Phys. Chem. B **115** (15), 4369-4377 (2011).
9. G. Murdachaew, C. J. Mundy, G. K. Schenter, T. Laino, and J. Hutter, "Semiempirical Self-Consistent Polarization Description of Bulk Water, the Liquid-Vapor Interface, and Cubic Ice," J. Phys. Chem. A **115** (23), 6046-6053 (2011).
10. R. Atta-Fynn, D. F. Johnson, E. J. Bylaska, E. S. Ilton, G. K. Schenter, and W. A. de Jong, "Structure and Hydrolysis of the U(IV), U(V), and U(VI) Aqua Ions from Ab Initio Molecular Simulations," Inorg. Chem. **51** (5), 3016-3024 (2012).

MOLECULAR ENVIRONMENTAL SCIENCES BEAMLINE

David K. Shuh, Hendrik Bluhm, Mary K. Gilles
Chemical Sciences Division, Lawrence Berkeley National Laboratory, Berkeley, CA 94720.
DKShuh@lbl.gov; HBluhm@lbl.gov; MKGilles@lbl.gov

I. Program Scope

The scientific themes at the Molecular Environmental Sciences (MES) Beamline (BL) at the Advanced Light Source (ALS) center around spatially-resolved and spectroscopic investigations of materials using soft X-ray techniques under realistic controlled environments of pressure and temperature. Scientific areas of investigation are: heterogeneous chemical reactions at solid and liquid interfaces; nanoscience (including nano-biogeochemistry); energy science (fuel cells, solar cell materials); aerosol and atmospheric science; heterogeneous catalysis; magnetization dynamics; actinide science; environmental science; atomic molecular and optical science; extraterrestrial science; science with novel in-situ reaction cells; and lastly, complementary interactions with other synchrotron radiation-based techniques and laboratory-based investigations. The MES Scanning Transmission X-ray Microscope (STXM) remains the world-wide flagship for scientific investigations utilizing soft X-ray STXM. Similarly, the MES Ambient Pressure X-ray Photoelectron Spectroscopy (APXPS) endstations are recognized leaders in studies of surfaces at pressures approaching 10 Torr in catalysis and environmental surface science.

The MES BL serves two branchlines with facility endstations (APXPS and STXM) that share beamtime from a 5-cm-period elliptical polarization undulator (EPU) providing soft X-ray photons from ~75 eV to 2000 eV. In addition, a second APXPS endstation is used as a platform for several different experimental chambers, among them a droplet train instrument for the investigation of liquid/vapor interfaces and a microscopy chamber for the development of 100 nm resolution, zone plate-based APXPS microscopy.

II. Recent Progress

The MES BL will be a new addition to the Condensed Phase and Interfacial Molecular Science (CPIMS) program in FY2013. Hence, only a general description of the types of work and the productivity are presented here. The MES BL is scientifically productive with an output of about 30 peer reviewed publications per year, of which about 10% are considered high profile. It has been the most highly-subscribed beamline at the ALS for several years. The high productivity results from the unique scientific capabilities of the state-of-the-art endstations combined with the user-friendly operation of the BL, the exceptional leadership expertise of the BL scientists, and the high-level of support given to users. The scientific success of the MES BL has inspired the construction of several new STXM and APXPS endstations at other synchrotrons in the USA as well as worldwide.

The MES BL and its staff support are integral to and important to the Chemical Sciences, Geosciences, and Biosciences Divisions as well other BES-supported research programs. In particular, it provides significant support for research efforts within CPIMS, the Chemical Sciences Division and Materials Sciences Division for Catalysis, Actinide Chemistry, Chemical Dynamics Beamline, Atomic, Molecular, and Optical Sciences, Combustion, and other DOE programs. The Beamline has a diverse and established

world-wide scientific user base supported by a range of funding sources. A Memorandum of Understanding with the ALS details the current allocations of beamtime between the ALS General Users (including the Approved Programs), MES BL staff, Development/Maintenance, and ALS Director's Discretionary time. General User proposals are accepted in accordance with normal, peer-reviewed ALS policies. In addition to providing support, several personnel to be associated with the CPIMS program have access to the beamline for individual scientific programs through an Approved Program with the ALS (D.K. Shuh, H. Bluhm, and M.K. Gilles).

III. Future Plans

The research of H. Bluhm will focus on the investigation of the physical chemistry of surfaces under operating conditions, in particular reactions at liquid/vapor and solid/vapor interfaces. The goal is a fundamental, molecular level understanding of chemical reactions at these interfaces, which play a crucial role in processes involved in energy generation, carbon dioxide sequestration, electrochemistry, as well as environmental science. Ongoing research addresses the hydroxylation and water adsorption of metal and metal oxide surfaces under ambient relative humidity, the functionalization and volatilization of carbonaceous species by ozone and hydroxyl radicals, as well as the reaction of organic molecules with ice surfaces. An important effort is also the continuing new development of new experimental methods (mainly based on soft X-ray spectroscopies) for the investigation of interfaces with increased spatial and temporal resolution, including time and spatially resolved simultaneous measurements of the electrical potential and surface chemistry in electrochemical devices.

Research for M.K. Gilles includes: continued development of in situ cells for soft X-ray spectroscopy (heating & liquid phase cells), studies on hybrid materials (with an emphasis on thin films), incorporation of photoactive materials into thin films (in particular metal organic framework materials), improved layer-by-layer synthesis of hybrid material thin films and their characterization, and examining the changes in bonding occurring during gas or water vapor uptake in thin films as well as atmospheric aerosols. Each of these projects also serves the larger scientific and user community. Advances in the in situ cell development will be initially available on a collaborative basis, with the longer intent to share these developments with other synchrotrons and user facilities. Work on hybrid material thin films has potential to complement research in a variety of field important to DOE missions (CO_2 sequestration, sensors, responsive materials).

The research of D. K. Shuh will investigate the chemical bonding in condensed phase *p*-, *d*-, 4*f*-metal light-atom materials and their reactions at interfaces to gain a further fundamental, molecular level understanding of their chemical bonding reactivity, and the interfacial interactions that bear directly on energy science. This research draws on the experience and insights derived from recent studies conducted with the 5*f*-materials with light atom constituents that need to be translated to species with lighter metal atoms (*p, d, f*) that have distinctly different chemical bonding characteristics and reactivity. Investigations will start with the 4*f*-metal species and materials (lanthanides) and move progressively towards lighter *p*-,*d*-metal materials. An overall objective is to transition from understanding electronic structure in *p*-, *d*-, 4*f*-metal light atom materials, to

predicting and controlling their physical properties and reactivity by fine-tuning the electronic interactions in the chemical bonds that will enable their utility for energy applications. Complementary studies will allow supporting soft X-ray theory and computation to be developed and validated. A further objective is to elucidate interactions of metal-light atom materials at interfaces with metal oxides, other metal-light atom materials, polymeric materials, nanoparticles, and organic-inorganic composites. All of the studies will use the in-situ and spatial resolution provided by the unique APXPS and STXM capabilities at the MES Beamline.

The ALS and MES BL 11.0.2 are supported by the Director, Office of Science and the Office of Basic Energy Sciences and the Division of Chemical Sciences, Geosciences, and Biosciences Division of the U.S. Dept. of Energy at LBNL under Contract Number DE-AC02-05CH11231, respectively.

IV. Selected Recent Beamline Publications 2010-2011 (not funded by CPIMS)
(Total number of publications in 2010-2011: 42)

1) G. Dupouy, T. Dumas, C. Fillaux, D. Guillaumont, P. Moisy, C. Den Auwer, C. Le Naour, E. Simoni, E.G. Fuster, R. Papalardo, E. Sanchez-Marcos, C. Hennig, A. Scheinost, S.D. Conradson, D.K. Shuh, T. Tyliszczak, *Molecular Solids of Actinide Hexacyanoferrate: Structure and Bonding*, Instit. Physics Conf. Series: Mater. Sci. Eng. **9**, 012026, 2010.
2) D.E. Bugaris, R. Copping, T. Tyliszczak, D.K. Shuh, J.A. Ibers, *$La_2U_2Se_9$: An Odered Lanthanide/Actinide Chalcogenide with a Novel Structure Type*, Inorg Chem., **49**, 2568 2010.
3) C. Fillaux, D. Guillaumont, J.-C. Berthet, R. Copping, D.K. Shuh, T. Tyliszczak, C. Den Auwer, *Investigating the Electronic Structure and Bonding in Uranyl Compounds by Combining NEXAFS and Quantum Chemistry*, Phys. Chem. Chem. Phys., **12**, 14253, 2010.
4) J.A. Bradley, E.R. Batista, K.S. Boland, C.J. Burns, D.L. Clark, S.D. Conradson, S.A. Kozimor, R. L. Martin, G. T. Seidler, D. K. Shuh, T. Tyliszczak, M. P. Wilkerson, L. E. Wolfsberg, P. Yang, *$NaReO_4$, an Intensity Standard for O K-edge Covalency Studies Using XAS and NRIXS Spectroscopy*, J. Amer. Chem. Soc., **132**, 13914 2010.
5) C.T. Angell, T.H. Bray, R. Yee, R. Copping, P.-Anders Glans, T. Joshi, A. Klimenko, S. Korbly, W.D. Kulp, E.B. Norman, D.K. Shuh, E. Swanberg, G.A. Warren, C. Wilson, *Nuclear Resonance Fluorescence of ^{237}Np*, Phys. Rev. C, **82**, 054310, 2010.
6) R.A. Zaveri, C.M. Berkowitz, F.J. Brechtel, M.K. Gilles, J.M. Hubbe, J R. Jayne, L.I. Kleinman, A. Laskin, S. Madronich, T.B. Onasch, M.S. Pekour, S.R. Springston, J.A. Thornton, A.V. Tivanski, D.R. Worsnop, *Nighttime chemical evolution of aerosol and trace gases in a power plant plume: Implications for secondary organic nitrate and organosulfate aerosol formation, NO_3 radical chemistry, and N_2O_5 heterogeneous hydrolysis*, J. Geo. Res. Atmos, 115 D12304, 2010. DOI:10.1029/2009JD013250
7) G. Caster, S. Kowarik, A.M. Schwartzberg, S.R. Leone, A. Tivanski, M.K. Gilles, *Quantifying Reaction Spread and X-ray Exposure Sensitivity in Hydrogen Silsequioxane Latent Resist Patterns with X-ray Spectromicroscopy*, J. Vac. Sci. Technol. B, **28**, 1304, 2010. DOI:10.1116/1.3514124
8) R.C. Moffet, T.R. Henn, A. Laskin, M.K. Gilles, *Automated Chemical Analysis of Internally Mixed Aerosol Particles Using X-ray Spectromicroscopy at the Carbon K-edge*, Anal. Chem., **82**, 7906, 2010. DOI: 10.1021/ac1012909
9) D.A. Knopf, B. Wang, A. Laskin, R.C. Moffet, and M.K. Gilles, *Heterogeneous Nucleation of Ice on Anthropogenic Organic Particles*, Geophys. Res. Lett., **37**, L11803, 2010. DOI:10.1029/2010GL043362.

10) C. Zhang, M.E. Grass, A.H. McDaniel, S.C. DeCaluwe, F. El Gabali, Z. Liu, K.F. McCarty, R.L. Farrow, M.A. Linne, Z. Hussain, G.S. Jackson, H. Bluhm, B.W. Eichhorn, *Measuring Fundamental Properties in Operating Solid Oxide Electrochemical Cells by Using in situ X-ray Photoelectron Spectroscopy*, Nature Maters., **9**, 944, 2010.
11) E.R. Mysak, D.E. Starr, K.R. Wilson, H. Bluhm, *A Combined Aerodynamic Lens/Ambient Pressure Photoemission Spectrometer for the On-stream Analysis of Aerosol Surfaces*, Rev. Sci. Instrum. **81**, 016106, 2010.
12) H. Bluhm, *Photoelectron Spectroscopy of Surfaces Under Humid Conditions*, J. Electron Spectrosc. Relat. Phenom. **177**, 71, 2010.
13) H. Bluhm, *X-ray Photoelectron Spectroscopy (XPS) for in situ Characterization of Thin Film Growth*, In: "*In situ Characterization of Thin Film Growth*, G. Koster, G. Rijnders (Eds.), Woodhead Publishing Ltd, Cambridge, UK, 2011, pp. 75-98.
14) D.E. Starr, D. Pan, J.T. Newberg, M. Ammann, E.G. Wang, A. Michaelidis, H. Bluhm, *Acetone Adsorption on Ice Investigated by X-ray Spectroscopy and Density Functional Theory*, Phys. Chem. Chem. Phys., **13**, 19988, 2011.
15) J.T. Newberg, D.E. Starr, S. Porsgaard, S. Yamamoto, S. Kaya, E.R. Mysak, T. Kendelewicz, M. Salmeron, G.E. Brown, Jr., A. Nilsson, H. Bluhm, *Auto-catalytic Surface Hydroxylation of MgO(100) Terrace Sites Observed Under Ambient Conditions*, J. Phys. Chem. C, **115**, 12864, 2011.
16) E.R. Mysak, J.D. Smith, J.T. Newberg, P.D. Ashby, K.R. Wilson, H. Bluhm, *Competitive Reaction Pathways for Functionalization and Volatilization in the Heterogeneous Oxidation of Coronene Thin Films by Hydroxyl Radicals and Ozone*, Phys. Chem. Chem. Phys. **13**, 7554, 2011.
17) K.R. Wilson, H. Bluhm, M. Ahmed, *Aerosol Photoemission*, In: "Fundamentals and Applications in Aerosol Spectroscopy," R. Signorell, J.P. Reid (Eds.), CRC Press, Boca Raton, 2011, pp. 367-399.
18) R. C. Moffet, A. V. Tivanski, M. K. Gilles, *Scanning Transmission X-ray Microscopy: Applications in Atmospheric Aerosol Research,* In: "Fundamentals and Applications in Aerosol Spectroscopy", R. Signorell, J.P. Reid (Eds.), CRC Press, Boca Raton, 2011, pps. 420-462.
19) J.T. Newberg, D.E. Starr, S. Porsgaard, S. Yamamoto, S. Kaya, E.R. Mysak, T. Kendelewicz, M. Salmeron, G.E. Brown, Jr., A. Nilsson, H. Bluhm, *Formation of Hydroxyl and Water Layers on MgO Films Studied with Ambient Pressure XPS*, Surf. Sci. **605**, 89, 2011.
20) M. J. K. Moore, H. Furutani, G. C. Roberts, R. C. Moffet, M. K. Gilles, B. Palenik, K. A. Prather, *Effect of Organic Compounds on Cloud Condensation Nuclei (CCN) Activity of Sea Spray Aerosol Produced by Bubble Bursting*, Atmospheric Environment, **45** (39), 7462-7469, 2011. DOI:10.1016/j.atmosenv.2011.04.034
21) Y. Liu, B. Minofar, Y. Desyaterik, E. Dames, Z. Shu, J. P. Cain, R. J. Hopkins, M. K. Gilles, H. Wang, P. Jungwirth, A. Laskin, *Internal Structure, Hygroscopic and Reactive Properties of Mixed Sodium Methanesulfonate - Sodium Chloride Particles*, Phys. Chem. Chem. Phys., **13**, 11846, 2011. DOI:10.1039/C1CP20444K.

Chemical Imaging and Dynamical Studies of Reactivity and Emergent Behavior in Complex Interfacial Systems

Steven J. Sibener
The James Franck Institute and Department of Chemistry; GCIS E-215
The University of Chicago, 929 East 57th St., Chicago, IL 60637
Email: s-sibener@uchicago.edu

Program Scope

This new program is exploring the efficacy of using molecular-level manipulation, imaging and scanning tunneling spectroscopy in conjunction with supersonic molecular beam gas-surface scattering to significantly enhance our understanding of chemical processes occurring on well-characterized interfaces. One program focus is on the spatially-resolved emergent behavior of complex reaction systems as a function of the local geometry and density of adsorbate-substrate systems under reaction conditions. Another focus is on elucidating the emergent electronic and related reactivity characteristics of intentionally constructed single and multicomponent atom- and nanoparticle-based materials. We are also examining emergent chirality and self-organization in adsorbed molecular systems where collective interactions between adsorbates and the supporting interface lead to spatial symmetry breaking. In many of these studies we are combining the advantages of scanning tunneling (STM) and atomic force (AFM) imaging, scanning tunneling local electronic spectroscopy (STS), and reactive supersonic molecular beams to elucidate precise details of interfacial reactivity that have not been observed by more traditional surface science methods. Using these methods, it will be possible to examine, for example, the differential reactivity of molecules adsorbed at different bonding sites in conjunction with how reactivity is modified by the local configuration of nearby adsorbates. At the core of this proposal resides the goal of significantly extending our understanding of interfacial atomic-scale interactions to create, with intent, molecular assemblies and materials with advanced chemical and physical properties. This ambitious program addresses several key topics in DOE Grand Challenge Science, including emergent chemical and physical properties in condensed phase systems, novel uses of chemical imaging, and the development of advanced reactivity concepts in combustion and catalysis including carbon management. These activities directly benefit national science objectives in the areas of chemical energy production and advanced materials development.

Recent Progress and Future Plans

1. Nanoparticle Assembled Clusters and Materials

In this theme we are using local probes to interrogate and intentionally assemble atom and nanoparticle-based clusters to form extended ensembles that exhibit emergent electronic and chemical behavior. Using our first generation cryogenically cooled STM we have assessed the electronic structure of quantum dots (semiconductor nanoparticles), and are presently extending these experiments to include nanoparticle structures adsorbed in different local ensembles. During the current grant period we learned about characterizing isolated clusters of differing size (monomers, dimers, trimers, islands, etc.); manipulation to form specific local ensembles is planned. These studies showed us both the promise and the difficulty involved in imaging nanoparticles with STM, with the difficulty arising from ligand contamination of the STM tip. Over the past year we decided to explore AFM for imaging and have found this route to be successful. The AFM image shown in **Figure 1** demonstrates our ability to examine dots of different size, here 6.5 PbSe mixed with 4.5 nm CdSe. We are focussing on films consisting of (i) differently sized but chemically identical nanoparticles and (ii) identically sized by chemically mixed binarys. (We gratefully acknowledge the synthetic efforts of grad student Sara Rupich and Prof. Dmitri Talapin, who have worked with us to

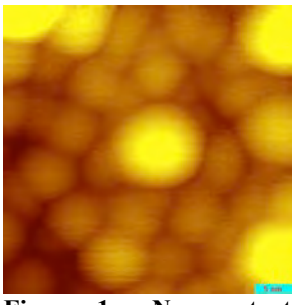

Figure 1. Non-contact AFM image of 6.5 nm PbSe and 4.5 nm CdSe quantum dots drop-casted on HOPG; scan size: 40nm × 40nm.

produce the nanoparticles needed for this project.) A key goal of these studies is to elucidate the local electronic spectra of nanoparticle assembled materials, and to see how variation in nanoparticle cores and ligand structure influence inter-nanoparticle electronic coupling. Going forward (using STS or conductive AFM measurements) we will examine supported nanoparticle arrays to see how these systems function as mesoscale electronic systems and catalysts, and especially how local cluster arrangements influence electronic structure and inter-dot communication.

2. Self Organizing Molecular Films

The Effect of Terminal Phenoxy Endgroups on Molecular Film Self-Organization

Self-assembled monolayers (SAMs) of 11-phenoxy undecanethiol on Au(111) were studied using scanning tunneling microscopy (STM), reflection absorption infrared spectroscopy (RAIRS), ellipsometry, and contact angle measurements before and after annealing in vacuum. The un-annealed phenoxy SAM appeared to be disordered under the STM while RAIRS showed that the SAM has relatively significant organization, indicating there is local disordering of the phenoxy groups at the film surface. After annealing, the SAM formed striped domains with a (5 x √3) rectangular structure with respect to the gold substrate. Molecularly-resolved STM images of the stripes were obtained and we were able to see that each stripe consists of two rows of molecules, **Figure 2**. Based on the results from all of the characterization techniques used here, we determined a structure for the stripes that involve gauche conformations and the phenyl rings interacting in a favorable edge-to-face configuration, **Figure 2c**. The chains within each stripe are close-packed to maximize the chain-chain van der Waals interaction. The molecules are tilted 50° from the surface normal for better van der Waals interaction with the gold substrate to compensate for some of the decreased chain-chain interactions due to the overall lower coverage. Whereas the initial SAM formation is driven by chain-chain interactions, the transition to the stripe phase is driven mainly by phenoxy-phenoxy interactions. These characteristics of the phenoxy SAMs are different from phenyl-terminated SAMs where the film is crystalline in the as-prepared state, and also from pyrrolyl-terminated SAMs where the STM results looked very similar but the results from their other techniques led to a different stripe structure. The importance of using multiple techniques to investigate SAM structures cannot be overemphasized. In sum, this study shows that mild annealing of aromatic SAMs can lead to drastic structural changes, and that aromatic interactions and electrostatic effects play an important role in determining the final structure.

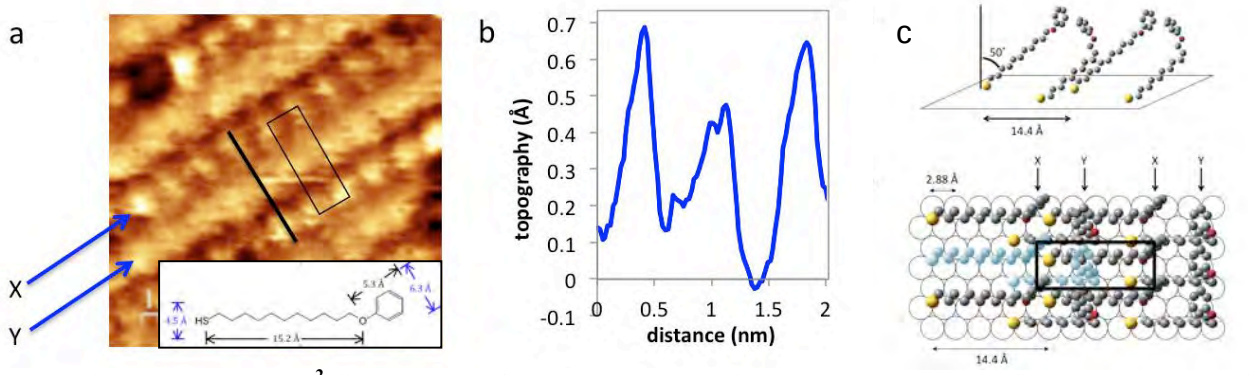

Figure 2. (a) A 5 x 5 nm^2 STM image of the stripe phase of an annealed phenoxy SAM. Two rows of molecules are visible within each stripe – one has clear dot-like features (labeled X) and the other is more decolocalized (labeled Y). The rectangle in the image indicates a unit cell of the (5 x √3) rectangular structure; Inset: molecular model. (b) Line scan over the black line in the STM image showing the height corrugation. (c) Schematics of our proposed structure of the phenoxy stripes.

Self-Organization of Multicomponent Systems

In this investigation C_{60} was solution-deposited onto phenoxy SAMs and studied with UHV-STM and STS; this study built directly on the knowledge we gained in our aforementioned study of phenoxy SAM structure. We observed that in the as-deposited state, the C_{60} was scattered inside the SAM, but when the

samples were annealed in UHV between 350 and 400 K, different C_{60} structures were formed, depending on whether the C_{60} was initially deposited on an un-annealed or an annealed phenoxy SAM, **Figure 3**. On an annealed SAM where the surface consists of a stripe phase, unique (2√3 x 4) rectangular islands were observed. A combination of confined motion at domain boundaries and defect sites and π-π interactions between the phenoxy group and C_{60} are responsible for this structure. On an un-annealed SAM, hexagonally close-packed (2√3 x 2√3)R30° islands and single lines of C_{60} running parallel to the stripes were observed, along with some small (2√3 x 4) rectangular islands. The different structures form as the phenoxy SAM makes a significant structural transformation from a dense phase to a stripe phase during annealing. The C_{60} that were able to segregate from the phenoxy molecules during the initial part of the anneal formed (2√3 x 2√3)R30° islands, while those that got caught in the middle of the stripe forming domain created lines. The ones that ended up stuck in domain boundaries or defect sites after most of the stripes had been formed interacted with phenoxy molecules that got trapped among them and/or with those at the edge of the stripe domains to form (2√3 x 4) rectangular islands. Based on the STM apparent heights, STS data, and the fact that all of the C_{60} structures are commensurate with the Au(111) substrate, we concluded that all of the C_{60} are adsorbed directly onto the gold. This study demonstrated the capability of functionalized alkanethiol SAMs to control the growth and structure of C_{60} islands during annealing depending on the structural changes of the SAM itself; by pre-annealing the SAM, the motion of the C_{60} can be confined and unique structures resulting from interactions between the SAM molecules and C_{60} can be produced. Future work will focus on the ability of functionalized SAMs to template C_{60} structures of interest for charge transfer characteristics in molecular-level systems.

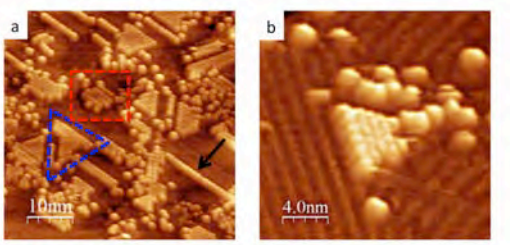

Figure 3. STM images of C_{60} deposited on an as-prepared phenoxy SAM and then annealed in vacuum: (a) 50 x 50 nm^2. The arrow is pointing at an example of a one-dimensional single C_{60} line. The blue triangle is placed around a (2√3 x 2√3)R30° hexagonally close-packed island. The red rectangle is placed around a rectangularly packed island in a pit. (b) A 20 x 20 nm^2 image of a (2√3 x 2√3)R30° island where domains of the phenoxy stripes surrounding it are clearly visible.

Emergent Chirality in Self-Organizing Materials

In this research theme we are examining emergent chirality and self-organization in molecularly adsorbed films. Ever since Pasteur first uncovered the direct correlation between the structure of a crystal and the handedness of its component molecules, researchers have been intrigued by the mechanisms of chiral separation. STM provides the ultimate technique for determination of the exact structure and chirality of adlayers on a substrate. The structure of an adlayer is the result of a delicate balance of lateral molecule-molecule interactions and adsorbate-substrate forces. The strength of the adsorbate-substrate interaction must be balanced such that adsorbed molecules are mobile enough to self-assemble into an organized array but greater than the adsorbate-adsorbate energy to allow two-dimensional crystallization. We are working with metalloporphyrin adlayers on Au(111) as such systems meet these criteria perfectly. They form well-ordered arrays on a variety of surfaces and are highly stable. These porphyrin arrays are especially interesting because they self-assemble at room temperature without the need for annealing, making them a likely candidate for technological applications. Our initial focus has been on NiTPP (nickel-2,3,7,8,12,13,17,18-octaethyl-21H,23H-porphine) and NiOEP (nickel-5,10,15,20-tetraphenyl-21H,23H-porphine) on Au(111). These molecules are achiral when isolated in the gas phase but we find that symmetry is broken when the molecules adsorb onto a surface in small clusters, where they form local chiral ensembles. Such racemic mixtures contain left- and right-handed domains for both porphyrins, indicating that the interplay of surface-adsorbate and intermolecular interactions induces chirality for the substrate-adsorbate system as a whole. We are pursuing not only general rules for the formation of racemic mixtures, but also methods of forcing (guiding) the system to form only one of the two mirror image structures. This might be achieved by the introduction of a "seed" chiral entity or, as shown in our recent publication, by the use of a high index crystal face. Here, we use a locally kinked

step as a symmetry-breaking template to lift the structural equivalence of the right- and left-handed racemic packing structures of NiTPP. In an effort to extend these initial findings to macroscopic dimensions, we have recently fabricated two enantiomorphic "mirror image" bulk chiral gold crystals with extended defects and kinks, Au(1070 1036 1035)^{R} and Au(1070 1036 1035)^{S}, ideally consisting of 14.1 nm wide terraces and straight step segments of 9.8 nm interspersed by single atom kinks. The adsorbate under investigation, NiTPP, has extent of ca. 1.4 nm; the ideal unit cell will therefore incorporate 70 molecules. It is our plan to use these new stepped crystals to guide the self-assembly of a macroscopic homochiral crystal. A surface structure whose chirality can be precisely controlled at the molecular level is immensely attractive to industrial techniques that fabricate enantiospecific reaction products or optically active materials.

3. Reaction Dynamics

This part of our program focuses on emergent chemical reactivity at interfaces. Recent exploratory measurements from our group have examined the partial oxidation of condensed phase arenes and unsaturated hydrocarbons on non-catalytic support substrates, and found substantial changes in the reactive potential energy barriers and the product distributions as compared with isolated molecule energetics. This raises a classic issue in the chemical sciences: how does molecular reactivity evolve when going from the single molecule level to the condensed state? Profound changes in electronic structure and energy relaxation pathways as a function of the local molecular environment lead to such emergent changes in reaction rates and mechanism. In these studies we have seen, for example, markedly different oxidative reaction pathways, activation energies, and product channels for several small hydrocarbons as compared to known gas-phase behavior. These preliminary studies have been done on "thermodynamic ensemble averages", that is, where we have measured reaction rates using molecular beam techniques while varying coverages and temperature without the benefit of local imaging or local electronic spectroscopy. In essence, there remains a remarkably incomplete understanding of molecular reactivity at interfaces as a function of local adsorbate density (coverage), i.e., *local ensemble structure*. We seek to change this situation. We are setting up to use scanning probe methods in conjunction with scattering, to directly correlate reactivity with local adsorbate and substrate geometry, and electronic structure. This will allow us to develop a more comprehensive understanding of emergent molecular reactivity with respect to the precise geometry of locally-adsorbed reactants.

References to Publications

- Mixing Up Surface Properties, Seth B. Darling and S. J. Sibener, *Physics Today*, 62, 88 (2009).
- Chiral Domains Achieved by Surface Adsorption of Achiral Nickel Tetraphenyl- or Octaethylporphyrin on Smooth and Locally Kinked Au(111), Lieve G. Teugels, L. Gaby Avila-Bront, and S.J. Sibener, *J. Phys. Chem. C* 115, 2826-2834 (2011).
- Rough Waters (First Place, AAAS Science/NSF Intl. Science & Engineering Visualization Challenge – Photography Category), Seth B. Darling and Steven J. Sibener, *Science* (Cover Story) 331, 852 (2011).
- Structural Investigations of the (5 x √3) Striped Phase of Annealed 11-Phenoxy Undecanethiol Self-Assembled Monolayers on Au(111), Miki Nakayama, Natalie A. Kautz, Tuo Wang, Hanqiu Yuan, S. J. Sibener, J. Phys. Chem. C 116, 6298-6306 (2012).
- Formation of Rectangular Packing and One-Dimensional Lines of C_{60} on 11-Phenoxy Undecanethiol Self-Assembled Monolayers on Au(111), Miki Nakayama, Natalie A. Kautz, Tuo Wang, Hanqiu Yuan, and S. J. Sibener, Langmuir 28, 4694-4701 (2012).

Water dynamics in heterogeneous and confined environments: Salt solutions, reverse micelles, and lipid multi-bilayers

James L. Skinner
Department of Chemistry
University of Wisconsin
Madison, WI 53706
skinner@chem.wisc.edu

Project Scope

Our goal is to understand the structure and dynamics of water, in its different phases, at the interfaces between these phases, and in confined and heterogeneous environments. To this end, linear and nonlinear vibrational spectroscopy is playing a very important role. We are developing techniques for calculating spectroscopic observables, and then using our results to analyze and interpret experiment.

Recent Progress

A. Bulk water

We have continued our studies of nonlinear vibrational spectroscopy for isotopic mixtures of bulk water, particularly dilute HOD in H_2O. In this system, the OD stretch is an isolated vibrational chromophore, and thus can report cleanly on the structure and dynamics of H_2O. We have calculated 2DIR spectra as a function of temperature, in collaboration with Tokmakoff and coworkers.[10] Together with experiment, our results determine the activation energy for hydrogen-bonding rearrangement dynamics. We have also shown how different levels of theory affect the calculation of anisotropic frequency-resolved pump-probe signals.[3] For neat H_2O, intramolecular and intermolecular vibrational coupling produce modest effects on the linear spectra, but dramatic effects on the anisotropic pump-probe signals.[5] In particular, for neat H_2O vibrational energy transfer causes the anisotropic pump-probe signal to decay 25 times faster than for HOD in H_2O, which is direct and convincing evidence for the importance of intermolecular vibrational coupling in neat H_2O.

B. Ice Ih

As is well known, there are at least 15 thermodynamically stable phases of ice, with ice Ih being the stable phase at one atmosphere pressure between 72 and 273 K. Ice Ih is a most interesting crystal indeed, as the hydrogen nuclei are disordered. We have been interested in using vibrational spectroscopy to assess the nature of this proton disorder. For the HOD/H_2O system, the proton disorder leads to inhomogeneous broadening of the OD spectrum.[4] The vibrational spectroscopy of neat H_2O is very rich, manifesting the competing effects of vibrational coupling and proton and thermal disorder. Our recent

work provides what we believe in the first assignment of the five different peaks in the IR and Raman spectra for single crystal ice Ih.[6]

C. Water liquid/vapor interface

Sum-frequency generation (SFG) spectroscopy has been used for nearly twenty years to probe the structure of the water liquid/vapor interface. Interpretation of experiment has been difficult for two reasons. First, studies on neat H_2O suffer from the effects of intramolecular and intermolecular vibrational coupling, as described above. Second, the sum-frequency intensity has contributions from the real and imaginary parts of the resonant and nonresonant susceptibilities. The first issue is alleviated by considering HOD in H_2O (or D_2O), while recent phase-sensitive detection techniques have allowed for direct measurement of the imaginary part of the resonant susceptibility. Experiments by Tian and Shen show the existence of a positive peak at low OH stretch frequency (for HOD in D_2O), and interpret this peak as arising from ice-like ordering at the liquid surface.

We had previously used the SPC/E simulation model to calculate the imaginary part of the susceptibility, and we did not find this positive low-frequency peak. We began to think that this resulted from a limitation of this and other two-body water simulation models. To this end, we developed a new model with explicit three-body interactions,[12] and used this model to recalculate the imaginary part of the susceptibility, this time finding good agreement with experiment (as shown).[11,13] We find that the positive low-frequency peak arises from cancelling positive and negative contributions from water molecules in different hydrogen-bonding environments, and does not reflect any ice-like ordering at the surface.

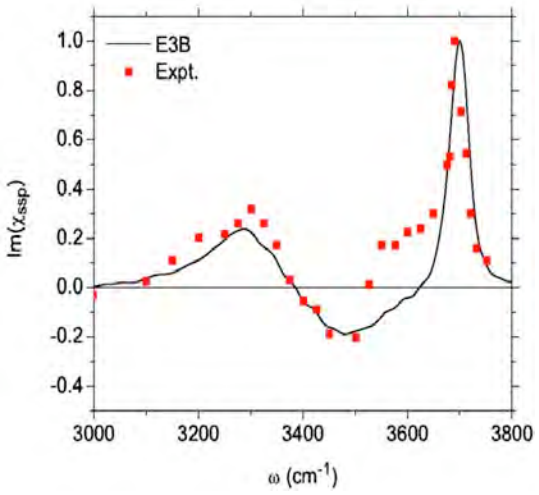

We have also collaborated with Benderskii and coworkers on understanding the peak frequencies of the free OD peak, for HOD in H_2O and for neat D_2O. Experimentally, the peak shifts to the blue by 17 cm^{-1} for the latter. We interpret this as arising from intramolecular coupling. We estimate that the frequency, of the other (hydrogen-bonded) OD group of the D_2O molecule with the free OD, is close to that of bulk water, providing experimental evidence for a very sharp liquid/vapor interface.[9]

D. Salt solutions

It is of great interest to understand how the dynamics of water is perturbed by anions and cations. To this end, we were interested in recent ultrafast spectroscopy experiments performed by Fayer and coworkers on sodium bromide solutions. They found that water

dynamics in 6M solution slows down by a factor of 3 or 4. Our calculations on this system were in reasonable agreement with experiment.[1] Moreover, we found that water structure and dynamics is hardly perturbed outside an ion's first solvation shell. We conclude, in agreement with recent sentiment, that the Hofmeister series reflects only local ordering of water molecules. The situation with divalent ions may be somewhat different.[7]

E. Reverse micelles

AOT reverse micelles provide beautiful model systems for studying nano-confined water. Depending on the ratio of water to surfactant concentrations, reasonably mono-disperse water nano-pools containing between 25 and several hundred thousand molecules can be created. FTIR experiments by Fayer and coworkers on the HOD/H_2O system show a red-shift of the absorption spectrum as micelle size decreases, and pump-probe experiments show a concomitant slow-down of the water rotational dynamics. We can qualitatively reproduce these effects with our models.[2] We interpret the slower rotational dynamics as resulting from "curvature-induced frustration".

F. Lipid multi-bilayers

A related system, for studying water near planar interfaces with headgroups, involves aligned hydrated lipid multi-bilayers. Experiments with DLPC lipids have been performed by Fayer and coworkers. FTIR line shapes now shift to the blue with decreasing hydration, because of stronger hydrogen bonding to lipid phosphate moieties. Rotational dynamics is also slowed down considerably with decreasing hydration level. We have reproduced these effects qualitatively with our models.[14-16] In doing so, we provide for a consistent calculation of all experimental observables within a unified theoretical framework.

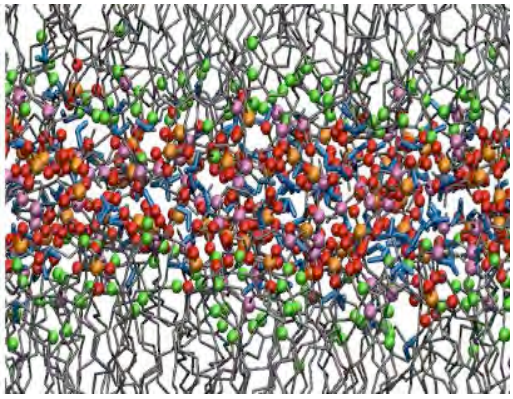

Future Plans

We plan to continue modeling salt solutions, moving on to divalent ions, and hydrated lipid bilayers, but focusing on anisotropy decay and THz spectroscopy. In addition, we plan to expand our scope to several new topics, including 1D and 2DSFG spectroscopy of water near the head-groups of lipid monolayers, and the vibrational spectroscopy of urea/water and other aqueous mixtures.

Selected publications acknowledging DOE support (October 1, 2009 - present)

1. Water structure, dynamics, and vibrational spectroscopy in sodium bromide solutions, Y.-S. Lin, B. M. Auer, and J. L. Skinner, J. Chem. Phys. **131**, 144511 (2009).
2. Vibrational spectroscopy and dynamics of water confined inside reverse micelles, P. A. Pieniazek, Y.-S. Lin, J. Chowdhary, B. M. Ladanyi, and J. L. Skinner, J. Phys. Chem. **113**, 15017 (2009).
3. On the calculation of rotational anisotropy decay, as measured by ultrafast polarization-resolved vibrational pump-probe experiments, Y.-S. Lin, P. A. Pieniazek, M. Yang, and J. L. Skinner, J. Chem. Phys. **132**, 174505 (2010).
4. IR and Raman line shapes for ice Ih. I. Dilute HOD in H_2O and D_2O, F. Li and J. L. Skinner, J. Chem. Phys. **132**, 204505 (2010).
5. Two-dimensional infrared spectroscopy and ultrafast anisotropy decay of water, T. l. C. Jansen, B. M. Auer, M. Yang, and J. L. Skinner, J. Chem. Phys. **132**, 224503 (2010).
6. IR and Raman line shapes for ice Ih. II. H_2O and D_2O, F. Li and J. L. Skinner, J. Chem. Phys. **133**, 244504 (2010); erratum J. Chem. Phys. **134**, 099901 (2011).
7. Following the motions of water molecules in aqueous solutions, J. L. Skinner, Science **328**, 985 (2010).
8. Vibrational energy relaxation of small molecules and ions in liquids, J. L. Skinner, Theor. Chem. Acc. **128**, 147 (2011).
9. Vibrational coupling and hydrogen bonding at the water surface revealed by isotopic dilution spectroscopy, I. V. Stiopkin, C. Weeraman, P. A. Pieniazek, J. L. Skinner, and A. V. Benderskii, Nature **474**, 192 (2011).
10. Collective hydrogen bond reorganization in water studied with temperature-dependent ultrafast infrared spectroscopy, R. A. Nicodemus, S. A. Corcelli, J. L. Skinner, and A. Tokmakoff, J. Phys. Chem. B **115**, 5604 (2011).
11. Surface of liquid water: Three-body interactions and vibrational sum-frequency spectroscopy, P. A. Pieniazek, C. J. Tainter, and J. L. Skinner, J. Am. Chem. Soc. **133**, 10360 (2011).
12. Robust three-body water simulation model, C. J. Tainter, P. A. Pieniazek, Y.-S. Lin, and J. L. Skinner, J. Chem. Phys. **134**, 184501 (2011).
13. Interpretation of the water surface vibrational sum-frequency spectrum, P. A. Pieniazek, C. J. Tainter, and J. L. Skinner, J. Chem. Phys. **135**, 044701 (2011).
14. Vibrational spectroscopy of water in hydrated lipid multi-bilayers. I. FTIR spectra and ultrafast pump-probe observables, S. M Gruenbaum and J. L. Skinner, J. Chem. Phys. **135**, 075101 (2011).
15. Vibrational spectroscopy of water in hydrated lipid multi-bilayers. II. 2DIR and peak-shift observables within different theoretical approximations, S. M Gruenbaum, P. A. Pieniazak, and J. L. Skinner, J. Chem. Phys. **135**, 164506 (2011).
16. Vibrational spectroscopy of water at interfaces, J. L. Skinner, P.A. Pieniazek, and S. M. Gruenbaum, Accounts of Chemical Research **45**, 93 (2012).

Generation, Detection and Characterization of Gas-Phase Transition Metal Containing Molecules (DE-FG02-04ER15603)

Timothy C. Steimle
Department of Chemistry and Biochemistry
Arizona State University
Tempe, Arizona 85287-1604
E-mail: tsteimle@asu.edu

I. Program Scope

Gas-phase transition metal containing molecules serve as ideal venues for testing computational methodologies being developed to predict chemical properties of more extended metal-containing catalysis because the properties of these simple molecules can be precisely derived from high-resolution spectroscopic measurements. The focus of this project is to determine geometric and electronic structure for both ground and low-lying excited states of these molecules from the analysis of high resolution electronic spectra. The determined properties include electronic state energies, bond lengths and angles, vibrational frequencies, permanent electric dipole moments, $\vec{\mu}_{el}$, magnetic dipole moments, $\vec{\mu}_m$, magnetic hyperfine interactions and radiative lifetimes. The $\vec{\mu}_{el}$ and $\vec{\mu}_m$ values are derived from the analysis of the spectral shifts and splittings induced by the application of either an external static electric (i.e. Stark effect) or magnetic (i.e. Zeeman effect) field. $\vec{\mu}_{el}$ gives insight into the polarity of the chemical bonds and $\vec{\mu}_m$ into the number of unpaired electrons. A knowledge of $\vec{\mu}_{el}$ and $\vec{\mu}_m$ is essential for developing schemes for kinetic energy manipulation (i.e. trapping) and enters into the description of numerous physical phenomena. The spatial distribution and nature of the chemically relevant valence electrons is garnered from analysis of the magnetic hyperfine interactions. The established synergism between experiments and theory for these simple molecules guides computations, particularly those based on density functional theory, for more extended chemical systems (e.g. clusters, nanoparticles and surfaces).

II. Recent progress

A. Platinum containing molecules: PtF and PtC

1. Microwave study of PtC (Publ.#9)

A high-level *ab initio* calculation performed by Minaev et al [PCCP **2**(2000) 2851] suggested that our previously assigned $A''^{1}\Sigma^{+}$ ($T_e \cong$ 13,200 cm^{-1}) and $A'^{1}\Pi$ ($T_e \cong$ 12,643 cm^{-1}) states of PtC were actually the $\Omega = 0^+$ and 1 components of a $^{3}\Pi$ state. Here we have used the analysis of the nuclear spin-rotation interaction parameter, C_I^{elec}, for the $X^{1}\Sigma^{+}$ state to probe the electronic state distribution. C_I^{elec} is given by 2nd order perturbation theory as:

$$C_I^{elec} = 4B\sum_n \frac{a_{0n}\left\langle X^{1}\Sigma^{+}\left|\hat{\mathrm{L}}_x\right|n\right\rangle^2}{E_n - E_0}. \qquad (1)$$

In Eq. 1 $a_{0n} = \left(\frac{\mu_0}{4\pi h}\right)\left(2g_I\mu_N\mu_B\right)\times\left\langle 0\left|r^{-3}\right|n\right\rangle$ with r being the position of the valence electrons relative to the nuclei with non-zero spin, $\hat{\mathrm{L}}_x$ is the component of the total electronic orbital angular momentum operator. It is evident form Eq. 1 that the location and nature of electronic states, $|n\rangle$, relative to the $X^{1}\Sigma^{+}$ state can be derived from an analysis of the C_I^{elec}. A molecular beam pump/probe microwave optical double resonance (PPMODR) technique was used to record the pure-rotational spectrum of the ^{194}Pt^{12}C, ^{195}Pt^{12}C and ^{196}Pt^{12}C isotopologues (Figure 1).
The determined C_I^{eff} (= 138(12) kHz) supports the re-assignment.

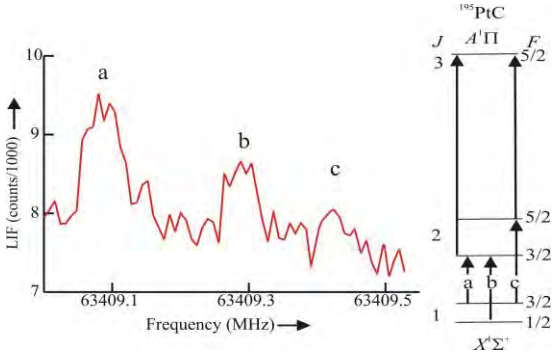

Figure 1. The pure rotational spectrum of $^{195}Pt^{12}C$ ($X\,^1\Sigma^+$,v=0) recorded using the PPMODR technique and associated energy levels. The rotational transitions in the $X\,^1\Sigma^+$ state("a-c") are detected as an increase in the laser induced fluorescence (LIF) signal of the $R(2)$ line of $A\,^1\Pi \leftarrow X\,^1\Sigma^+$ (0,0) band near 540 nm. The small splittings in the $X\,^1\Sigma^+$ state are due to the nuclear spin-rotation interaction.

2. Optical Stark study of PtF (Accepted JCP)

We have determined $\vec{\mu}_{el}$ and the ^{19}F(I=1/2) and ^{195}Pt(I=1/2) magnetic hyperfine interactions in the [11.9]Ω=3/2 and $X\,^2\Pi_{3/2}$ states of PtF. PtF has been the subject of two electronic structure predictions; Liu and Franke [J. Comp. Chem. **23**, 564 (2002)] and Zou, Liu and J.E. Boggs, [Dalton Trans., **39**, 2023 (2010)]. Both calculations predict that when spin-orbit coupling is taken into account the $^2\Pi_i$, $^2\Delta_i$, and $^2\Sigma^+$ states expected for a $Pt^+(5d^9)F^-(2p^6)$ configuration regroup into two sets of states separated by approximately 10,000 cm^{-1}: a low energy group having $|\Omega| = \frac{5}{2}$, $\frac{3}{2}$, and $\frac{1}{2}$ arising from the $d^4_{3/2}d^5_{5/2}\sigma^2_{1/2}$ superconfiguration and the high energy $|\Omega| = \frac{3}{2}$ and $\frac{1}{2}$ set from the $d^3_{3/2}d^6_{5/2}\sigma^2_{1/2}$ superconfiguration. The two theoretical predictions are inconsistent the observed hyperfine interaction (**Figure 2**)

Electric dipole moments of 2.47(11)D and 3.42(6)D for the [11.9]Ω=3/2 and $X\,^2\Pi_{3/2}$ states, respectively, were determined. The observed trend in $\vec{\mu}_{el}$ for the PtX (X= C,N,O,S and F) series strongly correlates with electronegativities (**Figure 3**) .

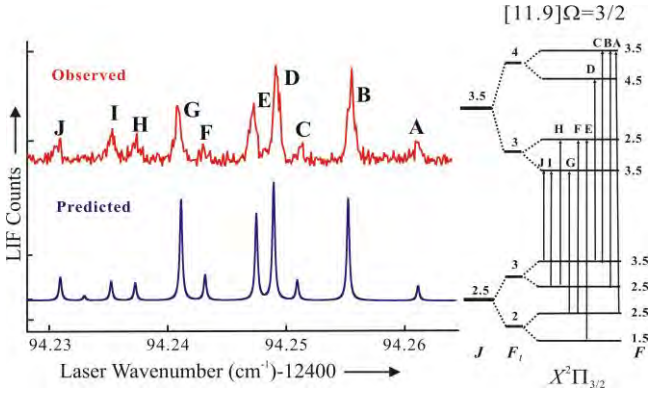

Figure 2. The observed and predicted spectra for the $R(2.5)$ (v=11933.4 cm^{-1}) branch feature of the for the Ω=3/2 ← $X^2\Pi_{3/2}$ (1,0) band of ^{195}PtF. The splitting is due to ^{195}Pt(I=1/2) and ^{19}F(I=1/2) hyperfine interaction. The determined hyperfine parameters $h_{3/2}(^{195}Pt)$(=706 MHz) and $h_{3/2}(^{195}Pt)$(=304MHz) are inconsistent with current theoretical prediction of 1820 MHz and 0 MHz.

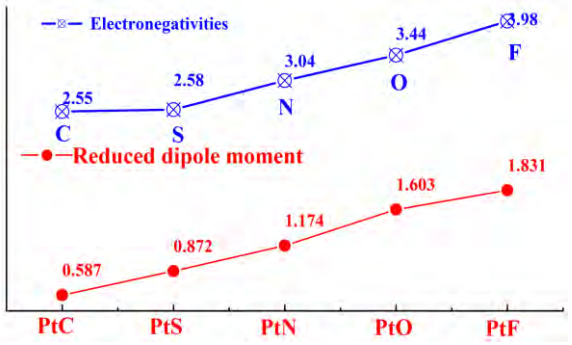

Figure 3. A comparison of the ground electronic state reduced dipole moment ($\equiv\mu_{el}/r$) for various Pt-containing molecules and the Pauling electronegativities. PtF is the most recent of the series we have investigated in DoE sponsored research. Although the qualitative agreement with simple concepts (e.g. electronegativities) is satisfying, the quantitative agreement with current theoretical predictions is generally poor.

B. Gold containing molecules: AuF

There are more than 20 reported electronic structure predictions for the ground state of gas-phase AuF, but only limited experimental information. We determined $\vec{\mu}_{el}$ of 4.148 (23)D and 2.210(60)D for the $X^1\Sigma^+$ (v=0) and [17.8] 0^+(v=0) states, respectively.

Table 1. $\vec{\mu}_{el}$ **for AuF ($X^1\Sigma^+$)**

Ref.	$\vec{\mu}_{el}$ (Debye)	Method
1	**4.148(23)**	**Exp. -Opt. Stark**
2	3.96	DFT-PBE
2	3.94	DFT-vdW
3	5.299	SC-NRPP-S
3	4.046	SC-SRPP-S
3	3.939	SC-SRPP-LANL
3	4.872	LC-SRPP-LANL
4	3.44	DFT-LDA
4	3.91	DFT- B3LYP
4	4.24	DFT-CAM/B3LYP

1) Present
2) E. M. Fernandez and L. C. Balba, *PCCP*, 2011, **13**, 20863.
3)P. Schwerdtfeger, et al, *JCP*, 2011, **134**, 204102.
4) E. Goll et al. *Phys. Rev. A,* 2007, **76**, 032507/1.

A comparison $\vec{\mu}_{el}$ for AuF ($X^1\Sigma^+$) with recent selected theoretical predictions is given in **Table 1**. Fernandez and Balba tested three non-local van der Waals (vdW) density functionals and compared them to gradient approximation functional PBE. Both methods underestimate $\vec{\mu}_{el}$. Schwerdtfeger et al tested numerous pseudo potentials (PP), functionals. The "small core-scalar relativistic pseudo potentials-Stuttgart (SC-SRPP-S) appears to performs best. The results of Goll et al demonstrate that the DFT-B3LYP and DFT-CAM/B3LYP give comparable level of agreement to our observation.

C. Iridium containing molecules: IrSi

Iridium, one of the rarest transition metal elements in the earth's crust, is a key component of automobile catalytic converters. We have recorded and analyzed the field-free and Stark spectra of the [17.4]7/2 ← $X^2\Delta_{5/2}$ (4,0) band. This is part of our effort of investigating the trends in the series of IrX (X=C,N,O, F, H, and Si). Electric dipole moments, bond lengths and hyperfine structure for this entire series has now been determined in our laboratory. We are currently collaborating with John Stanton (U. Texas-Austin) on the theoretical predictions for this series. The IrSi study is being performed in collaboration with Prof. Micheal Morse (U.Utah) who has recorded the REMPI spectra of numerous bands in the visible region.

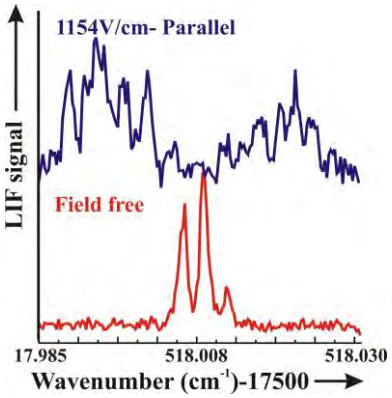

Figure 4. The $Q(3.5)$ line of the [17.4]7/2 ← $X^2\Delta_{5/2}$ (4,0) band near 18520 cm^{-1} of ^{193}IrSi recorded field free (bottom) and in the presence of a static 1154 V/cm electric field. The small splitting in the field-free spectrum is due to ^{193}Ir(I=3/2) magnetic hyperfine interactions. Interestingly, the interaction for the $X^2\Delta_{5/2}$ (v=0) state of IrSi is approximately a factor of 2 smaller than that for the $X^2\Delta_{5/2}$ (v=0) state of isovalent IrC [*J. Chem. Phys.* **104**, 8183 (1996). Analysis of the complex Stark spectrum is in progress

III. Future Plans

A. Metal dioxides/mass-resolved REMPI

We will expand our studies of transition metal dioxide, which to date have included TiO_2 (Publ. #1 and 6) and isovalent ZrO_2 (Publ. # 8). Little is known about other TM dioxides. The experimental photoelectron studies Prof. Lai-Sheng Wang (Brown University and Pacific Northwest Laboratories) of ScO_2, VO_2 ,CrO_2, MnO_2, FeO_2, NiO_2 and CuO_2 anions demonstrate that such species are chemically stable. A systematic search for these species will be performed using our newly constructed MS-REMPI spectrometer under construction. An analysis of the observed rotational fine structure will be used to confirm the assignment.

B. Iridium, gold and platinum molecules

We will continue our search for new Ir, Au and Pt containing molecules using laser induced fluorescence. A new pulsed dye laser system operating in the red spectral region has been installed and will be used for survey scans.

Publications of DOE sponsored research - 2009-present:

1. "Characterization of the $X^1A_1 - A^1B_2$ electronic state of titanium dioxide, TiO_2" H. Wang, T. C. Steimle, C. Apetrei and J. P. Maier, Phys. Chem. Chem. Phys. **11** 2649-2656 (2009).
2. "The Permanent Electric Dipole Moments and Magnetic g_e-Factors of PrO" H. Wang, C. Linton T. Ma, and T.C. Steimle, JCPA (2009), **113**13372-13378.
3. "Permanent Electric Dipole Moment of Cerium Monoxide." Colan Linton, Jinhai Chen Timothy C. Steimle Journal of Physical Chemistry A (2009), 113(47) 13379-13382.
4. "The permanent electric dipole moment of vanadium monosulfide" Xiujuan Zhuang and Timothy C. Steimle Journal of Chemical Physics (2010), 132(23), 234304/1-234304.
5. "Permanent electric dipole moment of copper monoxide, CuO" Xiujuan Zhuang, Sarah E. Frey and Timothy C. Steimle, Journal of Chemical Physics (2010), 132(23), 234312/1-234312/6.
6. "Visible Spectrum of Titanium Dioxide" Xiujuan Zhuang, Anh Le, Timothy C. Steimle Ramya Nagarajan, V. Gupta and J. P. Maier Phys. Chem. Chem. Phys. (2010), 12(45), 15018-15028.
7. "The permanent electric dipole moment in iridium monofluoride " X. Zhuang Colan Linton and T.C. Steimle J. Chem. Phys. (2010), 133(16), 164310/1-164310/6
8. " The visible spectrum of zirconium dioxide, ZrO_2", Anh Le, Timothy C. Steimle, Varun Gupta, Corey A. Rice, John P. Maier, Sheng H. Lin, and Chih-Kai Lin, J. Chem. Phys. (2011)) **135** 104303.
9. "The Pure Rotational Spectrum of Platinum Monocarbide, PtC" Chengbing Qin, Ruohan Zhang, Fang Wang and Timothy C. Steimle, Chem. Phys. Lett. 535,40 (2012).
10. "Optical Stark Spectroscopy of the 2_0^6 $\widetilde{A}^1A'' - \widetilde{X}^1A'$ Band of Chloro-Methylene, HCCl", T.C. Steimle, F. Wang, X. Zhuang and Z. Wang J. Chem. Phys. **136**, 114309 (2012) .

A Single-Molecule Approach for Understanding and Utilizing Surface and Subsurface Adsorption to Control Chemical Reactivity and Selectivity

E. Charles H. Sykes (charles.sykes@tufts.edu)
Department of Chemistry, Tufts University, 62 Talbot Ave, Medford, MA 02155

The second year research program has been focused on understanding the ability of single palladium atoms in and under the surface of industrially important alloys to promote hydrogenation reactions and using novel surface supported cobalt nanoparticles to understand cobalt's surface and subsurface chemistry [1-5]. Well-defined Pd, Co, Au and Cu systems are designed to be amenable to high resolution scanning probe studies, X-ray photoelectron spectroscopy, and chemical analysis of adsorbate binding, diffusion and reaction. In this way we can relate the atomic scale structure of these catalytically important systems to their electronic properties and surface chemistry. In terms of equipment, a state of the art temperature programmed reaction system built in year one is enabling us to relate the activity and selectivity of hydrogenation reactions on these model systems to their atomic scale structure.

Single Atom Alloys as a Strategy for Selective Heterogeneous Hydrogenations

Hydrogenation reactions are central to the petrochemical, fine chemical, pharmaceutical, and food industries and are of increasing interest in energy production and storage technologies. Typical heterogeneous catalysts often involve noble metals and alloys based on platinum, palladium, rhodium and ruthenium. While these metals are active at modest temperature and pressure, they are not always completely selective and are expensive. Facile dissociation of reactants and weak binding of intermediates are key requirements for efficient and selective catalysis. However, these two variables are intimately linked in a way that does not generally allow the optimization of both properties simultaneously.

We are interested in how the reactivity of a catalytically active metal is altered when it is atomically dispersed in a more inert host metal. In a series of low temperature scanning tunneling microscopy (LT STM), temperature programmed desorption/reaction (TPD/R) studies, we have investigated the formation of a class of bimetallic alloy systems, which we term single atom alloys, and their interaction with hydrogen (**Figure 1**). Two key characteristics of single atom alloys are: (i) one of the two components (in our case Pd) is present in the surface of the host metal at very low concentrations (0.01 monolayers) and (ii) the Pd atoms are thermodynamically more stable when surrounded by atoms of the host surface (i.e. no Pd dimers or trimers are present). Using desorption measurements we demonstrate that single atom alloys can act as very selective hydrogenation model catalysts. The mode of action involves the facile dissociation of hydrogen on individual Pd atoms and subsequent spillover of H atoms onto the Cu(111) surface. The selective hydrogenation of alkenes and alkynes takes place on the bare Cu(111) surface where the H atoms are weakly bound [1].

In marked contrast to the selective hydrogenation chemistry on single atom alloys, the hydrogenation of styrene and acetylene on 1 monolayer Pd/Cu(111) was found to be accompanied by an extensive decomposition of both molecular species and dramatically lower hydrogenation selectivities (**Figure 2**). Our results demonstrate that individual, isolated noble metal atoms can substantially influence the catalytic properties of less reactive metals, to the extent of converting an entirely inactive surface to an effective catalyst [1,7].

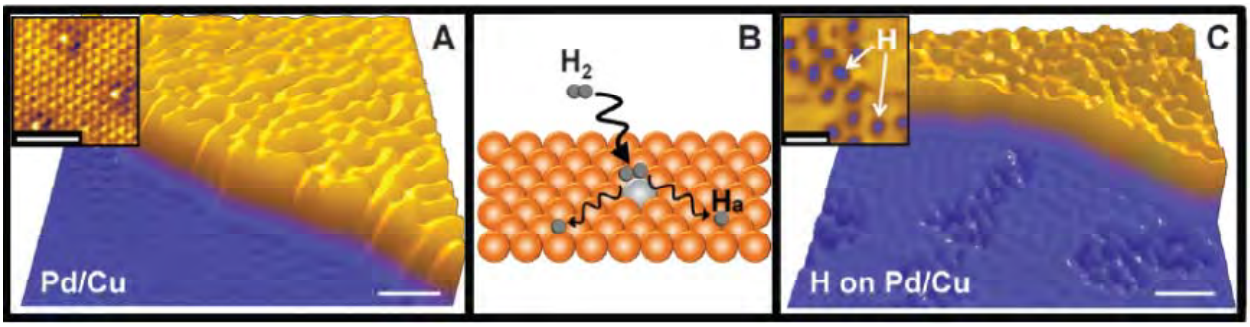

Figure 1. *STM images showing atomically dispersed Pd atoms in a Cu(111) surface and hydrogen atoms that have dissociated and spilled over onto the Cu surface. (A) Pd alloys into the Cu(111) surface preferentially above the step edges as evidenced by the rumpled appearance of the upper terrace (scale bar indicates 5 nm). (Inset) Atomic resolution of the Pd/Cu alloy on the upper terrace showing individual, isolated Pd atoms in the surface layer appearing as protrusions (scale bar, 2 nm). (B) Schematic showing H_2 dissociation and spillover at individual, isolated Pd atom sites in the Cu surface layer. (C) Islands of H atoms imaged after hydrogen uptake appear as depressed regions on the clean Cu(111) lower terrace (scale bar, 5 nm). (Inset) High-resolution image of individual hydrogen atoms on Cu(111) (scale bar, 2 nm). Images recorded at 5 K.*

From a practical application standpoint, the small amounts of precious metal required to produce single atom alloys generate a very attractive alternative to traditional bimetallic catalysts. While we have used a surface science approach to directly visualize the atomic-scale structure of the active sites and relate this information to hydrogenation reactivity/selectivity, we pose a challenge to the catalysis community to synthesize metal nanoparticles with trace amounts of an active element in order to generate single atom alloy surfaces capable of similar efficient and selective hydrogenation chemistry. We are currently expanding this approach to study the hydrogenation of saturated and unsaturated aldehydes and ketones in an effort to uncover how reaction with weakly bound hydrogen affects reaction selectivity in these systems. In a related line of work we are interested in how reversible adsorption of a spectator molecule at the atomic Pd sites can be used to control the hydrogen spillover pathway. This work will have interesting consequences for chemical reactions if hydrogen can be trapped on the Cu surface above its normal desorption temperature in a "superheated" form and may offer a new chemical method to enhancing hydrogen storage in systems with spillover via a non-equilibrium effect we term a "molecular cork" effect.

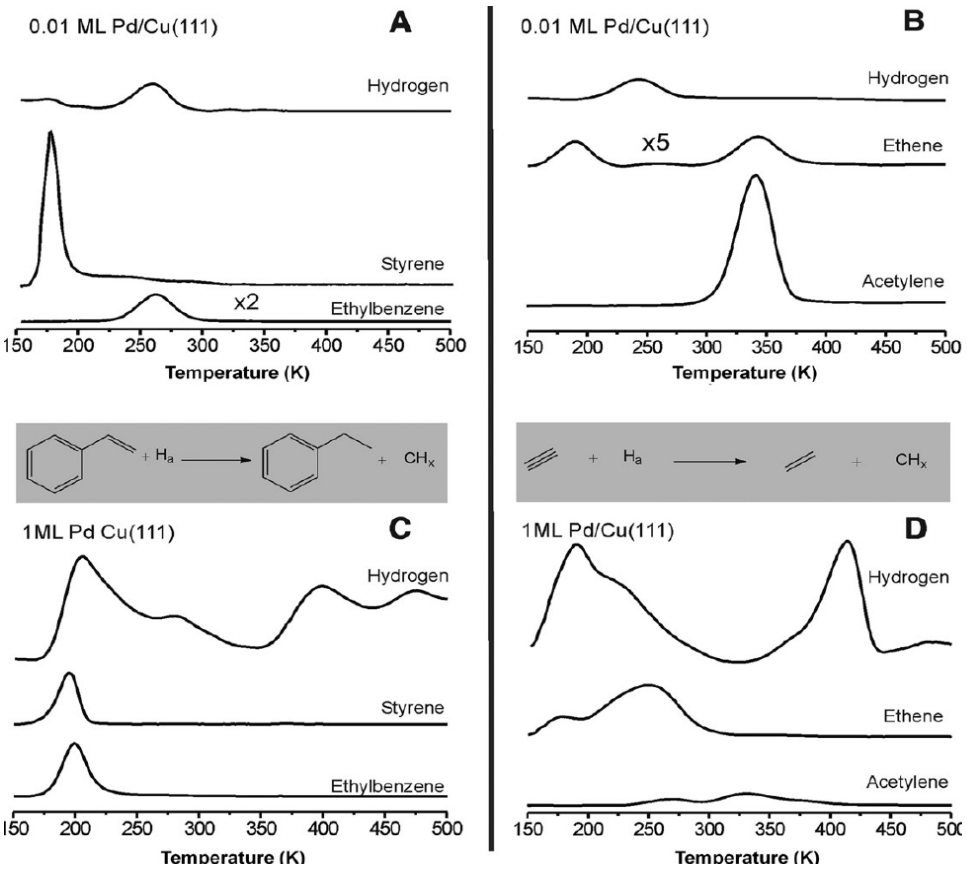

Figure 2. *Representative TPR data showing the increase in selectivity obtained by atomically dispersing Pd atoms in Cu vs. the extensive decomposition of the reactants on a 1 ML Pd layer. In all cases near saturation H_a was deposited at 85 K followed by 0.5 ML of the hydrocarbon at 150 K.*

Towards a Molecular Level Understanding of Fischer-Tropsch Synthesis on Cobalt Nanoparticles

Cobalt is an active metal for a variety of commercially and environmentally significant heterogeneously catalysed processes not least Fischer-Tropsch Synthesis. Despite its importance, Co's surface chemistry is less studied compared to other key industrial catalyst metals. This stems in part from the difficulties associated with single crystal preparation and stability. Recent advances in scanning probe microscopy have enabled the atomic scale study of the structural, electronic, and magnetic properties of well-defined Co nanoparticles on metal substrates. The physics of this system has been fairly well characterized to date, but its surface chemistry has scarcely been explored. Such systems offer an excellent platform to investigate the adsorption, diffusion, dissociation, and reaction of catalytically relevant molecules [2].

Fischer-Tropsch synthesis involves the formation of hydrocarbons via the catalytic conversion of syngas (carbon monoxide and hydrogen), which can be derived from biomass, and is itself a renewable energy resource. We have utilized a new method for preparing model cobalt catalysts

by depositing cobalt onto copper single crystals (an inert metal for FTS), yielding well-defined cobalt nanoparticles. Low-temperature scanning tunneling microscopy (LT-STM) enables us to study the interaction of syngas with well-defined cobalt nanoparticles controllably grown onto copper {111}, an inert metal for FTS. Hydrogen adsorbs dissociatively on the cobalt surfaces, and we have observed 3 unique coverage-dependent phases. We demonstrate that these phases can resolve crystal packing ambiguities of the underlying cobalt nanoparticles, a question that has been debated in the literature. Simultaneous exposure of the cobalt to H_2 and CO results in segregated islands of the adsorbates on the nanoparticle surface at 80 K, and we propose that atomic H blocks CO adsorption, causing the build-up of CO at the nanoparticle step edges. With increasing CO coverage, a two-dimensional phase compression of H by CO by spillover is observed, providing *the first direct* visualization of this long proposed phenomenon in a catalytically relevant system (**Figure 3**). Finally, our data suggest that FTS reactivity must be dominated by the available interface length between the two adsorbates, and thus, be subject to unforeseen kinetic restraints as a function of particle size. We have just submitted a joint paper on the subject in collaboration with the Talat Rahman Group who performed the theory work [6].

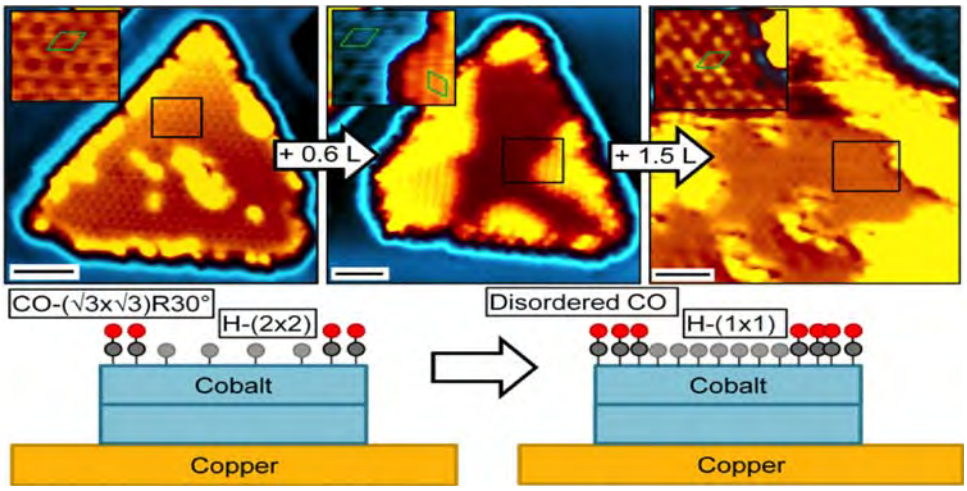

Figure 3. *Compression of H 2x2 overlayer on catalytic cobalt nanoparticle to a 1x1 induced by spillover of CO from the copper support.*

References:

1) "Isolated Metal Atom Geometries as a Strategy for Selective Heterogeneous Hydrogenations" - G. Kyriakou, M. B. Boucher, A. D. Jewell, E. A. Lewis, T. J. Lawton, A. E. Baber, H. L. Tierney, M. Flytzani-Stephanopoulos and E. C. H. Sykes - *Science*, **2012**, *335*, 1209-1212
2) Rediscovering Cobalt's Surface Chemistry" E. A. Lewis, A. D. Jewell, G. Kyriakou, E. C. H. Sykes - *Physical Chemistry Chemical Physics*, **2012**, *14*, 7215-7224
3) Molecular-Scale Surface Chemistry of a Common Metal Nanoparticle Capping Agent: Triphenylphosphine on Au(111)" - A. D. Jewell, E. C.H. Sykes and G. Kyriakou - *ACS Nano*, **2012**, *6*, 3545-3552
4) "Asymmetric Thioethers as Building Blocks for Chiral Monolayers" A. D. Jewell, H. L. Tierney, O. Zenasni, T. R. Lee and E. C. H. Sykes - *Topics in Catalysis* **2011**, *54*, 1357-1367
5) "An Atomic-scale View of Palladium Alloys and their Ability to Dissociate Molecular Hydrogen" A. E. Baber, H. L. Tierney, T. J. Lawton and E. C. H. Sykes - *ChemCatChem* **2011**, *3*, 607-614
6) "Visualization of Spillover-Induced Two-Dimensional Compression of Hydrogen by Carbon Monoxide" E. A. Lewis, D. Le, A. D. Jewell, C. J. Murphy, T Rahman and E. C. H. Sykes - *Submitted*

Understanding Nanoscale Confinement Effects in Solvent-Driven Chemical Reactions

Ward H. Thompson
Department of Chemistry, University of Kansas, Lawrence, KS 66045
Email: *wthompson@ku.edu*

Program Scope

It is now possible to synthesize nanostructured porous materials with a tremendous variety of properties, including sol-gels, zeolites, organic and inorganic supramolecular assemblies, reverse micelles, vesicles, and even proteins. The interest in these materials derives from their potential for carrying out useful chemistry (*e.g.*, as microporous and mesoporous catalysts with critical specificity, fuel cell electrodes and membranes, molecular sieves, and chemical sensors) and for understanding the chemistry in similar systems found in nature. Despite the advances in synthetic techniques, our understanding of chemistry in solvents confined in nanoscale cavities and pores is still relatively limited. Ultimately, one would like to design nanostructured materials adapted for specific chemical purposes, *e.g.*, catalysis or sensing, by controlling the cavity/pore size, geometry, and surface chemistry. To develop guidelines for this design, we must first understand how the characteristics of the confining framework affect the chemistry. Thus, the overarching question addressed by our work is *How does a chemical reaction occur differently in a nano-confined solvent than in a bulk solvent?*

Solvent-driven reactions, typically those involving charge transfer, should be most affected by confinement of the solvent. The limited number of solvent molecules, geometric constraints of the nanoscale confinement, and solvent-wall interactions can have dramatic effects on both the reaction energetics and dynamics. Our primary focus is thus on proton transfer, time-dependent fluorescence (TDF), and other processes strongly influenced by the solvent. A fundamental understanding of such solvent-driven processes in nano-confined solvents will impact many areas of chemistry and biology. The diversity among nanoscale cavities and pores (*e.g.*, in their size, shape, flexibility, and interactions with the solvent and/or reactants) makes it difficult to translate studies of one system into predictions for another.[3] Thus, we are focusing on developing a unified understanding of chemical dynamics in the diverse set of confinement frameworks, including nanoscale silica pores of varying surface chemistry.

Recent Progress & Future Plans

Reorientational Dynamics of Nanoconfined Hydrogen-bonded Liquids.

Reorientational motion of the solvent molecules is a key component in a wide variety of chemical processes, including solvation dynamics and proton transfer reactions. Thus, it is important to understand how liquid molecules rotate when confined within nanoscale frameworks. We have examined this question by examining the reorientational dynamics of water, methanol, and ethanol in identical model silica pores. In this work, we have collaborated with Damien Laage, École Normale Supérieure in Paris. Using the equilibrium densities obtained from grand canonical Monte

Carlo calculations, we have carried out molecular dynamics simulations for these three liquids in nanoscale silica pores of diameter $\sim$ 2.4 nm and varying surface chemistry (hydrophilic and hydrophobic). The results are generally expressed in terms of a reorientational correlation function, $C_2(t) = \langle P_2[\mathbf{e}(0)\cdot\mathbf{e}(t)]\rangle$ with $\mathbf{e}$ the OH unit vector, which provides a measure of the rotational times of the OH bonds in the liquid. A particularly interesting result for these systems is that the long-time decay of $C_2(t)$ for water confined in hydrophilic pores, Fig. 1, appears to follow a power law, *i.e.*, $C_2(t) \sim (t/\tau)^{\alpha}$. This is related to the hydrophilic surface chemistry since when the pore charges are "turned off" to yield an effectively hydrophobic pore, this long-time decay vanishes. In methanol and ethanol, the long-time decay appears to also exhibit a power-law decay, a feature that does *not* disappear when the pore charges are turned off. These results point to the differences in the fundamental reorientational dynamics of water and alcohols, suggesting that the methyl groups in the alcohols introduce steric effects that can alter the qualitative nature of the reorientation. We are continuing to examine these steric factors as well

This idea has led us to consider the origin of the differences in OH bond reorientational times in bulk liquid water and alcohols. Generally for linear alcohols, reorientation is slower the longer the alkyl chain. We have found that the extended jump mechanism developed for water, which predicts that the OH reorientation is governed by the switching of hydrogen-bonding partners and reorientation of intact hydrogen bonds, also describes reorientation in alcohols.[5] However, in alcohols the hydrocarbon moiety blocks the approach of potential new hydrogen-bond acceptors, significantly slowing down hydrogen-bond exchanges (or jumps). This excluded volume effect naturally increases with the size of the alkyl group. It does so to such a large degree for methanol and ethanol that the intact hydrogen bond reorientation becomes the dominant component compared to the contribution due to the hydrogen-bond jumps;[5] the opposite is the case for water where the jump contribution dominates over the intact hydrogen bond reorientation. We are further exploring the effect of alkyl chain size and configuration in higher alcohols on the OH reorientation and associated spectroscopic signatures. Preliminary results indicate the chain-length dependence of the mechanism is not straightforward.

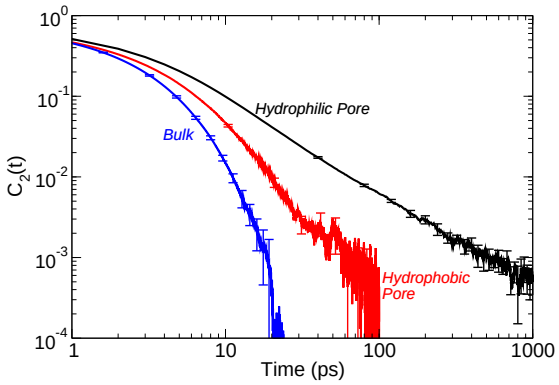

Figure 1: Reorientational correlation function, $C_2(t)$, for water in the bulk liquid (blue) and confined in hydrophilic (black) and hydrophobic (red) pores.

Solvation Dynamics in Nanoconfined Solvents.

Solvation dynamics in nanoconfined solvents are generally marked by dramatic changes relative to the corresponding bulk solvent. In particular, long time scales not seen in the bulk solvent – often as long as hundreds of picoseconds or several nanoseconds – are observed in the time-dependent fluorescence signal. A number of models have been proposed to explain the origin of this multi-exponential, long-time decay. However, clear comparisons of theoretical predictions with experimental measurements is lacking as is, by extension, a rigorous test of the models.[3] To address this, we have developed a number of models for both the dye molecule and the confining

framework to allow for more general exploration of the phenomena and driving forces involved in TDF experiments, and chemistry in general, in nanocc

We have calculated the free energy for a Stockmayer-type solute as a function of position in atomistic silica pores, using different solute dipole moments;[8] see Fig. 2. We found that the electrostatic interactions with the pore interface led to a dependence of the solute position distribution on the solute dipole. Moreover, in hydrophilic silica pores the fluorescence spectrum depends on the solute position. These results indicate that solute diffusion may contribute to the TDF signal and, more generally, that it will be a component of the mechanism for a number of chemical processes in nano confined solvents. The fact that this effect originates with the solute-pore interactions further suggests that the confining framework can be tuned to affect the chemistry of the confined liquid. Ongoing work includes comparing solvation dynamics in nanoconfined solvents with those at planar silica surfaces to separate interfacial and confinement effects and make better connections with experimental measurements. We are also exploring how the TDF response depends on the dye molecule properties and how this might be exploited to elucidate the solvation mechanism through multiple measurements with different dyes.

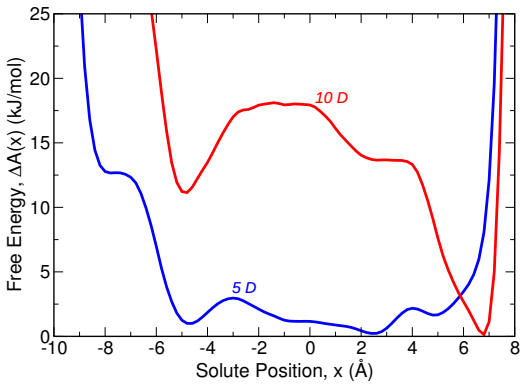

Figure 2: Free energy, $\Delta A(x)$, as a function of solute position along a slice across an ethanol-filled hydrophilic silica pore for a 5 D (blue) and 10 D (red) Stockmayer-type solute.

We have also examined the accuracy of linear-response and Gaussian statistics approximations for describing solvation dynamics generally and in nanoconfined solvents.[4] We have found that the dynamical linear-response approximation fails to describe the TDF signal in model nanoconfined solvent systems, while the assumption of Gaussian statistics gives quite accurate results.[4] We further investigated the differences between the static linear-response and Gaussian statistics approximations and found that the latter is the natural interpretation of excited-state equilibrium correlation functions. Finally, we showed how the Gaussian statistics approximation provides ways to test its accuracy based solely on equilibrium correlation functions. We are examining linear response approximations in more complex nanoconfined solvent systems, *e.g.*, silica pores, as well as testing the Gaussian statistics approximation and related insights for traditional models that exhibit linear-response violations.

Proton Transfer (PT).

We have been continuing our work on proton transfer reactions in nanoconfined solvents[2,3,6] by investigating approaches to more generally sample the reaction coordinate, both to identify transition state configurations and simulate infrared spectra.[6] Specifically, we have used an umbrella sampling approach based on the proton vibrational energy gap. This exploits the fact that for a PT reaction the energy gap between the vibrational ground and excited states of the transferring proton reaches a minimum at the transition state. We have implemented this umbrella sampling within mixed quantum-classical simulations to identify the transition state configurations and explore the reaction free energy curve and vibrationally nonadiabatic coupling. We have tested this

approach on a model phenol-amine proton transfer reaction complex in a solvent confined within a hydrophobic nanoscale cavity.[6] This sampling approach provides a direct and efficient way to calculate vibrational spectra and nonadiabatic couplings.

DOE-Supported Publications (2009 – present)

[1] X. Feng and W.H. Thompson, *J. Phys. Chem. C* **114**, 4279-4290 (2010). "Time-dependent Fluorescence in Nanoconfined Solvents. A Smoluchowski Equation Model Study"

[2] B.J. Ka and W.H. Thompson, *J. Phys. Chem. B* **114**, 7535-7542 (2010). "Nonadiabatic Effects on Proton Transfer Rate Constants in a Nanoconfined Solvent"

[3] W.H. Thompson, *Annu. Rev. Phys. Chem.* **62**, 599-619 (2011). "Solvation Dynamics and Proton Transfer in Nanoconfined Liquids"

[4] B.B. Laird and W.H. Thompson, *J. Chem. Phys.* **135** 084511 (2011). "Time-Dependent Fluorescence in Nanoconfined Solvents: Linear Response Approximations and Gaussian Statistics"

[5] A.A. Vartia, K.R. Mitchell-Koch, G. Stirnemann, D. Laage, and W.H. Thompson, *J. Phys. Chem. B* **115**, 12173-12178 (2011). "On the Reorientation and Hydrogen-Bond Dynamics of Alcohols"

[6] B.J. Ka and W.H. Thompson, *J. Phys. Chem. A* **116**, 832-838 (2012). "Sampling the Transition State of a Proton Transfer Reaction in Mixed Quantum-Classical Molecular Dynamics Simulations"

[7] D. Laage and W.H. Thompson *J. Chem. Phys.* **136**, 044513 (2012). "Reorientation Dynamics of Nanoconfined Water: Power-law Decay, Hydrogen-bond Jumps, and Test of a Two-State Model"

[8] A.A. Vartia and W.H. Thompson, *J. Phys. Chem. B* **116**, 5414-5424 (2012). "Solvation and Spectra of a Charge Transfer Solute in Nanoconfined Ethanol"

Structural Dynamics in Complex Liquids Studied with Multidimensional Vibrational Spectroscopy

Andrei Tokmakoff

Department of Chemistry, Massachusetts Institute of Technology, Cambridge, MA 02139
E-mail: tokmakof@MIT.edu

Water is a unique liquid due to the fact that it can form up to four hydrogen bonds, creating a loosely tetrahedral network of molecules whose connectivity evolves on ultrafast time-scales. It is the fluctuations of this network that allow water to rapidly solvate nascent charge and to participate in chemical reactions. Moreover, it is predicted that the breakage and rearrangement of hydrogen bonds plays a major role in charge transport in water and is an intrinsic element of proton transport. The goal of our research is to develop ultrafast spectroscopic probes of the hydrogen bonding network of water and to use these probes to obtain a mechanistic understanding of how water dynamics influence proton transport in water and aqueous solvation. Our work during the past year has focused on the development of a 2D IR interferometer using broadband IR, and initial applications to the study of water dynamics, and proton transport in aqueous acids and bases.

Our interest is revealing the mechanism by which water hydrogen bond dynamics mediates the structure and diffusion of protons in water. In the case of an excess proton (H^+) or hydroxide (OH^-, a proton hole), the transport of the ion is anomalously fast diffusion due to the ability to transfer a proton to or from neighboring water molecules, a process known as the Grotthuss mechanism. Simulations have suggested that hydrogen bond rearrangements play a key role in guiding proton transfer processes involving these ions. However, experimental work that is able to directly capture proton motion is lacking due in large part to the difficulty of finding probes that can measure the timescales and mechanism of transfer.

Proton transfer in strong acids has been primarily treated in the framework of two limiting hydrated proton configurations – the Eigen species where a proton is localized as a three coordinate hydronium species, and the Zundel species where a proton is equally shared between two water molecules. Ultrafast infrared spectroscopy is a powerful tool for studying proton transfer because strong aqueous acids and bases exhibit extremely broad and featureless transitions that span most of the mid-infrared region of the spectrum from ~900 cm^{-1} to 3400 cm^{-1} due to a large distribution of rapidly exchanging protonated configurations. A linear infrared spectrum of HCl in H_2O shows a continuum absorption on the red side of the OH stretch vibration that ranges down to hundreds of wavenumbers. Riding on top of the acid continuum is a 1750 cm^{-1} feature from the flanking water molecules in the Zundel species, and a 1200 cm^{-1} feature from the proton shuttling in the Zundel species. In the OH stretching region, the stretching vibration of the flanking water molecules of the Zundel species absorb around 3200-3400 cm^{-1} and the hydronium stretching mode is around 2500-3000 cm^{-1}.

To access all of these transitions in ultrafast time-resolved spectroscopy, we have developed the use of a broadband mid-infrared probe for use in nonlinear vibrational spectroscopy. By focusing 25 femtosecond 800 nm light pulses, together with their first two harmonics, in dry air, we can generate a plasma that radiates mid-infrared light which has spectral intensity from 4000 cm^{-1} down to the terahertz region and a pulse duration of <100 femtoseconds. These pulses are used as the probe pulse in two-dimensional IR spectroscopy and IR pump-probe experiments. The 45 femtosecond pump pulses in the 3000-3600 cm^{-1} region are generated using an optical parametric amplifier. This unique experiment allows us to correlate, in a time resolved way, high frequency stretching modes in liquids with all of the vibrational modes present in the mid-IR region.

We performed pump-probe experiments on HCl in H_2O using pump pulses between 3150 cm^{-1} and 3500 cm^{-1} with 400 cm^{-1} of bandwidth that excite the OH stretching vibration of strong and weak hydrogen bonds in acid solutions, followed by broadband IR probe pulses. For excitation at 3400 cm^{-1}, where we primarily excite bulk water molecules and the flanking waters of the Zundel species, we see an instantaneous response from the bending modes of water and the flanking water molecules of the shared proton species due to anharmonic bend-stretch coupling. Pumping the system with excitation pulses at 3100 cm^{-1}, where we are primarily exciting the Eigen configuration, shows HCl concentration-dependent sub-100 fs relaxation of the entire broad continuum absorption between 1300 cm^{-1} and 3000 cm^{-1}. Polarization dependent measurements show that this continuum feature is aligned with the excitation, providing evidence that we are exciting the asymmetric stretch of a distorted hydronium resulting. This suggests that the continuum could be a result of transient excursions of protons toward double-well (shared) configurations. The fast decay of the continuum probably arises from electric field fluctuations of the environment due to the librational motions of the surrounding water molecules that transiently distort the proton transfer potential. These results have direct implications on the stability of Eigen and Zundel proton complexes in water and the time-scale for their exchange.

We have also studied the continuum absorption of hydroxide solutions with femtosecond broadband IR spectroscopy. On addition of NaOH in H_2O, a broad continuum absorption grows across the entire mid-IR region. Along with it, a shoulder grows in at ~2850 cm^{-1} which is most probably due to the O-H stretching vibration of the H_2O molecule hydrogen bonded to the OH^- ion. The broad continuum is generally attributed to different proton deficient species. We performed pump-probe and 2D IR experiments on NaOH in H_2O with pump pulses between 2900 cm^{-1} and 3400 cm^{-1} and probed the mid-IR region between 1300-4000 cm^{-1}. The magic angle pump-probe data shows a transient absorption in the entire mid-IR region on addition of NaOH to H_2O which decays on a very fast timescale of 100-150 fs. This effect is more pronounced when the red side of the O-H stretching vibration is pumped, exciting the strongly hydrogen bonded species preferentially. The potential of a proton becomes a symmetric double well from an asymmetric one when it becomes equally shared between two OH moieties from a H_2O molecule hydrogen bonded to an OH^- ion. This fast timescale is probably associated with shuttling of protons resulting in a fluctuation of the proton potential.

We are also studying both neat and isotopically dilute water extensively. For the isotopically dilute liquid (i.e. HOD in D_2O), we directly observe vibrational coupling between the OH stretch and the HOD bend as well as coupling to low frequency librational modes. We also see coupling between the OH stretch and the overtone of the bend, suggesting the presence of a Fermi resonance whereby fundamental and overtone vibrations mix giving rise new oscillations.

Neat H_2O is markedly different, showing extremely strong coupling to the HOH bend as well as very broad induced absorptions upon exciting the OH stretching vibration. This suggests that the vibrational energy surface of water is extremely anharmonic and that a simple normal mode picture is not valid for this complex liquid. To further examine the nature of the stretch-bend coupling, we made polarization sensitive measurements where the relative polarization of the pump and probe were varied. The results show that there is no polarization dependence between the coupling of the bend and the stretch. This remarkable feature can be explained by having OH stretching vibrations which are delocalized over many water molecules (thus averaging over the bend orientation). This result corroborates theoretical predictions of delocalized stretching vibrations in water.

In addition to the work on water, DOE support contributes to our work to develop structure based spectroscopic models for 2D IR spectroscopy. We actively develop MD simulation based models for the linear IR and 2D IR spectroscopy of water and aqueous solutes, including peptides and proteins.

DOE Supported Publications (2008-2012)

1. Ganim, Z.; Chung, H. S.; Smith, A. W.; DeFlores, L. P.; Jones, K. C.; Tokmakoff, A., Amide I Two-Dimensional Infrared Spectroscopy of Proteins. *Acc. Chem. Res.* **2008,**
2. Roberts, S. T.; Petersen, P. B.; Ramasesha, K.; Tokmakoff, A., The dynamics of aqueous hydroxide ion transport probed via ultrafast vibrational echo experiments. In *Ultrafast Phenomena XVI*, Corkum, P.; Silvestri, S. D.; Nelson, K. A.; Riedle, E.; Schoenlein, R. W., Eds. Springer: Berlin, 2009; pp 481-483.
3. Petersen, P. B.; Roberts, S. T.; Ramasesha, K.; Nocera, D. G.; Tokmakoff, A., Ultrafast N-H Vibrational Dynamics of Cyclic Doubly Hydrogen-Bonded Homo- and Heterodimers. *J. Phys. Chem. B* **2008,** *112* (42), 13167-13171.
4. DeFlores, L. P.; Ganim, Z.; Nicodemus, R. A.; Tokmakoff, A., Amide I '-II ' 2D IR Spectroscopy Provides Enhanced Protein Secondary Structural Sensitivity. *J. Am. Chem. Soc.* **2009,** *131* (9), 3385-3391.
5. Roberts, S. T.; Petersen, P. B.; Ramasesha, K.; Tokmakoff, A.; Ufimtsev, I. S.; Martinez, T. J., Observation of a Zundel-like transition state during proton transfer in aqueous hydroxide solutions. *PNAS* **2009,** *106* (36), 15154-15159.
6. Roberts, S. T.; Ramasesha, K.; Tokmakoff, A., Structural rearrangements in water viewed through two-dimensional infrared spectroscopy. *Acc. Chem. Res.* **2009,** *42* (9), 1239-1249.
7. Nicodemus, R. A.; Ramasesha, K.; Roberts, S. T.; Tokmakoff, A., Hydrogen Bond Rearrangements in Water Probed with Temperature-Dependent 2D IR. *J. Phys. Chem. Letters* **2010**, *1*, 1068-1072.
8. Ramasesha, K.; Nicodemus, R. A.; Mandal, A.; Tokmakoff, A., Orientational Dynamics of Water Probed with 2D-IR Anisotropy Measurements. In *Ultrafast Phenomena XVII*, Jonas, D.; Riedle, E.; Schoenlein, R.; Chergui, M.; Taylor, A., Eds. Springer: Berlin, 2010; (accepted).
9. "A Source for Ultrafast Continuum Infrared and Terahertz Radiation," Poul B. Petersen and Andrei Tokmakoff, *Optics Letters*, **35** (2010) 1962–1964.
10. "Feature Article: Melting of a β-hairpin peptide using isotope-edited 2D IR spectroscopy and simulations," Adam W. Smith, Joshua Lessing, Ziad Ganim, Chunte Sam Peng, Andrei Tokmakoff, Santanu Roy, Thomas L. C. Jansen, and Jasper Knoester, *Journal of Physical Chemistry B*, in press.
11. "A Fast-Scanning Fourier Transform 2D IR Interferometer," Sean T. Roberts, Joseph J. Loparo, Krupa Ramasesha, and Andrei Tokmakoff, *Optics Communications*, **284** (2011) 1062–106.
12. "Proton Transfer in Concentrated Aqueous Hydroxide Visualized using Ultrafast Infrared Spectroscopy," Sean T. Roberts, Krupa Ramasesha, Poul B. Petersen, Aritra Mandal, and Andrei Tokmakoff, *Journal of Physical Chemistry A*, **115** (2011) 3957-3972.
13. "Collective Hydrogen Bond Reorganization in Water Studied with Temperature-Dependent Ultrafast Infrared Spectroscopy," Rebecca A. Nicodemus, S. A. Corcelli, J. L. Skinner, and Andrei Tokmakoff, *Journal of Physical Chemistry B*, **115** (2011) 5604-5616.
14. "Ultrafast 2D IR Anisotropy of Water Reveals Reorientation during Hydrogen-Bond Switching," Krupa Ramasesha, Sean T. Roberts, Rebecca A. Nicodemus, Aritra Mandal and Andrei Tokmakoff, *Journal of Chemical Physics*, **135** (2011) 054509.

15. “A phenomenological approach to modeling chemical dynamics in nonlinear and two-dimensional spectroscopy,” Krupa Ramasesha, Luigi De Marco, Andrew D. Horning, Aritra Mandal and Andrei Tokmakoff, *Journal of Chemical Physics*, **136** (2012) 134507-1-11.
16. “Identifying residual structure in intrinsically disordered systems: A 2D IR spectroscopic study of the GVGXPGVG peptide,” Joshua Lessing, Santanu Roy, Mike Reppert, Marcel Baer, Dominik Marx, Thomas La Cour Jansen, Jasper Knoester, and Andrei Tokmakoff, *Journal of the American Chemical Society*, **134** (2012) 5032–5035.

The Role of Electronic Excitations on Chemical Reaction Dynamics at Metal, Semiconductor and Nanoparticle Surfaces

John C. Tully
Department of Chemistry, Yale University, 225 Prospect Street, P. O. Box 208107, New Haven, CT, 06520-8107 USA
john.tully@yale.edu

Program Scope

Achieving enhanced control of the rates and molecular pathways of chemical reactions at the surfaces of metals, semiconductors and nanoparticles will have impact in many fields of science and engineering, including heterogeneous catalysis, photocatalysis, materials processing, corrosion, solar energy conversion and nanoscience. However, our current atomic-level understanding of chemical reactions at surfaces is incomplete and flawed. Conventional theories of chemical dynamics are based on the Born-Oppenheimer separation of electronic and nuclear motion. Even when describing dynamics at metal surfaces where it has long been recognized that the Born-Oppenheimer approximation is not valid, the conventional approach is still used, perhaps patched up by introducing friction to account for electron-hole pair excitations or curve crossings to account for electron transfer. There is growing experimental evidence that this is not adequate. We are examining the influence of electronic transitions on chemical reaction dynamics at metal and semiconductor surfaces. Our program includes the development of new theoretical and computational methods for nonadiabatic dynamics at surfaces, as well as the application of these methods to specific chemical systems of experimental attention. Our objective is not only to advance our ability to simulate experiments quantitatively, but also to construct the theoretical framework for understanding the underlying factors that govern molecular motion at surfaces and to aid in the conception of new experiments that most directly probe the critical issues.

Recent Progress

Independent Electron Surface Hopping

In the previous years of this grant, we developed the Independent Electron Surface Hopping (IESH) approach to nonadiabatic dynamics at metal surfaces, using the NO/Au system as a benchmark, with direct comparisons to experimental studies by Alec Wodtke and coworkers. IESH is applicable in cases of strong coupling where the electronic friction model is suspect, and has been demonstrated to accurately reproduce the results of detailed molecular beam experiments on vibrationally inelastic scattering of nitric oxide from the (111) surface of gold. However, in its original form, IESH represents a closed system without energy flow outside of the local region of explicitly included substrate atoms. We have developed two “thermostats” for introducing energy flow to the bulk, one for phonons and the other for electronic excitations. This extends the applicability of IESH to energetic or highly exothermic processes at surfaces where the deposited energy could otherwise be trapped and influence the outcomes. In addition, it allows ultrafast laser induced chemistry at surfaces to be simulated, where electrons

may be initially produced in a non-thermal distribution and electron-phonon equilibration may compete with local reactivity.

Vibrational Fano Resonances in Dipole-Bound Anions

The experimental group of Mark Johnson, Yale University, has obtained unique spectral characterizations of dipole-bound water cluster anions as a function of the number of water molecules in the cluster. These spectra are obtained using an "action spectroscopy" which detects the loss of the electron when the infrared laser excites an O-H vibration. The energy of the O-H stretch is sufficient to detach the weakly bound electron. The electron can also be detached via a second direct photodetachment pathway, however. This leads to an interference effect that results in asymmetric "Fano" vibrational lineshapes. In collaboration with Mark Johnson, we have explored the origins of these Fano resonances that arise due to non-adiabatic coupling of vibrational modes in dipole-bound anions. We developed a simple one-electron model of a dipole-bound anion, consisting of a point dipole and an auxiliary potential to represent the excess electron interaction with the neutral core. Nuclear motion was introduced by assuming harmonic vibration that modulates the dipole moment. When the model is parameterized to simulate water anions the resultant photodetachment lineshapes closely resemble those observed experimentally, with the asymmetry parameter q approximately equal to -1. Other parameterizations were explored for the model and it was found that changing the auxiliary potential can strongly affect q and even change its sign. The sign and magnitude of q was found to reflect a competition between two outgoing electron wave function channels, an s-like channel that produces negative q and a p-like channel that produces positive q.

Future Plans

The goals of our research program include completing our studies of the NO-Au system and more general investigations of nonadiabatic behavior at metal and semiconductor surfaces, described below.

1. Carry out a systematic comparison of 3 methods for simulating nonadiabatic dynamics at metal surfaces: electronic friction dynamics, Ehrenfest (self-consistent field) dynamics, and IESH dynamics. We will carry out this comparison using the NO/Au Hamiltonian we have employed for our comparisons with the Wodtke experiments. We also plan to repeat this systematic comparison for hydrogen atom scattering from metal surfaces as described below. The electronic friction model is basically the weak-coupling limit of the Ehrenfest theory. Ehrenfest invokes nuclear motion on an effective potential energy surface that is a weighted average of potential surfaces corresponding to different electronic configurations. IESH is a surface hopping model that invokes stochastic hops between individual potential energy surfaces, with hopping probabilities determined by electronic transition probabilities. The widespread use of the electronic friction model justifies documenting its accuracy in a well-defined comparison, and the extent to which it may be improved by not making the weak coupling assumption, i.e., by carrying out Ehrenfest dynamics exactly, is an unsettled question.

2. Extend the NO/Au IESH calculations to semiconductor surfaces and to metal surfaces with varying work functions. Calculating the required ground and excited potential energy surfaces and nonadiabatic couplings for each new chemical system is a daunting task. In order to obtain qualitative insights about general trends, we plan to use the NO/Au interactions we derived previously, with simple alterations. We can change the effective work function of the metal simply by altering the asymptotic energy of the negative ion state relative to the neutral state. This will not properly incorporate the chemical differences between the surfaces of copper, silver, platinum, etc., but it may give us a preliminary view of the sensitivity of energy transfer rates to the work function and, perhaps more importantly, suggest fruitful experiments. Similarly, we can introduce a band gap in the substrate electron density of states, again using the NO/Au interactions, in order to obtain an initial glimpse of vibrational energy transfer at semiconductor surfaces. This may reveal, for example, insight into the competition between electronic and phonon mechanisms of energy transfer.

3. Develop methods for computing "diabatic" potential energy surfaces and their off-diagonal couplings for molecules interacting with surfaces. The IESH method appears capable of accurately simulating nonadiabatic dynamics at metal and semiconductor surfaces, provided the required input is available and reliable. The necessary input is a diabatic Hamiltonian matrix that accurately represents the charge and excited states of the molecule embedded in the continuum of conduction band levels, and does so for all relevant molecule and surface atom positions. For NO interacting with the gold surface, we were able to construct a satisfactory diabatic Hamiltonian using density functional theory with the application of fictitious electric fields to modulate the energies of ionic states. This procedure is not applicable to most systems of experimental interest, however. The most critical challenge to further progress is to develop more generally applicable ab initio procedures for computing the necessary diabatic Hamiltonians. We propose to further develop and apply Constrained Density Functional Theory (CDFT) for this purpose. CDFT is conceptually simple; a DFT calculation is carried out with an imposed constraint, such as constraining the net local charge on a molecule to be minus one. This will produce the lowest energy potential energy surface consistent with this charge constraint. This can be repeated with different constraints to produce diagonal elements of the desired diabatic Hamiltonian. However, there are unsolved issues with computing the off-diagonal elements, including the absence of a proper wave function in DFT and non-orthogonality of Kohn-Sham determinants corresponding to different constraints. We will address these issues. In particular, we are exploring the possibility of enforcing orthogonality via an additional constraint. As we overcome these obstacles, we will apply this approach to hydrogen atom scattering from metals, as described below. We will also apply CDFT with spin constraints to oxygen atoms and oxygen molecules interacting with metals surfaces. For both of these cases, transitions between the ground state triplet and low-lying singlet states may occur without spin-orbit interactions via a two-electron exchange with the conduction band, possibly with major implications to chemical reactivity.

4. Inelastic scattering of hydrogen atoms from silver and gold surfaces. The hydrogen atom is the simplest example of an open shell species. While the interaction of an H atom with a metal surface does not exhibit all of the complexities of more complicated systems, because of its simplicity it affords an excellent opportunity to develop and test computational approaches for simulating atom-surface dynamical events. Equally importantly, the experimental group of Alec Wodtke (Göttingen) is planning an extensive molecular-beam study of this system, with the objective of producing detailed and quantitative data about angular distributions, inelasticity, temperature dependence, etc. We will carry out extensive calculations of the potential energy surfaces and nonadiabatic couplings for these systems, using both DFT and quantum chemical methods. Note that since DFT is in practice based on a density arising from a single-determinant Kohn-Sham wavefunction, it may not correctly portray the open-shell nature of the hydrogen atom which requires the intermixing of at least two electronic configurations (spin up and spin down), and perhaps three if the hydrogen negative ion plays a significant role. As mentioned above, we will simulate scattering dynamics with electronic friction, Ehrenfest and IESH methods, and compare each to the Wodtke experiments. This will be the most complete study to date of the role of nonadiabaticity in atom-metal interactions and the accuracy of current theories of nonadiabatic dynamics.

References to Publications of DOE-Sponsored Research since October 1, 2009

1. N. Shenvi, S. Roy and J. C. Tully, "Dynamical Steering and Electronic Excitation in NO Scattering from a Gold Surface", *Science* **326**, 829-832 (2009).

2. R. Cooper, C. Bartels, A. Kandratsenka, I. Rahinov, N. Shenvi, K. Golibrzuch, Z. S. Li, D. J. Auerbach, J. C. Tully and A. M. Wodtke, "Multiquantum Vibrational Excitation of NO Scattered from Au(111): Quantitative Comparison of Benchmark Data to Ab Initio Theories of Nonadiabatic Molecule-Surface Interactions", *Angewandte Chemie-Int. Ed*. **51**, 4954-4958 (2012).

3. S. T. Edwards, M. A. Johnson and J. C. Tully, "Vibrational Fano resonances in dipole-bound anions", *J. Chem. Phys*. **136**, 154305 (2012).

Ab-initio description of chemical transformations in condensed phase

Marat Valiev
Environmental Molecular Sciences Laboratory and
Pacific Northwest National Laboratory
902 Battelle Blvd.
Mail Stop K9-90
Richland, WA 99352
marat.valiev@pnl.gov

Our research efforts[1-8] are focused on developing fundamental understanding of factors that govern chemical transformations in condensed phase. These include bond breaking/making transformations that occur during reaction processes, as well as characterization of excited states pertinent to UV spectroscopy.

An integral part of our approach is development of advanced simulations methods that can deliver accurate description of electronic degrees of freedom relevant for a given chemical process, while taking into account surrounding environment in a way that does not impede efficiency of the calculations.[3] Conventional chemistry approaches are not very well suited for this task, and our strategy has been to utilize multi-physics methods, where the level of theory is not fixed but varies throughout the system. Parts of the system that undergo chemical transformation are described using quantum-mechanical (QM) models that explicitly include electron degrees of freedom theories. Regions where chemical identity of constituents remains intact are described based on classical parameters. The latter typically is typically based on molecular mechanics (MM) description leading to the QM/MM approach.

Even with the simplifications provided by QM/MM approach, computational expense of free energy calculations remains significant. One solution to this problem that we have developed in the past consists in shifting bulk of statistical sampling to intermediate effective Hamiltonians via thermo-dynamical cycles. Another solution, that we are currently investigating, is based on developing an alternative description of the environment based on one-dimensional reference interaction site model (1D RISM). Unlike continuum dielectric description, this description retains information about internal structure of the constituents, but utilizes density distributions functions in lieu of explicit sampling intrinsic to MM description. We have implemented this methodology into NWChem, and applied it to study of solvation structure and hydration free energies of several organic solutes.[1] (see Fig. 1)

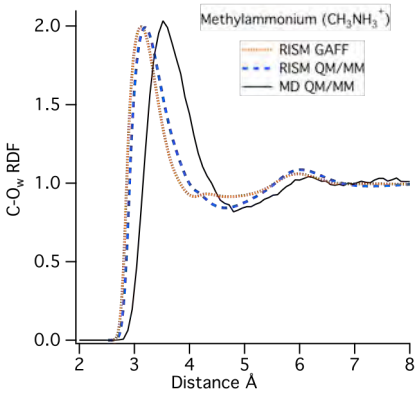

Figure 1: Methyl carbon–water oxygen (C–Ow) radial distribution function for methylammonium obtained QM/MM RISM method.

Using QM/MM free energy methods we have continued our investigation of chemistry of chlorinated hydrocarbons (CHC's) in aqueous solutions.[6-8] These chemicals are widely used in industrial applications (solvents, pesticides, electrical insulators, etc.) and account for a major fraction of the organic pollutants. The long degradation time impedes the experimental characterization, leading to significant uncertainty in understanding reaction mechanisms. Our investigation is focused on reactions between $CH_{4-n}Cl_n$(n = 2-4) with OH- -- one of important pathways for CHC decomposition in aqueous solution. Our results show that aqueous environment leads to substantial elevation of activation free energy and subsequently slow decomposition rates. Our analysis shows that in addition to solvation energy, an important contribution to reaction profile comes from solvent-induced polarization of the reactive region.

Chemistry of radical species in aqueous solution is important research area relevant to to nuclear energy production and remediation. Collaborating with experimental efforts led by Dr. Lymar at BNL we are investigating NO based radical species in aqueous solution. Following our prior studies of hyponitrite radical (N2O2-) and nitrosyl hyponitrite (N3O3-) species, we have expanded our investigation to more complex system -- diazeniumdiolates (X[N(O)NO]–). The distinguishing feature of these compounds is their ability to slowly release NO and/or its congeneric nitroxyl. The mechanisms of these processes remain obscure, and we are addressing this issue using combined experimental theoretical approach. We have completed initial studies focusing on molecular mechanism for decomposition of amino diazeniumdiolates (amino NONOates: R2N[N(O)NO]–, where R = -N(C2H5)2) in aqueous solution. Our results show that upon protonation the primary decomposition channel involves N5 (amino position)-protonated tautomer (see Figure 2).

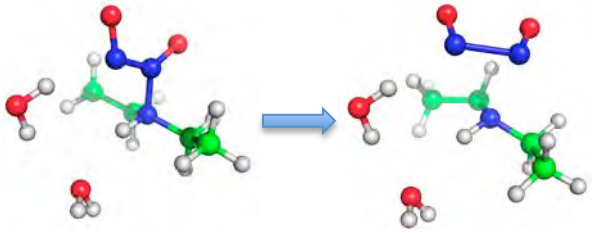

Figure 2: Decomposition mechanism of amino diazeniumdiolates

Collaborators on this project include S. K. Kathmann, B. C. Garrett, G. K. Schenter, Xuebin Wang, and Sergei Lymar. Some of the work was performed using the Molecular Science Computing Facility in the Environmental Molecular Sciences Laboratory, a national scientific user facility sponsored by the Department of Energy's Office of Biological and Environmental Research, located at Pacific Northwest National Laboratory (PNNL). Battelle operates PNNL for DOE.

1 G. N. Chuev, M. Valiev, and M. V. Fedotova, 'Integral Equation Theory of Molecular Solvation Coupled with Quantum Mechanical/Molecular Mechanics Method in Nwchem Package', *Journal of Chemical Theory and Computation,* 8 (2012), 1246-54.

2 G. Murdachaew, M. Valiev, S. M. Kathmann, and X. B. Wang, 'Study of Ion Specific Interactions of Alkali Cations with Dicarboxylate Dianions', *Journal of Physical Chemistry A,* 116 (2012), 2055-61.

3 M. Valiev, E. J. Bylaska, N. Govind, K. Kowalski, T. P. Straatsma, H. J. J. Van Dam, D. Wang, J. Nieplocha, E. Apra, T. L. Windus, and W. de Jong, 'Nwchem: A Comprehensive and Scalable Open-Source Solution for Large Scale Molecular Simulations', *Computer Physics Communications,* 181 (2010), 1477-89.
4 M. Valiev, and S. V. Lymar, 'Structural and Mechanistic Analysis through Electronic Spectra: Aqueous Hyponitrite Radical (N2o2-) and Nitrosyl Hyponitrite Anion (N3o3-)', *Journal of Physical Chemistry A,* 115 (2011), 12004-10.
5 H. J. J. van Dam, W. A. de Jong, E. Bylaska, N. Govind, K. Kowalski, T. P. Straatsma, and M. Valiev, 'Nwchem: Scalable Parallel Computational Chemistry', *Wiley Interdisciplinary Reviews-Computational Molecular Science,* 1 (2011), 888-94.
6 D. Y. Wang, M. Valiev, and B. C. Garrett, 'Ch2cl2+Oh- Reaction in Aqueous Solution: A Combined Quantum Mechanical and Molecular Mechanics Study', *Journal of Physical Chemistry A,* 115 (2011), 1380-84.
7 T. T. Wang, H. Y. Yin, D. Y. Wang, and M. Valiev, 'Hybrid Quantum Mechanical and Molecular Mechanics Study of the S(N)2 Reaction of Ccl4 + Oh- in Aqueous Solution: The Potential of Mean Force, Reaction Energetics, and Rate Constants', *Journal of Physical Chemistry A,* 116 (2012), 2371-76.
8 H. Y. Yin, D. Y. Wang, and M. Valiev, 'Hybrid Quantum Mechanical/Molecular Mechanics Study of the S(N)2 Reaction of Ch3cl+Oh- in Water', *Journal of Physical Chemistry A,* 115 (2011), 12047-52.

This page is intentionally left blank

Probing the Actinide-Ligand Binding and the Electronic Structure of Gaseous Actinide Molecules and Clusters Using Anion Photoelectron Spectroscopy

PI: Lai-Sheng Wang

Department of Chemistry
Brown University
324 Brook Street
Providence, RI 02912
Email: lai-sheng_wang@brown.edu

Program Scope

The broad scope of this program is to better understand actinide chemistry using new spectroscopic techniques and to provide accurate spectroscopic data for the validation of new theoretical methods aimed at actinide chemistry. This program contains three thrust areas:

* probing ligand-uranyl (UO_2^{2+}) interactions in gaseous anionic complexes in the form of $[UO_2L_x]^{n-}$ produced by electrospray ionization
* probing the electronic structure and bonding of inorganic and organometallic compounds of actinides in the gas phase using electrospray and anion photoelectron spectroscopy
* probing the metal-metal bonding and size-dependent electronic structures in U_x^- and $U_xO_y^-$ clusters as a function of size and composition.

Understanding the chemistry of the actinide elements, in particular, uranium, is of critical importance to the mission of DOE. We have developed a number of experimental apparatuses, including a magnetic-bottle photoelectron spectroscopy instrument equipped with a laser vaporization supersonic cluster source, a photoelectron imaging apparatus with a laser vaporization cluster source, and a combined photoelectron imaging and magnetic-bottle instrument equipped with an electrospray ionization source and low temperature ion trap. This suite of state-of-the-art instruments are uniquely suitable to investigate the three classes of actinide compounds. Photodetachment involves removal of electrons from occupied molecular orbitals and probes directly the electronic structure and chemical bonding properties of the underlying molecular species. Photoelectron spectroscopy of anions yields electron affinities, vibrational information, and low-lying electronic state information for the corresponding neutral species. The application of *anion* photoelectron spectroscopy to actinide molecules opens up new research opportunities and yields systematic electronic structure and spectroscopic information that can be used to verify computational methods and advance our understanding of the reactivity, structure, and bonding of actinide molecules.

Recent Progress (FY2011)

This program commenced in August 2011. During the first funding year, we have focused on the first two thrust areas and have studied $[UO_2F_4]^{2-}$ and its H_2O and CH_3CN solvated species, UF_5^- and UF_6^- complexes, and $[UO_2Cl_4]^{2-}$. Preliminary data have been obtained on a number of other uranyl complexes with different ligands.

Observation and investigation of the uranyl tetrafluoride dianion ($UO_2F_4^{2-}$) and its solvation complexes with water and acetonitrile. Bare uranyl tetrafluoride ($UO_2F_4^{2-}$) and its solvation complexes by one and two water or acetonitrile molecules have been observed in the

gas phase using electrospray ionization and investigated by photoelectron spectroscopy and *ab initio* calculations. The isolated $UO_2F_4^{2-}$ dianion is found to be electronically stable with an adiabatic electron binding energy of 1.10 ± 0.05 eV and a repulsive Coulomb barrier of ~2 eV. Photoelectron spectra of $UO_2F_4^{2-}$ display congested features due to detachment from U–O bonding orbitals and F 2p lone pairs. Solvated complexes by H_2O and CH_3CN, $UO_2F_4(H_2O)_n^{2-}$ and $UO_2F_4(CH_3CN)_n^{2-}$ (n = 1, 2), are also observed and their photoelectron spectra are similar to those of the bare $UO_2F_4^{2-}$ dianion, suggesting that the solvent molecules are coordinated to the outer sphere of $UO_2F_4^{2-}$ with relatively weak interactions between the solvent molecules and the dianion core. Both DFT and CCSD(T) calculations are performed on $UO_2F_4^{2-}$ and its solvated species to understand the electronic structure of the dianion core and solute-solvent interactions. The strong U–F interactions with partial (d-p)π bonding are shown to weaken the U=O bonds in the $[O=U=O]^{2+}$ unit. Each H atom in the water molecules forms a H-bond to a F atom in the equatorial plane of $UO_2F_4^{2-}$ (**Fig. 1**), while each CH_3CN molecule forms H-bonds to two F ligands and one axial oxygen.

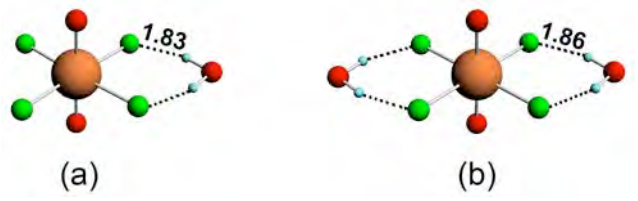

Fig. 1. Optimized structures of (a) $UO_2F_4(H_2O)^{2-}$ (C_{2v}) and (b) $UO_2F_4(H_2O)_2^{2-}$ (D_{2d}) using density functional theory. The H-bond lengths are in Å.

Photoelectron spectroscopy and theoretical studies of UF_5^- and UF_6^-. The UF_5^- and UF_6^- anions are produced using electrospray ionization (**Fig. 2**) and investigated by photoelectron spectroscopy and relativistic quantum chemistry. An extensive vibrational progression is observed in the spectra of UF_5^-, indicating significant geometry changes between the anion and the neutral ground states. Franck-Condon factor simulations of the observed vibrational progression yield an accurate electron affinity of 3.82 ± 0.05 eV for UF_5, which is an important thermodynamic value, but was not accurately known before. Relativistic quantum calculations using density functional and *ab initio* theories are performed on UF_5^- and UF_6^- and their neutrals. The ground states of UF_5^- and UF_5 are found to have C_{4v} symmetry, but with a large U−F bond length change. The ground state of UF_5^- is a triplet state ($^3B_2$) with the two 5f electrons occupying a $5f_{z3}$-based $8a_1$ highest occupied molecular orbital (HOMO) and the $5f_{xyz}$-based $2b_2$ HOMO-1 orbital. The detachment cross section from the $5f_{xyz}$ orbital is observed to be extremely small and the detachment transition from the $2b_2$ orbital is more than ten times weaker than that from the $8a_1$ orbital at the photon energies available. The UF_6^- anion is found to be octahedral, similar to neutral UF_6 with the extra electron occupying the $5f_{xyz}$-based a_{2u} orbital. Surprisingly, no photoelectron spectrum could be observed for UF_6^- due to the extremely low detachment cross section from the $5f_{xyz}$-based HOMO of UF_6^-.

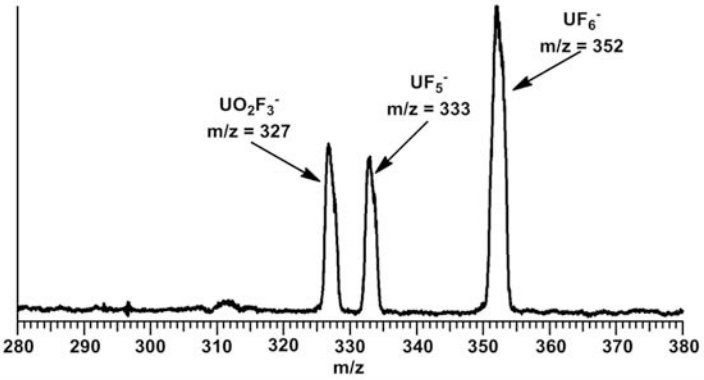

Fig. 2. Electrospray mass spectrum for $UO_2F_3^-$, UF_5^-, and UF_6^-.

Photoelectron spectroscopy and the electronic structure of the uranyl tetrachloride dianion: $UO_2Cl_4^{2-}$. The uranyl tetrachloride dianion ($UO_2Cl_4^{2-}$) is one of the most important uranyl complexes in solution. We observed it in the gas phase using electrospray ionization and investigated its electronic structure using photoelectron spectroscopy and

relativistic quantum chemical calculations and compared it to that of $UO_2F_4^{2-}$. Photoelectron spectra of $UO_2Cl_4^{2-}$ are obtained at various photon energies and congested spectral features are observed. The free $UO_2Cl_4^{2-}$ dianion is found to be highly stable with an adiabatic electron binding energy of 2.40 eV. *Ab initio* calculations are carried out and used to interpret the photoelectron spectra and elucidate the electronic structure of $UO_2Cl_4^{2-}$. The calculations show that the frontier molecular orbitals in $UO_2Cl_4^{2-}$ are dominated by the ligand Cl 3p orbitals, while the U-O bonding orbitals are much more stable. The electronic structure of $UO_2Cl_4^{2-}$ is found to be quite different from that of $UO_2F_4^{2-}$. The frontier orbitals of $UO_2Cl_4^{2-}$ mainly consist of ligand 3p type orbitals, whereas the frontier orbitals of $UO_2F_4^{2-}$ are dominated by U-O bonding orbitals as a result of stronger uranyl-F bonding. The electron binding energy of $UO_2Cl_4^{2-}$ is found to be much higher than that of $UO_2F_4^{2-}$ due to the reduced intramolecular Coulomb repulsion in $UO_2Cl_4^{2-}$, as well as the stronger uranyl-F bonding in $UO_2F_4^{2-}$.

Future Plans

In the future, we will continue to investigate UO_2^{2+} complexed with halides and other ligands. We plan to examine the periodic trend from L = F to I. We have found that we can also produce UCl_x^- and UCl_6^{2-} complexes using our electrospray ionization source. We will study the chemical bonding and electronic structures of these species and compare them with the corresponding fluoride complexes. We have obtained a pure uranium laser ablation target. We plan to start experiments on simple U_x^- clusters and uranium oxide clusters ($U_xO_y^-$) produced by using a laser vaporization supersonic cluster source.

More importantly, we have built a second generation cryogenic ion trap to be coupled with our electrospray photoelectron spectroscopy apparatus. This new trap is an improved version over our original cryogenic ion trap still under operation at PNNL. This cryogenic ion trap will allow us to create cold actinide complexes from the electrospray ion source and should significantly enhance the energy resolution and accuracy of our photoelectron spectroscopy experiments.

Publications resulted from joint CPIMS and HEC support (FY 2011)

1. "Observation and Investigation of the Uranyl Tetrafluoride Dianion ($UO_2F_4^{2-}$) and Its Solvation Complexes with Water and Acetonitrile" (P. D. Dau, J. Su, H. T. Liu, J. B. Liu, D. L. Huang, J. Li, and L. S. Wang), *Chem. Sci*. **3**, 1137-1146 (2012).

2. "Photoelectron Spectroscopy and Theoretical Studies of UF_5^- and UF_6^-" (P. D. Dau, J. Su, H. T. Liu, D. L. Huang, F. Wei, J. Li, and L. S. Wang), *J. Chem. Phys.* **136**, 194304 (2012).

3. "Photoelectron Spectroscopy and the Electronic Structure of the Uranyl Tetrachloride Dianion: $UO_2Cl_4^{2-}$" (P. D. Dau, J. Su, H. T. Liu, D. L. Huang, J. Li, and L. S. Wang), *J. Chem. Phys.* , in press (2012).

This page is intentionally left blank

Chemical Kinetics and Dynamics at Interfaces

Cluster Model Investigation of Condensed Phase Phenomena

Xue-Bin Wang

Chemical & Materials Sciences Division, Pacific Northwest National Laboratory, P.O. Box 999, MS K8-88, Richland, WA 99352. E-mail: xuebin.wang@pnnl.gov

Program Scope

This program is aimed at obtaining a microscopic understanding of solution chemistry and condensed phase phenomena using gas phase clusters as model systems. Ionic and molecular (including hydrated) clusters with molecular specificity, selected sizes, and controlled compositions are ideal model systems to understand condensed phases processes and obtain molecular-level understanding of environmental materials, solution chemistry, atmospheric aerosols, and biological functions involving these species. Our primary experimental technique is a cold and temperature-controlled photoelectron spectroscopy (PES) coupled with electrospray ionization (ESI), which is used to produce complex anions, including multiply-charged anions, and solvated clusters with multiple compositions from solution samples. The precise control of ion temperatures in the range from 10 K to room temperature has facilitated not only the enhancement of the photoelectron spectroscopic resolution and precision, but also the investigation of new temperature-dependent phenomena. Experiments and *ab initio* calculations are synergistically combined to

- Obtain a molecular-level understanding of the solvation and stabilization of complex singly- and multiply-charged anions important in condensed phases
- Probe ion specific interactions with biological implications
- Study temperature-dependent conformation changes and isomer populations of complex solvated clusters
- Understand the molecular processes and initial steps of dissolution of salt molecules in polar solvents
- Investigate intrinsic electronic structures of environmentally and catalytically important species and reactive diradicals.

The central theme of this research program lies at obtaining a fundamental understanding of environmental materials and solution chemistry important to many primary DOE missions (waste storage, subsurface and atmospheric contaminant transport, catalysis, etc.), and enhances scientific synergies between experimental and theoretical studies towards achieving such goals.

Recent Progress

Study of Ion Specific Interactions of Alkali Cations with Dicarboxylate Dianions. Alkali metal cations (M^+) often show pronounced ion specific interactions and selectivity with macromolecules in biological processes, colloids, and interfacial sciences, but a fundamental understanding about the underlying microscopic mechanism is still very limited. The ion-pair interaction between M^+ and carboxylate has been a particular topic of great interest, partly due to the important biological implications of the remarkable metal selectivity (Na^+ versus K^+ ion channels) present in normal functioning of life. We reported a direct probe of interactions between M^+ and dicarboxylate dianions, $^-O_2C(CH_2)_nCO_2^-$ (D_n^{2-}) in the gas phase by combined PES and ab initio electronic structure calculations on nine M^+–D_n^{2-} complexes (M = Li, Na, K; n = 2, 4, 6). PES spectra show that the electron binding energy (EBE) decreases in the

order of $Li^+ > Na^+ > K^+$ for complexes of $M^+–D_2^{2-}$, whereas the order is changed to $Li^+ < Na^+ \approx K^+$ when M^+ interacts with a more flexible D_6^{2-} dianion. Theoretical modeling suggests that M^+ prefers to interact with both ends of the carboxylate $–COO^–$ groups by bending the flexible aliphatic backbone, and the local binding environments are found to depend upon backbone length *n*, carboxylate orientation, and the specific cation M^+. The observed variance of EBEs reflects how well each specific dicarboxylate dianion accommodates each M^+. This work demonstrates the delicate interplay among several factors (electrostatic interaction, size matching, and strain energy) that play critical roles in determining the structures and energetics of gaseous clusters as well as ion specificity and selectivity in solutions and biological systems.

Probing Electronic Structures of Diradicals: meta-Benzoquinone and $(CO)_4$. Electron affinities (EAs) and electronic structures of benzoquinone molecules (BQs) are crucial information in understanding a wide range of applications involving these molecules from biological photosynthesis to energy conversion processes. We carried out a systematic spectroscopic probe on the electronic structures and EAs of all three isomers (*o*-, *m*-, and *p*-BQs) employing PES and *ab initio* electronic structure calculations. Similar spectral pattern was observed in the *o*- and *p*-$BQ^{\bullet-}$ spectra, each revealing a broad ground state feature and a large band gap, followed by well-resolved excited states peaks. In contrast, the spectrum of *m*-$BQ^{\bullet-}$ is distinctly different from its two congeners, with no clear band gap and a much higher EA. Accompanying theoretical calculations confirmed experimental EAs and band gaps, and further unraveled a triplet ground state for *m*-BQ in contrast to singlet ground states for *o*- and *p*- isomers. The diradical nature of *m*-BQ, consistent with its non-Kekulé structure, is primarily responsible for the observed high EA and also explains its nonexistence in bulk materials.

On the other hand, despite a seemingly simple and Kekulé appearance, cyclobutanetetraone (C_4O_4) has been predicted to have a very low-lying triplet state among four low-lying electronic states. Determining the energetic ordering of these states and the ground state of $C_4O_4^-$ theoretically has been proven to be considerably challenging. The most reliable theoretical calculations by Borden and co-workers predicted surprisingly a triplet ground state for $(CO)_4$. But such prediction remained to be confirmed experimentally. We recently conducted a low temperature (20K) PES approach to obtain electronic structure of $(CO)_4$ molecule. Well resolved spectra were obtained at both 193 and 266 nm. Combined with the theoretical studies by Borden and co-workers, our PES study reveals that $(CO)_4$ indeed has a triplet ground state with diradical character. The two low-lying excited states of C_4O_4 are also determined to be $^1A_{1g}$ (8π), and $^1B_{2u}$ with the term values of (6.27 ± 0.5 kJ/mol) and $^1B_{2u}$ (13.50 ± 0.5 kJ/mol), respectively. The obtained spectroscopic information is valuable to benchmark high-level *ab initio* methods.

Hydrogen Bonded Arrays: The Power of Multiple Hydrogen Bonds. Many enzymes catalyze a wide variety of chemical processes by using two or even three hydrogen bonds to a single oxygen atom in what is commonly referred to as an oxyanion hole. The energies of these hydrogen bonding interactions are important in catalysis but are not well understood. In collaboration with Kass and co-workers at University of Minnesota, we used PES to directly probe the energetic consequences of hydrogen bond arrays in small covalently bound model compounds, and the experimental results are compared to computational predictions. We find that in a series of monodeprotonated polyhydroxyalcohols (i.e., polyols) the strengths of the hydrogen bond arrays systematically increase with the number of hydroxyl groups from 1 to 3 and for 6. That is, an oxygen anion center is stabilized most effectively by up to 3 hydrogen bond donors, but in the process the donor groups become better hydrogen bond acceptors. The resulting hydrogen-bonded network can provide a large energetic stabilization that may lead to catalytic rate enhancements and greater acidities and basicities than those measured in water.

Photoelectron Spectroscopic Investigation on Atmospherically Important Halogen Oxide Radicals: $BrO_{2,3}$ and IO_{2-4}. Higher halogen oxides (XO_n, $n \geq 2$) are important species involved in the ozone

depletion and other atmospheric reactions by photodissociation to generate halogen atoms or halogen monoxides. The detailed electronic structure information of these species is therefore much needed to understand and model related photochemistry upon solar radiation. To date, our knowledge about the electronic states of XO_n is largely based on theoretical predictions, in particular for bromine and iodine oxides, which is at least partially due to the fact that some of the radicals are not even thermodynamically stable and therefore haven't been studied spectroscopically. By taking advantage of the ubiquity of XO_n^- in solutions, we 'fished out' these anions from solutions via ESI, and investigated ground and excited states of the corresponding neutral radicals by PES in the gas phase. Furthermore, because PES can access optically "dark" states complementary to the absorption spectroscopy, the low-lying "dark" states directly involved in the photochemistry and photodissociation processes of these species in the stratosphere are also unraveled. Our work represents the first experimental (spectroscopic) probe aimed at providing direct energetic information to characterize these excited states in comparison with available theoretical predictions and in discussion with their atmospheric implications.

Zeise's Anion and Its Br- and I-Analogs: A Combined Gas-Phase Photoelectron Spectroscopic and Theoretical Study. Zeise's anion, $[PtCl_3(C_2H_4)]^-$ is the quintessential organometallic compound first synthesized by William Zeise in the 1820s. We carried out the first PES study of Zeise's anion, and its Br- and I- analogs in the gas phase. Well-resolved and rich spectral features are obtained for each species, yielding detailed electronic structure information, which is assigned with the aid of high-level electronic structure calculations at the coupled cluster level of theory. The electron binding energies of $[PtX_3(C_2H_4)]^-$ are found to decrease with the size of halogen (4.57, 4.51, and 4.18 eV for X = Cl, Br, and I, respectively). The calculations indicate a synergistic η^2 interaction [with interaction strengths of 1.54 (Cl), 1.37 (Br) and 1.10 eV (I)] between the perpendicular C_2H_4 fragment and the nearly horizontal planar PtX_3^- anions, resulting in activating the ethylene molecule. The detailed insights of the chemical bonding and underlying electronic structure can be used to benchmark interactions between olefins and transition metal complexes, which are crucial to a wide range of catalytic processes.

Future Directions

The main thrust of our BES program will continue to be on cluster model studies of condensed phase phenomena in the gas phase. The experimental capabilities that we have developed give us the opportunity to attack a broad range of fundamental chemical physics problems pertinent to ionic solvation and solution chemistry. In particular, the temperature control will allow us to study different isomer populations and conformation changes of environmentally important hydrated clusters as a function of temperature. We will also be able to study physisorption of various gas molecules onto negatively-charged anions. The physisorption of H_2 and CO_2 are of particular interest because of relevance to identifying potential H_2 and CO_2 storage materials by providing fundamental energetic and structural information between these two gases and different types of molecules. Another major direction is to use gaseous clusters to model ion-specific interactions in solutions and initial nucleation processes relevant to atmospheric aerosol formation. While we will continue to explore the new capabilities of temperature control, we also plan to initiate new research directions in the coming years to study excited state properties of solvated clusters to model possible aerosol photochemistry and high-energy processes at interfaces.

References to Publications of DOE CPIMS Sponsored Research (10/1/2009 - present)

1. XB Wang, YL Wang, J Yang, XP Xing, J Li, and LS Wang, "Evidence of Significant Covalent Bonding in $Au(CN)_2^-$." *Journal of the American Chemical Society* 131(45), 16368-16370 (2009).

2. MM Meyer, XB Wang, CA Reed, LS Wang, and SR Kass, "Investigating the Weak to Evaluate the Strong: An Experimental Determination of the Electron Binding Energy of Carborane Anions and the Gas Phase Acidity of Carborane Acids." *Journal of the American Chemical Society* 131, 18050-18051 (2009).

3. XB Wang, C Chi, M Zhou, IV Kuvychko, K Seppelt, AA Popov, SH Strauss, OV Boltalina, and LS Wang, "Photoelectron Spectroscopy of $C_{60}F_n^-$ and $C_{60}F_m^{2-}$ (n = 17, 33, 35, 43, 45, 47; m = 34, 46) in the Gas Phase and the Generation and Characterization of C_1-$C_{60}F_{47}^-$ and D_2-$C_{60}F_{44}$ in Solution." *Journal of Physical Chemistry A* 114, 1756-1765 (2010).

4. XB Wang, K Kowalski, LS Wang, and SS Xantheas, "Stepwise Hydration of the Cyanide Anion: A Temperature-Controlled Photoelectron Spectroscopy and Ab Initio Computational Study of $CN^-(H_2O)_n$, n = 2-5." *Journal of Chemical Physics* 132(12), 124306 (2010).

5. YL Wang, XB Wang, XP Xing, F Wei, J Li, and LS Wang, "Photoelectron Imaging and Spectroscopy of MI_2^- (M = Cs, Cu, Au): Evolution from Ionic to Covalent Bonding." *Journal of Physical Chemistry A* 114, 11244-11251 (2010).

6. XB Wang, Q Fu, and J Yang, "Electron Affinities and Electronic Structures of *o*-, *m*-, and *p*-hydroxyphenoxyl Radicals: A Combined Low-Temperature Photoelectron Spectroscopic and Ab Initio Calculation Study." *Journal of Physical Chemistry A* 114, 9083-9089 (2010).

7. Q Fu, J Yang, and XB Wang, "On the Electronic Structures and Electron Affinities of the m-Benzoquinone (BQ) Diradical and the o-, p-BQ Molecules: A Synergetic Photoelectron Spectroscopic and Theoretical Study" *Journal of Physical Chemistry A* 115, 3201-3207 (2011).

8. XB Wang and SS Xantheas, "Photodetachment of Isolated Bicarbonate Anion: Electron Binding Energy of HCO_3^-", *Journal of Physical Chemistry Letters* 2, 1204-1210 (2011).

9. H Wen, GL Hou, W Huang, N Govind, and XB Wang, "Photoelectron Spectroscopy of Higher Bromine and Iodine Oxide Anions: Electron Affinities and Electronic Structures of $BrO_{2,3}$ and IO_{2-4} Radicals", *Journal of Chemical Physics* 135, 184309 (2011).

10. A Shokri, JC Schmidt, XB Wang, and SR Kass, "Hydrogen Bonded Arrays: The Power of Multiple Hydrogen Bonds", *Journal of the American Chemical Society* 134, 2094-2099 (2012).

11. JC Guo, G Hou, SD Li, and XB Wang, "Probing the Low-lying Electronic States of Cyclobutanetetraone (C_4O_4) and its Radical Anion: A Low-Temperature Anion Photoelectron Spectroscopic Approach", *Journal of Physical Chemistry Letters* 3, 304-308 (2012).

12. G Murdachaew, M Valiev, SM Kathmann, and XB Wang, "Study of Ion Specific Interactions of Alkali Cations with Dicarboxylate Dianions", *Journal of Physical Chemistry A* 116, 2055-2061 (2012).

13. IV Kuvychko, JB Whitaker, BW Larson, TC Folsom, NB Shustova, SM Avdoshenko, YS Chen, H Wen, XB Wang, L Dunsch, AA Popov, SH Strauss, and OV Boltalina, "Substituent Effects in a Series of 1,7-$C_{60}(R_F)_2$ Compounds (R_F = CF_3, C_2F_5, n-C_3F_7, i-C_3F_7, n-C_4F_9, s-C_4F_9, n-C_8F_{17}): Electron Affinities, Reduction Potentials and E(LUMO) Values Are Not Always Correlated", *Chemical Science* 3, 1399-1407 (2012).

14. GH Hou, H Wen, KA Lopata, W Zheng, K Kowalski, N Govind, XB Wang, and SS Xantheas, "A Combined Gas-Phase Photoelectron Spectroscopic and Theoretical Study of Zeise's Anion and Its Br- and I-Analogs", *Angewandte Chemie International Edition* 51, 6356-6360 (2012).

Free Radical Reactions of Hydrocarbons at Aqueous Interfaces

Principal Investigator: Kevin R. Wilson
Lawrence Berkeley National Laboratory, 1 Cyclotron Road, MS 6R2100, Berkeley, CA 94720
Email: krwilson@lbl.gov

Program Scope

Although there are some exquisite X-ray, non-linear optical and molecular beam scattering probes of liquid interface structure, new and innovative methods for measuring chemical reactions occurring at liquid surfaces are clearly needed to advance our understanding of how molecular structure, reaction depth and solute ions govern molecular weight growth and degradation of organic molecules at water and electrolyte interfaces. This project will probe the surface chemistry of hydrocarbons molecules residing on micron-sized aqueous droplets exposed to gas phase hydroxyl radicals using ambient pressure X-ray photoelectron spectroscopy and surface sensitive mass spectrometry. This program aims to:

(1) Quantify the link between molecular structure and surface reactivity at an aqueous interface using model hydrocarbon architectures (e.g. isomers)

(2) Determine how the presence and distribution of interfacial ions control the surface reactivity of a hydrocarbon at an aqueous interface.

This work broadly supports the Department of Energy's Basic Energy Sciences program to better assess, mitigate and control the efficiency, utilization, and environmental impacts of energy use. This work seeks a rigorous molecular understanding of how heterogeneous reaction pathways lead to either bulk solvation of a surface active organic molecule or its removal from the interface through decomposition into gas phase products. These fundamental processes are critical for understanding the chemical fate of hydrocarbon byproducts of energy use and consumption.

Motivation

Chemical reactions occurring at interfaces govern a wide array of environmentally and technologically important processes in electrochemistry, fuel cells, catalysis, soot formation and oxidation, aerosol aging, electron transport across membranes, lipid peroxidation, and corrosion. In many of these systems hydrocarbon radicals (e.g. R·, RO·, RO_2·) play key chemical roles as initiators or propagators of surface reactions or as reactive intermediates. In the gas phase the exact distribution of stable reaction products depends sensitively upon the molecular structure, transition states and the multitude of reactions pathways available for these radical intermediates. For surface reactions, simple predictions of interfacial reactivity based solely upon chemical structure (e.g. the number and kind of molecular reactive sites in an isolated gas phase molecule) are often inaccurate by many orders of magnitude, since interfacial molecular orientation and solvent structure all play significant and complex roles in controlling the activation energy of a surface reaction. Thus, new molecularly incisive probes of organic/aqueous interfaces are clearly needed to achieve the sufficient molecular detail necessary to formulate quantitative surface free radical reaction mechanisms.

Technical Approach and Progress to Date

Atmospheric pressure mass spectrometry and ambient pressure (up to 5 Torr) X-ray photoelectron spectroscopy will be used in conjunction with a droplet train flow reactor for detailed measurements of interfacial free radical chemistry. Micron-sized droplets produce liquid surfaces that are contaminate-free, and constantly refreshed. Droplet streams or trains inherently provide the time structure for quantifying the heterogeneous kinetics. Unlike previous uses of droplet trains, the key innovation of this proposal is to combine two surface sensitive techniques to probe the air/hydrocarbon/water interface directly during a heterogeneous reaction.

A new atmospheric pressure ionization source, known as DART (Direct Analysis in Real Time), has been recently developed and is now commercially available. A DART source produces a heated stream of helium atoms containing a fraction metastable species (He^*) that form protonated water clusters which collide with a solid or liquid surface to both desorb and ionize material. These ions are then transported into an atmospheric pressure mass spectrometer for mass analysis. DART is extremely sensitive (picomole), quantitative, and provides clear molecular signatures of the chemical constituents of complex liquid and solid samples, such as urine, pharmaceutical drug tablets, and self-assembled monolayers. The DART source will be coupled to an existing atmospheric pressure mass spectrometer to obtain molecularly detailed surface mass spectra of reactants and products as they are forming at the aqueous droplet interface. Initial results to date have shown that the ion signal produced by DART for nanometer sized organic droplet streams is proportional to surface area with an estimated probing depth of 2-10 nm for a 200 nm diameter droplet.

Hydrocarbon radicals will be formed at the droplet surface via reactive collisions with OH radicals. Mass spectral changes in the surface chemical composition (reactant decay and the formation of interfacial products) will then be measured in real time. From these measurements heterogeneous kinetics will be quantified and through a detailed analysis of the reaction products, their formation rates and branching ratios detailed surface reaction mechanisms will be formulated.

In companion experiments, synchrotron-based ambient pressure X-ray photoelectron spectroscopy (XPS) will be used to quantify the elemental composition and functional group distribution as a function of interfacial depth (0.8-2 nm). In addition to surface sensitive chemical information, these measurements allow radial concentration profiles in hydrocarbons/aqueous droplets to be quantified, thus providing a depth-resolved view of the aqueous interface as it is chemically transformed. These kinds of measurements might reveal differences in how reactants, radical intermediates and products might be distributed (surface, subsurface and bulk) at the droplet interface during a reaction. Furthermore, these experimentally derived concentration profiles, obtained using synchrotron XPS, can be directly compared to interfacial distributions produced by Molecular Dynamics simulations to further refine the predictive capabilities of these computer models for capturing interfacial reactions of large hydrocarbons in an aqueous solution.

Together these techniques are expected to have the required surface sensitivity and molecular specificity to explore, in fundamentally new ways, the heterogeneous chemistry of hydrocarbons at aqueous interfaces.

Future Plans

Quantifying the link between molecular structure and surface reactivity

Experiments will be designed to isolate how molecular structure of a hydrocarbon radical controls its spatial distribution and overall reactivity at an aqueous interface. The general approach can be illustrated by a simple example of pentanol ($C_5H_{12}O$), of which there are eight structural isomers. The –OH group in each isomer is located at different points along the carbon backbone yielding a collection of molecules (straight vs. branched) with a distinct distribution of reactive sites (i.e. the number of primary, secondary, and tertiary carbon atoms in each isomer). Furthermore, the location of the hydrophilic -OH group (terminal vs. branched) in each isomer may play a critical role in controlling the orientation and distribution of each isomer at the aqueous interface. These factors might enhance surface reactivity, stabilize unique transition states and lead to novel product formation pathways for certain isomeric structures that would not be observed in the gas phase. This approach will be used for a variety of hydrocarbon structures to isolate how the interfacial reactivity of hydrocarbon radicals depend upon the kinds and number of functional groups (e.g. aliphatic vs. aromatic), carbon number, molecular weight, etc.

Interfacial molecular weight growth and oxidative degradation reaction pathways

Determining the rate at which a surface active hydrocarbon molecule is chemically transformed to either become solvated in the bulk solution or broken down into small gas phase species will be a key objective of future work. This will be done through careful measurements of how the rate of heterogeneous oxygen addition (molecular weight growth) competes with surface reaction channels that lead to carbon and/or oxygen loss (decomposition) from the interface. Such measurements would be key steps in understanding and predicting interfacial reaction pathways to identify the atmospheric and terrestrial sinks of hydrocarbons emitted by energy production and use.

Surface solvation structure and the interfacial reactivity of hydrocarbon radicals

The addition of solute molecules (e.g. NaI) has been previously shown to modify the solvation structure of the liquid water surface, through the preferential adsorption of large polarizable anions to the interface. A key question to be addressed is: how does the presence of inorganic solutes modify the reactivity of a hydrocarbon radical or ion at an interface? One might expect that anions or cations at or near the liquid water interface might lead to changes in the interfacial distribution and orientation of a hydrocarbon at the surface. Such changes might play important roles in altering the kinds and availability of hydrocarbon reactive sites at the interface.

This page is intentionally left blank

Ionic Liquids: Radiation Chemistry, Solvation Dynamics and Reactivity Patterns

James F. Wishart
Chemistry Department, Brookhaven National Laboratory, Upton, NY 11973-5000
wishart@bnl.gov

Program Definition

Ionic liquids (ILs) are a rapidly expanding family of condensed-phase media with important applications in energy production, storage and consumption, including advanced devices and processes and nuclear fuel and waste processing. ILs generally have low volatilities and are combustion-resistant, highly conductive, recyclable and capable of dissolving a wide variety of materials. They are finding new uses in dye-sensitized solar cells, chemical synthesis, catalysis, separations chemistry, batteries, supercapacitors and other areas. Ionic liquids have dramatically different properties compared to conventional molecular solvents, and they provide a new and unusual environment to test our theoretical understanding of primary radiation chemistry, charge transfer and other reactions. We are interested in how IL properties influence physical and dynamical processes that determine the stability and lifetimes of reactive intermediates and thereby affect the courses of reactions and product distributions. We study these issues by characterization of primary radiolysis products and measurements of their yields and reactivity, quantification of electron solvation dynamics and scavenging of electrons in different states of solvation. From this knowledge we wish to learn how to predict radiolytic mechanisms and control them or mitigate their effects on the properties of materials used in nuclear fuel processing, for example, and to apply IL radiation chemistry to answer questions about general chemical reactivity in ionic liquids that will aid in the development of applications listed above.

Soon after our radiolysis studies began it became evident that the slow solvation dynamics of the excess electron in ILs (which vary over a wide viscosity range) increase the importance of pre-solvated electron reactivity and consequently alter product distributions and subsequent chemistry. This difference from conventional solvents has profound effects on predicting and controlling radiolytic yields, which need to be quantified for the successful use under radiolytic conditions. Electron solvation dynamics in ILs are measured directly when possible and estimated using proxies (e.g. coumarin-153 dynamic emission Stokes shifts or benzophenone anion solvation) in other cases. Electron reactivity is measured using ultrafast kinetics techniques for comparison with the solvation process.

A second important aspect of our interest in ionic liquids is how their unusual sets of properties affect charge transfer and charge transport processes. This is important because of the many applications of ionic liquids in devices that operate on the basis of charge transport. While interest in understanding these processes in ionic liquids is growing, the field is still in an early stage of development. We are using donor-bridge-acceptor systems to study electron transfer reactions across variable distances in a series of ionic liquids with a range of structural motifs and whose dynamical time scales vary from moderately fast to extremely slow, and to compare them with conventional solvents.

Methods. Picosecond pulse radiolysis studies at BNL's Laser-Electron Accelerator Facility (LEAF) are used to identify reactive species in ionic liquids and measure their solvation and reaction rates. This work is aided greatly by the recent development of Optical Fiber Single-Shot (OFSS) detection at LEAF by A. Cook (DOI: 10.1063/1.3156048) and its forthcoming extension into the NIR regime. IL solvation and rotational dynamics, and electron transfer reactions are measured by TCSPC in the laboratory of E. W. Castner at Rutgers Univ. Picosecond transient absorption measurements of excited state dynamics and electron transfer reactions are done in the laboratory of R. Crowell (BNL). Diffusion rates of anions, cations and solutes are obtained by PGSE NMR in S. Greenbaum's lab at Hunter College, CUNY and by Castner's group at Rutgers. We have extensive collaborations with other major groups in ionic liquid synthesis, physical chemistry, simulations and radiation chemistry.

Ionic liquid synthesis and characterization. Our work often involves novel ILs that we design to the requirements of our radiolysis and solvation dynamics studies and are not commercially available. We have developed in-house capabilities and a network of collaborations (particularly with S. Lall-Ramnarine of Queensborough CC and R. Engel of Queens College) to design, prepare and characterize ILs in support of our research objectives. Cation synthesis is done with a CEM microwave reactor, resulting in higher yields of purer products in much shorter time than traditional methods. We have assembled an instrumentation cluster including DSC, TGA, viscometry, AC conductivity, Karl Fischer moisture determination and ESI-mass spec (for purity analysis and radiolytic product identification). The cluster serves as a resource for our collaborators in the New York Regional Alliance for Ionic Liquid Studies and other institutions (Penn State, ANL). Our efforts are substantially augmented by student internships from the BNL Office of Educational Programs, particularly the VFP (formerly FaST) program, which brings collaborative faculty members and their students into the lab for ten weeks each summer. Since 2003, a total of 34 undergrads, two graduate students, one pre-service teacher, one high school student and four junior faculty have worked on IL projects in our lab, many of them for more than one summer.

Recent Progress

Electron solvation and pre-solvated reactivity in ionic liquids.[5] On time scales of a nanosecond or less, radiolytically-generated excess electrons in ionic liquids undergo solvation processes and reactions that determine all subsequent chemistry and the accumulation of radiolytic damage. Using picosecond pulse-probe and OFSS detection methods, we observed and quantified the solvation response of the electron in 1-methyl-1-butyl-pyrrolidinium bis(trifluoromethylsulfonyl)amide and used it to understand electron scavenging by duroquinone in terms of the competition between electron solvation and pre-solvated electron capture. (with A. Cook, BNL)

Electron transfer (ET) in ionic liquids.[6] Photoinduced charge-separation reactions in a system comprised of an N,N-dimethyl-1,4-phenylenediamine donor, proline bridge and coumarin 343 acceptor (DMPD-pro-C343) were studied as a function of temperature and viscosity and analyzed using a distribution of exponential lifetimes. The ET kinetics were distributed broadly in the ILs and narrowly in CH_3CN and CH_3OH. The results showed the complexity of simple reactions in IL systems and in the case of the most viscous IL, the effects of overlapping dynamical and ET time scales. (with H. Y. Lee and E. W. Castner, Rutgers)

Tuning ionic liquid properties independent of structural changes.[2] In the interest of developing sets of isostructural ionic liquids with different viscosities and therefore different dynamical properties for studies of chemical reactivity, we prepared ammonium and phosphonium NTf_2 salts with the same alkyl side chains and compared their properties and OKE spectra. Viscosities of the phosphonium ILs were roughly half those of the ammonium salts, which the OKE analysis attributed to a weaker interionic interaction arising from the larger ionic volume. (with H. Shirota, Chiba U.)

Future Plans

Cage escape and recombination in ILs. The early steps of photoinduced reactions often involve a competition between recombination and escape of the photoproducts, whether they are radicals or charge-separated states, which largely determines the quantum efficiency of energy capture and in some cases, photodegradation yields in catalytic systems. Compared to molecular solvents, ionic liquids may show unusual dynamical effects in cage relaxation, in addition to slower cage escape due to higher viscosity. In previous work, we observed such effects in the photolysis of *ortho*-chloro-hexaarylbisimidazole (*o*-Cl-HABI, L-L in the adjacent scheme) where quantum yields of the lophyl radical (L•) were much lower in three ILs than in DMSO. Work by others showed that recombination of

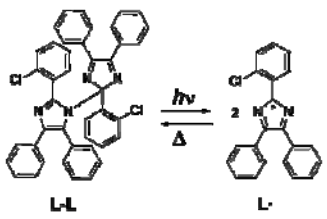

lophyl radical pairs that are covalently constrained in a near-optimal configuration is quite slow ($t_{1/2}$ = 33 ms, $\Delta G^{\neq}$ = 65.5 kJ/mol) due to the large structural rearrangement required. We would like to know if ILs promote recombination through slower cage structural relaxation, holding the radical pair close to the transition state configuration for a longer time, and whether the viscosity-lengthened cage escape time promotes recombination of the relaxed pair through interactions with the IL environment. The OFSS system is critical to this effort because the diffusive recombination of lophyl radicals takes many seconds in ILs and in ordinary solvents, making typical repetitive pump-probe experiments completely impractical. In contrast, OFSS provides picosecond-resolution, 5-nanosecond-range transient absorption data using relatively small numbers of shots that can be collected at arbitrarily long delays in-between. With this advantage, we will examine the kinetics of cage escape and recombination in ILs of different viscosities, and the effects of slow IL relaxation dynamics on the planarization of the lophyl radical, which provides the very large reorganization barrier for radical dimerization. (Collaboration with Prof. V. Strehmel (U. of Applied Sci., Krefeld, Germany) and A. Cook and D. Polyanskiy (BNL))

Effects of ionic liquids on intramolecular ET processes. Over the years, we have successfully used oligoproline-bridged electron donor-bridge-acceptor (D-B-A) systems to probe various aspects of the energetics and distance dependence of ET processes. As noted above,[6] we are using these D-B-A systems to study how ET processes are affected by ionic liquids and showed how slow IL dynamics leads to distributed ET kinetics as predicted by theory. The question of local environment effects (dynamical and energetic) is very important in ILs because of their molecular-scale polar/non-polar heterogeneity. To explore these aspects, we will use D-B-A systems of different charge types, which we expect to occupy different regions within the IL. The neutral DMPD-pro-C343 system undergoes photoinduced charge separation to form a zwitterion, followed by charge recombination during the back electron transfer. Building on the previous emission work,[6] we are using picosecond transient absorption techniques to observe the back ET process and any forward ET processes too fast for TCSPC, and we are extending the bridge length to look for effects of IL structural heterogeneity on both processes. For comparison, we will use the charged $[(bpy)_2Ru^{II}MCbpy\text{-}(pro)_n\text{-}ampyRu^{III}(NH_3)_5]^{5+}$ (n = 1,2) system we have studied extensively in water, which should preferably be located in the polar region of the IL. The $(bpy)_2Ru^{II}MCbpy$ center is an excited state electron donor, so the forward and back ET reactions are charge-shift (2+,3+/3+,2+). (J. Wishart, with R. Crowell (BNL, psec TA), E. W. Castner (Rutgers, TCSPC) and R. Rachid (Fordham, synthesis))

Scavenging and solvation processes of pre-solvated electrons in ionic liquids. Our early work in the reactivity of excess electrons in ionic liquids demonstrated the importance of pre-solvated electron scavenging in trying to understand and predict the distributions of early radiolysis products and radiolytic damage accumulation. It was also clear that the slower relaxation dynamics of ILs made them excellent media for the general study of fundamental radiolysis processes without the need to use cryogenic techniques, in combination with the advanced instrumentation of the LEAF Facility. As noted above,[5] we have recently connected our observed electron solvation dynamics to the kinetics of electron scavenging. In other preliminary work we have observed that selected scavengers (e.g., nitrate, benzophenone) in ILs show different reaction profiles towards the various precursor states to the solvated electron. Different scavenger reactivities towards pre-solvated and solvated electrons have been known empirically for many years and cryogenic kinetic work by Jonah and Lewis showed specific mechanistic differences between scavengers similar to what we have seen in ILs. However, the combination of extended IL dynamical time scales and the time resolution of the LEAF OFSS detection system, coupled with the fact that it uses only small amounts of samples that do not have to be flowed, as well as the ability of ILs to dissolve polar and nonpolar scavengers, provides a unique opportunity to characterize the fundamental reactivity of pre-solvated electron species and understand how the properties of scavengers control their reaction profiles. This knowledge will permit the design of better systems to control radiation-induced reactivity, for example in the processing of radioactive materials (whether in ionic liquids or not), in systems for radiation processing and sterilization, and during long-term exposure to space, for example.

Studies of structure and reaction dynamics in ionic liquids using EXAFS and femtosecond spectroscopy. In collaboration with R. Crowell, R. Musat and D. Polyanskiy, photoionization of Br– anion in neat and diluted bromide ionic liquids is being used to probe the dynamics of excess electrons and excited states. Static and time-resolved Br EXAFS is employed to study the structure of the ionic liquid and the dynamics and reactivity of the Br atom formed by the photoionization. The results can be applied to understanding analogous iodide systems of interest in dye-sensitized solar cells.

Publications on ionic liquids

1. *Radiation Chemistry and Photochemistry of Ionic Liquids*, K. Takahashi and J. F. Wishart in "Charged Particle and Photon Interactions with Matter" Y. Hatano, Y. Katsumura and A. Mozumder, Eds. Taylor & Francis, (2010) Ch. 11, pp 265-287.
2. *Heavy Atom Substitution Effects in Non-Aromatic Ionic Liquids: Ultrafast Dynamics and Physical Properties* H. Shirota, H. Fukazawa, T. Fujisawa, and J. F. Wishart, *J. Phys. Chem. B*, **114,** 9400-9412 (2010)
3. *Ionic Liquids and Solids with Paramagnetic Anions,* B. M. Krieger, H. Y. Lee, T. J. Emge, J. F. Wishart, E. W. Castner, Jr., *Phys. Chem. Chem. Phys.*, **12**, 8919-8925 (2010)
4. *Exploring the Effect of Structural Modification on the Physical Properties of Various Ionic Liquids,* S. I. Lall-Ramnarine, J. L. Hatcher, A. Castano, M. F. Thomas, and James F. Wishart in "ECS Transactions - Las Vegas, NV, Vol. 33, Molten Salts and Ionic Liquids 17" Fox, D., *et al.*, Eds.; The Electrochemical Society, Pennington, NJ, (2010) pp. 659 - 665.
5. *Electron solvation dynamics and reactivity in ionic liquids observed by picosecond radiolysis techniques* J. F. Wishart, A. M. Funston, T. Szreder, A. R. Cook and M. Gohdo, *Faraday Discuss.* **154**, 353-363 (2012).
6. *A Comparison of Electron-Transfer Dynamics in Ionic Liquids and Neutral Solvents* H. Y. Lee, J. B. Issa, S. S. Isied, E. W. Castner, Jr., Y. Pan, C. L. Hussey, K. S. Lee and J. F. Wishart, *J. Phys. Chem. C,* **116**, 5197-5208 (2012).

Publications on other subjects

7. Book: "Recent Trends in Radiation Chemistry," J. F. Wishart and B. S. M. Rao, Eds.; World Scientific, Singapore, (2010). (ISBN 978-981-4282-07-9)
8. *Ultra-fast pulse radiolysis methods,* J. Belloni, R. A. Crowell, Y. Katsumura, M. Lin, J.-L. Marignier, M. Mostafavi, Y. Muroya, A. Saeki, S. Tagawa, Y. Yoshida, V. De Waele, and J. F. Wishart in "Recent Trends in Radiation Chemistry," J. F. Wishart and B. S. M. Rao, Eds. Ch. 5, pp 121-160, World Scientific, Singapore, (2010).
9. *Application of External-Cavity Quantum Cascade IR Lasers to Nanosecond Time-Resolved Infrared Spectroscopy of Condensed-Phase Samples Following Pulse Radiolysis*, D. C. Grills, A. R. Cook, E. Fujita, M. W. George, J. M. Preses, and J. F. Wishart, *Appl. Spect.* **64**, 563-570 (2010), cover publication.

Guest-host interactions in molecular systems with emphasis in energy applications

Sotiris S. Xantheas
Chemical & Materials Sciences Division, Pacific Northwest National Laboratory
902 Battelle Blvd., Mail Stop K1-83, Richland, WA 99352
sotiris.xantheas@pnnl.gov

The objective of this research effort is to develop an understanding of the factors controlling the affinity and selectivity of several molecular hosts to a variety of guest molecules with a particular emphasis on energy applications. The molecular level details of the various prototype guest/host systems, as probed experimentally via spectroscopic techniques and obtained theoretically by various levels of electronic structure theory, play an important role in the assessment of the accuracy of the latter. This information is subsequently used to model the guest/host interactions in complex molecular hosts such as hydrate lattices.

Calixarenes (CAs) are cyclic oligomers built with phenol units. They are recognized as molecular receptors and form a variety of complexes with metal ions, anions and neutral molecules. CAs have a cavity defined by benzene rings and form *endo*-complexes with hydrophobic molecules and cations through both CH-π and charge-π interactions. In addition, CAs have hydroxyl groups at their lower rim. These OH groups are strongly hydrogen (H)-bonded with each other, resulting in the stabilization of the cone conformation. The balance of the interaction between the guest molecule (G in Figure 1) and either the benzene or the hydroxyl group site is very subtle. For example, though it was expected that Calixarenes (C4A) and aliphatic molecules form *endo*-complexes (i.e. the aliphatic molecule lies inside the CA cavity), recent NMR studies revealed that the complex exists as the *exo*-complex having the N^+–H---O^- form (i.e. the aliphatic molecule is located outside the cavity and it is H-bonded to the OH groups). These molecular host/guest systems are ideal test beds for probing the nature of the underlying intermolecular interactions, by switching on and off several of its components upon changing the molecular guest (G = Ar, H_2O, NH_3, C_2H_4, N_2, CH_4). When used in conjunction with various electronic structure calculations, the measured structural (via the interpretation of the IR spectra) and energetic results for these complexes provide important information regarding the performance of different levels and approximations of electronic structure theory in reproducing the subtle balance of those interactions.

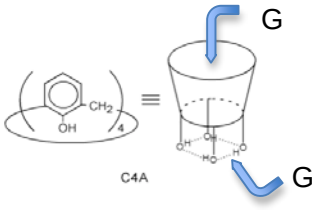

Fig. 1. The two bonding scenarios of a molecular guest (G) to the host Calix[4]arene (C4A).

Table 1 lists the computed energy difference (in cm^{-1}) between the more stable *endo*- and *exo*-isomers of C4A-H_2O. The structures of these two isomers are determined from two very different classes of interactions, namely OH-π and hydrogen bonding interactions, two of the most important ones in the modeling of aqueous biological systems. High levels of electronic

Level of Theory	ΔE(inside-outside), cm^{-1}
MP2 / CBS (*NWChem*)	1052 ± 10
CCSD(T) / CBS est. (*NWChem*)	(838 ± 10)
PBE / TZVP (*CP2K*)	-86
BLYP / TZVP (*CP2K*)	45
BLYP – D / TZVP (*CP2K*)	389
B3LYP / cc-pVTZ (*Gaussian09*)	-828
M06L / cc-pVTZ (*Gaussian09*) / Truhlar	1388
M06HF / cc-pVTZ (*Gaussian09*)	1244
M062X / cc-pVTZ (*Gaussian09*)	1222
B97D / cc-pVTZ (*Gaussian09*) / Grimme	1329
wB97 / cc-pVTZ (*Gaussian09*) / Head-Gordon	583
wB97X / cc-pVTZ (*Gaussian09*)	271
wB97XD / cc-pVTZ (*Gaussian09*)	**964**

Table 1. Calculated energy difference (in cm^{-1}) between the *endo*- (more stable) and *exo*-isomers of C4A-H_2O at various levels of theory.

structure theory that include electron correlation (MP2, CCSD(T)) are used to establish the yardsticks by which other lower levels of theory (such as various Density Functionals) are measured. It is seen that dispersion-corrected functionals are needed to reproduce the trend of the more accurate CCSD(T) results, with some of the most "popular" functionals (BLYP, PBE, B3LYP) producing inaccurate results.

Hydrogen hydrate, a clathrate hydrate generated from hydrogen guest molecules inside hydrate host lattices, is one of the promising hydrogen storage materials. Its applicability as a low-cost hydrogen storage alternative providing a higher storage capacity is still debated because of issues related to its thermal stability near ambient conditions. The maximum hydrogen capacity of the hydrogen hydrate is 5.3 wt. % (mass H_2 per mass H_2O) for cubic structure II (sII) at pressures of P=300 MPa and temperatures of T=250 K [4, 5], a value that is close to the US DOE's 2015 goal of 5.5 wt. %. Experiments have previously indicated that up to four H_2 molecules can occupy the large cages and up to two H_2 molecules the smaller cages. However, the high-pressure requirement for the stability of the hydrogen hydrate, places a limiting constraint on its practical application. An alternative approach to reduce the storage conditions near ambient conditions (e.g. at P=5 MPa and T=280 K) is to use binary hydrate with hydrogen and tetrahydrofuran (THF) with the expense of dramatically reducing the hydrogen storage capacity down to ~ 2 wt.%. A scientific challenge is therefore associated with devising ways to increase the hydrogen storage capacity in hydrogen hydrates near ambient conditions.

We have used dispersion-corrected density functionals to model the accommodation of molecular hydrogen inside the "structure I" (sI) hydrate lattice. The unit cell of this lattice comprises of of two units of the D- (5^{12}) $(H_2O)_{20}$ cage and six units of T- ($5^{12}6^2$) $(H_2O)_{24}$, cage resulting in a periodic unit cell of 46 water molecules with $Pm\bar{3}n$ crystallographic symmetry (α ~12Å). Our first principles MP2 calculations suggest that the gas phase D- and T-cages can accommodate *up to* 5 and 7 hydrogen guest molecules, respectively. One reason for the lower hydrogen capacity of ~5.3 wt. % (mass H_2 per mass H_2O) in the periodic lattice found during experiments, is the release of hydrogen guest molecules to the vapor interface through the hexagonal faces of the larger (T- and H-) cages. Larger guest molecules, such as CH_4 for the (sI) hydrate and THF for the (sII) hydrate, inside the larger cages were found to block the release of hydrogen via the hexagonal faces. In comparison to hydrogen hydrate, which is stable at higher pressures of 300 MPa and lower temperatures of 250 K, methane hydrate is stable near ambient conditions (i.e. at 275 K and 5 MPa). Therefore the hydrogen hydrate could be more stabilized by the presence of larger molecules in the T- and H-cages. In this manner these coated guest hydrates could enhance the thermal physical stability of hydrogen hydrate and allow for the possibility of its practical and industrial applications as hydrogen storage. Finally, since hydrogen hydrate forms a (sII) instead of a (sI) hydrate lattice, coating with larger guest molecules (e.g. THF) might be required.

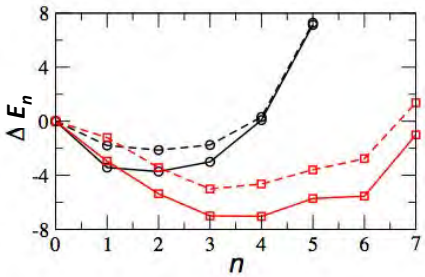

Fig. 2. The binding energies of gas phase $(H_2)_n$@D-cage (black lines, open circles) and $(H_2)_n$@T-cage (red lines, open squares) as a function of the number of hydrogen guest molecules (n) embedded in the host cages. Solid lines: MP2/aug-cc-pVDZ. Dashed lines: BLYP-D/TZV2P.

Most of the hydrogen was found to migrate to adjacent cages via the hexagonal rings, since the migration via (rigid) pentagonal rings is a much higher energy (25 kcal/mol) process.

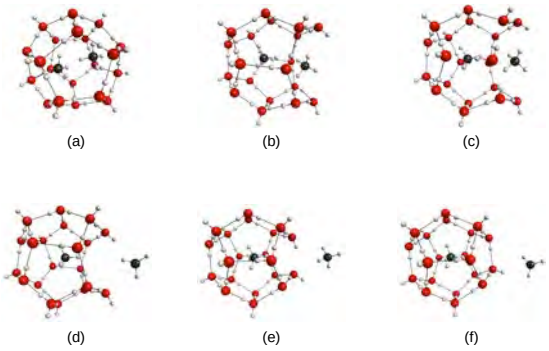

Fig. 3. Snapshots during geometry optimization of a gas phase D-cage with 2 CH_4 molecules: (a) initial configuration (2 CH_4 molecules inside D-cage), (f) final configuration (1 CH_4 molecule inside and one outside). Panels (b)-(e): intermediate steps showing the extrusion of a CH_4 molecule from the D-cage via the breaking of a hydrogen bond of one of the pentagonal faces.

However, an alternative, lower energy hydrogen migration mechanism via broken/reformed pentagonal rings was found to occur via the following steps: (1) a hydrogen bond in the pentagonal ring breaks, (2) one hydrogen molecule migrates to a neighboring cage by slipping through this broken hydrogen bonding network and (3) the broken hydrogen bond is reformed. In this way, the large energy required for the migration of hydrogen molecules via pentagonal rings without breaking any hydrogen bonds is circumvented. This molecular mechanism is similar to the one found for the expulsion of a second methane molecule from a gas phase D-cage (initially containing two CH_4 molecules). It is known that the simple hydrate of methane always occupies the small (5^{12}) cavity of the (sI) lattice and that it will also enter the large ($5^{12}6^2$) cavity of that structure. Future studies will explore the mechanism for the exchange of CH_4 with CO_2 in hydrate lattices.

Acknowledgements: This research was performed in part using the computational resources of the National Energy Research Supercomputing Center (NERSC) at Lawrence Livermore National Laboratory and the Molecular Sciences Computing Facility (MSCF) at the Environmental Molecular Sciences Laboratory, a national scientific user facility sponsored by the Department of Energy's Office of Biological and Environmental Research located at Pacific Northwest National Laboratory. Battelle operates PNNL for the US Department of Energy.

References to publications of DOE sponsored research (2010 - present)

1. N. Hontama, Y. Inokuchi, T. Ebata, C. Dedonder-Lardeux, C. Jouvet, and S. S. Xantheas, "Structure of the Calix[4]arene-(H_2O) cluster: The World's Smallest Cup of Water", *Journal of Physical Chemistry A* **114**, 2967 (2010)
2. X.-B. Wang, K. Kowalski, L.-S. Wang and S. S. Xantheas**,** "Stepwise hydration of the cyanide anion: A temperature-controlled photoelectron spectroscopy and *ab-initio* computational study of $CN^-(H_2O)_n$ (n = 2-5)", *Journal of Chemical Physics* **132**, 124306 (2010)
3. R. Kusaka, Y. Inokuchi, S. S. Xantheas and T. Ebata, "Structures and Encapsulation Motifs of Functional Molecules Probed by Laser Spectroscopic and Theoretical Methods", Invited Review article, Special issue on Laser Spectroscopy and Sensing, *Sensors* **10**, 3519 (2010)
4. T. Ebata, N. Hontama, Y. Inokuchi, T. Haino, E. Aprà and S. S. Xantheas, "Encapsulation of Ar_n clusters by Calix[4]arene: *Endo*- vs. *exo*-complexes" *Physical Chemistry Chemical Physics* **12**, 4569 (2010)
5. F. Paesani, S. Yoo, H. J. Bakker and S. S. Xantheas, "Nuclear Quantum Effects in the reorientation of water" *Journal of Physical Chemistry Letters* **1**, 2316 (2010)
6. E. G. Bakalbassis, E. Malamidou-Xenikaki, S. Spyroudis and S. S. Xantheas, "Dimerization of Indanedioneketene to Spiro-oxetanone: A Theoretical Study", *Journal of Organic Chemistry* **75**, 5499 (2010)
7. S. S. Xantheas, M. S. Gordon, "A Tribute to Klaus Ruedenberg", Klaus Ruedenberg special issue, *Journal of Physical Chemistry A* **114**, 8489 (2010)
8. V.-A. Glezakou, S. T. Elbert, S. S. Xantheas and K. Ruedenberg, "Analysis of bonding patterns in the valence isoelectronic series O_3, S_3, SO_2 and OS_2 in terms of oriented quasi-atomic molecular orbitals" Klaus Ruedenberg special issue (invited), *Journal of Physical Chemistry A* **114**, 8923 (2010)

9. S. Pandelov, J. C. Werhahn, B. M. Pilles, S. S. Xantheas, and H. Iglev, "An empirical correlation between the enthalpy of solution of aqueous salts and their ability to form hydrates", *Journal of Physical Chemistry A* **114**, 10454 (2010). Journal cover
10. S. Yoo, E. Aprà, X.-C. Zeng and S. S. Xantheas, "Lowest-Energy Structures of Water Clusters $(H_2O)_{16}$ and $(H_2O)_{17}$ from high-level ab initio calculations", *Journal of Physical Chemistry Letters* **1**, 3122 (2010)
11. J. C. Werhahn, S. Pandelov, S. Yoo, S. S. Xantheas, H. Iglev, "Dynamics of Confined Water Molecules in Aqueous Salt Hydrates", in *Ultrafast Phenomena XVII,* M. Cherqui, D. M. Jonas, E. Riedle, R. W. Schoenlein, A. J. Taylor (Eds.), Oxford University Press, pp. 463-465 (2011)
12. S. Yoo and S. S. Xantheas, "The Effect of Dispersion Corrections on the Melting Temperature of Liquid Water", Communiction to the Editor, *Journal of Chemical Physics* **134**, 121105 (2011). Featured in the *Virtual Journal of Biological Physics Research*. 5th most downloaded paper in April 2011
13. X.-B. Wang and S. S. Xantheas, "Photodetachment of Isolated Bicarbonate Anion: Electron Binding Energy of HCO_3^-", *Journal of Physical Chemistry Letters* **2**, 1204 (2011)
14. S. Yoo and S. S. Xantheas**,** "The Role of Hydrophobic Surfaces in Altering Water-Mediated Peptide-Peptide Interactions in an Aqueous Environment" Victoria Buch Memorial Issue (invited), *Journal of Physical Chemistry A* **115**, 6088 (2011)
15. J. C. Werhahn, S. Pandelov, S. S. Xantheas, H. Iglev, "Dynamics of Weak, Bifurcated and Strong Hydrogen Bonds in Lithium Nitrate Trihydrate", *Journal of Physical Chemistry Letters* **2**, 1633 (2011)
16. S. Kaneko, Y. Inokuchi, T. Ebata, E. Aprà and S. S. Xantheas, "Laser Spectroscopic and Theoretical Studies of Encapsulation Complexes of Calix[4]arene", *Journal of Physical Chemistry A,* **115**, 10846 (2011)
17. A. Whiteside, S. S. Xantheas, M. Gutowski, "Is Electronegativity a Useful Descriptor for the "Pseudo-Alkali-Metal" NH_4?", *Chemistry A European Journal* **17**, 13197 (2011). Journal cover. Highlighted in Royal Society of Chemistry's "*Chemistry World*", http://www.rsc.org/chemistryworld/News/2011/September/23091104.asp 23 September 2011; Included as a Feature Article in *DOE Pulse*, #356, Feb. 13, 2012: http://www.ornl.gov/info/news/pulse/no356/feature.shtml
18. J. Liu, W. H. Miller, G. S. Fanourgakis, S. S. Xantheas, I. Sho and S. Saito, "Insights in Quantum Dynamical Effects in the Infrared Spectroscopy of Liquid Water from a Semiclassical Study with an Ab Initio-Based Force Field", *Journal of Chemical Physics* **135**, 244503 (2011)
19. S. Yoo and **S**. S. Xantheas, "Structures, Energetics and Spectroscopic Fingerprints of Water Clusters *n*=2-24" *Handbook of Computational Chemistry,* J. Leszczynski (ed.), Springer Science+Business Media B. V., ISBN 978-94-007-0710-8, pp. 761-792 (2012)
20. S. Yoo and **S. S. Xantheas**, "Enhancement of Hydrogen Storage Capacity in Hydrate Lattices", *Chemical Physics Letters,* **525-526**, 13-18 (2012). Editor's Choice article. Featured in DOE's *In Focus* online publication: http://science.energy.gov/news/in-focus/2012/02-06-12/, Science Daily, EV Driven, Deixis magazine (Computational Science at the National Laboratories) http://www.deixismagazine.org/2012/07/twice-stuffed-permafrost/?utm_source=rss&utm_medium=rss&utm_campaign=twice-stuffed-permafrost
21. R. L. Sams, S. S. Xantheas, and T. A. Blake, "Vapor Phase Infrared Spectroscopy and *ab initio* Fundamental Anharmonic Frequencies of Ammonia Borane", *Journal of Physical Chemistry A* **116**, 3124 (2012)
22. G.-L. Hou, H. Wen, K. Lopata, W.-J. Zheng, K. Kowalski, N. Govind, X.-B. Wang, and S. S. Xantheas, "Zeise's Anion and Its Br- and I-Analogs: A Combined Gas-Phase Photoelectron Spectroscopic and Theoretical Study", Communication to the Editor, *Angewandte Chemie International Edition* **51**, 6356 (2012)
23. S. S. Xantheas, "Low-lying energy isomers and global minima of aqueous nanoclusters: Structures and corresponding spectroscopic features of the pentagonal dodecahedron $(H_2O)_{20}$ and $(H_3O)^+(H2O)_{20}$", Special issue on "Nano-Thailand: Nanotechnology for A Sustainable World" (invited), *Canadian Journal of Chemical Engineering* **90**, 843 (2012)
24. D. S. Lambrecht, L. McCaslin, S. S. Xantheas, E. Epifanovsky, and M. Head-Gordon, "Refined energetic ordering for sulfate-water (n=3-6) clusters using high-level electronic structure calculations", Peter Taylor Special Issue (invited), *Molecular Physics*, in press (2012)

Towards single molecule stimulated Raman scattering detection

Sunney Xie, Gary Holtom, Dan Fu
Dept. of Chemistry and Chemical Biology, Harvard University
12 Oxford Street, Cambridge, MA 0213, Cambridge, MA 02138
E-mail: xie@chemistry.harvard.edu

Single molecule spectroscopy and imaging has profoundly deepened our understanding of basic chemical and biological processes. Tremendous progress has been made in the last two decades in single-molecule spectroscopy techniques, especially based on fluorescence detection. The heavy reliance on fluorescence detection for single-molecule spectroscopy is taken for granted by virtue of background free detection. However, most molecules are not naturally fluorescent. Labeling those molecules could be either difficult or affect their function, thus preventing the direct study of those molecules. Therefore, it is important to explore other avenues in single molecule detection and imaging.

Recent success of single molecule absorption detection further motivated us to tackle the larger challenge: single molecule Raman detection. Raman scattering is an inelastic light scattering process that reveals chemical information. Well-resolved vibrational bands are sensitive to both electronic and molecular structure changes. We aim to use stimulated Raman scattering spectroscopy to achieve single molecule Raman scattering detection. Previously we have achieved an SRS detection limit of 50 μM for retinyl palmitate with 1 sec integration time. We have employed two different approaches to further improve the sensitivity of our current SRS system.

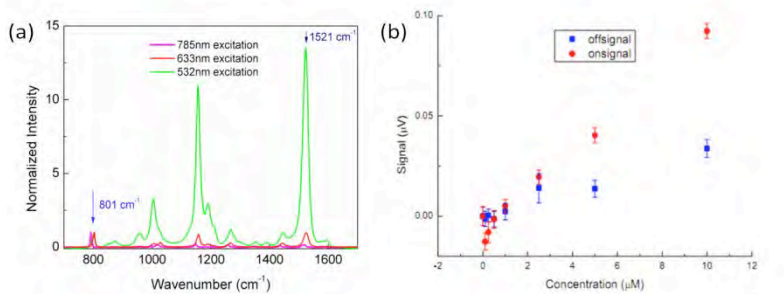

Figure 1: (A) Spontaneous Raman spectra of 1mM β-carotene dissolved in cyclohexane normalized by the solvent peak at 801 cm^{-1}. The C=H stretching peak is at 1521 cm^{-1}. (B) SRS on resonance (1521 cm^{-1}) and off resonance (1501 cm^{-1}) signals from β-carotene at different concentrations. Integration time is 100 ms.

The first approach utilizes near-resonance effect to increase the Raman cross-section. We used visible picosecond lasers as both pump and Stokes beam to excite the SRS of the β-carotene molecule, which has strong absorption near 470 nm. Based on spontaneous Raman measurement (Figure 1a), we observed that visible excitation at 532 nm presents an increase in cross-section of more than 400 fold compared to excitation at 785 nm, at the same excitation power. We measured the detection limit with near-resonant SRS using a flow cell. Solutions of β-carotene in ethanol at increasing concentrations were flowed through a home-made flow cell and the SRS signals were recorded with a lock-in amplifier (100ms time constant). Figure 1(b) shows the concentration-dependent SRS signal. A detection limit of 1μM can be achieved. We also noticed a substantial contribution of off-resonance signal, which is very likely coming from two-color two photon absorption.

The second approach we have undertaken to improve sensitivity is using chirped femtosecond lasers as excitation sources. Stimulated Raman scattering efficiency depends on a number of parameters other than wavelength, including spectral bandwidth, pulse duration and repetition rate. A common laser source for SRS imaging is a saturable absorbed mode-locked Nd:YVO_4 laser which has a pulse duration of 7ps and a synchronous pumped optical parametric oscillator (OPO) with similar output pulse duration. This

pulse duration is a few times longer than the vibrational lifetime of typical chemical bonds, which reduces the excitation efficiency. We adopted a different laser system for SRS excitation. The laser system we used is a home-built Yb:KGW femtosecond laser and a synchronously pumped femtosecond OPO (Figure 2a). In order to reduce the excitation bandwidth, we chirped both lasers with appropriate lengths of glass rods to about 2ps in pulse duration. We demonstrated theoretically and experimentally that the excitation efficiency of this laser system is equivalent to picosecond laser systems with the same pulse duration. With shorter pulse duration, we were able to achieve higher sensitivity at the same power level. In addition, this system allows us to incorporate a frequency modulation (FM) scheme that can effectively remove non-Raman contribution (Figure 2b-c). As an example, we have demonstrated that FM-SRS can image DNA directly in mammalian cells at the fingerprint frequency 790 cm^{-1}.

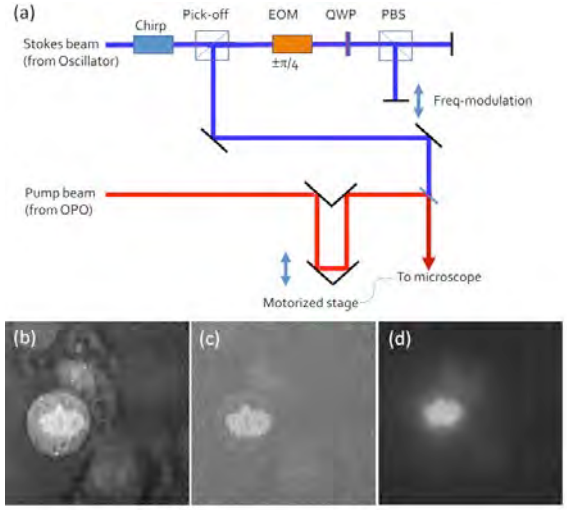

Figure 2: (a) FM-SRS based on chirped femtosecond lasers. The Stokes beam is modulated by an electro-optical modulator and a polarization beamsplitter. The delay of the retroreflecting mirror determines the probed Raman frequency. By changing the relative delay of the two retroreflecting mirrors after the PBS, an effective frequency modulation is applied. (b) SRS image of a mitotic HeLa cell obtained from a single SRS arm probing at 790 cm^{-1}. (c) FM-SRS image of the same cell with the relative Raman shift separated by 20 cm^{-1}. (d) DAPI epi-fluorescence image of the same cell shows the same contrast of the condensed chromosomes.

In summary, we have already achieved single molecule detection sensitivity for absorption using a pump-probe type imaging technique. SRS spectroscopy and microscopy uses a similar detection scheme and has already achieved 50μM detection sensitivity. We are further pushing the sensitivity limit of SRS detection towards single molecule. In theory, near-resonance enhancement could provide up to 400-fold increase in detection sensitivity for β-carotene. We have already improved it to 1μM. A new laser system based on chirped femtosecond laser excitation could also improve the sensitivity as well as eliminating non-Raman background such as absorption. We believe that with further technical developments, we will ultimately achieve the goal of single molecule Raman detection.

Publications of DOE/BES sponsored research

1. Fu, Dan; Holtom, Gary; Freudiger, Christian W.; Xu, Zhang; Xie, X. Sunney "Fast Fast Raman spectral imaging using chirped femtosecond lasers" *J. Phys. Chem*, *submitted* (2012).
2. Chong, Shasha; Min, Wei; Xie, X. Sunney "Ground-State Depletion Microscopy: Detection Sensitivity of Single-Molecule Optical Absorption at Room Temperature" *J. Phys. Chem. Lett*. **1**, 3316-3322 (2010).
3. Saar, Brian G.; Zeng, Yining; Freudiger, Christian W.; Liu, Yu-San; Himmel, Michael E.; Xie, X. Sunney; Ding, Shi-You "Label-Free, Real-Time Monitoring of Biomass Processing with Stimulated Raman Scattering Microscopy" *Angew. Chem. Int. Ed.* **49**, 5476-5479 (2010).
4. Min, Wei; Jiang, Liang; Xie, X. Sunney "Complex Kinetics of Fluctuating Enzymes: Phase Diagram Characterization of a Minimal Kinetic Scheme" *Chem. Asian J.* **5**, 1129-1138 (2010).
5. Lu, Sijia; Min, Wei; Chong, Shasha; Holtom, Gary R.; Xie, X. Sunney "Label-free imaging of heme proteins with two-photon excited photothermal lens microscopy" *Appl. Phys. Lett.*, **96**, 113701 (2010).

DYNAMICS AND KINETICS OF PHOTO-INITIATED CHEMICAL REACTIONS

Hua-Gen Yu (hgy@bnl.gov)
Chemistry Department, Brookhaven National Laboratory, Upton, NY 11973-5000

Program Scope

The purpose of this project is the development and application of computational dynamics and kinetics methods for studying the photochemistry and photophysics processes at liquid and/or solid surfaces. We are interested in developing new dynamics and kinetics models using the molecular and quantum wavepacket dynamics approach and mathematical graph theory, and in applying these models to specific chemical systems related to solar energy conversion. We focus particularly on the processes at semiconductor and nanoparticle surfaces initiated by ultra-violet (UV) or near UV radiation. Here, we aim to construct a general theoretical framework for understanding the energy and chemical evolution of the photo-initiated processes at those surfaces. This project also carries out electronic structure calculations using modern DFT methods to explore the energetics and optical properties of these systems of interest. The research will be done in collaboration with experimentalists at BNL and elsewhere.

Recent Progress

The origin of band gap narrowing of wurtzite GaN/ZnO solid solutions

In collaboration with Dr. Han at BNL CFN, we have carried out a combined experimental and theoretical study for understanding the mechanism of band gap narrowing of GaN/ZnO solid solutions and/or nanocrystals, an important solar fuel material. The GaN-rich GaN/ZnO solid solution was discovered by Domen et al. to be a stable and efficient photocatalyst for water splitting in the visible region in 2005. Recently, our experimental results show that the solid solutions have an even distribution of (ZnO) units among the (GaN) wurtzite frameworks. The GaN/ZnO nanocrystals have the narrowest band gap of 2.21 eV.

Although there are several mechanisms proposed for the band gap narrowing of GaN/ZnO based on DFT calculations, the mechanism is still in extensive debate, partially owing to the ambiguity of the standard DFT methods using the LDA and/or GGA approach. Because the standard DFT methods have a typical flaw that often predicts a rather small band gap for semiconductors such as GaN and ZnO. The theoretical studies of the properties of GaN/ZnO solid solutions have been severely hampered. In order to overcome this drawback, we have developed a hybrid DFT method (bBLYP) optimized for the GaN and ZnO systems. The optimal method can accurately describe the band gaps of both GaN and ZnO bulk materials as well as the properties of some relevant small molecules. The method has successfully been applied for studying the evolution of the band gaps from molecules to bulk materials, and the mixture effect on the band gaps of GaN/ZnO nanoparticles. It was found that the appropriate treatment of exchange functional is very important.

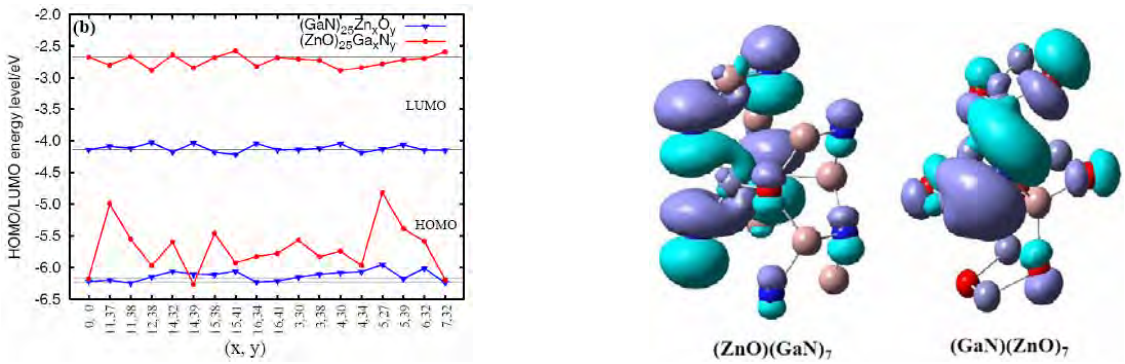

Figure 1 (**Left**) *The HOMO and LUMO energy levels of the* $(GaN)_{25}(ZnO)$ *and* $(ZnO)_{25}(GaN)$ *wurtzite crystal-like nanoparticles; and* (**Right**) *Highest occupied crystal orbitals (HOCOs) of GaN/ZnO wurtzite solid solutions in a* $(ZnO)(GaN)_7$ *or* $(GaN)(ZnO)_7$ *supercell.*

By using this accurate and unambiguous DFT method, we have explored the mechanism of band gap narrowing. It was found that the band gap narrowing in GaN/ZnO is mainly attributed to the upward shifting of the HOMO or HOCO energy levels as shown in Fig. 1 (left). The detailed molecular orbital investigations show that the upward shifting of HOMO/HOCO energy levels is driven by the formation of a chemically bound π-like localized orbital (see the right panel in Fig.1) over a Ga-N-Zn fragment in addition to the p-d repulsion, which is apparently different from the previous proposed mechanisms. In the future, we are going to study the photocatalytic water splitting processes at illuminated aqueous surfaces of GaN/ZnO solid solutions.

The stability of boron nitride-carbon sheets

The boron nitride sheet is isoelectronic with the graphene sheet, but they have dramatically different electronic properties. Mixed BN-C sheets might have band gap engineering applications in electronics and optics. In this work, we (with Dr. Han at CFN) did a combined experimental and theoretical study to understand the structures of carbon units in BN sheets. The theoretical calculations were done using the B3LYP DFT method, based on a circumcoronene-like model. The Raman spectra, structures, and their relative stability are displayed in Fig.2. Results clearly demonstrated that the most stable BN–C sheet is **III** with an armchair linked C–B/N structure. In other words, the armchair linked structure is energetically preferable so that there is a

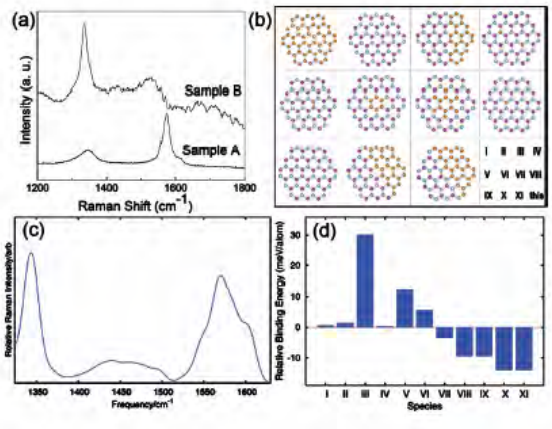

Figure 2. (a) Experimental Raman spectra of BN-C sheets; (b) the C (brown), B (purple), and N (blue) skeletons of circumcoronenelike sheets studied in this work. Their labeling map is given in the right-bottom panel; (c) simulated Raman spectrum of the armchair-connected BN–C species (**III**); (d) calculated relative stability of the BN–C sheets among the group in (b).

relatively large fraction in BN–C sheets, or higher Raman intensities as shown in Fig.2 (a) and (c). Furthermore, Fig. 2(d) shows that the occurrence of embedded C2 and benzene C6 units is likely. This finding supports the experimental observations by Krivanek et al. (O.L. Krivanek et al. *Nature* (London) 464 (2010) 571) and Ci et al. (L. Ci et al. *Nature Mater*. 9 (2010) 430). Indeed, the finding of the armchair connection of graphene fragments to BN can be understood by the fact that graphene sheets with armchair edges are metallic. In addition, the weaker C–B and C–N bond strengths relative to C–C are consistent with the redshift of the Raman peak around 1580 cm^{-1}.

Future Plans

Quantum wavepacket and kinetics studies of photoinduced dynamics of O_2 on TiO_2(110)

One ongoing project is to carry out quantum wavepacket dynamics and kinetics calculation for studying the photoinduced dynamics of the $O_2/TiO_2(110)$ system in collaboration with the BNL Surface Chemical Dynamics Group. This research is an extension of research from our gas-phase molecular dynamics studies toward the gas/solid interface. Here, we will focus on the non-adiabatic effects resulting from the interactions between the photo-excited electrons and the adsorbed molecules on surfaces, and on the electron-hole (e^--h^+) recombination in the TiO_2 case. The non-adiabatic effects will be investigated using a time-dependent wavepacket approach based on the Luntz et al.'s and/or Lara-Castlells and Krause's models (e.g. *J. Chem. Phys*. 118 (2003) 5098; 124 (2006) 244702). The hot electron dynamics at surfaces will be simulated in a kinetics manner. We have developed a kinetic graph theory (KGT) method for studying the e^--h^+ recombination of TiO_2. Preliminary results show that the photocatalytic efficiency is mainly limited by the fast delocalization of excited electrons and their recombination with holes.

The interactions between O_2 and reduced $TiO_2(110)$ surface have been investigated by using a DFT method, based on a compact O_2-$(Ti_{15}O_{28}OH)^-$ cluster model. It has a comparable band gap with that of the TiO_2 crystal. Results show that the triplet state of the reduced $TiO_2(110)$ surface with an O-vacancy is more stable (about 0.22 eV) than the singlet one. An oxygen molecule can strongly chemically adsorb at the vacancy site via either a parallel (in O_2^{2-}) or perpendicular (in O_2^-) structure, where the former is slightly more stable (by about 0.38 eV). Although the dissociated product channel of O_2 at the vacancy site is

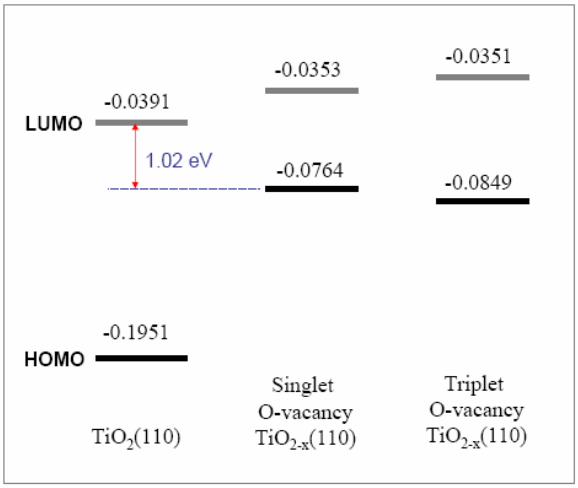

Figure 3. Relative HOMO/LUMO energy levels (in au w.r.t. vacuum) of $TiO_2(110)$ model with/without an O-vacancy.

slightly preferable in energy, the dissociation process has to overcome a classical barrier. Figure 3 shows the HOMO and LUMO energy levels of the cluster model with/without the vacancy, which demonstrates the n-type doping character of O-vacancy.

Publications since 2010

W.-Q. Han, Z. Liu and H.-G. Yu, *Synthesis and optical properties of GaN/ZnO solid soulution nanocrystals*, App. Phys. Lett. **96**, 183112 (2010).

H.-G. Yu, *An optimal density functional method for GaN and ZnO*, Chem. Phys. Lett. **512**, 231 (2011).

W.-Q. Han, H.-G. Yu, Z. Liu, *Convert graphene sheets to boron nitride and boron nitride-carbon sheets via a carbon-substitution reaction*, App. Phys. Lett. **98**, 203112 (2011).

G. Nyman and H.-G. Yu, *Quantum approaches to polyatomic reaction dynamics*, Int. Rev. Phys. Chem. (accepted, 2012).

Participant List

Participant List

Dr. Musahid Ahmed
Lawrence Berkeley National Laboratory
mahmed@lbl.gov
http://www.lbl.gov/LBL-Programs/CSD/directory/bio_ahmed_m.html

Professor Scott Anderson
University of Utah
anderson@chem.utah.edu
http://www.chem.utah.edu/directory/faculty/anderson.html

Professor Krishnan Balasubramanian
California State University East Bay and University of Houston
krishnan.balasubramanian@csueastbay.edu
http://www.mcs.csueastbay.edu/~kbalasub/

Dr. David Bartels
Notre Dame Radiation Laboratory
David.M.Bartels.5@nd.edu
http://www.rad.nd.edu/faculty/bartels.htm

Dr. Ali Belkacem
Lawrence Berkeley National Laboratory
abelkacem@lbl.gov
http://www.lbl.gov/csd/directory/bio_belkacem_a.html

Dr. Hendrik Bluhm
Lawrence Berkeley National Laboratory
hbluhm@lbl.gov
http://www.lbl.gov/csd/directory/bio_bluhm_h.html

Dr. Nicholas Camillone
Brookhaven National Laboratory
nicholas@bnl.gov
http://www.bnl.gov/chemistry/bio/Camillone%20IIINicholas.asp

Dr. Ian Carmichael
Notre Dame Radiaton Laboratory
carmichael.1@nd.edu
http://www.rad.nd.edu/faculty/carmichael.htm

Dr. Michael Casassa
US DOE/Basic Energy Sciences
michael.casassa@science.doe.gov
http://science.energy.gov/bes/csgb/about/staff/dr-michael-p-casassa/

Professor David Chandler
Lawrence Berkeley National Laboratory
chandler@berkeley.edu
http://gold.cchem.berkeley.edu/David/David/David_Chandler.html

Dr. Daniel Chipman
Notre Dame Radiation Laboratory
chipman.1@nd.edu
http://www.rad.nd.edu/faculty/chipman.htm

Dr. Andrew Cook
Brookhaven National Laboratory
acook@bnl.gov
http://www.chemistry.bnl.gov/sciandtech/PRC/acook/cook.html

Dr. Robert Crowell
Brookhaven National Laboratory
crowell@bnl.gov
http://www.bnl.gov/chemistry/bio/CrowellRobert.asp

Professor Tanja Cuk
Lawrence Berkeley National Laboratory
tanjacuk@berkeley.edu
http://www.cchem.berkeley.edu/tkgrp/tanja.html

Dr. Liem Dang
Pacific Northwest National Laboratory
liem.dang@pnnl.gov
http://www.pnl.gov/science/staff/staff_info.asp?staff_num=5604

Professor Michael Duncan
University of Georgia
maduncan@uga.edu
http://maduncan.myweb.uga.edu/

Dr. Michel Dupuis
Pacific Northwest National Laboratory
michel.dupuis@pnnl.gov
http://www.pnl.gov/cmsd/staff/staff_info.asp?staff_num=5599

Professor Kenneth Eisenthal
Columbia University
kbe1@columbia.edu
http://www.columbia.edu/cu/chemistry/fac-bios/eisenthal/faculty.html

Professor Mostafa El-Sayed
Georgia Institute of Technology
melsayed@gatech.edu
http://www.chemistry.gatech.edu/faculty/El-Sayed/

Professor James Evans
Ames Laboratory
evans@ameslab.gov
http://www.ameslab.gov/cbs/evans

Professor Michael Fayer
Stanford University
fayer@stanford.edu
http://www.stanford.edu/group/fayer/

Dr. Gregory Fiechtner
DOE/Basic Energy Sciences
gregory.fiechtner@science.doe.gov
http://science.energy.gov/bes/csgb/about/staff/dr-gregory-j-fiechtner/

Mr. John L. Fulton
Pacific Northwest National Laboratory
john.fulton@pnnl.gov
http://www.pnl.gov/cmsd/staff/staff_info.asp?staff_num=5587

Dr. Bruce Garrett
Pacific Northwest National Laboratory
bruce.garrett@pnnl.gov
http://www.pnl.gov/science/staff/staff_info.asp?staff_num=5496

Professor Phillip Geissler
Lawrence Berkeley National Laboratory
geissler@cchem.berkeley.edu
http://www.cchem.berkeley.edu/plggrp/index.html

Dr. Mary K. Gilles
Lawrence Berkeley National Laboratory
MKGilles@lbl.gov
http://www.lbl.gov/csd/directory/bio_gilles_mk.html

Professor Mark Gordon
Ames Laboratory
mark@si.msg.chem.iastate.edu
http://www.ameslab.gov/cbs/mark

Dr. Jeffrey Guest
Argonne National Laboratory
jrguest@anl.gov
http://nano.anl.gov/docs/people/guest.pdf

Dr. Alexander Harris
Brookhaven National Laboratory
alexh@bnl.gov
http://www.bnl.gov/chemistry/bio/HarrisAlex.asp

Professor Mark Hersam
Northwestern University
m-hersam@northwestern.edu
http://www.hersam-group.northwestern.edu/

Dr. Wayne Hess
Pacific Northwest National Laboratory
wayne.hess@pnnl.gov
http://www.pnl.gov/science/staff/staff_info.asp?staff_num=5505

Professor Wilson Ho
University of California, Irvine
wilsonho@uci.edu
http://www.physics.uci.edu/~wilsonho/whoghp.htm

Dr. Frances Houle
Lawrence Berkeley National Lab
FAHoule@lbl.gov
http://www.lbl.gov/LBL-Programs/CSD/introduction/contacts.html

Dr. Libai Huang
Notre Dame Radiation Laboratory
lhuang2@nd.edu
http://www.rad.nd.edu/faculty/huang.htm

Professor Bret Jackson
University of Massachusetts Amherst
jackson@chem.umass.edu
http://www.chem.umass.edu/faculty/jackson.html

Dr. Ireneusz Janik
Notre Dame Radiation Laboratory
ijanik@nd.edu
http://www.rad.nd.edu/faculty/Janik.htm

Professor Caroline Chick Jarrold
Indiana University
cjarrold@indiana.edu
http://cjarrold.chem.indiana.edu/

Dr. Cynthia J. Jenks
Ames Laboratory
cjenks@ameslab.gov
http://www.ameslab.gov/cbs/cjenks

Professor Mark Johnson
Yale University
mark.johnson@yale.edu
http://www.chem.yale.edu/faculty/johnson.html

Professor Kenneth Jordan
University of Pittsburgh
jordan@pitt.edu
http://www.pitt.edu/~jordan/

Dr. Shawn Kathmann
Pacific Northwest National Laboratory
shawn.kathmann@pnnl.gov
http://www.pnl.gov/science/staff/staff_info.asp?staff_num=5601

Dr. Bruce Kay
Pacific Northwest National Laboratory
bruce.kay@pnnl.gov
http://www.pnl.gov/science/staff/staff_info.asp?staff_num=5530

Professor Munira Khalil
University of Washington
mkhalil@chem.washington.edu
http://depts.washington.edu/chem/people/faculty/mkhalil.html

Dr. Greg Kimmel
Pacific Northwest National Laboratory
gregory.kimmel@pnnl.gov
http://www.pnl.gov/science/staff/staff_info.asp?staff_num=5527

Dr. Jay LaVerne
Notre Dame Radiation Laboratory
Jay.A.LaVerne.1@nd.edu
http://www.rad.nd.edu/faculty/laverne.htm

Professor H. Peter Lu
Bowling Green State University
hplu@bgsu.edu
http://www.bgsu.edu/departments/chem/faculty/hplu/peterlu.htm

Dr. Sergei Lymar
Brookhaven National Laboratory
lymar@bnl.gov
http://www.bnl.gov/chemistry/bio/LymarSergei.asp

Diane Marceau
DOE/Basic Energy Sciences
diane.marceau@science.doe.gov
http://science.energy.gov/bes/csgb/about/staff/

Dr. John Miller
Brookhaven National Laboratory
jrmiller@bnl.gov
http://www.chemistry.bnl.gov/SciandTech/PRC/miller/miller.html

Dr. Christopher Mundy
Pacific Northwest National Laboratory
chris.mundy@pnnl.gov
http://www.pnl.gov/science/staff/staff_info.asp?staff_num=5981

Professor Richard Osgood
Columbia University
osgood@columbia.edu
http://www.ee.columbia.edu/fac-bios/osgood/faculty.html

Dr. Mark Pederson
DOE/Basic Energy Sciences
mark.pederson@science.doe.gov
http://science.energy.gov/bes/csgb/about/staff/dr-mark-r-pederson/

Professor Hrvoje Petek
University of Pittsburgh
petek@pitt.edu
http://www.ultrafast.phyast.pitt.edu/Home.html

Professor Eric Potma
University of California, Irvine
epotma@uci.edu
http://chem.ps.uci.edu/~potma/research.htm

Professor Krishnan Raghavachari
Indiana University
kraghava@indiana.edu
http://raghavachari.chem.indiana.edu/

Dr. Eric Rohlfing
DOE/Basic Energy Sciences
eric.rohlfing@science.doe.gov
http://science.energy.gov/bes/csgb/about/staff/dr-eric-a-rohlfing/

Professor Richard Saykally
University of California Berkeley
saykally@berkeley.edu
http://www.cchem.berkeley.edu/rjsgrp/

Dr. Gregory Schenter
Pacific Northwest National Laboratory
greg.schenter@pnnl.gov
http://www.pnl.gov/science/staff/staff_info.asp?staff_num=5615

Professor Steven Sibener
Univerity of Chicago
s-sibener@uchicago.edu
http://sibener-group.uchicago.edu/

Dr. Wade Sisk
US DOE/Basic Energy Sciences
wade.sisk@science.doe.gov
http://science.energy.gov/bes/csgb/about/staff/dr-wade-sisk/

Professor James Skinner
University of Wisconsin
skinner@chem.wisc.edu
http://www.chem.wisc.edu/~skinner/

Professor Timothy Steimle
Arizona State University
tsteimle@asu.edu
http://www.public.asu.edu/~steimle/

Professor Charles Sykes
Tufts University
charles.sykes@tufts.edu
http://ase.tufts.edu/chemistry/sykes/frameSet.html

Professor Ward Thompson
University of Kansas
wthompson@ku.edu
http://web.ku.edu/~wthompson/Thompson_Group_Home.html

Professor Andrei Tokmakoff
Massachusetts Institute of Technology
tokmakof@mit.edu
http://web.mit.edu/~tokmakofflab/

Professor John Tully
Yale University
john.tully@yale.edu
http://www.chem.yale.edu/~tully/

Dr. Marat Valiev
Pacific Northwest National Laboratory
marat.valiev@pnnl.gov
http://emslbios.pnl.gov/bios/biosketch.nsf/bynameinit/valiev_m

Professor Lai-Sheng Wang
Brown University
lai-sheng_wang@brown.edu
http://casey.brown.edu/chemistry/research/LSWang/

Dr. Xue-Bin Wang
Pacific Northwest National Laboratory
xuebin.wang@pnnl.gov
http://emslbios.pnl.gov/bios/biosketch.nsf/bynameinit/wang_x

Professor Michael White
Brookhaven National Laboratory
mgwhite@bnl.gov
http://www.bnl.gov/chemistry/bio/WhiteMichael.asp

Dr. Kevin R. Wilson
Lawrence Berkeley National Laboratory
krwilson@lbl.gov
http://www.lbl.gov/csd/directory/bio_wilson_kevin.html

Dr. James Wishart
Brookhaven National Laboratory
wishart@bnl.gov
http://www.chemistry.bnl.gov/SciandTech/PRC/wishart/wishart.html

Professor X. Sunney Xie
Harvard University
xie@chemistry.harvard.edu
http://bernstein.harvard.edu/

Dr. Sotiris Xantheas
Pacific Northwest National Laboratory
sotiris.xantheas@pnl.gov
http://www.pnl.gov/science/staff/staff_info.asp?staff_num=5610

Dr. Hua-Gen Yu
Brookhaven National Laboratory
hgy@bnl.gov
http://www.bnl.gov/chemistry/bio/YuHua-Gen.asp